SURFACE PHASE BEHAVIOR OF PHOSPHOLIPID MONOLAYERS AT THE AIR/WATER INTERFACE AND INTERACTIONS WITH LUNG ANNEXIN I

by

SANDY KOPPENOL

A thesis in partial fulfillment of the
requirements for the degree of

Doctor of Philosophy
(Pharmacy)

at the
UNIVERSITY OF WISCONSIN-MADISON
1996

SURFACE PHASE BEHAVIOR OF PHOSPHOLIPID MONOLAYERS AT THE AIR/WATER INTERFACE AND INTERACTIONS WITH LUNG ANNEXIN I

Sandy Koppenol

Under the supervision of Professor George Zografi

at the University of Wisconsin-Madison

Mixtures of zwitterionic and anionic phospholipids spread as monolayers on an aqueous subphase were used as model systems to study the interaction of a phospholipid-binding protein, lung annexin I (LAI), with phospholipids. The objectives were to (1) determine the surface miscibility of mixtures of zwitterionic dipalmitoylphosphatidylcholine (DPPC) with unsaturated phosphatidylcholines and with saturated and unsaturated phosphatidylglycerols (PG) at pH 7.4, 25°C in the absence and presence of Ca^{2+} and; (2) study the influence of monolayer composition and phase behavior on the interaction of LAI. The miscibility of the binary monolayers was determined by analysis of surface pressure, π, as a function of surface density, measurement of equilibrium spreading pressures, and by direct observation of phase behavior using fluorescence microscopy. The interaction of LAI with phospholipids was studied by injecting the protein beneath the monolayer and monitoring changes in the surface pressure, $\Delta\pi$, and the phase behavior of the monolayer, and by imaging LAI adsorbed to mica-supported phospholipid bilayers using atomic force microscopy (AFM).

Phospholipids with identical acyl chains mix ideally while mixtures of saturated and unsaturated lipids show nonideal miscibility when the polar groups are the same, or phase separation when the headgroups are different. The amount of phase separation increases with increasing π, increasing ratios of DPPC in the monolayer and with the

addition of Ca^{2+} to the subphase. Measurements of $\Delta\pi$ indicate that LAI penetrates PG monolayers in a Ca^{2+}-dependent manner up to $\pi \approx 20$mN/m but that it shows no such effects with DPPC. At $25<\pi<35$mN/m, adsorption of LAI condensed the POPG (1-palmitoyl-2-oleoyl-phosphatidylglycerol) monolayers resulting in a negative $\Delta\pi$, while no changes in π were observed at higher π with DPPG (dipalmitoylphosphatidyl-glycerol) monolayers. AFM measurements with DPPG LB films formed by monolayers at $\pi = 35$mN/m show that LAI remains associated with DPPG even when excluded from the monolayer. LAI increased surface phase separation in binary monolayers of DPPC and POPG at low π, while at high π LAI promoted surface miscibility. In contrast, no significant changes in π or on the phase equilibria of the monolayer were observed with an LAI mutant in which a portion of the N-terminus had been removed. This suggests that the N-terminus is directly involved in the LAI-anionic phospholipid interaction.

APPROVED:

Date April 13, 1996

George Zografi

George Zografi, Professor

Acknowledgments

I would like to thank Professor Zografi for giving me the opportunity to work on this project. His systematic approach to research and his careful attention to detail were important to the development of this project. I also greatly appreciate the many hours he spent working with me to write proposals and work on various presentations.

I would also like to acknowledge Professor Yu for all of his insight into this project. Dr. Yu's interest in my education began even before I arrived on campus. His encouraging letter played a key role in swaying my decision to attend UW. Ever since my arrival on campus he has treated me as a member of his research group.

I also attribute much of my development as a scientist to the various members of the pharmaceutics department. I not only learned a lot of science from them but, I had fun doing it. Gwen Mlynek and Ching-Yi Chow helped to make graduate school life a lot more bearable by celebrating all kinds of holidays with me and making sure that I wasn't going hungry on a day to day basis. Gwen was also key in making sure I got some exercise by coaxing me to take a break and go to aerobics. Karen Mangasarian has been a great support ever since the first day that I arrived. She introduced me to the joys of working late into the wee hours of the morning, Her surprise visits back to Madison from the Big Apple were always a treat. Rashid Mosavin shared a big portion of his life with me and his patience and understanding throughout our friendship made life a lot easier. Although Marco Lolli was only here for a short time, we had loads of good times especially when we went out in his "dream car." New Year's celebrations are not the same without him and Alberto. Gary "Bucky" Anderson's constant words of encouragement (harassment?) helped make those difficult days go by a little faster. Fortunately, my tenure at Wisconsin overlapped with those of the trio from Professor Connors' lab, Ray Skwierczynski, Michael Mulski and, Jason LePree. I owe part of my

survival of quantum mechanics and statistical mechanics to Ray. He should be a teacher. Mike was always there for reality checks. Jay helped me out in ways too numerous to list. The best thing about Jay was his great personality, he added a lot of life to the department. Jay and the rest of the night shift, Sheri Shamblin, Gwen Mlynek, and John Hill, made experimenting in the lab late at night an adventure. The fourth floor gang also made lab life a lot more enjoyable. Gedi Vidugiris' big smile and bear hugs always cheered me up when I was feeling down. Martha Brown's sense of humor and willingness to listen to me ramble during preparation of this thesis were commendable. My very special thanks to John Hill for unending scientific and emotional support. He was very patient and understanding of my irrational behavior during my stress attacks. His amiable personality makes him unique in this department. He is one of the few people who can work really hard and have fun doing it. His encouragement and enthusiasm not only helped me through graduate school but got me an awesome postdoc position in Seattle.

I was lucky enough to have worked with three outstanding research labs. Pete Ellingson, Sanghoon Kim, Sangsoo Park, Alan Esker, Jingwen Ma and Zhihao Yang of Professor Yu's research group were very helpful in giving me feedback from a physical chemist's viewpoint. Dr. Tsao provided me with protein and he always made me feel very welcome in his lab. He made this project very interesting by keeping us up to date on the exciting implications that our biophysical work had on important biochemical and clinical events involving the protein. I would also like to acknowledge all of the members of Professor Zografi' s group, past and present. They helped me to mature as a scientist and were always over anxious to help me. My first monolayer was spread with the help of Mehran Yazdanian who still is counseling me to this day. Churn-Shiouh Gau and Mark Sacchetti were also key to my development as a surface scientist. Cynthia Oksanen, Azita Saleki-Gerhardt, Valssios Andronis, Negar Sadrzadeh, and Aye

Khin-Khin were also really great labmates. I especially acknowledge Sheri Shamblin for companionship both in and out of the lab. I am sure that I would not have made it this far without Sheri's constant encouragement and fun-loving attitude.

Finally, I would like to acknowledge my parents, Caroline and Peter, and my brother Hank for their understanding and encouragement throughout my graduate career.

Financial support was provided by the Glaxo/American Association of Colleges of Pharmacy, the American Foundation for Pharmaceutical Education (Edwin L. Newcomb Memorial Fellowship), and the Pharmaceutical Research and Manufacturers of America Foundation, Inc.

Table of Contents

List of Figures

List of Tables

Chapter I

Introduction

Lung Surfactant Composition and Function

Lung surfactant is a complex mixture of phospholipids and proteins that play an important physiological role in the pulmonary system. Phospholipids comprise approximately 90% of human lung surfactant by weight and phosphatidylcholines (PC) are the most abundant (70-80%); approximately 60% of the PCs are disaturated with 1, 2-dipalmitoyl-*sn*-glycero-3-phosphocholine (DPPC) being the most common. Lung surfactant also contains an unusually large amount (up to 10%) of phosphatidylglycerol (PG) which is the second most abundant group of phospholipids (Keough, 1985; Hawgood and Clements, 1990; Hills, 1990). Interestingly, in other tissues PG only occurs in minute amounts. Lung surfactant also contains small amounts of phosphatidylethanolamine (PE), phosphatidylinositol (PI), and phosphatidylserine (PS) (Green, Phillips et al., 1973). Very little variation in surfactant components are observed among various adult mammalian species (Schlame, Casals et al., 1988). However, immature mammalian lung surfactant and infants suffering from respiratory distress syndrome have surfactant that is characterized by a high percentage of PI and little or no PG, suggesting that PG specifically improves surfactant quality (Hallman, Enhorning et al., 1985).

Synthesis of lung surfactant components occurs in the endoplasmic reticulum of the Type II cell of the lung (for review see (Wright and Clements, 1987)) (Figure 1.). The products are transferred as vesicles ("small lamellar bodies") via the Golgi

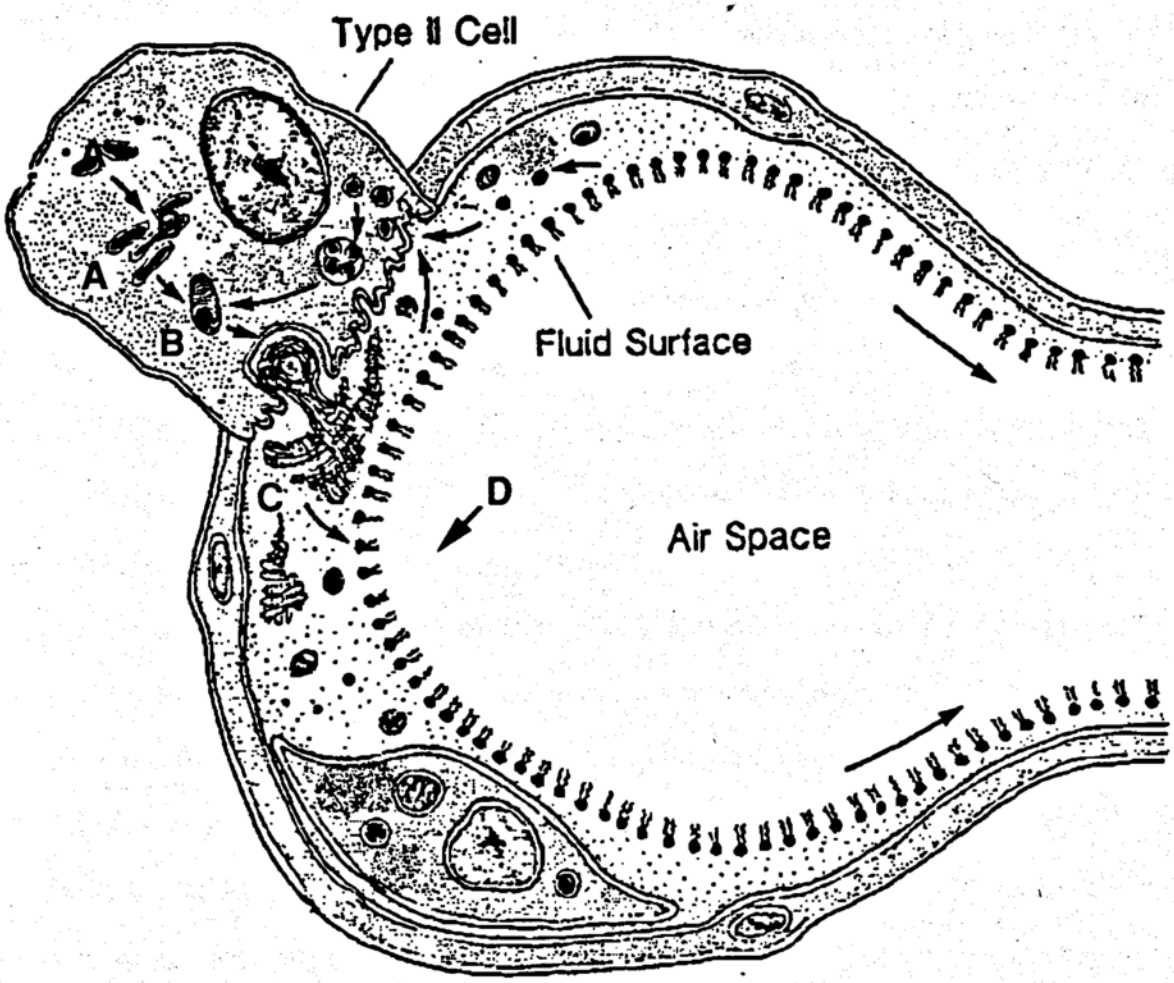

Figure 1. Schematic illustration of the alveolus of the lung. A. Golgi apparatus B. Lamellar body C. Tubular myelin D. Lung surfactant monolayer

apparatus and assembled into lamellar bodies, the intracellular storage granules. Within the lamellar bodies, the surfactant is believed to be tightly packed in multilayer arrays with a protein core and it has been suggested that lipid remodeling may occur within this structure to produce the high levels of DPPC found in surfactant (Batenburg, 1992). By some yet unknown exocytotic process, the surfactant then is secreted by way of these lamellar bodies into the liquid lining of the alveolus (the terminal unit of the lung where gas exchange occurs) and expands into a complicated three-dimensional lattice-like structure called tubular myelin. Tubular myelin then undergoes a transformation to form a monolayer of surfactant at the air/alveolus interface. There are approximately 300 million alveoli which comprise 70-90 m^2 of surface area. At the end of the breathing cycle, some components are taken back into Type II cells, possibly in the form of small vesicles and multivesicular bodies, and again are stored in lamellar bodies (Wright and Clements, 1987; Hawgood and Clements, 1990) To date, there is a significant lack of knowledge about the details of how any of these processes take place.

The primary role of lung surfactant is to reduce the surface tension, γ, at the air/alveolus interface, thereby preventing the alveoli from collapsing during exhalation (Goerke, 1974; Hills, 1990). A reduction in γ prevents collapse by keeping the pressure gradient, ΔP, across the alveolus wall constant as the radius, r, is decreased., This is described by the Laplace equation (Adamson, 1990):

$$\Delta P = \frac{2\gamma}{r}. \qquad (1)$$

There are also strong indications that lung surfactant is involved in the host-defense system of the lung (Van Iwaarden, Welmers et al., 1990)

The best known clinical manifestation of a lack of functioning surfactant is respiratory distress syndrome (RDS) which occurs in the mature adult population and is also the leading cause of mortality in premature infants. This has led to an interest in the development of an artificial lung surfactant which consists of a mixture of the minimum number of components that can meet the physiological and physical chemical requirements of natural surfactant. The current understanding of the natural surfactant suggests that any artificial lung surfactant must meet the following requirements (Bangham, Morley et al., 1979): (1) the monolayer formed by the materials must be capable of achieving very low surface tension and be stable in that state for significant periods of time; and (2) the spreading and formation of the monolayer over the air/alveolus interface must be rapid (Keough, 1984) Achieving these requirements demands two very different types of molecules so that a delicate balance of different lipids is necessary for proper function.

It has been suggested that the first requirement can be met by a monolayer film that is enriched in DPPC since it has been demonstrated that pure DPPC monolayers form incompressible, highly elastic films that upon rapid compression are capable of reducing γ to close to 0 mN/m at high surface densities. Although the mechanism is not completely clear, it has been proposed that "squeeze out" of non-DPPC lipids occurs as the monolayer is compressed via the action of certain ions and/or proteins(Watkins, 1968; Hawco, Coolbear et al., 1981; Hawco, Davis et al., 1981; Boonman, Machiels et al., 1987; Van Liempd, Boonman et al., 1987; Fleming and Keough, 1988; Pastrana, Mautone et al., 1991; Yu and Possmayer, 1992; Rana, Mautone et al., 1993). The second requirement can be achieved with lipids that are more "liquid-like" or "fluid" and are thus capable of destabilizing bilayer and multilayer phases, the precursors of the alveolar monolayer. It is generally accepted that the unsaturated lipids which spontaneously form expanded, compressible

monolayers and consist primarily of PC and PG in lung surfactant accomplish this role and facilitate the adsorption and spreading of the surfactant monolayer (Fleming and Keough, 1988; Yu and Possmayer, 1992). Exogenously introduced artificial surfactant replacements have been designed along these lines with limited amounts of long-term success (Van Golde, Batenburg et al., 1988)

Also associated with extracellular lung surfactant are the surfactant proteins, designated SP-A, SP-B, SP-C, and SP-D, whose exact functions are still unclear (for review, see (Van Golde, Batenburg et al., 1988; Hawgood and Clements, 1990)). SP-A and SP-D are hydrophilic while SP-B and SP-C are hydrophobic. They appear to facilitate a number of the steps in the process of delivering surfactant to the alveolus and having it efficiently spread at the air/alveolus interface (Hawgood and Clements, 1990) In vitro experiments have demonstrated that SP-A SP-B, and SP-C interact synergistically to enhance the adsorption of phospholipids. SP-A may participate in the transformation of the lamellar body to tubular myelin and it may be important in the regulation and of the secretion and clearance of surfactant lipids and in the alveolar defense mechanism (Van Golde, Batenburg et al., 1988). SP-D, the most recently identified surfactant associated protein is hypothesized to have functions similar to those of SP-A .

Monolayers as Model Phospholipid Assemblies

Monolayers at the Air/Water Interface

Mixtures of phospholipids as self-assembled monolayers on an aqueous subphase have traditionally been used as structural models of biological membranes. They also serve as useful models of bilayer systems such as vesicles and multilayer structures,

i.e. the lamellar body associated with the lung surfactant system. The study of phospholipid monolayers has led to an increased understanding of the functional role of lipid bilayers in biological systems, and how the lateral organization of the lipid matrix affects physical properties and biological functions of these systems. Monolayer studies are advantageous since they can be performed in a well-defined system by controlling variables such as surface density, ionic conditions of the subphase, temperature and surface composition (Möhwald, 1990)

Phospholipid monolayers are typically formed on aqueous surfaces by dissolving the lipids in a volatile solvent and depositing known amounts on an aqueous surface of known surface area at a constant temperature. The surface concentration, Γ, in molecules per unit area is altered by varying the number of molecules for a fixed total area or by varying the available area with a fixed number of molecules. Surface tension, γ, at the air-water interface before and after spreading the monolayer is measured using the Wilhelmy plate method. The difference between the surface tension of the clean surface, γ_o, and the surface tension of the monolayer-covered surface, γ, is the surface pressure, Π. By relating the surface pressure to $1/\Gamma$ or area per molecule, A, one can construct a "surface phase diagram" conjugate to the more familiar three dimensional pressure vs. volume phase diagram. Spreading of a monolayer can also be performed without a solvent for most lipids. When a material which spreads spontaneously is placed on a water surface, molecules leave the bulk phase and diffuse out over the liquid. In the presence of excess bulk material, spreading will continue until the surface pressure reaches the "equilibrium spreading pressure," or πe. The equilibrium value is characteristic of the substance being spread and varies with temperature (Jalal, Zografi et al., 1980). It depends on the relative magnitude of the intermolecular forces between the molecules in the monolayer at the air/water interface i.e. interaction with water, and those that favor the retention of the molecules in a bulk phase, i.e. crystal energies.

Molecules in monolayers can exist in different states which are analogous to three dimensional solids, liquids, and gases (for review, (Gaines, 1966; Adamson, 1990)). These different states reflect the different degrees of molecular order which result from intermolecular forces between the monolayer film-forming molecules and the interactions of these molecules with the subphase. A schematic surface phase diagram or Π-A diagram of a monolayer is given in Figure 2 (Birdi, 1989) At high molecular areas, the monolayer exists in a gaseous state where the area per molecule is large compared to the actual molecular area so that there are essentially no intermolecular interactions. As the area per molecule is decreased, a liquid-like monolayer is formed where the hydrocarbon portion of the molecule now extends into the air and eventually becomes perpendicular to the plane of the subphase surface. There are two distinguishable types of liquid films. The first is termed liquid expanded (LE) and it is schematically illustrated in curve a. It is formed via a first-order transition from the gaseous state and has a relatively high compressibility. In this state, the hydrocarbon chains are believed to be in a highly fluid, mobile state (Phillips and Chapman, 1968) A further decrease in the area per molecule will cause the monolayer film to undergo another first-order phase transition to a liquid condensed (LC) state (Pallas and Pethica, 1985; Hifeda and Rayfield, 1992). In this state, the acyl chains are more ordered and the monolayer now has a lower compressibility. A monolayer also can pass directly from a gaseous state to a LC state, as is illustrated in Figure 2 (Birdi, 1989), curve b, depending on temperature and the presence of electrolytes in the subphase. A further decrease in area per molecule yields an incompressible solid film which represents the closest packing of the hydrocarbon chains. If the area per molecule is decreased further, film collapse (Π_c) occurs and the molecules are forced out of the monolayer to form a new bulk phase. Experimentally, it has been found that some monolayers can be compressed to surface pressures that are considerably higher

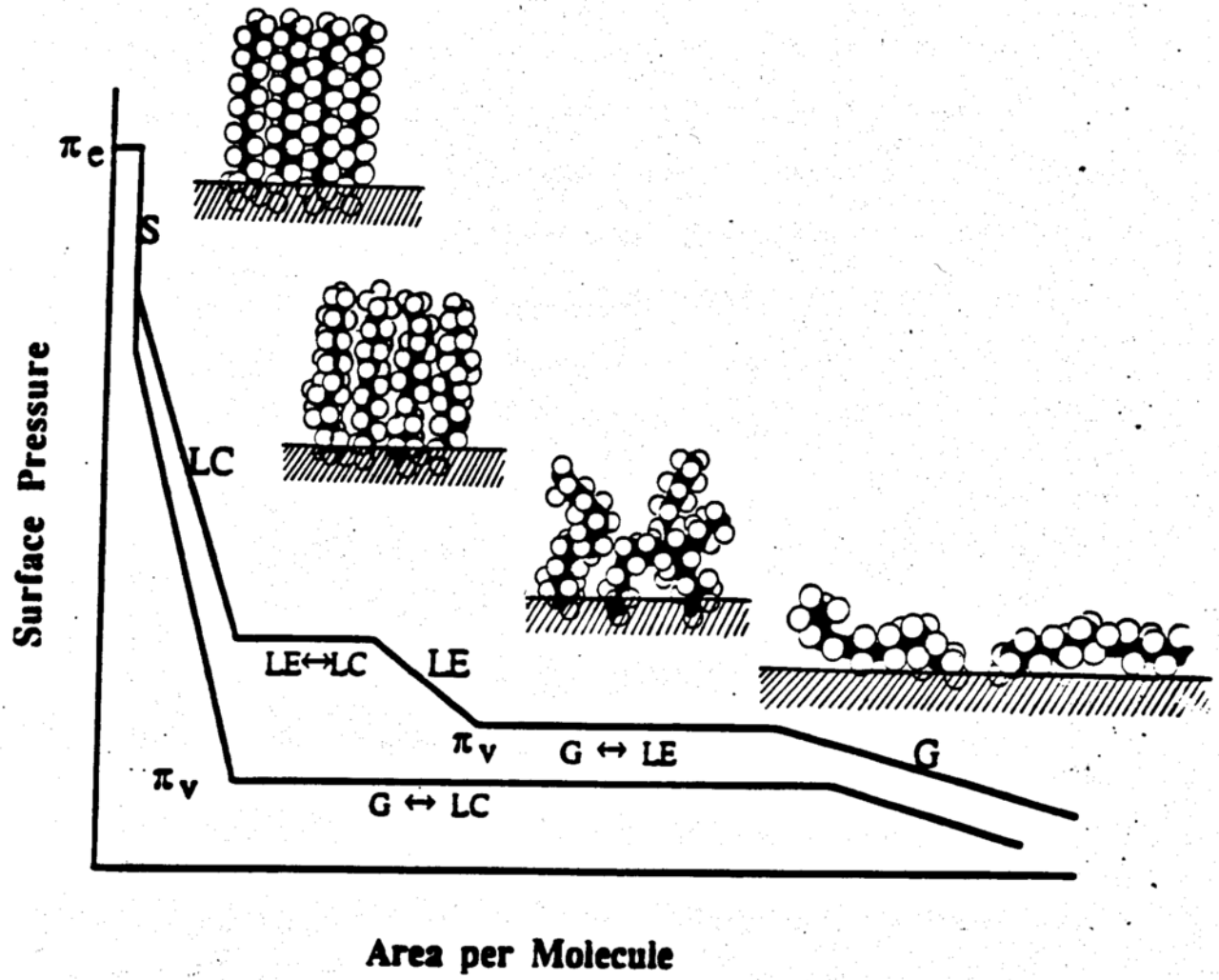

Figure 2. Schematic π-A diagram. G: gas, LE: liquid expanded, LC: liquid condensed, S: solid, π_e: equilibrum spreading pressure, π_v: surface vapor pressure Taken from (Birdi, 1989).

than their equilibrium spreading pressures. This primarily occurs with lipids whose stable bulk phase is a crystalline solid at the temperature of the experiment or for phospholipids with a gel to a liquid crystalline phase transition temperature that is above the temperature of the experiment (Gaines, 1966). These overcompressed monolayers can be extremely stable with respect to the bulk phase. It has been suggested that the slow attainment of equilibrium between the film and the bulk phase, when approached from the film side, could result from the absence of suitable crystal nuclei or from a higher energy, and hence higher spreading pressure, of the aggregates formed in the collapsed film as compared to the stable crystals (Gaines, 1966).

Binary Monolayers at the Air/Water Interface

Biological self-assemblies, such as membranes and vesicles, generally contain mixtures of phospholipids that vary with respect to both their polar headgroup and their acyl chains. One important characteristic of mixtures of lipids is their relative tendency to be homogeneously mixed or completely immiscible with the formation of separate domains within the bilayer. The presence of immiscibility or lateral phase separation of membrane phospholipids creates instabilities or "surface defects" at the domain boundaries which can influence processes that occur at the membrane interface (Eklund, Vuorinen et al., 1988; Yu and Possmayer, 1992) In model biomembranes, phase separation has been shown to enhance permeability, binding of proteins, and fusion of phospholipid vesicles (Eklund, Vuorinen et al., 1988) Lateral phase separation also can profoundly affect the electrical properties of the membrane. For example, the formation of domains of charged lipids affects the charge distribution in the lipid layer to create regions of high negative or positive charge density which may then serve as recognition sites for proteins (Reichert, Ringsdorf et

al., 1992). Therefore, a systematic investigation of mixtures of lipids containing different headgroups and/or acyl chains would provide insight into the phase behavior of lipids as they may exist *in vivo*.

The first question that must be considered in any study of a two component monolayer system concerns the miscibility of the components in the monolayer. Figure 3 schematically illustrates a miscible monolayer (Figure 3A), and an immiscible monolayer (Figure 3B) that has completely phase separated although, partial phase separation can occur. Finally, "squeeze-out" of one component from the interface (Figure 3C) can also occur but would only be expected at $\pi > \pi_c$.

From the surface phase diagrams, an analysis of miscibility can be made in two ways. First, for binary systems exhibiting either ideal mixing or complete immiscibility, the dependence of the average molecular area, A_{av}, on the composition of the monolayer should obey the additivity rule (for review (Gaines, 1966; Adamson, 1990))i.e.,

$$A_{av} = N_1A_1 + N_2A_2 \qquad (2)$$

where A_1 and A_2 are the area per molecule, respectively, of each of the single components at a constant surface pressure and N_1 and N_2 are their corresponding mole fractions. Deviations from the additivity rule indicate the presence of interactions between components of the mixed monolayer and therefore miscibility. One also can express this equation in terms of excess area, A^E, i.e.,

$$A^E = A_{12} - A_{av}$$

or

$$A^E = A_{12} - (N_1A_1 + N_2A_2) \qquad (3)$$

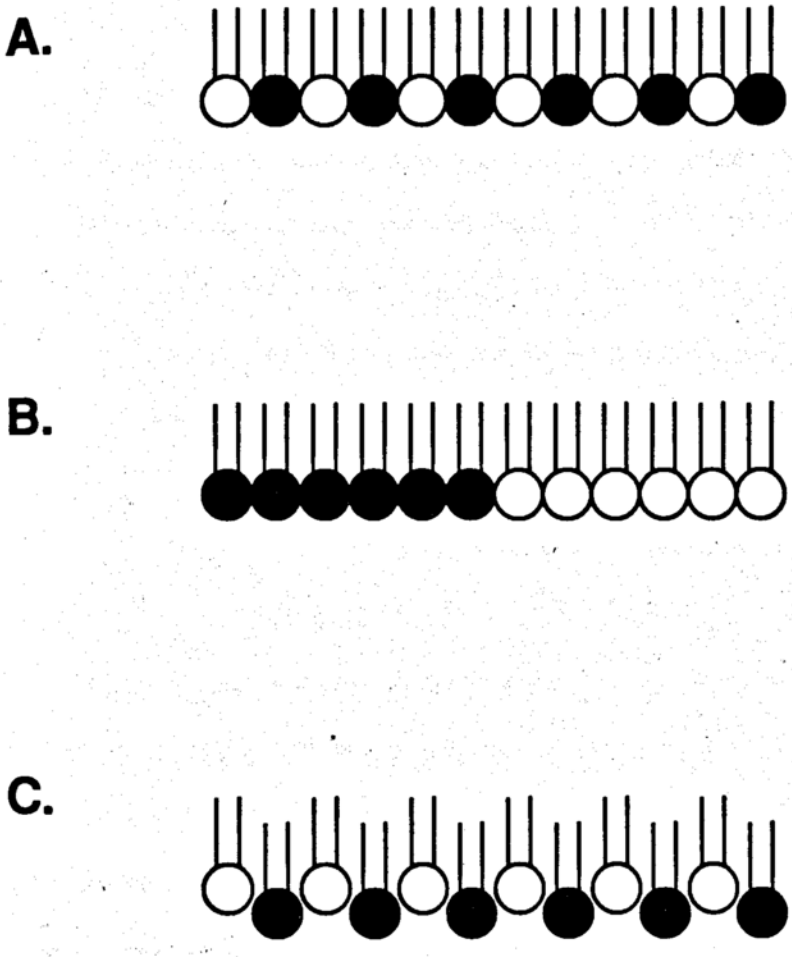

Figure 3. Schematic illustration of the possible phase behavior in binary monolayers.
A. Miscible monolayer B. Immiscible or phase separated monolayer
C. "Squeeze out " of one monolayer component.

where A_{12} is the actual area per molecule of the mixed monolayer. Therefore, if $A^E=0$ there is either ideal mixing or complete immiscibility. If $A^E>0$, there are positive deviations from the predicted area of equation (1) caused by the presence of repulsive interactions between unlike molecules of the mixed monolayer. On the other hand, attractive interactions cause deviations to be negative and $A^E<0$. The interpretation of such positive and negative deviations are made in a manner completely analogous to the explanations given for positive and negative deviations from Raoult's law in three dimensions (Gaines, 1966).

Miscibility also can be determined by the Gibbs phase rule, modified for application to insoluble monolayers by Crisp (Crisp, 1949);

$$F = C - P^B - P^S + 1 \qquad (4)$$

where F is the number of degrees of freedom in the system, C is the number of components and, P^B and P^S are the number of bulk and surface phases, respectively, at constant external pressure and temperature. This equation is useful in determining miscibility when applied to mixed monolayers that undergo a phase transition from an expanded to a condensed phase. For example, applying equation (4) in a region of coexistence in a binary mixed monolayer and assuming miscible components in both surface phases, we have C=3 (lipid 1, lipid 2, aqueous subphase), $P^B=1$ (aqueous subphase), and $P^S=2$ (expanded and condensed monolayer phases), yielding F=1. Thus, if components 1 and 2 are miscible, the phase transition pressure, Π_t, should vary continuously with the composition of the monolayer. If Π_t is invariant with composition, F=0 and thus in one of the surface phases the components are immiscible and another surface phase must be present, $P^S=3$ (Pagano and Gershfeld, 1972). The

phase rule is also useful in the determination of miscibility at the point of monolayer collapse (Crisp, 1949). In the simplest case of a single component film, C = 2, P^B=2, P^S =1, hence F = 0, and the equilibrium spreading pressure, π_e, is invariant at the collapse. In binary mixtures, if two miscible components exist in the surface film, equilibrated to an excess phase which is a solution of one component in the other, C = 3, P^B=2, P^S =1, hence F = 1. At each surface composition, there is a characteristic value of π_e. If the two components are immiscible then, there is an additional bulk phase and F = 0, and π_e is invariant. Knowledge of the mixing properties of the lipids in the bulk can thus predict *a priori* the extent of miscibility of the components in the surface.

Once it has been established that the components of the film are miscible under equilibrium conditions, a quantitative analysis of the intermolecular interactions can be obtained by the calculation of thermodynamic excess functions. From thermodynamics, we know that the molar free energy of mixing, ΔG_{mix}, consists of two contributions, i.e.,

$$\Delta G_{mix} = \Delta G^I + \Delta G^E \qquad (5)$$

where ΔG^I is the ideal molar Gibbs free energy of mixing and ΔG^E is the excess molar Gibbs free energy of mixing. We may define an ideal mixed monolayer in exact analogy with the definition of ideal bulk solutions.

$$\Delta G^I = RT \sum_i N_i \ln N_i \qquad (6)$$

For a two component mixture, this equation becomes;

$$\Delta G^I = RT\,(N_1 \ln N_1 + N_2 \ln N_2) \qquad (7)$$

To apply this equation to mixed monolayers, we must assume that at low surface pressures (as Π goes to 0), ideal mixing of monolayer components will occur.

The molar Gibbs excess free energy of mixing can be calculated from the surface phase diagrams as derived by Goodrich (Goodrich, 1957) i.e.,

$$\Delta G^E = \int_0^{\Pi} (A_{12}\text{-}N_1A_1\text{-}N_2A_2)\, d\Pi \qquad (8)$$

However, care should be taken in applying equation (10) to all mixed monolayers. Steric factors are not considered in Goodrich's treatment and can give misleading results when applied to mixtures of molecules of very different shape or size (Shah and Capps, 1968; Shah and Schulman, 1968) A more exact, although less practical, equation for calculating ΔG^E, derived by Motomura (Motomura, Sekita et al., 1974; Motomura, 1980), takes into account the presence of water in the monolayer mixture.

Miscibility can also be determined by direct observation of the monolayer by fluorescence microscopy, a technique that is becoming widely used to examine monolayer homogeneity (for review (Eklund, Vuorinen et al., 1988; McConnell, 1991; Stine and Knobler, 1992; Stine and Stratmann, 1992; Stine, 1994)). The technique is based on the partitioning of a small amount of a fluorescently labeled lipid into the less ordered phase that is created when two surface phases separate. With this method, it is possible to visualize coexisting phases and domain structures that can only be inferred from π-A isotherms, surface potential, and other techniques. The technique is relatively easy to use and provides a lateral resolution on the order of a few micrometers. More recently, domain morphology and dynamics have been addressed theoretically using models which consider the competition between electrostatic forces and line tension (McConnell, 1991).

Many biological systems, such as those of interest in this study, consist of mixtures of zwitterionic and anionic phospholipids. In such systems surface phase separation has been shown to occur because of the immiscibility of the hydrocarbon chain structure, or by the interaction of the anionic headgroups with positively charged species such as calcium ion or cationic peptides and proteins (Eklund, Vuorinen et al., 1988; Mittler-Neher and Knoll, 1989). Previous studies of the thermal properties of mixtures of saturated PC and PG bilayers (Findlay and Barton, 1978) and the surface phase diagrams of monolayers (El Mashak, Lakhdar-Ghazal et al., 1982; Nag, Rich et al., 1994) have demonstrated that no surface phase separation occurs when the acyl chains are identical, e.g. dipalmitoylphosphatidylcholine (DPPC) and dipalmitoylphosphatidylglycerol (DPPG), with and without the presence of calcium ion (Ca^{2+}). While the mixing of these lipids is essentially ideal, in the absence of Ca^{2+} there are small nonidealities which favor phase separation when Ca^{2+} is added (Nag, Rich et al., 1994). Surface phase separation in PC/PG monolayers and bilayers has been found to occur in mixtures where the saturated acyl chains differ by 4 carbons or more, and in the presence of a strong anion-complexing cation (El Mashak, Lakhdar-Ghazal et al., 1982). The relatively high compatibility of the PC and PG headgroups, in the absence of such complexing ions, has been attributed to the possible formation of hydrogen bonds between the phosphate and hydroxyl groups of these mixtures (El Mashak, Lakhdar-Ghazal et al., 1982). Clearly, therefore, acyl chain structure is a major determinant of mixing tendencies in such systems.

Very often biological bilayer assemblies, such as lung surfactant, contain mixtures of saturated acyl chains, e.g. DPPC, and unsaturated chains, e.g. 1-palmitoyl-2-oleoyl phosphatidyl-choline or -glycerol (POPC or POPG) (Hawco, Davis et al., 1981). Unsaturated phospholipids are believed to play an important role in imparting increased mobility or fluidity to monolayers and bilayers of saturated phospholipids,

and this increase in fluidity is believed to be important for many events that involve phospholipid assembly. For example, unsaturated lipid species are believed to play a critical role in the spontaneous spreading of lung surfactant at the air/alveolus interface (Bangham, Morley et al., 1979; Hawco, Davis et al., 1981; Keough, 1984).

The mixing tendencies of PC and PG phospholipids where one of the phospholipids is saturated and the other lipid unsaturated have been studied to a limited extent. It has been shown by thermal analysis, for example, that bilayer gel phase immiscibility occurs in equimolar mixtures of DPPC or DSPC (distearoylphosphatidylcholine) and either POPC or DOPC (dioleoylphosphatidyl-choline) (Davis, Coolbear et al., 1980; Curatolo, Sears et al., 1985). Studies of a mixed monolayer of equimolar amounts of DPPC and DOPC by Phillips et. al. (Phillips and Chapman, 1968) and analysis of surface pressure versus area per molecule (π-A) isotherms reveal a nonideal miscibility to surface pressures as high as 20 mN/m, while Nag and Keough (Nag, Boland et al., 1991) using fluorescence microscopy report the appearance of condensed domains at surface pressures of 14 mN/m and higher upon continuous compression when relatively short equilibration times are allowed. These domains grow in size with surface pressure and are believed to be enriched in DPPC. Only a single study with bilayers containing various proportions of DPPC and POPG has been reported (Wiedmann, Salmon et al., 1993), and it has been shown that in the absence of Ca^{2+} these lipids appear to be miscible. To date, no systematic studies of DPPC mixed with unsaturated PG systems in monolayers with and without Ca^{2+} have been reported.

Monolayers on Solid Supports

Supported multilayers (Figure 4), Langmuir-Blodgett films, (Roberts, 1990) formed by transferring monolayers onto solid supports are also useful models for studying bilayer assemblies and can serve as excellent substrates for binding and imaging of macromolecules (Egger, Ohnesorge et al., 1990; Fare, Palmer et al., 1992). A freely supported phospholipid bilayer separated from the support by ultrathin water layers (≈10Å) can be deposited onto a hydrophilic solid support such as freshly cleaved mica (Sackmann, 1996). Because they are immobilized, these films can be used with a variety of surface-sensitive techniques, such as scanning probe microscopy (Meyer, Howald et al., 1991; Chi, Anders et al., 1993; Chi, Fuchs et al., 1994), which cannot be used at a fluid interface. The common methods of multilayer assembly of phospholipids on solid surfaces are monolayer transfer by the Langmuir-Blodgett technique (Von Tscharner and McConnell, 1981; McConnell, Watts et al., 1986)and by vesicle spreading (Brian and McConnell, 1984). The Langmuir-Blodgett technique involves lowering the support through a condensed monolayer, which is being held at a constant surface pressure, at the air/water interface in a Langmuir-Blodgett trough. The support can be kept in a vertical position or horizontal, "face down," immersion can be used (Figure 4) (McConnell, Watts et al., 1986; Roberts, 1990). Alternatively, a supported bilayer can be prepared by allowing small unilamellar vesicles to come into contact with a clean hydrophilic support. The vesicles apparently fuse with one another on the surface to form the bilayer assembly. The continuity of the supported film is highly dependent on the smoothness of the substrate (McConnell, Watts et al., 1986). Unfortunately, supported planar films are not free from defects and imaging experiments using electron microscopy and atomic force microscopy reveal that film defects can range in size from 50 nm to a few

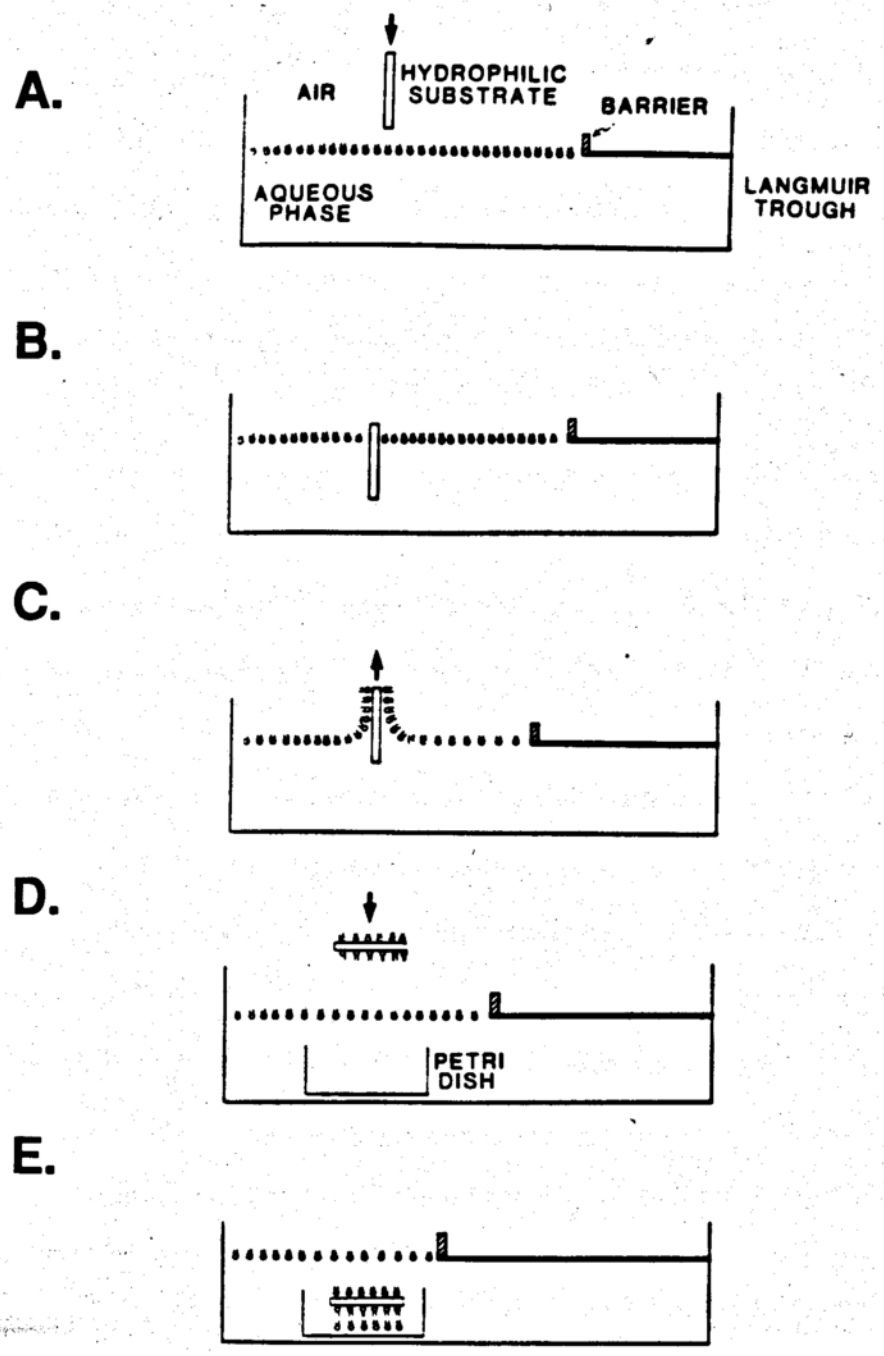

Figure 4. Preparation of supported planar bilayers by the Langmuir-Blodgett technique. A, B. The hydrophillic support is lowered through the monolayer, with no significant change in the surface pressure. C. Vertical transfer of the first monolayer. D. Horizontal or " face down" transfer of the second monolayer. Taken from (McConnell, 1986).

micrometers (Hansma, Gould et al., 1991; Garnaes, Schwartz et al., 1992; Peltonen, He et al., 1992; Bourdieu, Ronsin et al., 1993; Kajiyama, Oishi et al., 1994). Supported films appear to have long-term stability in air over the course of several months since they do not undergo significant structural changes in lattice structure or defect number upon aging (Zasadzinski, Viswanathan et al., 1994).

Interaction of Peptides and Proteins with Lipid Monolayers

Most studies of the interaction of soluble surface-active compounds, dissolved in the subphase, with insoluble lipid monolayers are carried out at a constant surface area. The protein is injected below a phospholipid film that is being held at a constant initial surface pressure (π_i) and an increase in surface pressure is measured due to the penetration of the protein into the interface ($\Delta\pi = \pi_{final} - \pi_i$). The pressure at which $\Delta\pi = 0$ is the penetration capacity of the protein and is the pressure at which the protein becomes excluded from the lipid monolayer. The influence of parameters such as initial surface pressure, ionic strength, and lipid identity on the change in surface pressure can give information on the nature of the protein-lipid interaction i.e. the lipid specificity of the protein (Goddard and Schulman, ; Pethica, 1955).

The surface excess of an adsorbed solute at an interface, in principle, can be calculated from surface pressure data using thermodynamics by means of the Gibbs equation;

$$d\pi = RT\Gamma_I d\log a_I + RT\Gamma_S d\log a_S \qquad (9)$$

where Γ is the surface concentration, a is activity and I refers to the insoluble monolayer and S to the species present in solution (including water and its ionization products) (Pethica, 1955). Thus, the change in surface pressure after injection of the

protein is not a quantitative measurement of protein penetration alone (Alexander and Barnes, 1980), having contributions from the insoluble monolayer as well as the species being adsorbed from solution. In penetration experiments, where adsorption is occurring at a surface at which an insoluble monolayer exists, calculation of surface quantities is difficult because the activity of a monolayer component in the bulk phase most often can be neither controlled nor measured (Pethica, 1955; Alexander and Barnes, 1980; Hall, 1986).

Several researchers have reduced equation (9) using several assumptions. Pethica (Pethica, 1955), for example, has reduced equation (9) to;

$$\left(\frac{\partial \pi}{\partial \ln m_s}\right)_{A,n_i^\sigma} = \left(\frac{\hat{A}_I}{\hat{A}_I - \overline{A}_I}\right) RT\Gamma_S \qquad (10)$$

where m_S is the molality of the species in solution, "A" is the area of the surface n_i^σ is the surface excess of component I, $\hat{A}_I$ is the area per molecule of I and $\overline{A}_I$ is the partial molar area of the monolayer in the absence of any adsorbed species. This equation assumes that there is low monolayer coverage (i.e. the first term in equation (9) is negligible) and the bulk concentration of the adsorbing species is low and thus the molality of the adsorbing species can be substituted for its activity in equation (9). Alexander and Barnes (Alexander and Barnes, 1980), using different assumptions, derived an expression that is more broadly applicable.

$$\left(\frac{\partial \pi}{\partial \ln m_S}\right)_{A,n_i^\sigma} = \frac{RT}{\overline{A}_S}\left[1 - \frac{RT\hat{A}_I\left(\partial \overline{A}_I / \partial \pi\right)}{\left(\hat{A}_I - \overline{A}_I\right)\overline{A}_I\left(\hat{A}_I - \overline{A}_I + \overline{A}_S\right)}\right]^{-1} \qquad (11)$$

In this equation, $\overline{A}_S$ is the partial molar area of the species being adsorbed from solution, defined by the following equation;

$$\frac{\hat{A}_I \Gamma_S}{\hat{A}_I - \overline{A}_I} = \frac{1}{\overline{A}_S} \qquad (12)$$

from which Γ_S can be calculated. Equation (11) assumes that the surface excess of the adsorbing species is much less than the surface excess amount of insoluble monolayer and that the compressibilities of the insoluble monolayer and a monolayer formed from the adsorbing species are the same. When experimental data obtained for the penetration of cholesterol monolayers by dodecylsulphate were evaluated it was shown that equation (11) could accurately predict the surface excess of an adsorbed species, relative to direct measurements (Gaines, 1966), when the surface is dilute in adsorbed species, or in regions where the monolayer is dilute, i.e. high area/molecule, and the species being adsorbed is of relatively high concentration. In equations (10) and (11), a value for $\overline{A}_I$ is required. This term can only be evaluated by assuming that the area/molecule of the penetrated monolayer is the same as that of the insoluble monolayer at the same surface pressure. This assumption is best made when $\left(\partial\overline{A}_I / \partial\pi\right)$ is small, which holds true with highly incompressible monolayers. For, cases in which the above assumptions cannot be made, other direct methods, such as the use of radioactive tracers, must be applied to calculate the surface excess of surfactant (Gaines, 1966).

The above analysis assumes that the entire molecule or a constant portion of the molecule is penetrating the monolayer regardless of the initial surface pressure. However, there are at least three possible types of protein-lipid monolayer interactions

that can occur and the type of interaction may vary with the film state of the monolayer, i.e. its surface density or compressibility (Colacicco, 1968; Quinn and Dawson, 1970). First, whole molecules of protein can penetrate the lipid film and occupy the same area as those of the protein spread at the air/water interface (Figure 5A). This type of interaction would be favored with expanded lipid monolayers. Second, above a certain film pressure, a portion of each protein molecule, probably the hydrophobic side chains, may penetrate the film such that the change in surface pressure is much smaller than in the first case (Figure 5B). This generally occurs around the collapse pressure of the pure protein monolayer at the air/water interface Lastly, at high surface pressures, adsorption without penetration occurs (Figure 5C). Some researches (Quinn and Dawson, 1970) have also suggested that the latter mode of interaction can occur even at low surface pressures, suggesting that the peptide bonds of the protein are associated with the polar group of a lipid molecule through hydrogen bonding.

Annexins

General Studies

The annexins are a group of structurally related, calcium dependent phospholipid-binding proteins that were discovered in the 1980s (for review (Geisow, Walker et al., 1987; Klee, 1988; Romisch and Paques, 1991; Ernst, Mall et al., 1994; Perretti, 1994)). These intracellular proteins are ubiquitous and have been isolated from both the plant and animal kingdoms suggesting that they function in a broad range of biological processes. Many in vitro activities of annexins have been found, however,

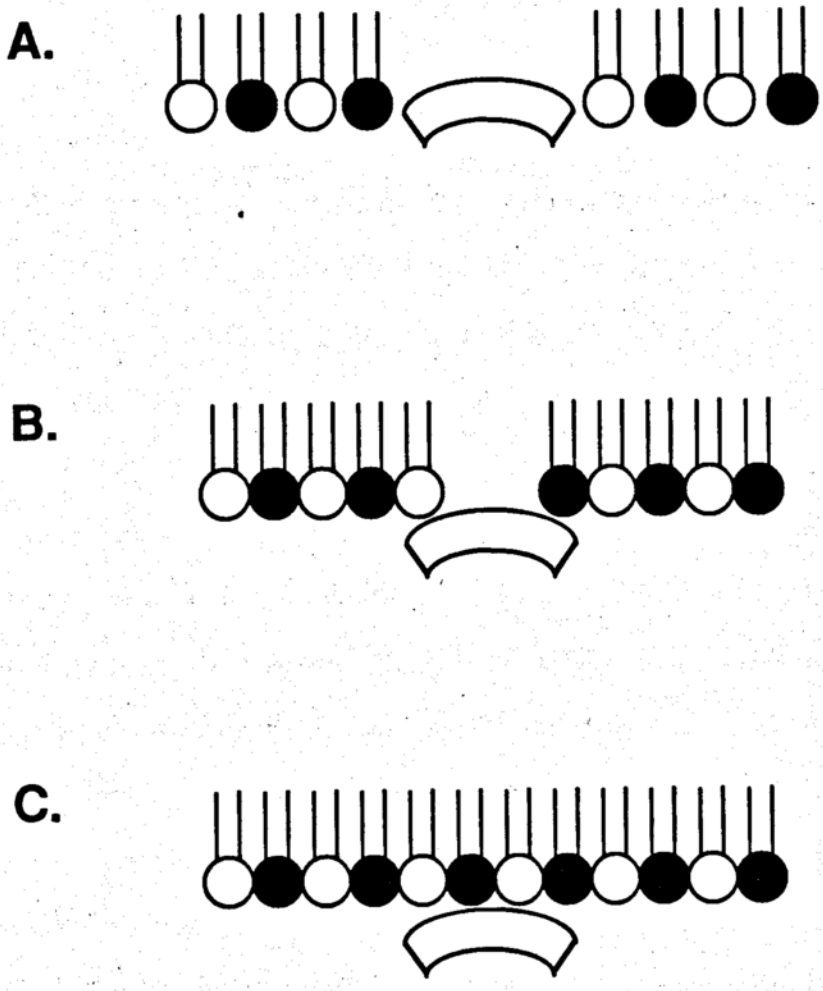

Figure 5. Schematic illustration of the possible types of protein-lipid interactions. A. Penetration of the entire protein. B. Partial penetration of the protien. C. Adsorption of the protein beneath the monolayer.

the exact functions of annexins are not yet known (Ráynal and Pollard, 1994). In all proposed functions, it is believed that phospholipid binding is involved. Some annexins, i.e. annexin V, have anticoagulant properties which can be described by the "displacement model." In the displacement model, not only can annexin prevent blood coagulation factors from binding to the surfaces of vesicles and platelets, a necessary step in the coagulation cascade, but it can also displace most coagulation factors from surfaces due to its higher binding constant (Andree, Reutelingsperger et al., 1990; Andree, Stuart et al., 1992). By inhibiting phospholipase A2 penetration into an interface, a necessary requirement for the enzyme to act, some annexins, i.e. annexins I and II, may be able to mediate the inflammatory response (Davidson and Dennis, 1992; Raynal and Pollard, 1994). Annexin I has been shown to promote fusion and may therefore be involved in exocytosis (Blackwood and Ernst, 1990; Zaks and Creutz, 1990; Burgoyne and Morgan, 1992; Francis, Balazovich et al., 1992; Pollard, Guy et al., 1992; Meers, Mealy et al., 1993). Annexins V and VII may form calcium-specific voltage-gated channels (Pollard, Guy et al., 1992; Rojas, Arispe et al., 1992). Finally, there is evidence that annexins may be involved in membrane-cytoskeleton interactions (Raynal and Pollard, 1994).

The ability of annexins to mediate vesicle aggregation and fusion may be an important function for lung associated annexin-like proteins. The mechanism by which annexin-mediated membrane fusion occurs is poorly understood. It has been suggested in the literature (Meers, Mealy et al., 1992) that the process must entail binding to the membrane, possible oligomerization or conformational changes of the protein, aggregation of vesicles, and finally actual fusion of membranes. Figure 6A depicts aggregation mediated by protein-protein interactions but is unlikely unless the protein-protein contacts are irreversible. Figure 6B would require a Ca^{2+}-independent interaction of the N-terminal side of the annexin with membrane phospholipids.

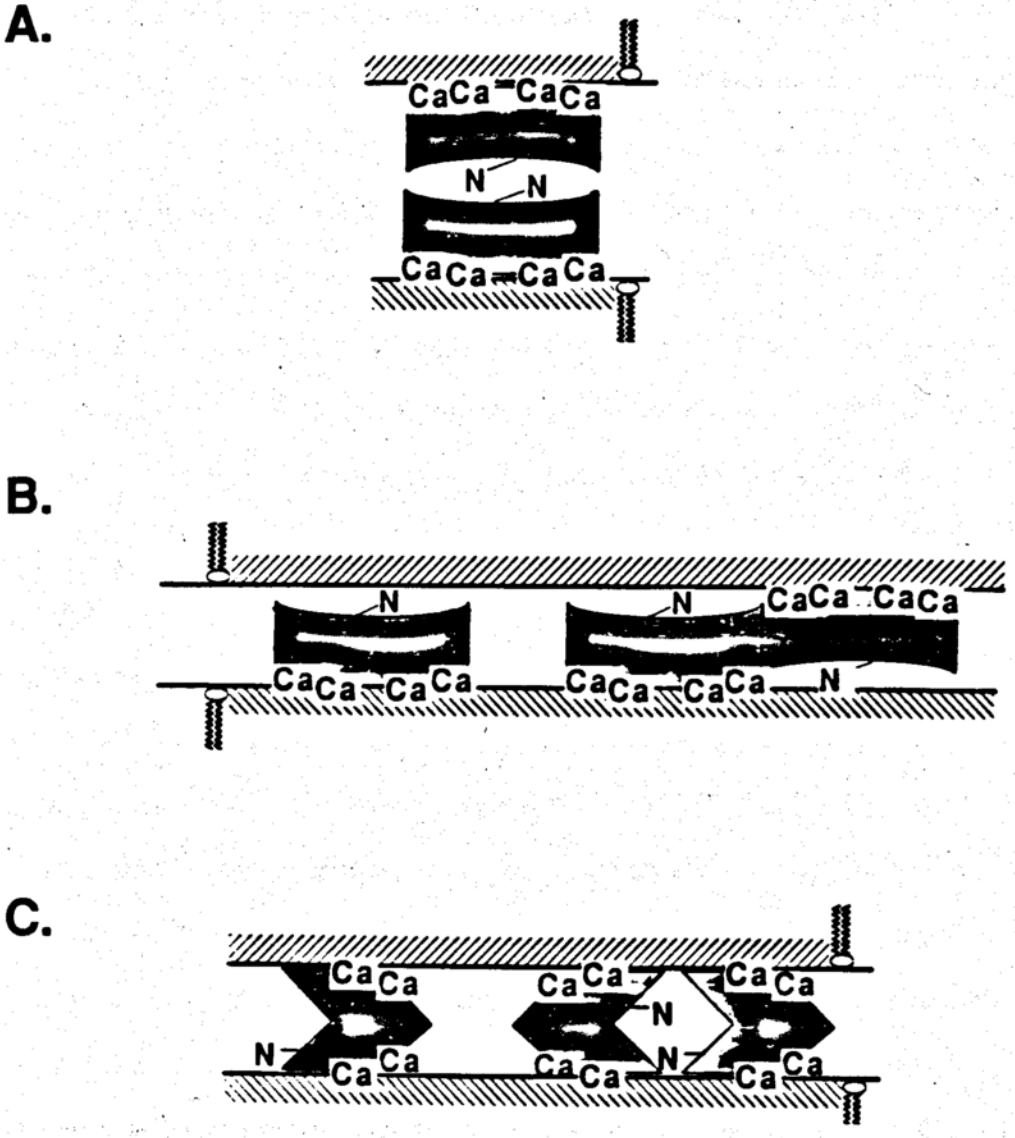

Figure 6. Models for annexin-mediated vesicle aggregation. A. Vesicular aggregation which depends soley on protein-protein interactions after initial binding of annexin. B. Each annexin molecule is able to make simultaneous contact with two bilayers with either one contact made with the N-terminal face of the molecule or through lateral protein-protein interactions. C. Binding of one molecule to two bilayers via an unknown conformational change in protein structure.
Taken from (Meers, 1992).

Figure 6C also requires that each face of the protein can interact with the membrane and that lateral protein-protein interactions also play a role. The model in Figure 6C shows that if a conformation significantly different from that of the original annexin structure could occur, then, each monomer could contact more than one bilayer. To date, none of the above models can be ruled out. Aggregation and fusion experiments using chimeric annexins and mutant annexin I have demonstrated that the ability of annexin I to promote membrane aggregation and fusion is highly sensitive to changes in the structure of the N-terminal domain suggesting that the N-terminus plays an important role in the annexins ability to promote fusion (Andree, Willems et al., 1993).

The products of ten different genes of the annexin family have been found in mammals to date. Their ability to bind calcium and phospholipid is linked to their common primary structure. Each annexin has a unique N-terminal domain, also called the "tail," and a C-terminal domain, named the "core" (Figure 7). The core of the molecule strictly defines the protein as part of the annexin family. The core contains 4 (or 8 in the special case of annexin VI) tandem repeat domains that contain ≈ 70 amino acids which are 40-60% identical in amino acid sequence within the annexin family in mammals with low interspecies differences (Romisch and Paques, 1991; Ernst, Mall et al., 1994; Raynal and Pollard, 1994). The overall sequence of the annexin core is hydrophilic due to an abundance of polar and charged amino acids. It has isoelectric points that range from 4.8 to 7.8 (Geisow, Walker et al., 1987; Pollard, Guy et al., 1992). In contrast, the N-terminal domain is highly variable and is considered the regulatory region of the protein since it contains the major sites for phosphorylation, proteolysis and interaction with other proteins (Schlaepfer and Haigler, 1987; Ando, Imamura et al., 1989; Hoekstra, Buist-Arkema et al., 1993; Wang and Creutz, 1994).

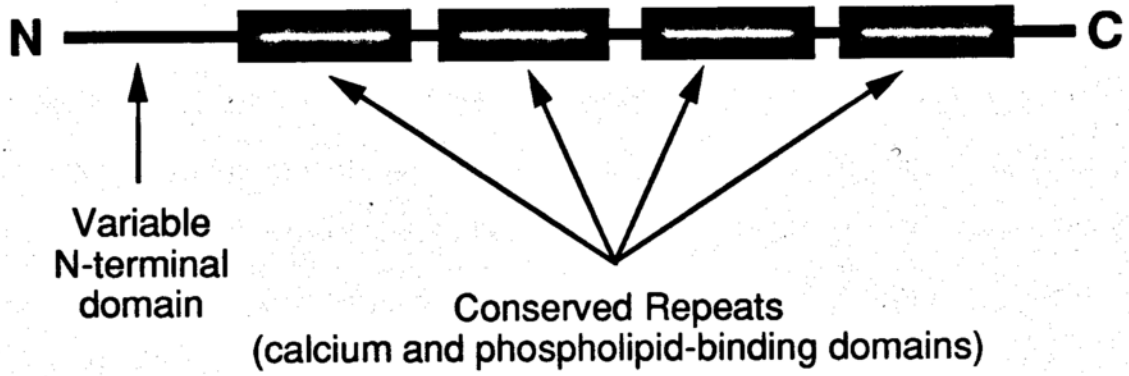

Figure 7. Schematic illustration of the conserved annexin structure.

Three dimensional crystals of annexins I, IV, V, and VI have been obtained however, annexin I (Weng, Luecke et al., 1993), V (Huber, Berendes et al., 1992; Bewley, Boustead et al., 1993; Sopkova, Renouard et al., 1993), and XII (Luecke, Chang et al., 1995) are the only annexins whose structures have been solved by x-ray crystallography. Human placental annexin I (synonyms: lipocortin I, p35, calpactin II, chromobindin 9) is a 35-40 kDa protein which has an isoelectric point of 6.5-6.8 (Raynal and Pollard, 1994). The current model of N-terminally truncated human placental annexin I has the same overall topology as annexin V . It consists of four compact structurally homologous domains and two connecting strands. Each domain consists of five α-helices, A, B, C, D, and E (Figure 8) consisting of 7-15 amino acids and connected by short sequences that are 10 amino acids or less. Helices A and B and helices D and E form two parallel helix-loop-helix folds while helix C lies perpendicular to the other four helices. The connecting strands link domains I and IV and II and III to form two modules of two domains. The two domains within each module form tight hydrophobic contacts, while interactions between the two modules are made mostly by hydrophilic side chains. A hydrophilic channel is formed between the four domains. The four domains pack together to form a slightly curved plate with two faces, one convex and one concave. (Figure 9). All of the loops of the helix-loop-helix motif are located on the convex face of the molecule and contain the calcium binding sites. Although the N-terminal region is not present in the crystal structure of annexin I, the crystal structure for annexin V reveals that the N-terminus is located on the concave side of the molecule and is thus directed away from the binding surface, possibly close to the hydrophilic channel (Weng, Luecke et al., 1993).

Experiments reveal that most annexins have at least three calcium-binding sites; the calcium sites are typically found in domains II and IV and one in either domain I

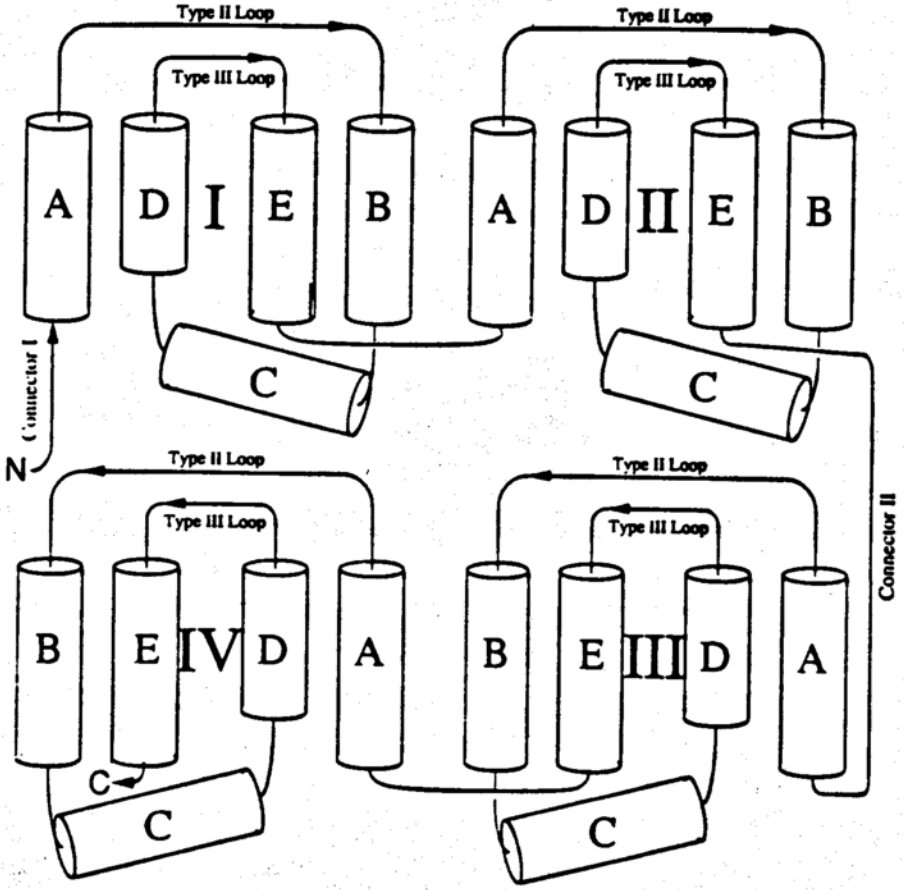

Figure 8. Topological structure of human placental annexin I. Taken from (Weng, 1993).

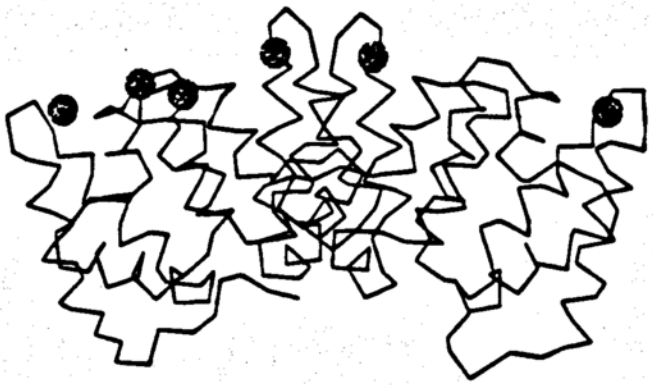

Figure 9. Side view of human placental annexin I. Dark circles represent the six observed calciums.
Taken from (Weng, 1993).

or III (Huber, Berendes et al., 1992). The calcium is bound to the loops of negatively charged amino acids that protrude from clefts on the convex face of the annexin (Huber, Berendes et al., 1992; Huber, Berendes et al., 1992). These calcium sites have structural similarity to the sites found on PLA_2 (Thunnissen, AB et al., 1990) which may explain the ability of annexin to inhibit this enzyme. The six calcium binding sites of annexin I fall into two classes: type II and type III (Figure 10). Type II sites are located on the A to B loop of domains II, III, and IV and are all found to bind calcium ions. The coordination of the type II sites is octahedral and consists of three peptide oxygens from the AB loops with the (K, R), (G, R)-X-G-T sequence and the bidentate ligands from the acidic group of either aspartate or a glutamate 39 residues downstream in the sequence (Figure 10). The remaining two calcium coordinating sites show electron density for water molecules. These type II sites are similar to the phospholipid-binding site of PLA_2. Not all of the loops that contain the type III site conformation are occupied by calcium. The D to E loop of domains I and IV form the two type III sites that bind calcium. The calcium ions in these type III sites coordinate to two backbone carbonyl oxygens and one acidic side chain. Water molecules have been found at most of the remaining three coordinating sites to complete the octahedral coordination. Finally, an unusual site is formed in the A to B loop of domain I. Instead of forming a type II site like the other A to B loops, this site has type III calcium binding geometry. This exception is due to the absence of the required negatively charged residue 39 residues downstream from the A to B loop (Weng, Luecke et al., 1993). Purified human lipocortin I obtained from placenta has a K_d for calcium that is greater than 1 mM in the absence of phospholipid, however, binding is significantly enhanced in the presence of phosphatidylserine to give an apparent K_d of 10-90 μM (Raynal and Pollard, 1994). The binding of calcium has been shown to induce conformational changes within the molecule as detected by

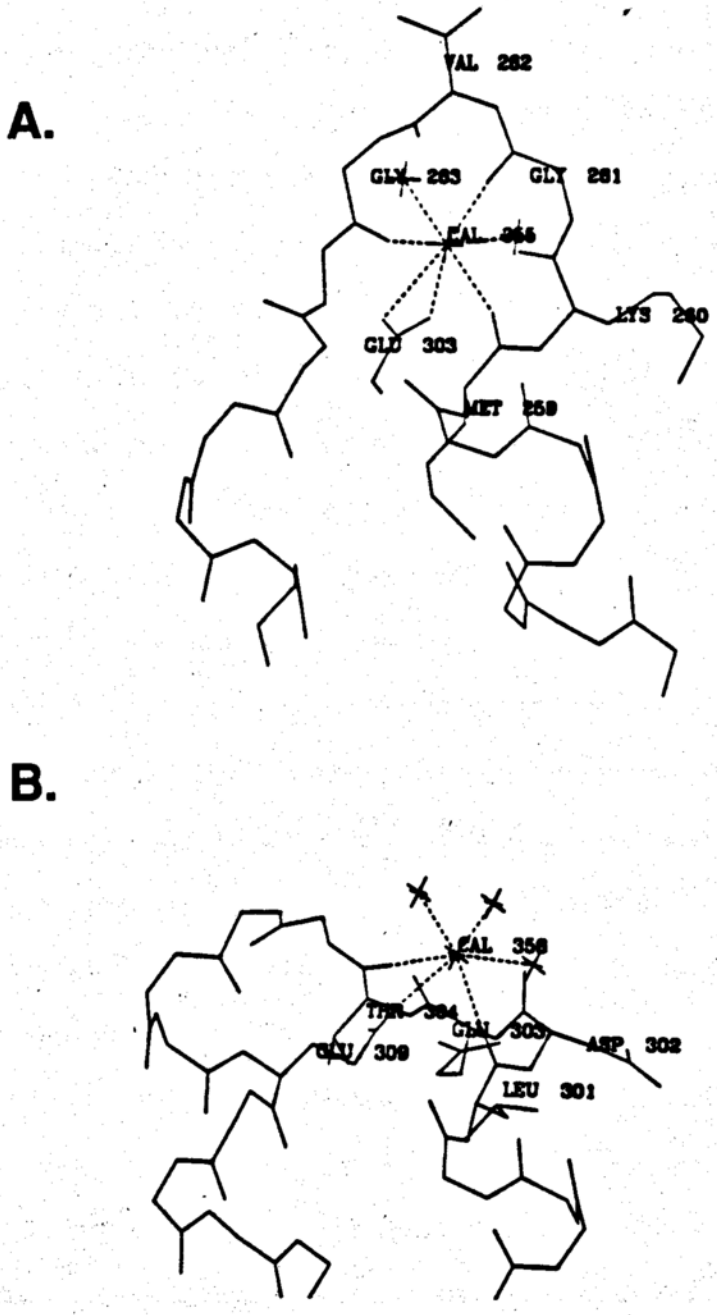

Figure 10. Comparison of the two types of calcium binding sites in human placental annexin I. A. Type II binding site. B. Type III binding site. Taken from (Weng, 1993).

ultraviolet spectroscopy. Phosphorylation or limited proteolysis of the N-terminus of the protein has been shown to alter the calcium requirements of annexin (Ando, Imamura et al., 1989; Wang and Creutz, 1994) for binding and/or ability to aggregate membranes. This suggests a regulatory role for the N-terminus despite the fact that it is not directly involved in calcium binding.

Annexins have also been studied in the presence of phospholipid surfaces (Newman, Tucker et al., 1989; Brisson, Mosser et al., 1991; Mosser, Ravanat et al., 1991; Driessen, Newman et al., 1992; Lecompte, Bouix et al., 1994; Pigault, Follenius-Wund et al., 1994) using annexin V or VI as model proteins. Typical data from experiments of annexin interactions with monolayers of phospholipids are shown in Figure 11. Small increases in surface pressure are observed which are attributed to steric or perhaps electrostatic perturbation of the lipid monolayer and perhaps partial penetration (Newman, Tucker et al., 1989) Experiments using vesicles as model membrane systems show that the annexins preferentially bind to anionic lipids such as phosphatidic acid, phosphatidylglycerol, phosphatidylinositol, phosphatidylserine. Binding of annexin V to the zwitterionic headgroup phosphatidylcholine only occurrs at very high calcium concentrations, i.e. >100mM (Tait, Gibson et al., 1989; Andree, Reutelingsperger et al., 1990; Junker and Creutz, 1993) whereas, no binding is observed between annexin I and vesicles composed of PE or PC. From these data, it has been suggested that the annexins interact with the polar head groups of the lipids, and the interaction is largely ionic in nature (Meers, Daleke et al., 1991; Lecompte, Bouix et al., 1994). In this model, phospholipid binding was hypothesized to occur by the replacement of two calcium bound water molecules by the phosphoryl and ester oxygens of the phospholipid. This model was further supported by the observation that phospholipid binding is reversible upon addition of EDTA (Andree, Reutelingsperger et al., 1990). This model also suggests that the whole surface of the

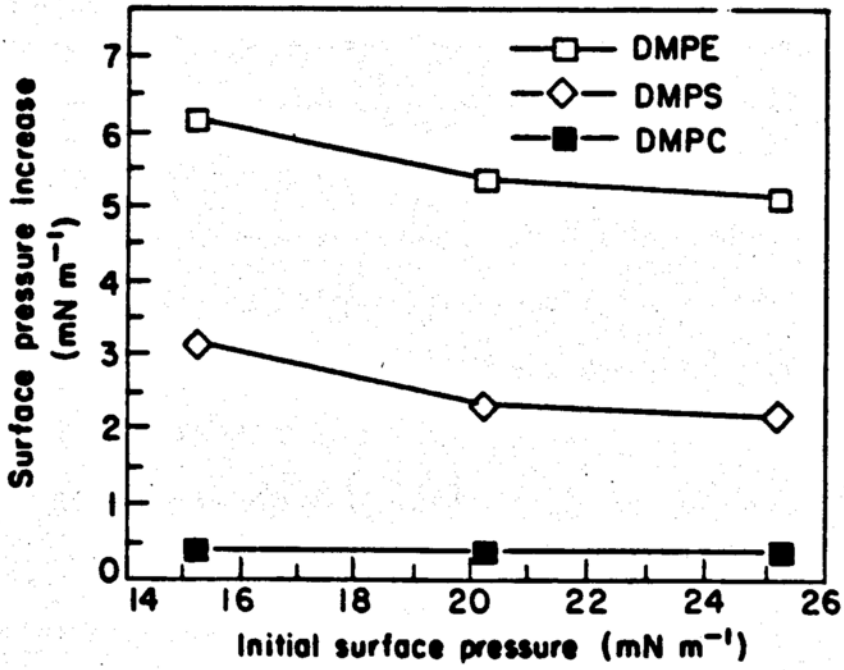

Figure 11. Increase in surface pressure ($\Delta\pi$) relative to the initial surface pressure of the lipid monolayer (π_i) after injection of annexin VI.
Taken from (Newman, 1989).

annexin is involved in binding and this can explain why binding to monomeric phospholipids was observed to be more than 10^5-fold weaker than binding to phospholipid vesicles (Tait, Gibson et al., 1989). The calcium concentration required for the binding of annexin I to the different phospholipids varies with the phospholipid headgroup in the order PA < PI ≈ PS. It has been suggested that factors such as the type of ion contributing the charge and headgroup size are important determinants for annexin binding (Junker and Creutz, 1994). Junker and Creutz hypothesized that annexin binding is a two step process involving adsorption to a membrane surface followed by the coupled binding of calcium and specific lipids. Finally, the ability to mediate binding of annexin V to PS/PC bilayers is highly specific for calcium. The use of other divalent cations results in decreased binding in the order $Cd^{2+} > Zn^{2+} > Mn^{2+} > Co^{2+} > Ba^{2+} > Mg^{2+}$ (Andree, Reutelingsperger et al., 1990). The high specificity for calcium binding could be the result of the presence of a calcium-binding cleft in the annexin molecule; the size of the cleft could determine the size of the binding divalent ion (Tait, Gibson et al., 1989)

Phospholipid binding with annexin may also involve a direct protein-phospholipid interaction. By monitoring the spectral properties of single tryptophan residue located on the concave face of annexin I and close to the convex face of annexin V, it was found that calcium binding in domain III of annexin V Induced a relocation of the calcium-binding loop regions causing the exposure of only the domain III tryptophan that is located on the convex face of the protein to solvent (Concha, Head et al., 1993; Meers and Mealy, 1994; Sopkova, Gallay et al., 1994). This hydrophobic residue may play a role in the interaction between the sn-2 acyl chain of the phospholipid and the protein causing the annexin to become inserted into lipid layers and serving as an anchor for the protein (Concha, Head et al., 1993; Lecompte, Bouix et al., 1994). Experiments using site-directed mutagenesis suggests that there may also be a direct

protein-phospholipid interaction between a conserved basic site on the annexin (most likely conserved lysine residues which flank the calcium binding sites) and the acidic phospholipid (Trave, Quignard et al., 1994).

Two-dimensional crystals of annexins IV, V, and VI when bound to phospholipid layers have been observed using electron microscopy (Newman, Tucker et al., 1989; Brisson, Mosser et al., 1991; Mosser, Ravanat et al., 1991; Driessen, Newman et al., 1992). These proteins have been found to crystallize on specific lipid monolayers and different annexins crystallize on different monolayers. The two-dimensional projection maps revealed that the annexins crystallize with the symmetry of the plane group p3 and form a network of trimers that form a triskelion-like motif (Figure 12) which may occur via disulfide dimerization (Huber, Berendes et al., 1992; Huber, Berendes et al., 1992) The two-dimensional structure was found to be similar to the three-dimensional structure suggesting that annexins attach to phospholipid membranes without substantial structural change (Brisson, Mosser et al., 1991; Mosser, Ravanat et al., 1991), thus supporting the hypothesis that the convex face of annexin lies closest to the lipid monolayer. Annexin V has unit cell dimensions: a = b = 94 Å and is composed of two staggered domains of similar size, about 40 Å by 20 Å. Both domains have two subdomains. The four resolved subunits are hypothesized to represent the folding units that correspond to the four amino acid repeating segments as mentioned previously (Mosser, Ravanat et al., 1991). Each annexin V molecule occupies approximately 2550 to 2740 $Å^2$ (Andree, Reutelingsperger et al., 1990; Mosser, Ravanat et al., 1991) and is estimated to involve approximately 30-60 phospholipid molecules (Andree, Reutelingsperger et al., 1990; Meers, Mealy et al., 1993) although only 3-5 acidic lipids are necessary for their attachment (Huber, Berendes et al., 1992; Huber, Berendes et al., 1992; Junker and Creutz, 1993). Less annexin was found to bind to small unilamellar vesicles than to planar bilayers or large

A.

B.

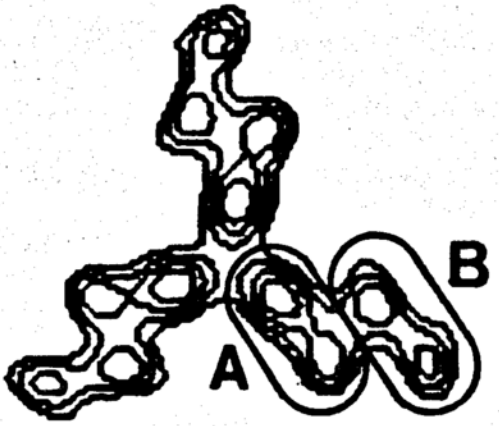

Figure 12. A. Two-dimensional projection maps from annexin V crystals bound to a dioleoylphosphatidylserine monolayer. A unit cell with its origin located at the triskelion center is outlined. B. Projected structure of an annexin V trimer. Contours represent protein density Each of the domains A and B, indicated for 1 annexin molecule are composed of two subdomains. Each subdomain is postulated to represent the folding unit corresponding to a single 70 amino acid residue repeat.
Taken from (Mosser, 1991).

vesicles. Binding of annexins to large phospholipid vesicles, with low surface curvature, resulted in the formation of facets on the vesicles which are believed to form as sheets of annexin molecules bound to the surface of the bilayer (Andree, Stuart et al., 1992). A comparison of the thickness of the annexin V molecule obtained from 3D reconstructions corresponds well with the thickness of the crystal structure of the membrane bound protein suggesting peripheral binding of annexin V without substantial penetration of the membrane (Voges, Berendes et al., 1994).

The binding of annexins to monolayers or bilayers of phospholipids was found to significantly affect phospholipid distribution and fluidity within the lipid layer (Junker and Creutz, 1993; Gilmanshin, Creutz et al., 1994) In a study involving annexin IV, the changes in bilayer fluidity and the lateral organization of PG in PG/PC vesicles upon annexin binding was monitored using a PG derivative that contained the fluorophore pyrene, which exhibits fluorescence sensitive to molecular collision frequency. Decreases in lateral mobility of the lipids resulting from binding to larger macromolecules should result in decreased eximer fluorescence, while increases in local pyrene-PG concentration which might result from preferential localization of pyrene-PG lipids to distinct regions should result in increased excimer fluorescence. The authors observed a decrease in the average diffusion constant of the pyrene-PG molecules in vesicles that contained PG alone and lateral segregation of pyrene-PG in PG/PC mixtures upon addition of annexin molecules (Junker and Creutz, 1993). A separate study (Gilmanshin, Creutz et al., 1994) involving the measurement of lateral lipid diffusion using fluorescence recovery after photobleaching (FRAP) in mixed POPC and POPG planar bilayers also measured a reduction in lateral diffusion and evidence for lateral phase separation of the lipids upon addition of the annexin IV. Furthermore, more annexin IV was required to observe phase separation in the POPC-rich mixtures as opposed to the POPG-rich mixtures. Finally, a study with annexin V

demonstrated that annexin V binding decreased the lateral mobility of the lipids in vesicles however, no changes in the lateral organization were observed (Meers, Daleke et al., 1991).

Lung Annexin I

Recently, Tsao has purified and characterized two calcium-dependent phospholipid-binding proteins from rabbit lung cytosolic fraction, a 33 and a 36 kDa protein (Tsao, 1990). Partial amino acid sequencing and cross reaction with antibodies to various annexin proteins reveals that the 36kDa protein has homology with annexin I (Tsao, Chen et al., 1994). This lung phospholipid-binding protein or lung annexin I (LAI) is slightly smaller (36 vs. 37 kDa) and more acidic (pI 6.0 vs. 6.9) than recombinant human annexin 1. Tsao has also isolated a breakdown product of LAI (LAI-bp). It has a pI of 8.5 and a molecular weight of 33 kDa due to the cleavage of approximately 30 of the N-terminal amino acids. It is recognized by polyclonal antibodies to annexin I (Tsao personal communication). *In vitro*, the 33kDa phospholipid-binding protein (PLBP), LAI and human annexin I demonstrate the ability to inhibit PLA_2 activity (Tsao, Foo et al., 1990; Tsao, Hull et al., 1991) and cause aggregation and fusion of a variety of membranes (Tsao, 1990). In contrast, the breakdown protein shows no vesicle aggregation activity (Tsao personal communication).

Lung annexin I and 33kDa PLBP inhibit PLA_2 function, *in vitro*, when DOPC/PG vesicles or monolayers are used as substrates (Tsao, Hull et al., 1991). Two mechanisms by which this inactivation occurs have been proposed and the exact details are controversial. Initially, a "substrate depletion" model was proposed for the mechanism whereby the annexin binds to the phospholipids and thus prevents the

penetration of PLA_2 into the interface, a requirement for the enzyme to act. More recently (Kim, Kim et al., 1994), a "specific interaction" mechanism has been proposed and evidence has been collected which suggests there exists a direct interaction between PLA_2 and annexin I.

Lung annexin I and 33kDa PLBP may also function to promote membrane aggregation and fusion, an event which plays an important role in many biological processes such as exocytosis. In the presence of calcium, both proteins have the ability to aggregate certain negatively charged unilamellar liposomes (i.e. PG and PS) but not neutral phosphatidylcholine liposomes (Tsao, 1990). The two proteins show different specificities for phospholipid headgroups. For example, LAI aggregated liposomes containing PS better than the 33kDa PLBP. Both proteins poorly aggregated liposomes that contained PI or phosphatidic acid. Aggregation activity with both proteins increased upon increasing the amount of negatively charged PG. Aggregation activity increase upon increasing the Ca^{2+} concentration for 33kDa PLBP, reached a maximum level below 10 mM and remained at that level through 0.1 M Ca^{2+}. LAI, on the other hand, showed increasing aggregation activity with increasing Ca^{2+} up to 5mM Ca^{2+}, but activity was markedly reduced by higher Ca^{2+} concentrations. No aggregation activity is observed for either protein when up to 10 mM Mg^{2+} or Mn^{2+} are used. They are able to fuse neutral PC unilamellar liposomes to acceptor multilamellar liposomes (egg PC, cholesterol, dicetyl phosphate). This fusion activity was stimulated 4-5 times by the presence of PG, PI, or PS with LAI but did not affect the fusion activity of 33kDa PLBP. Interestingly, both proteins fused [^{14}C] PC unilamellar liposomes to lamellar bodies and surfactant from lung lavage 13-16 times more than synthetic phospholipid vesicles. The above results coupled with an observed difference in the amino acid composition of these two proteins indicates that LAI and 33kDa PLBP are indeed different proteins (Tsao, 1990).

Tsao has found that the amount of LAI in the soluble fraction of 25-day fetal lungs comprises 0.04% of total soluble protein, while in the more developed adult lung it is 0.3%, thus linking LAI to lung surfactant development. It was also shown that LAI is primarily associated with the lamellar bodies within the Type II cells. These findings suggest that LAI plays a role in surfactant biogenesis, namely, that it aids in the assembly of lamellar bodies possibly through its ability to mediate membrane aggregation and fusion of the surfactant components (Tsao, Chen et al., 1994). High concentrations of LAI-bp have been associated with several lung diseases including bronchopulmonary dysplasia and cystic fibrosis (Tsao personal communication).

The surface activity of LAI, in the absence of lipids, was determined in the absence and presence of calcium over the protein concentration range of 0.25-4.9 μg/ml using the Wilhelmy plate method to measure surface tensions and a surface radioactivity detection method (Tsao, Foo et al., 1990; Tsao, Gau et al., 1993) to measure surface counts of ^{14}C-labeled LAI which were then converted to surface concentration. (Radioactive labeling did not affect the ability of LAI to cause aggregation or fusion and did not affect intrinsic surface activity as measured by its ability to decrease surface tension). It was found that LAI is intrinsically surface active reaching surface concentrations as high as 1.91 mg/m^2 for the concentrated solutions, which is high when compared with other well-studied surface active proteins (MacRitchie, 1990). It is interesting to note that calcium, which is required for LAI activity, increases the surface activity of the protein. Furthermore, increasing the calcium concentration to 10 or 20 mM did not produce any further changes in equilibrium Π values (Tsao, Gau et al., 1993).

Stable insoluble monolayers of LAI were spread from aqueous solution using the Trurnit method (Trumit, 1960). The π-A isotherm was similar in the presence and absence of 5 mM $CaCl^2$ and reached surface pressures of $\approx$ 23 mN/m at a surface

concentration of ≈ 3.7 mg/m^2. The surface pressure, surface longitudinal elasticity, and surface longitudinal viscosity were measured using the Wilhelmy plate method and electrocapillary wave diffraction technique (Tsao, Gau et al., 1993). Changes in the surface viscoelasticity were found between low (1.22 mg/m^2) and slightly higher surface concentrations (1.59 mg/m^2). It was found that at the lower surface concentration, just before the protein chains assume close packing arrangement, almost purely elastic behavior is observed with or without added calcium. At higher surface concentrations, where the protein chains are most likely beginning to undergo some conformational changes due to the very close packing, significant changes in the viscoelastic properties occur which are very sensitive to the presence of calcium.

Statement of the Problem

The first part of this thesis examines the mixing behavior of anionic and zwitterionic phospholipids in monolayers, particularly mixtures of saturated and unsaturated phosphatidylcholines (PC) and phosphatidylglycerols (PG). These two lipid headgroups constitute a large part of lung surfactant and their mixing tendencies are critical to an understanding of the structural properties of lung surfactant. No comprehensive study of these lipids spread as monolayers has been performed and the few studies that have been carried out appear to be in disagreement, (e.g. mixing of DPPC and DOPC). In this study, a systematic investigation of the mixing behavior of DPPC and various unsaturated derivatives of PC and PG as mixed monolayers in the absence and presence of Ca^{2+} at various lipid compositions will be made through the measurement of π-A isotherms, πe, and the use of fluorescence microscopy. The working hypothesis to be tested is that mixing of phospholipids in a monolayer of a saturated lipid, such as DPPC, with a lipid that contains at least one unsaturated acyl chain, will show either miscibility with positive deviations from ideality, or surface phase separation. Furthermore, tendencies for such nonidealities or phase separation will be greater when a.) the headgroups are different, i.e. PC and PG, b.) when Ca^{2+} is added to a system containing an anionic phospholipid, and c.) when the composition of the mixture is increased with regard to the disaturated lipid.

The second focus of this thesis research is to examine the possible role by which lung annexin I (LAI) operates intracellularly to affect lipid storage and release. Experiments will be performed to examine certain aspects of the hypothesis of Tsao (Raynal and Pollard, 1994) that LAI is involved in the assembly and storage of lung

surfactant within the type II epithelial cells, specifically that this protein plays a role in the formation of lamellar bodies, surfactant storage granules, and subsequent delivery of surfactant to the alveolus. The lamellar bodies are formed via the fusion of small vesicles that are transported by the Golgi apparatus from the endoplasmic reticulum and can release their surfactant contents by way of fusion with the membrane of the Type II cell. Tsao has shown that LAI can mediate fusion of synthetic unilamellar vesicles to lamellar bodies and surfactant from lung lavage (Romisch and Paques, 1991). It is of great interest to determine the molecular mechanism by which LAI is able to mediate fusion i.e. its ability to bind phospholipids in a calcium-dependent manner and elicit structural changes within the lipid monolayer to facilitate fusion.

This study, therefore will attempt to gain a fundamental understanding of the macroscopic and microscopic structure of well-defined phospholipid-LAI systems and their relationships to composition and environment as they might exist in the lung surfactant system using well-characterized spread monolayers of phospholipids of varying composition. The experiments performed will examine the hypothesis of Tsao given above by investigating a.) LAI-phospholipid monolayer interactions in the absence and presence of calcium ions to determine the extent, if any, of lipid specificity and calcium sensitivity and b.) the effect of LAI binding on certain structural features of model phospholipid monolayers that might relate to the fusion process i.e. monolayer surface phase behavior. Lipid specificity, the role of calcium, and indirect measurements of perturbations of the monolayer, i.e. expansion or condensing of the lipid monolayer, will be made through measurements of changes in the surface pressure of monolayers upon injection of the protein into the subphase. It is expected that LAI will interact specifically with anionic phospholipids in a calcium-dependent manner and therefore affect the distribution of phospholipids in the mixed anionic/zwitterionic monolayer. The changes in the distribution of lipids will then

affect monolayer structure which will be monitored using fluorescence microscopy. Selected results obtained with LAI will be compared with analogous experiments performed with a similar lung phospholipid-binding protein (33kDa PLBP) and a mutant LAI which has been associated with several lung diseases and does not display any aggregation activity. The experiments involving the mutant LAI will test the hypothesis presented in the literature that the N-terminus affects phospholipid binding despite its distant proximity to the phospholipid binding face of the protein.

Chapter II
Experimental

Materials

Lipids

The phospholipids used in this study were 1, 2-dipalmitoyl-*sn*-glycero-3-phosphocholine (DPPC), 1-palmitoyl-2-oleoyl-*sn*-glycero-3-phosphocholine (POPC), 1, 2-dioleoyl-*sn*-glycero-3-phosphocholine (DOPC), 1, 2-dipalmitoyl-*sn*-glycero-3-phospho-rac-glycerol (DPPG), 1-palmitoyl-2-oleoyl-*sn*-glycero-3-phospho-rac-glycerol (POPG), and 1, 2-dioleoyl-*sn*-glycero-3-phospho-rac-glycerol (DOPG), soy plant phosphatidylinositol (PI), and 1-palmitoyl-2-[12-[(7-nitro-2-1,3-benzoxadiazol-4-yl)amino] dodecanoyl-*sn*-glycero-3-phosphocholine (NBD-PC) (Avanti Polar Lipids, Inc., Alabaster, AL) which all had stated purities of 99+% and were used as received. The phosphatidylglycerols (PG) and phosphatidylinositol (PI) were supplied as their sodium salts. The supplier performed two EDTA partitions at high sodium concentration to remove calcium and ammonium ions from the PG lipids. They have a residual calcium content of between 10-40 ppm, as analyzed by the supplier. Therefore, a typical lipid solution of 0.7 mg/ml would contain at most 8×10^{-7} M calcium. The soy plant PI has a composition consisting of a variety of acyl chains. The acyl chain composition, as reported by the Avanti Polar Lipids, Inc. is 16:0 (29.50%), 18:0 (8.18%), 18:1 (5.70%), 18:2 (47.26%), 18:3 (7.18%) and 2.18% other.

Chloroform (99.9%, Aldrich) was used as the spreading solvent for all lipids except DPPG and was used as received. DPPG was dissolved in chloroform : methanol (99.9%, Fisher Scientific) : water (98.9 : 1 : 0.1). The surface purity of the

chloroform was checked by spreading the solvent on water and monitoring surface tension as the surface was compressed. No decrease in surface tension was observed so it was assumed that no significant amounts of any surface active material were present. In previous work (Yazdanian, 1990)some of the chloroform was distilled two additional times, and it was found that the original and doubly distilled samples gave identical surface pressure. All solutions were stored at -20°C. The saturated lipids were stored up to one year whereas the unsaturated lipids were stored for no more than six months.

Subphase

The water used throughout these studies was triply distilled. The house-distilled water was passed through a Barnstead PCS filtration system that contains an organic removal cartridge, two mixed ion exchange resin cartridges, a super organic removal cartridge, and a 0.2 μm filter. The water was then distilled two times, once from an alkaline potassium permanganate solution and once from a dilute sulfuric acid solution. The collected water was then stored in a glass container. The calcium content of the triply distilled water was analyzed by atomic emission spectroscopy with an inductively coupled plasma source. The calcium ion content was found to be less than 9.5 ppb (or less than 2×10^{-7} M calcium).

The subphase pH was controlled with a 10 mM Tris (hydroxymethyl) aminomethane (Tris) (99.9%, Sigma Chemical Company) buffer that was adjusted to pH 7.4 with 1N HCl (A.C.S reagent grade, Aldrich). Selected experiments were performed with added calcium chloride (99.99+%, Aldrich) or ethylenediaminetetraacetic acid (EDTA) (99.5%, A.C.S. reagent, Aldrich).

Lung Proteins

Isolation and Purification

All lung proteins were the generous gifts of Dr. Francis H.C. Tsao[§]. Two Ca^{2+}-dependent phospholipid-binding proteins (PLBPs), 36 kDa lung annexin I (LAI) (pI 6.0) and 33 kDa PLBP (pI 5.5), extracted from rabbit lung cytosolic fraction were purified to homogeneity. Details of the isolation have been given elsewhere (Tsao, 1990). Briefly, the proteins were precipitated from a lung soluble fraction of adult rabbit lungs and applied to a Sephadex G-100 column. The protein content of the eluted fractions was estimated from absorbance measurements at 280 nm. The protein fractions were then pooled and ultrafiltered through an Amicon Diaflo ultrafilter with an Amicon UM 10 membrane (10,000 molecular weight cutoff). The condensed protein solution was applied to a phenyl Sepharose column and ultrafiltered again using the Amicon UM 10 membrane and by Amicon Centricon™-10 microconcentrators. High purity protein samples were then obtained by applying the protein solution to a Spherogel TSK phenyl-5PW (10μm particle size) column that was assembled onto a gradient HPLC system.

Rabbit lung annexin I breakdown protein (Anx-I-bp) was prepared from purified LAI by the removal of about 30 N-terminal amino acids to yield a 33 kDa protein with a pI of 8.5. The proteins were stored in concentrated form (typically 5 μg/ μl) in silanized centrifuge tubes at -70°C in 0.01 M Tris-HCl buffer containing 5 mM 2-mercaptoethanol, 1 mM EDTA and 0.15 M NaCl at pH 7.4 (buffer A). Prior to use, the protein was diluted to 5 μg/10 μl to provide a means for more accurate measurement of the protein solution.

[§] Department of Pediatrics, University of Wisconsin Perinatal Center, Meriter Hospital-Park, 202 South Park Street, Madison, WI 53715, USA.

Activity Assay

The activity of the protein was assayed by measuring the transfer of [^{14}C]DPPC/ [^{3}H]triolein from unilamellar liposomes to multilamellar liposomes. Details are given elsewhere (Tsao, 1990) Briefly, the reaction mixture consisted of radiolabelled unilamellar liposomes as the donor, multilamellar liposomes as the acceptor, and protein solution. The control consisted of all the components except protein. The reaction was initiated by adding $CaCl_2$ with vortexing. The samples were then centrifuged and the supernatant, containing unreacted donor liposomes, was removed and discarded. The pellet, containing the acceptor multilamellar liposomes was washed with buffer and resuspended by vortexing. An aliquot of the lipid dispersion was transferred to a scintillation vial for counting the radioactivity's of ^{3}H and ^{14}C. Using this assay, no significant loss in activity of LA I was detected after storage of the protein at -20°C for two months and at 25°C for 8 hours after dilution of the protein to 1μg/ 2μl.

Determination of protein concentration

Protein concentration was determined using bicinchoninic acid (BCA) and bovine serum albumin (BSA) as the protein standard. Bicinchoninic acid, sodium salt, is a stable, water-soluble compound capable of forming an intense purple complex with cuprous ion (Smith, Krohn et al., 1985). The reagent can be used as an analytical method for the detection of protein by monitoring the reaction of protein with alkaline Cu^{2+} (biuret reaction) i.e.

$$\text{Protein} + Cu^{2+} \xrightarrow{OH-} Cu^{1+}$$

$$Cu^{1+} + \text{BCA} \longrightarrow \text{BCA} - Cu^{1+}\text{complex}$$

The color produced from this reaction is stable and was found to increase in a linear fashion over a broad range of increasing protein concentrations. It has the advantage over the method of Lowrey since this reagent has a greater tolerence toward commonly encountered interferences such as nonionic detergents and buffer salts. The stability of the reagent and the resulting chromophore also allows a simple, one-step analysis. One modification to the standard protocol had to be made to use this reagent with LAI. BCA was found to react with thiol reagents in a linear and reproducible manner (Hill and Straka, 1988). Therefore, because the protein's storage buffer contained mercaptoethanol, the procedure had to be modified by preincubating the protein solution with iodoacetamide prior to addition of the BCA protein reagent. In the presence of a 10-fold molar excess of iodoacetamide over the thiol species, the reaction of the BCA with the thiol is prevented. The details of the procedure can be found in Appendix A.

Methods

Cleaning

All glassware was washed with distilled water, soaked in concentrated sulfuric acid containing an inorganic oxidizer (Nochromix, Godax Laboratories, Inc.) for at least 24 hours, rinsed thoroughly with distilled-deionized water, and dried in an oven. The Teflon trough and barrier were cleaned in a similar fashion approximately every two weeks. The platinum plate was stored in concentrated hydrochloric acid and was rinsed and then heated by gas flame prior to use.

Surface Pressure Measurement

Surface pressure was measured by the Wilhelmy plate technique (Gaines, 1966) using a sand-blasted platinum plate (2.58 x 1.0 x 0.1 cm or 2.55 x 1.0 x 0.1 cm) and a Teflon trough (28.5 x 11.1 x 1.0 cm or 17.0 x 5.75 x 1.0 cm) that was mounted to an aluminum base. It was enclosed in a box to reduce drafts and dust and to maintain a high relative humidity (>80%). The temperature in the box for all experiments was 23 to 25°C and the temperature of the aqueous subphase was controlled with a thermostated water bath (Lauda model RM6) which circulated water at 25.0 ± 0.1 °C through a glass coil at the bottom of the trough. Just before an experiment was performed, the surface was suctioned to remove any surface contaminants. The platinum plate, which is connected to a balance by a thin wire, was lowered so that it just touched the liquid surface. The change in mass of the plate was then measured using either a Cahn 2000 electrobalance (Cahn Co., Paramount, CA) with a chart recorder (Kipp&Zonen model BD40) or by an Ohaus GA 200-D electronic balance (Ohaus Corp., Florham Park, NJ) equipped with an RS232 port and interfaced to a Macintosh Plus computer. The surface tension, γ in mN/m, was calculated by the following equation;

$$\gamma = \frac{mg}{2L} \qquad (13)$$

where m (in mg) is the mass of the meniscus (the difference between the mass of the plate in water - mass of the dry plate), g is the gravitational constant (0.98) and L is the length of the plate (in cm). The surface tension of the pure subphase, γ_o, was always recorded first and was found to be 71.9 ± 0.2 mN/m, in agreement with the expected value of 71.97 mN/m at 25 °C.

The lipid solutions were spread using a Hamilton microsyringe (Hamilton Co., Reno, NV) and allowed to equilibrate anywhere between 30 minutes to 24 hours

depending on the lipid identity and state of the monolayer. Mixed monolayers were deposited using a mixed spreading technique (Dörfler, 1990), where both lipids are dissolved into a single spreading solution. The equilibrium surface tension, γ, was determined when the change in mass of the plate was less than 1 mg (or less than 0.2 mN/m) in one hour * . The area per molecule, A, was varied by three methods: (1) continuous addition of lipid molecules (after the attainment of equilibrium) to a surface of constant area, (2) stepwise reduction of surface area with a movable barrier with a fixed amount of deposited material (compression method), and (3) repeated cleaning and spreading of the monolayer film to a given surface concentration (single-shot method). Surface pressure ($\gamma - \gamma_0$) versus area isotherms were constructed using each of the three methods. Using DPPC as a model, good agreement between all three methods was observed in both the expanded and condensed regions of the monolayer however, some deviation was observed between the single-shot method and the compression method in the phase transition regions. In the phase transition region, the single-shot method showed a constant surface pressure as the area per molecule was reduced while the compression method showed a slight rise (approximately 0.5 mN/m) in surface pressure as the area per molecule was reduced as has been reported in the literature (Pallas and Pethica, 1985; Chen, Sano et al., 1986).

Equilibrium Spreading Pressure

Mixtures of lipids were dissolved in chloroform at room temperature and the solvent was removed at 45°C under vacuum using a Büchi Rotavapor (Brinkman, Westbury, NY). The samples were purged with argon and stored at -20°C prior to use. Solid material was sprinkled onto the clean surface and the surface pressure due

* For monolayers with limited stability, the mass of the plate remained constant for less time.

to the spreading monolayer was measured as described above. Final π_e values where chosen when changes in π were less than 0.2 mN/m per hour, and when the value was independent of the amount of excess bulk material on the surface.

Fluorescence Microscopy at the Air/Water Interface

Each of the single-component films and the binary mixed films were examined with the fluorescence microscope to investigate monolayer surface phase behavior. In order to use this technique1 mol% of the dye NBD-PC was added to the spreading solution. The monolayer mixture was spread and allowed to equilibrate anywhere from 15 minutes to several hours as described above. Studies at this level of dye concentration reveal a negligible effect of the dye on the monolayer π-A diagram, as shown in Figures 13 and 14 for a single component and a binary mixture, respectively. Good agreement between the curves is observed at low to intermediate surface pressures however, some deviation is observed at higher pressures. This discrepancy is most likely due to the expulsion of the dye molecules at higher surface pressures which would shift the π-A isotherm slightly to the left due to the calculation of an area/molecule that is smaller than what is actually present at the interface.

The fluorescence microscope was constructed from a commercially available microscope (Micromaster, Model E, Fisher Scientific, Pittsburgh, PA) (Figure 15)and is similar in design to those constructed previously (Peters and Beck, 1983; Meller, 1988; Riegler, 1988; Nag, Boland et al., 1990; Stine and Knobler, 1992). In order to minimize surface flow during observation, a moveable circular Teflon barrier was devised (Kim and Yu, 1992) to confine a small area of the surface. Temperature of the subphase was maintained by circulating thermostated water (Lauda model RM6) through a glass coil placed in the bottom of the trough. Surface pressure measurement

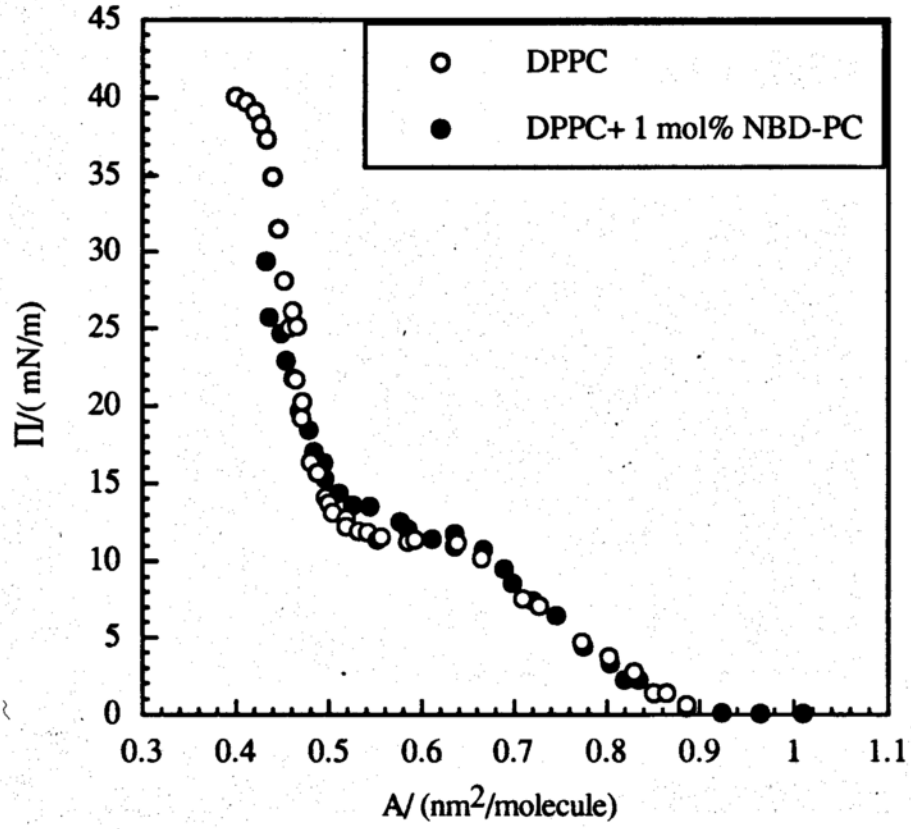

Figure13. The π-A isotherm for DPPC with (filled circles) and without (empty circles) 1 mol% NBD-PC on a water subphase at 25°C.

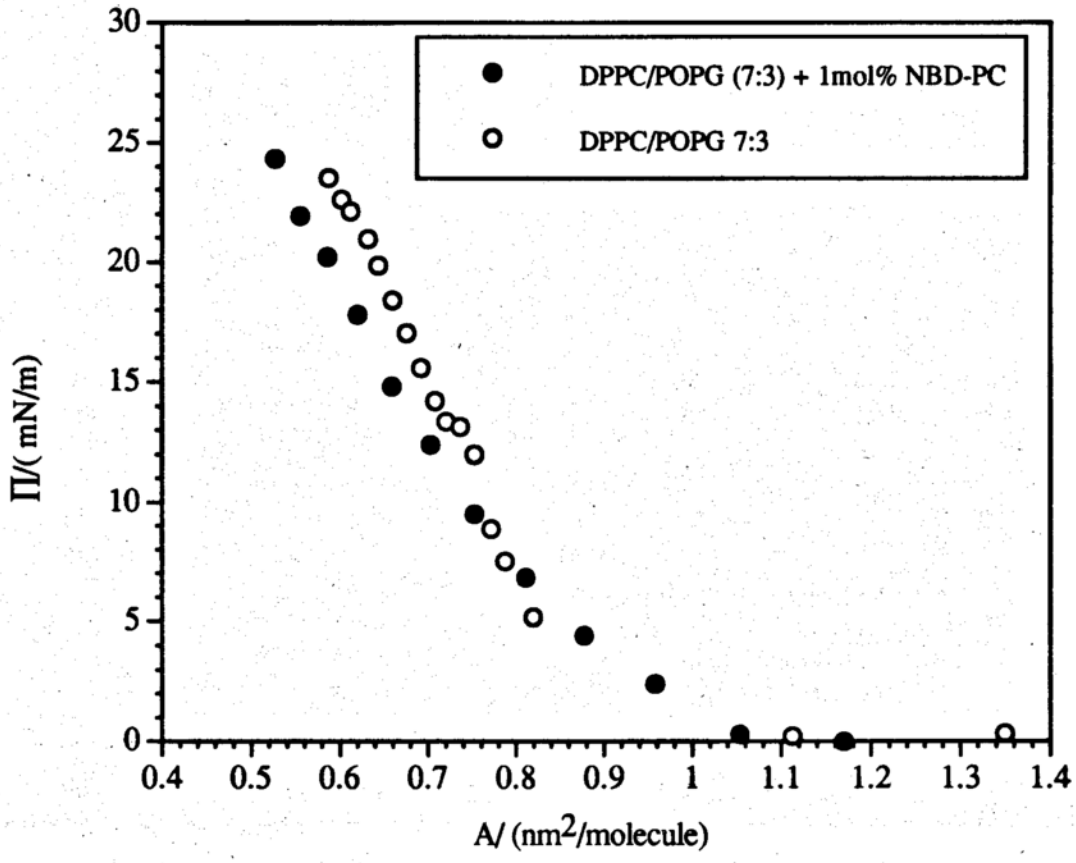

Figure 14. The π-A isotherm for DPPC/POPG (7:3) mixture with (filled circles) and without (empty circles) 1 mol% NBD-PC spread on a 10 mM Tris-HCl, pH 7.4, 15 mM NaCl at 25°C.

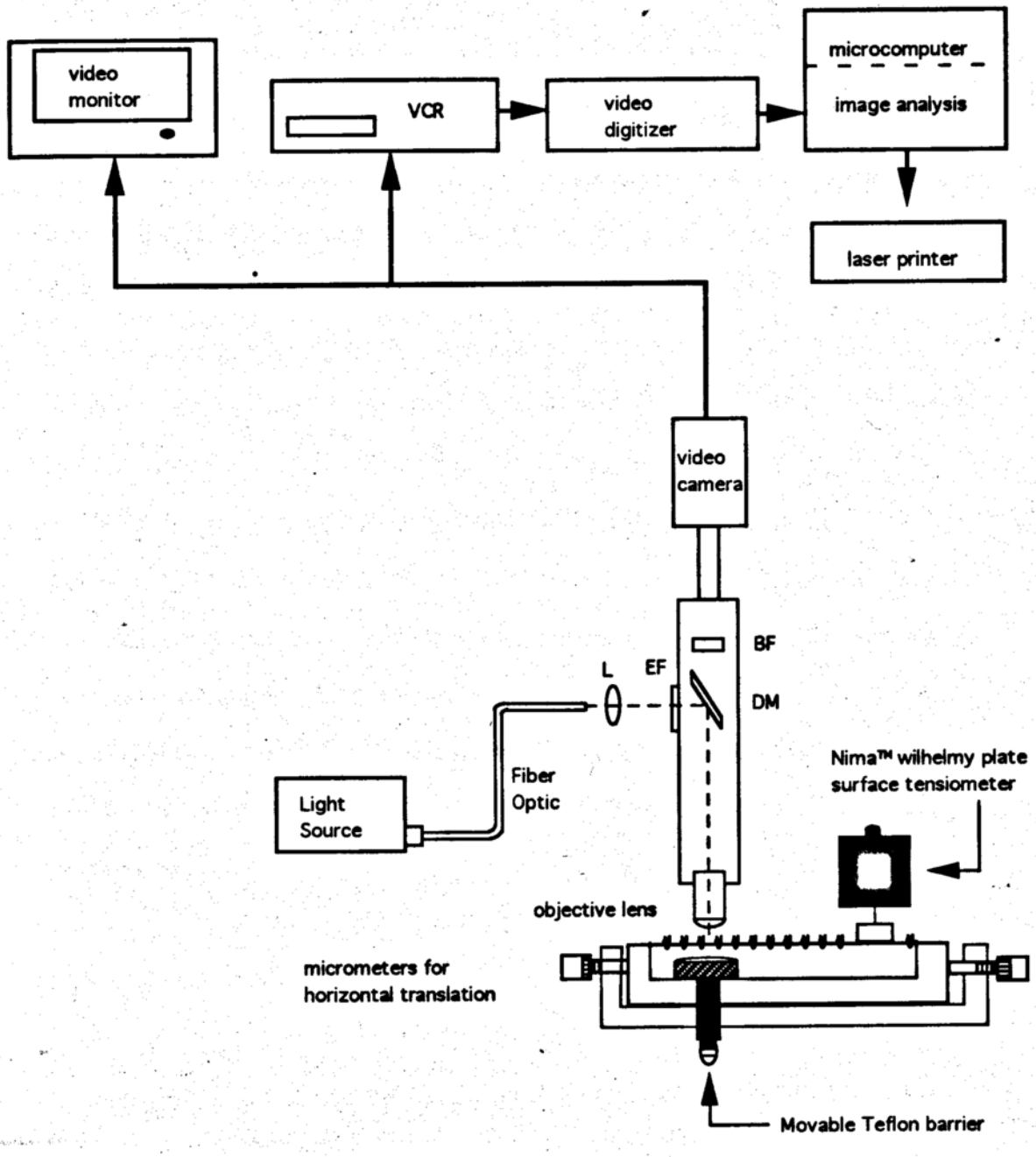

Figure 15. Schematic illustration of the fluorescence microscope. L: lens, EF: excitation filter, DM: dichroic mirror, BF: barrier filter.

was made using a Nima pressure transducer (Nima, Inc., Coventry, England). The excitation light from a tungsten-halogen lamp (Fiber-Lite, Dolan-Jenner Industries Inc.) passes through a filter (Zeiss Inc., Thornwood, NJ) which only passes light of wavelength, λ, 480 ± 20 nm. This light is reflected down to the water surface via a dichroic mirror (Zeiss Inc.) which only reflects light of $\lambda = 480 \pm 20$ nm. The fluorescence from the surface is collected by the objective lens (40x) (Fisher Scientific) and passes through the dichroic mirror, which only passes light with $\lambda >$ 500 nm, and an additional barrier filter (Zeiss Inc.), which also only passes light with $\lambda > 500$ nm. The microscope is connected to a video camera (Optronics Engineering, Goleta, CA) via a video relay lens (10x) (Fisher Scientific) and the image is viewed on a monitor (Apple monitor III) and stored onto video tape (Mitsubishi HS-U65). Images were captured using a Mac Vision video digitizer and Mac Vision image processing software (Koala Acquisitions, Inc.). Image analysis was performed using NIH Image software (v. 1.55) available from the National Institutes of Health (Washington DC).

Injection of Protein Beneath Lipid Monolayers

Experiments measuring the change in surface pressure upon injection of the protein into the subphase beneath the lipid monolayer were made using a specially designed small volume($\approx$ 35 ml) trough illustrated in Figure 16. Details of the construction are given in Figures 17-19. The monolayer is spread on one side of the Teflon barrier. The subphase temperature is maintained using a refrigerated constant temperature circulator (VWR model 1165, VWR, West Chester, PA) which circulates water through channels located in the aluminum base (see Figure 19). The surface pressure of the monolayer at equilibrium is then obtained. The protein is then injected

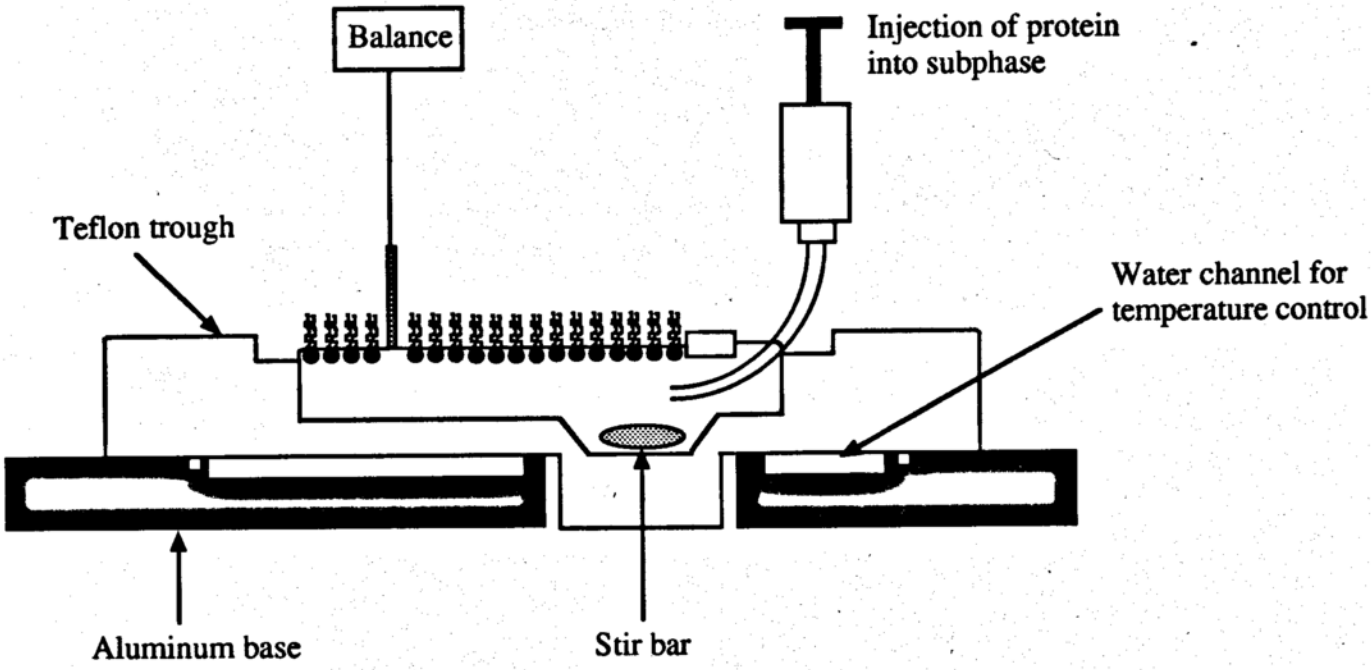

Figure 16. Schematic illustration of th monolayer trough used for experiments involving the injection of protein into the subphase.

a.

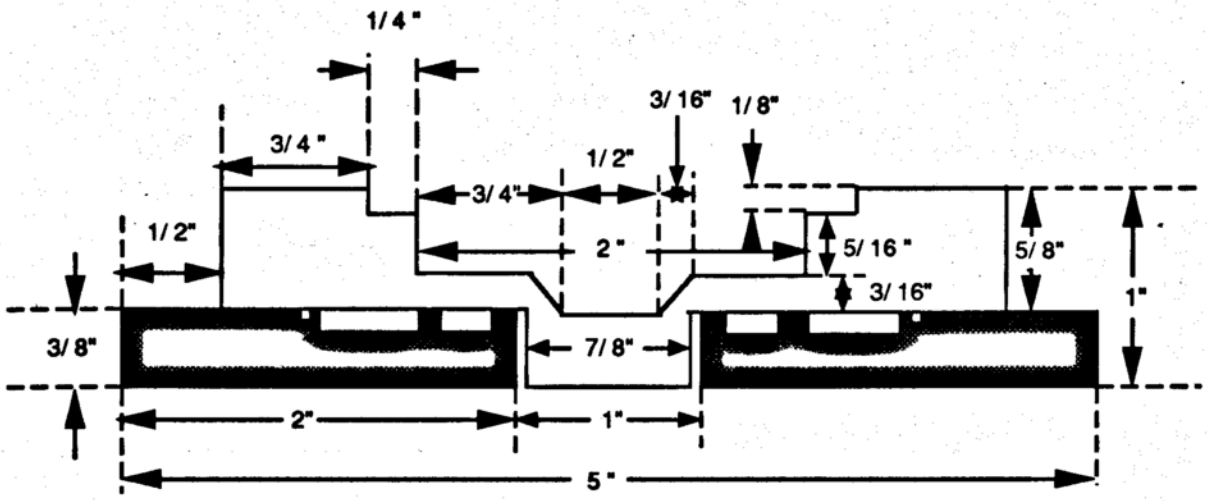

b.

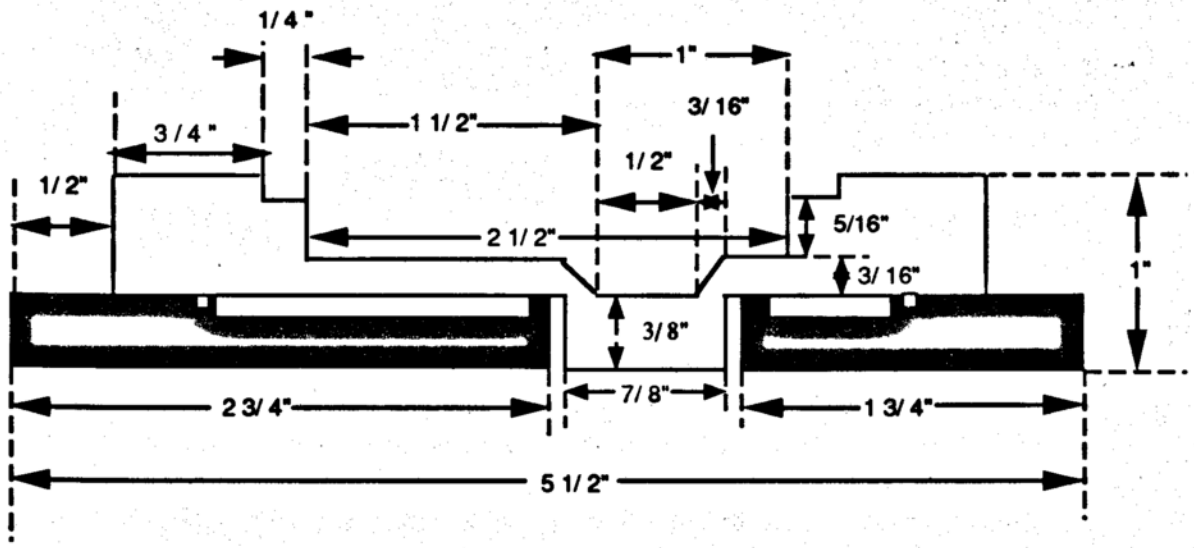

Figure 17. Dimensions for the design of the trough used in protein experiments. Cross section of the short side (a.) and the long side (b.).

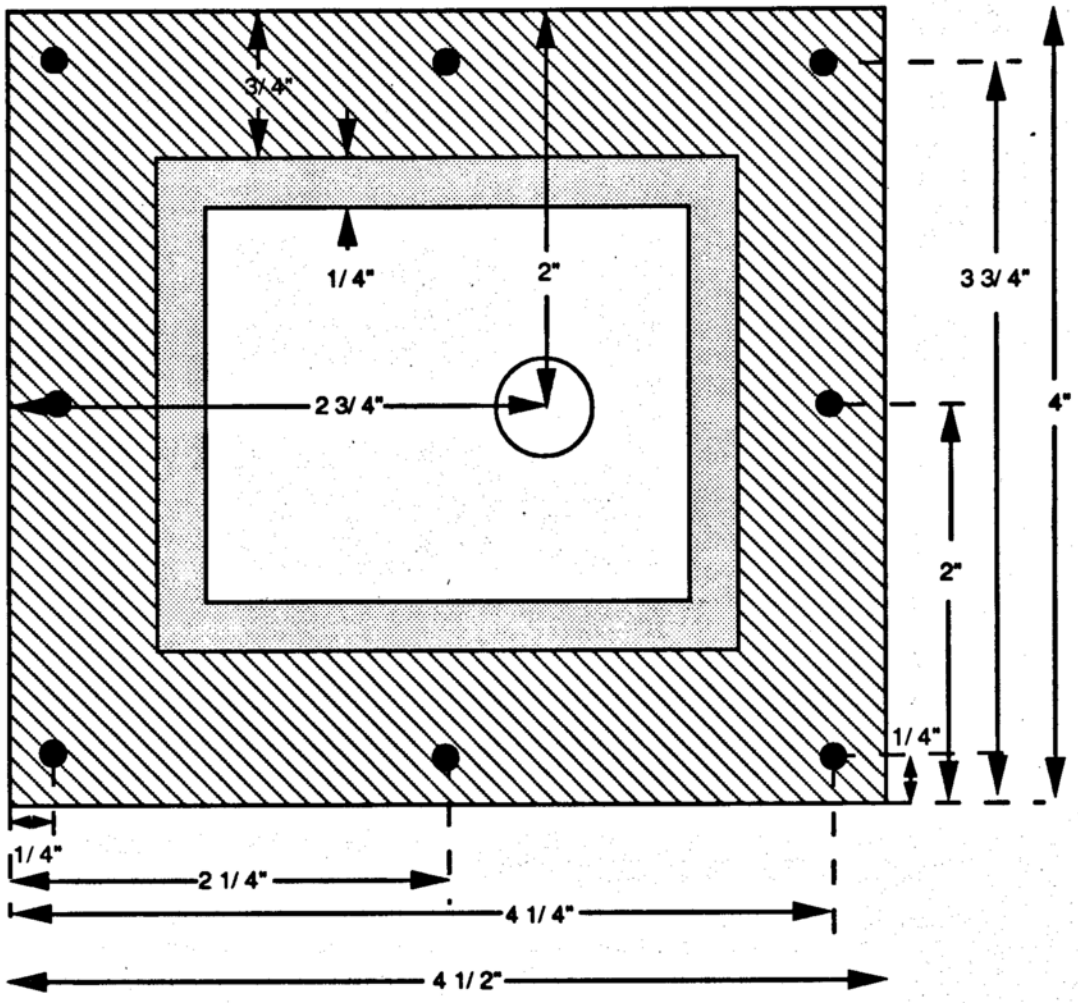

Figure 18. Dimensions for the design of the trough used in protein experiments (top view).

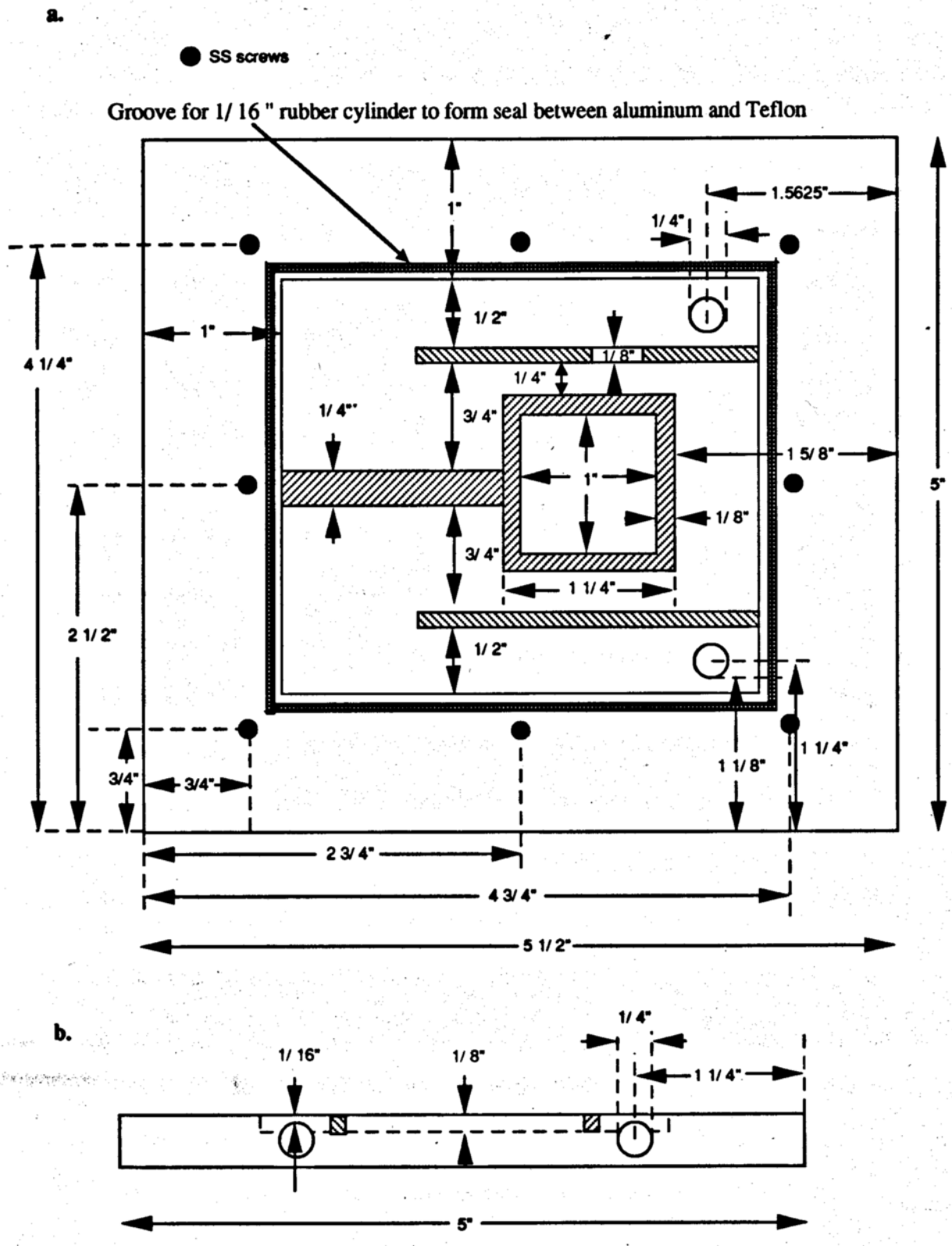

Figure 19. Top view of the aluminum base (a.) and side view of the aluminum base (b.) of the trough used in protein experiments.

into the subphase from the opposite side of the barrier and the subphase is stirred by placing the trough on a Thermolyne nuova II stirrer (Barnstead/Thermolyne, Dubuque, IA) and placing a stir bar (3mm in diameter, 10 mm in length) into the well of the trough (Figure 16). Separate experiments performed by injecting methylene blue into the subphase revealed that homogeneous mixing in the subphase is obtained after stirring for 5 minutes at a setting of 5. An experiment performed with lycopodium powder (Flinn Scientific, Inc., Batavia, Ill) sprinkled at the interface revealed that minimal disruption at the interface accompanies stirring. The equilibrium final surface pressure is then measured typically 15-24 hours after injection of the protein.

The trough was also designed so that it could be place onto the stage of the fluorescence microscope. However, due to its difference in design, the movable circular barrier could not be used with this trough. An alternate approach to control surface flow during microscopic observation was used based on a design previosly reported in the literature (Peters and Beck, 1983; Meller, 1988). A mask (Figure 20) was designed which captures a portion of the monolayer in a small circular cutout in a removable Teflon piece. A canal from the surrounding monolayer to the circular cutout ensured equilibration of the monolayer both inside and outside of the circular area.

Preparation of Supported Phospholipid Bilayers

Supported planar bilayers were prepared by successive transfer of two monolayers from the air/water interface by vertical dipping. Regular multilayers of phospholipids can be dipped successfully using this method provided that the monolayer is condensed (Green, Phillips et al., 1973). A DPPG monolayer was spread at the

a.

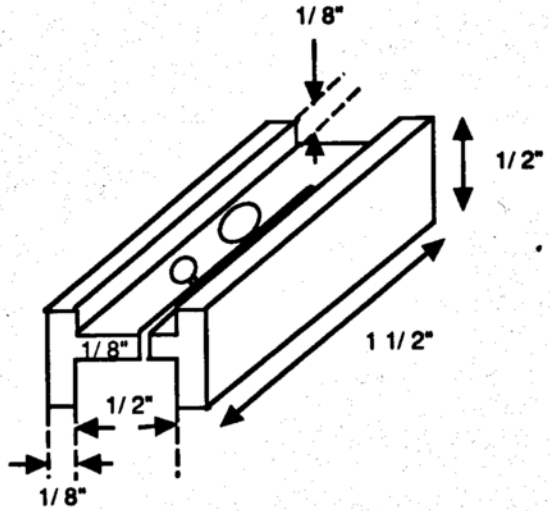

b.

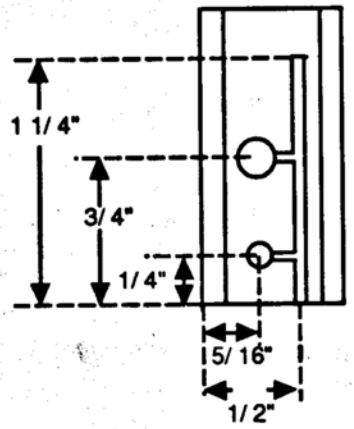

canal width = 2 mm (≈ 0.078")
small hole = 3 mm (≈ 0.118")
large hole = 5 mm (≈0.197")

Figure 20. Dimensions of the mask used for protein experiments using the fluorescence microscope. Front view of the mask (a.) and top view of the mask (b.)

air/water interface to a surface pressure of approximately 35mN/m and allowed to equilibrate at least one hour to ensure the evaporation of the spreading solvent. The subphase consisted of 10 mM Tris-HCl buffer, pH 7.4, 25°C and 5 μM Ca^{2+}, unless otherwise specified. The monolayer was spread at the air/water interface of a Langmuir trough equipped with a movable barrier whose movement was controlled by a feedback mechanism that maintained the monolayer at a constant surface pressure to within 0.1 mN/m (Sacchetti, Yu et al., 1993). The freshly cleaved mica (scratch-free muscovite mica from Asheville-Schoemaker, P.O Box 318, Newport News, VA machined into discs 0.390" ± 0.005" in diameter, 0.012"-0.015" thick) substrate was stored beneath the water surface. After equilibration of the monolayer, the substrate was then pulled vertically through the interface at a speed slow enough to allow water to drain from the surface. The substantial drop in surface pressure observed was compensated by a reduction in the area of the trough controlled via the feedback electronics. The substrate was then lowered vertically through the monolayer and again the surface pressure decreased and the trough area was reduced to compensate. The bilayer covered mica was then deposited at the bottom of the trough and the remainder of the monolayer was suctioned from the trough. The buffer was removed and the bilayer-coated mica was allowed to air dry.

Atomic Force Microscopy of Supported Phospholipid Monolayers

The atomic force microscope (AFM) is a scanning probe microscope that is capable of resolving surface detail of nonconducting materials down to the atomic level. It was invented by Binnig, Quate, and Gerber (Binnig, Quate et al., 1986) in 1986 after the development of the scanning tunneling microscope. The AFM records interatomic forces between the apex of a tip and atoms in a sample as the tip is

scanned over the surface of the sample (Figure 21A) (for review see (Marti, Drake et al., 1987; Hansma, Elings et al., 1988; Gould, Drake et al., 1990; Ruger and Hansma, 1990; Frommer and Meyer, 1991; Radmacher, Tillmann et al., 1992; Lal and John, 1994)). In the experiments described below, the AFM is being operated in a mode (i.e. constant-deflection or constant-force mode) that senses the repulsive forces between the tip and sample. The tip actually touches the sample, much like the stylus of a record player touches the surface of a record. However, for the AFM, the tip is much sharper theoretically with one molecule at its apex, and the tracking force is much smaller so that the tip can trace over individual atoms without damaging the surface of the sample.

The small repulsive tracking forces between the tip and the sample, usually in the range of 10^{-6} to 10^{-9} N are recorded by measuring minute deflections of the cantilever. The deflection of the tip is translated into a detectable signal through the use of an optical lever system (Figure 21B). A laser beam reflects off the cantilever, the angular direction of which changes as the tip undergoes deflections. The reflected beams are captured and converted into electrical signals by position sensitive photodetectors. The optical lever amplifies the deflection signal up to 1,000-fold, so that even a deflection of <1 nm can be measured.

Using an appropriate feedback system, the deflection of the cantilever can be kept constant. The feedback loop changes the height of the sample by adjusting the voltage applied to the *z* portion of the *xyz* piezoelectric scanner. The amount of change (z) corresponds to the topological height of the sample at each point in the *x*-*y* raster. Combining the information from the three coordinates generates the three dimensional image. So, the AFM image obtained is essentially an isoforce relief of the sample.

Mica samples were imaged with a commercial AFM (Nanoscope III, Digital Instruments, Santa Barbara, CA) equipped with a D-type scan head, which provides a

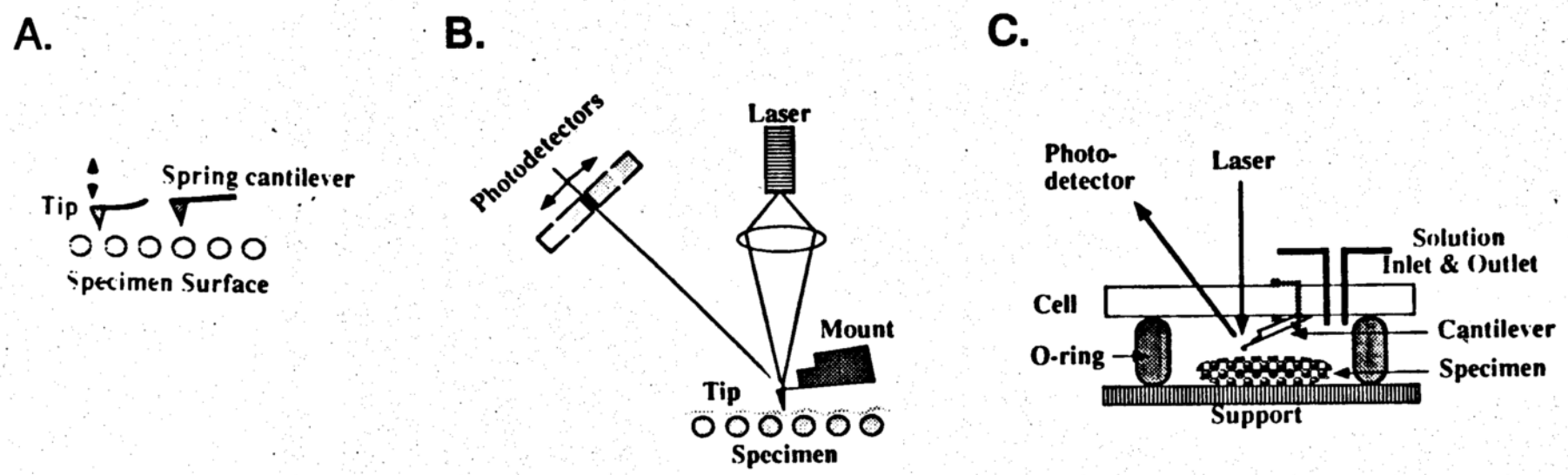

Figure 21. Schematics of the operating principle of an atomic force microscope. A. The force sensor consisting of sharp tip mounted onto a cantilever spring. B. Optical deflection detection system. C. AFM fluid cell. Both the cantilever and specimen are immersed in fluid.
Taken from (Lal, 1994).

maximum scan size of 12 x 12 μm. Images were obtained at room temperature either in air or under solution using a glass fluid cell attachment (Digital Instruments) (Figure 21C). Imaging in a fluid environment has the advantage that the surface tension force (due to adsorbed layers of water to a sample) are abolished, thus reducing the necessary imaging force which contributes substantially to the stability of the sample and the resolution that can be achieved (Zasadzinski, Viswanathan et al.; 1994). The fluid cell, silicone rubber inlets, O-rings, and polypropylene connectors were rinsed with triple distilled water prior to use. The samples were mounted onto a 1 cm steel disk with an adhesive and placed on the sample stage of the AFM which has a magnet in the base. Imaging was performed with silicon nitride cantilevers that were either 200 μm wide (spring constant, k = 0.12 N/m) for experiments involving the protein or 100 μm wide (k = 0.58 N/m) for imaging of clean mica. The laser was aligned to the tip of the cantilever and the position sensitive photodiodes were aligned to the deflected beam. The tip was brought into close contact with the sample and the fluid cell could be attached at this point. For experiments performed on areas of < 50 nm^2, the instrument was mounted on a concrete block and suspended from a tripod. The instrument was then engaged and a force calibration curve was generated to ensure proper engagement of the tip. The imaging force was calculated by multiplying the distance the sample had to be withdrawn in order for the tip to be snapped free from the surface and the spring constant of the cantilever. Typical imaging forces were 8-12 nN.

Chapter III

The Surface Phase Behavior of Phospholipids at the Air/Water Interface

Results

Single component systems

Equilibrium spreading pressures

Table I lists the equilibrium spreading pressures, π_e, and the collapse pressure, π_c, the maximum surface pressure to which the monolayer can be compressed and remain stable, and the corresponding molecular area, A_{min}, the closest packing dimensions attainable in a monolayer. All experiments were performed on 10 mM Tris-HCl, pH 7.4, 25°C. Reasonable agreement between π_e and π_c is observed except with the disaturated lipids, DPPC and DPPG, which exhibited π_e values of zero. Whereas, all other phospholipids have gel-to -liquid transition temperatures, T_m, below 25°C, DPPC and DPPG both have T_m values of 41°C and hence cannot spread over any reasonable time period without the aid of a spreading solvent. The addition of 5 mM $CaCl_2$ to the subphase caused negligible effects on π_e or π_c in all cases.

Surface pressure vs. area isotherms and fluorescence microscopy

Fluorescence microscopic and π-A measurements revealed complete homogeneity for all of the liquid-expanded monolayers, i.e. POPC, DOPC, POPG, and DOPG in the presence and absence of 5 mM $CaCl_2$ over the entire surface pressure range examined. In contrast, the π-A isotherms and fluorescence microscopy reveal that for DPPC (Figure 22) and DPPG monolayers, in both the absence (Figure 23) and presence of 5 mM $CaCl_2$ (Figure 24), undergo an LE to LC phase transition at 25°C

Table I. Single Component Monolayers

Lipid	π_e / (mN/m)	π_{max} / (mN/m)	A_{min} / (nm^2/molecule)
DPPC	0	40	0.42
POPC	29	30	0.57
DOPC	28	23	0.74
DPPG	0	43	0.42
POPG	43	44	0.54
DOPG	32	23	0.73

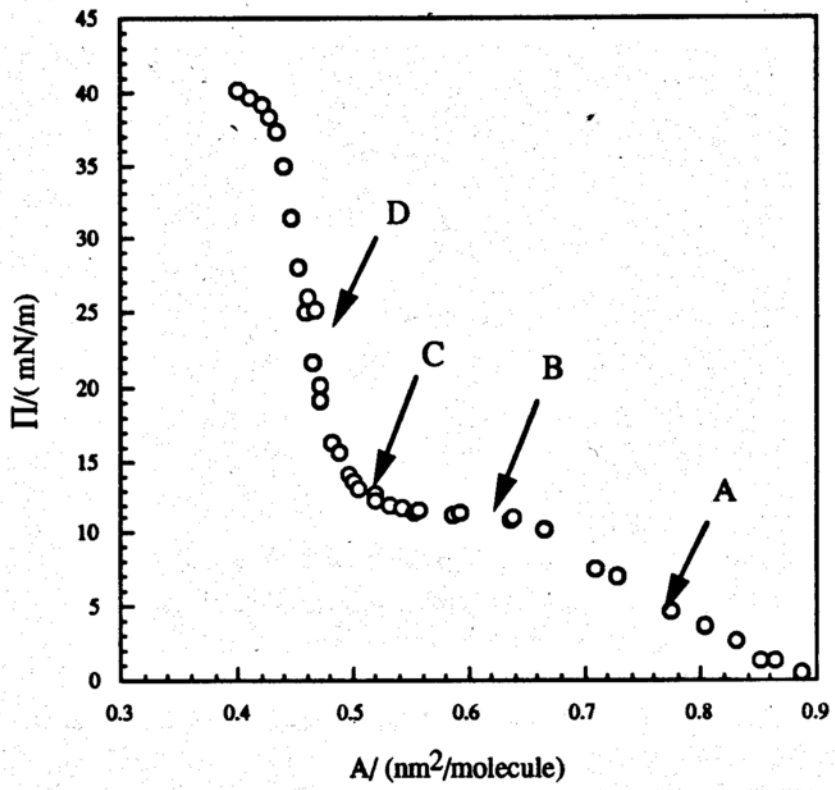

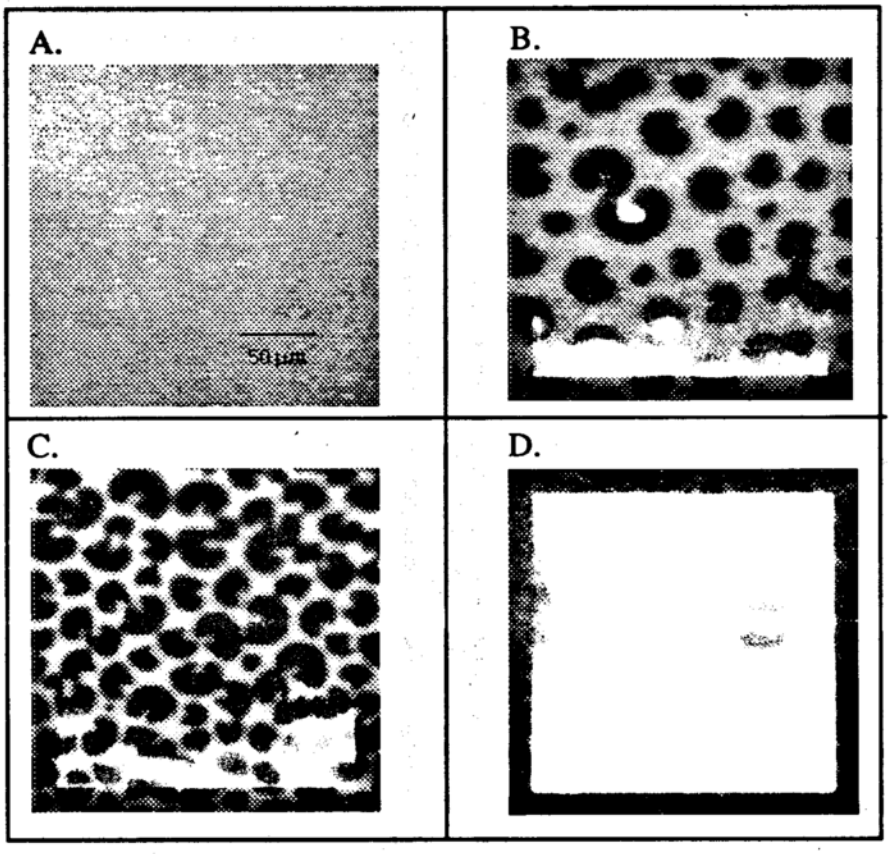

Figure 22. The π-A isotherm (top) and fluorescence images for DPPC spread on 10 mM Tris-HCl, pH 7.4, 25°C and 15 mM NaCl. The images are obtained at (A.) 4.0 mN/m, (B.) 10.5 mN/m, (C.) 11.6 mN/m, and (D.) 25.0 mN/m,

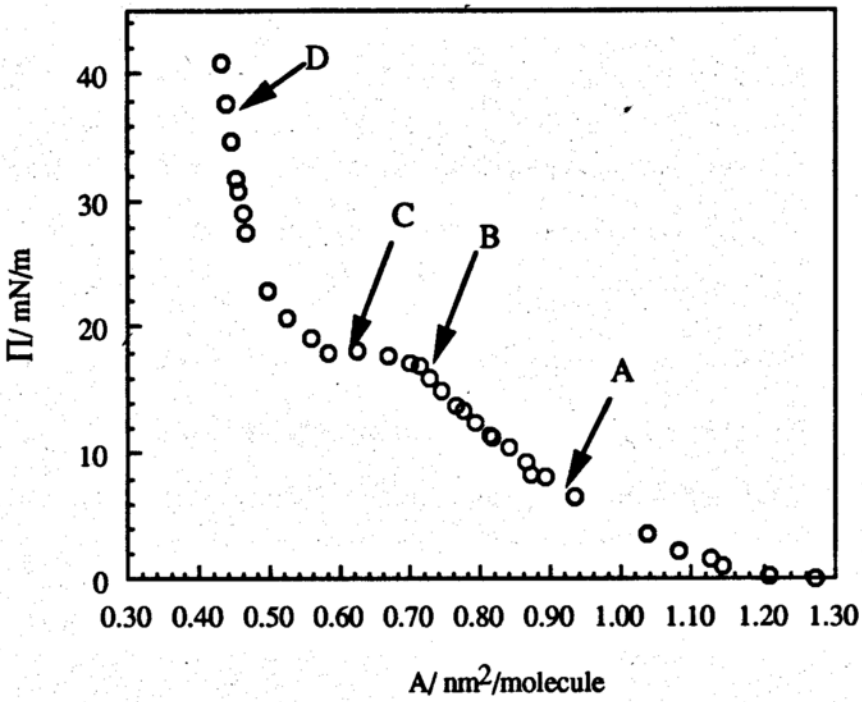

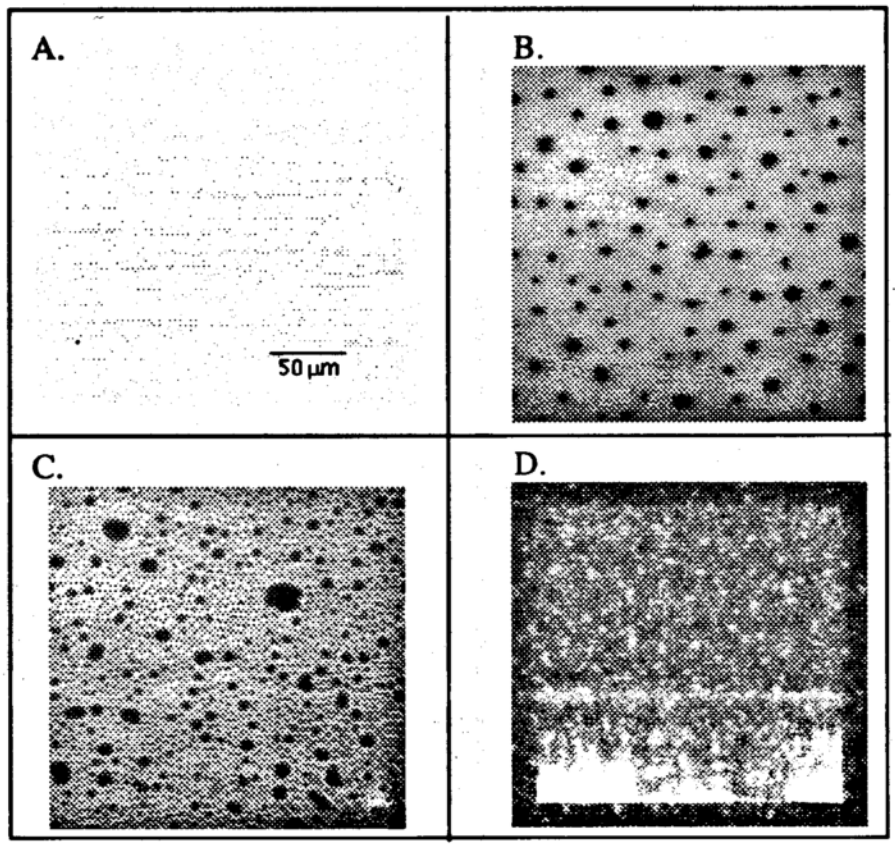

Figure 23. The π-A isotherm (top) and fluorescence images (bottom) for DPPG spread on 10 mM Tris-HCl, pH 7.4, 25°C and 15 mM NaCl. The images are obtained at (A.) 6.4 mN/m, (B.) 13.5 mN/m, (C.) 19.8 mN/m, and (D.) 36.8 mN/m,

in agreement with results obtained in the literature (Hendrickson, Fan et al., 1983; MacRitchie, 1990; Kim and Yu, 1992). The coexistence of phases could readily be viewed by fluorescence microscopy as has also been previously documented in the literature (McConnell, 1991). The addition of 5 mM $CaCl_2$ to the subphase of the anionic DPPG monolayer condensed the monolayer film, but did not affect the LE to LC phase transition (Figure 24). The domains appeared coalesced in the presence of Ca^{2+}, most likely due to the shielding of electrostatic repulsions that are believed to maintain the separated domains.

Binary Mixtures

Equilibrium spreading pressures

Table II lists the equilibrium spreading pressure, π_e, the collapse pressure, π_c, and the corresponding molecular area at π_c, A_{min}, for binary mixtures of DPPC with DPPG, unsaturated phosphatidylcholines and the corresponding phosphatidylglycerol phospholipids at a variety of molar ratios. All experiments were performed on 10 mM Tris-HCl, pH 7.4, 25°C. Reasonable agreement between π_e and π_c is observed except with the disaturated lipid mixture of DPPC and DPPG. Again, this result could be anticipated since DPPC and DPPG both have T_m values of 41°C and hence cannot spread over any reasonable time period at 25°C without the aid of a spreading solvent. The addition of 5 mM $CaCl_2$ to the subphase caused negligible effects on π_e or π_c in all cases. The πe, or πc, values for the DPPC/PC mixtures are, within experimental error, the same regardless of composition. The values measured for the DPPC/PG mixtures vary with composition, decreasing with increasing amounts of DPPC.

Surface pressure vs. area isotherms and fluorescence microscopy

The π-A isotherms and the phase behavior as determined from fluorescence microscopy were obtained for a series of binary mixed monolayers of DPPC with DPPG

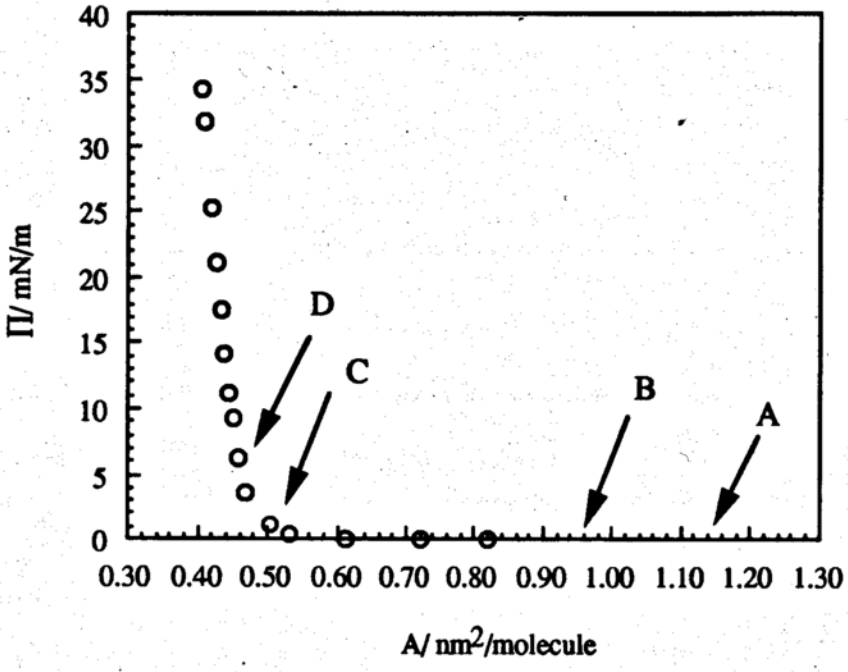

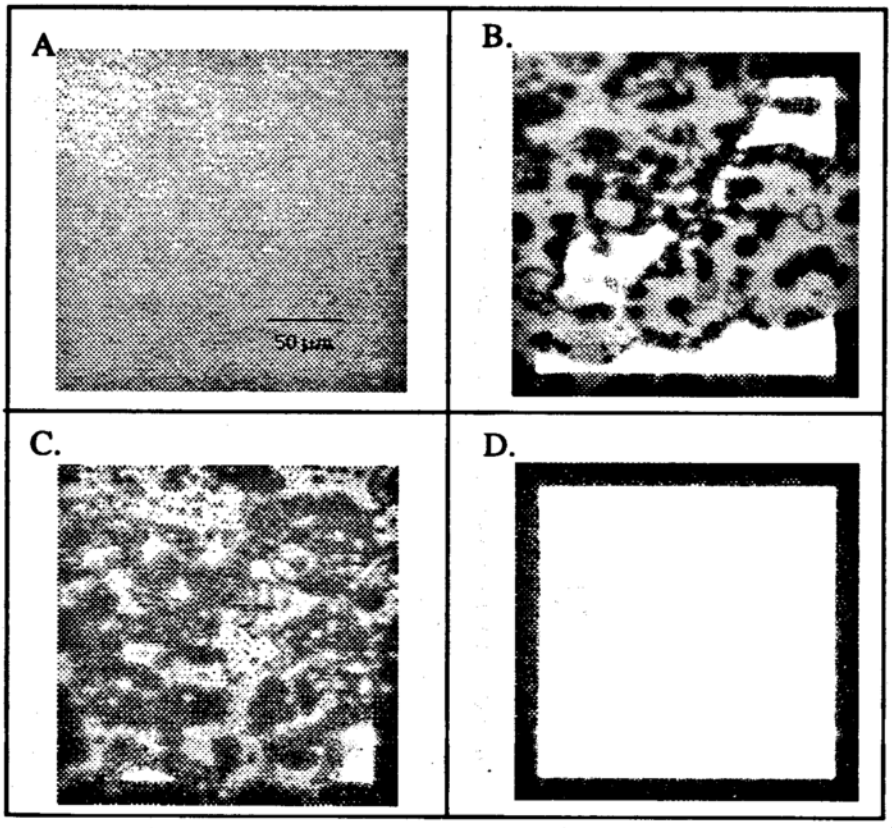

Figure 24. The π-A isotherm (top) and fluorescence images for DPPG spread on 10 mM Tris-HCl, pH 7.4, 25°C and 5 mM $CaCl_2$. The images are obtained at (A.) 0 mN/m, (B.) 0.5 mN/m, (C.) 1.6 mN/m, and (D.) 6.6 mN/m,

Table II Binary Mixed Monolayers

Lipid	π_e / (mN/m)	π_{max} / (mN/m)	A_{min} / (nm^2/molecule)
DPPC/DPPG (1:1)	0	38	0.42
DPPC/POPC (1:1)	29	32	0.53
DPPC/POPC (7:3)	27	25	0.55
DPPC/DOPC (1:1)	34	36	0.58
DPPC/DOPC (7:3)	32	30	0.55
DPPC/POPG (1:9)	39	40	0.65
DPPC/POPG (3:7)	46	40	0.65
DPPC/POPG (1:1)	27	25	0.60
DPPC/POPG (7:3)	20	22	0.60
DPPC/POPG (9:1)	10	12	0.72
DPPC/DOPG (3:7)	29	26	0.76
DPPC/DOPG (1:1)	12	16	0.80
DPPC/DOPG (7:3)	16	24	0.73

or with unsaturated phosphatidylcholines or the corresponding phosphatidylglycerol phospholipids at an equimolar ratio.

Same Acyl Chains/Different Headgroups The π-A isotherms and fluorescence microscopic images for an equimolar mixture of DPPC/DPPG were obtained in the absence (Figure 25), and presence (Figure 26) of 5 mM $CaCl_2$. The mixture, in the absence and presence of $CaCl_2$, exhibits an LE to LC phase transition at a surface pressure that is intermediate to those observed for each individual component. The surface pressure in the phase transition region for this mixture was also found to increase slightly with the mean area per molecule. Fluorescence microscopy reveals a homogeneously bright LE phase and an essentially homogeneous dark LC phase at high pressures. Similar phase behavior was noted in the presence of 5mM $CaCl_2$.

Different Acyl Chains/Same Headgroups The effects of introducing unsaturation into the acyl chains of one component, while keeping the polar headgroup constant, has been studied using equimolar mixtures of DPPC/POPC and DPPC/DOPC spread on 10 mM Tris-HCl, pH 7.4, 25° C and 15 mM NaCl. Both mixtures were shown to form expanded monolayers (Figure 27) and to be unaffected by the addition of 5 mM $CaCl_2$ to the subphase. Fluorescence microscopy revealed no stable domain formation in either mixture up to $\pi \approx 20$mN/m both in the absence and presence of 5 mM $CaCl_2$.

Different Acyl Chains/Different Headgroups The effect of simultaneously changing the polar headgroup and adding unsaturation to the lipid that is being mixed with DPPC has been studied using mixtures of DPPC/POPG and DPPC/DOPG. The π-A isotherms and the surface phase behavior of these systems, in the absence and presence of 5 mM $CaCl_2$, were examined. Partial phase separation occurred at π as low as 1 to 2 mN/m in equimolar mixtures of DPPC/POPG, in both the absence (Figure 28) and presence (Figure 29) of 5 mM $CaCl_2$. The amount of phase

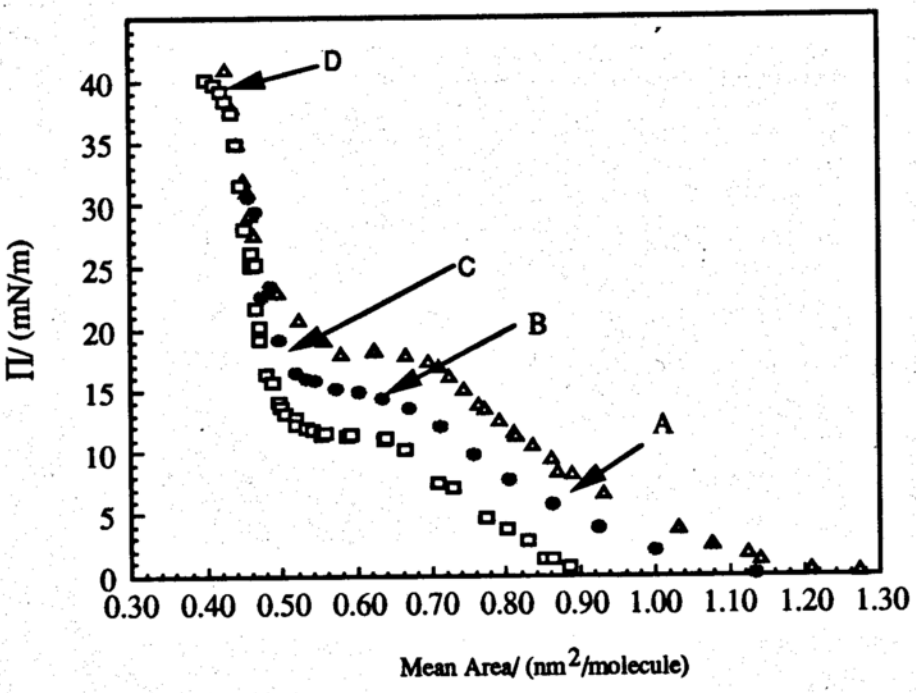

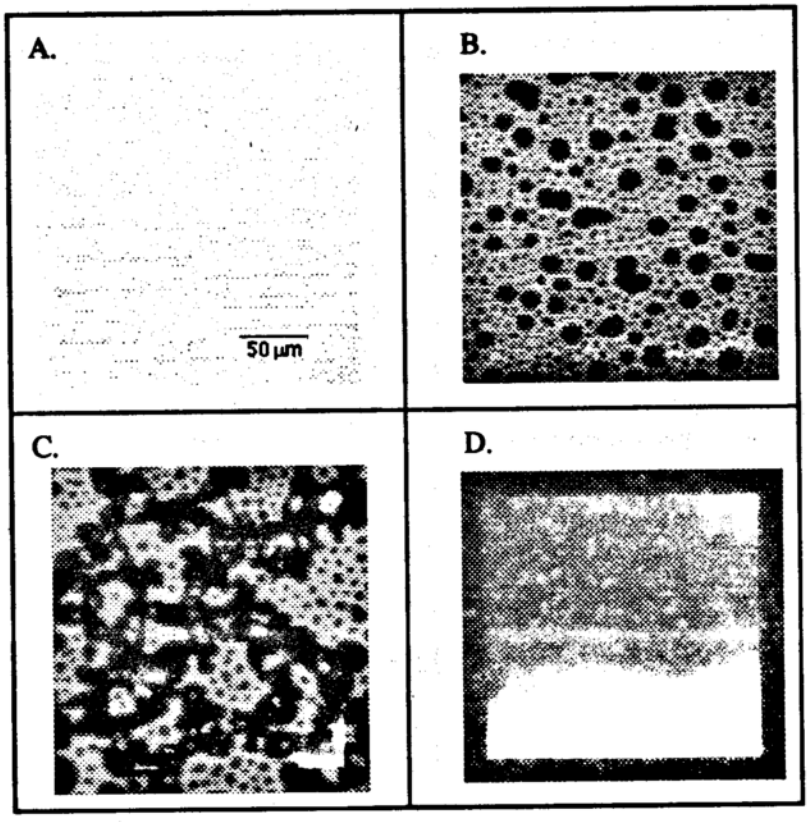

Figure 25. The π-A isotherm (top) and fluorescence images for DPPC/DPPG (1:1) spread on 10 mM Tris-HCl, pH 7.4, 25°C and 15 mM NaCl. The images are obtained at (A.) 5.0 mN/m, (B.) 15.3 mN/m, (C.) 19.5 mN/m, and (D.) 40.8 mN/m,

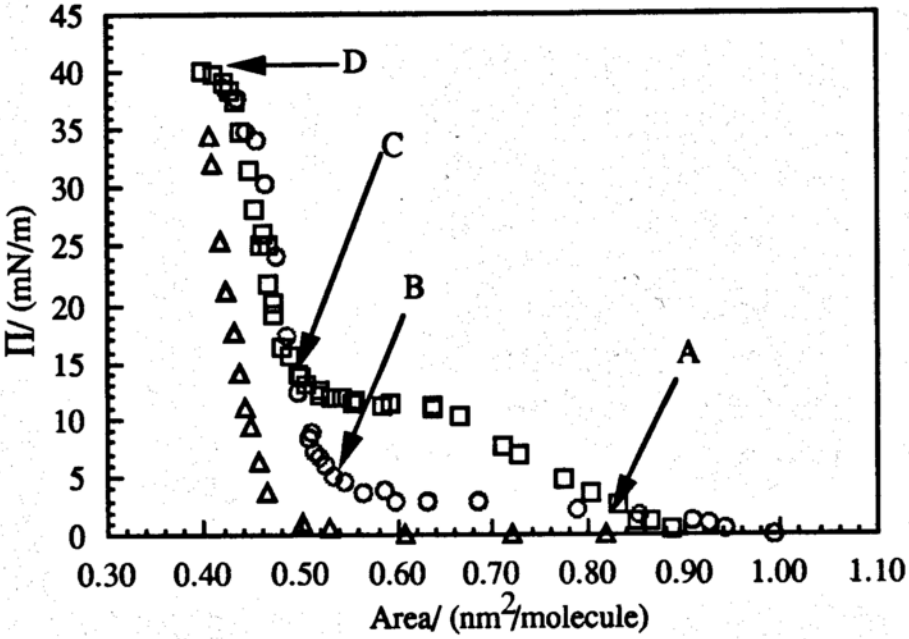

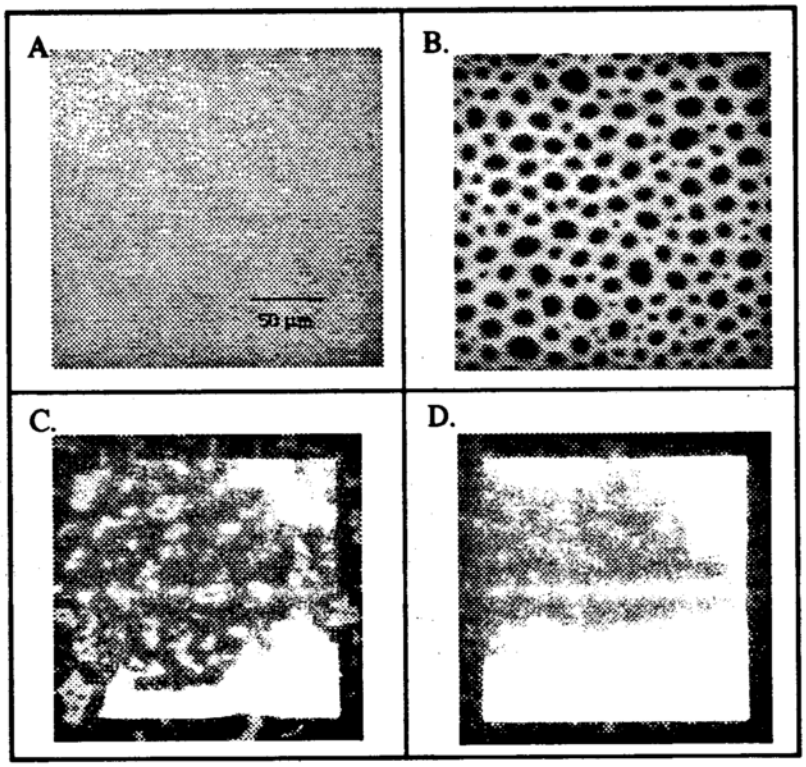

Figure 26. The π-A isotherm (top) and fluorescence images for DPPC/DPPG (1:1) spread on 10 mM Tris-HCl, pH 7.4, 25°C and 5 mM $CaCl_2$. The images are obtained at (A.) 0 mN/m, (B.) 4.3 mN/m, (C.) 12.5 mN/m, and (D.) 40.8 mN/m,

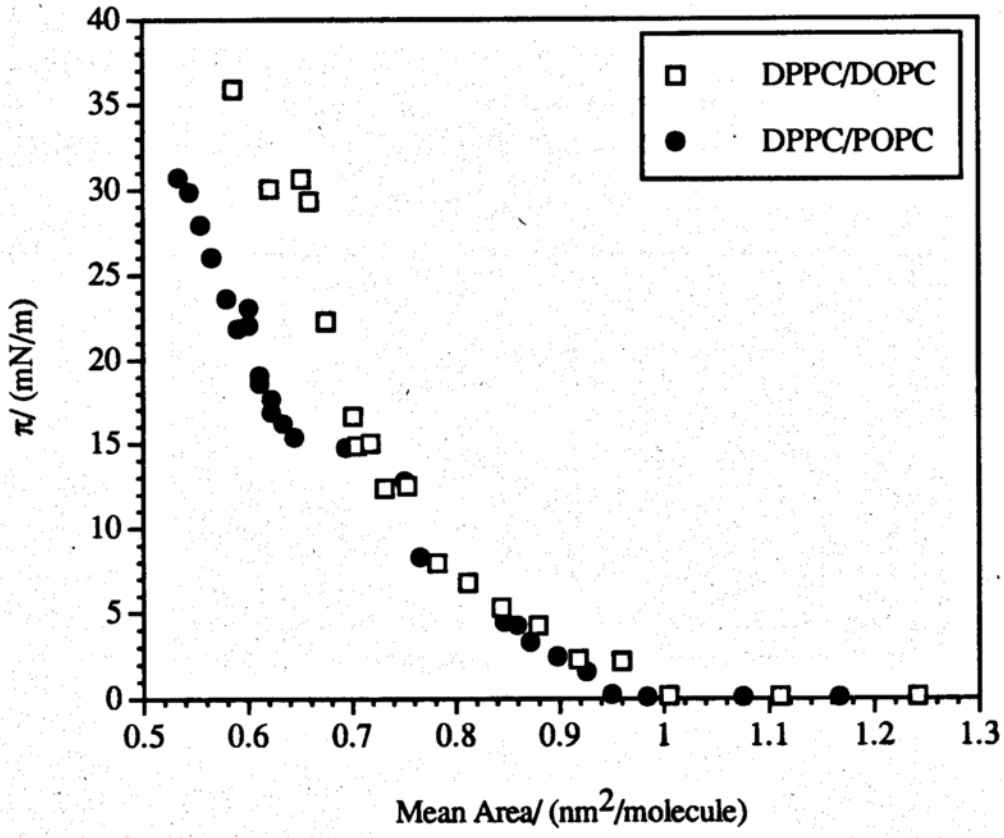

Figure 27. The π-A isotherm for DPPC/POPC (1:1) and DPPC/DOPC (1:1) spread on 10 mM Tris-HCl, pH 7.4, 25° C and 15 mM NaCl.

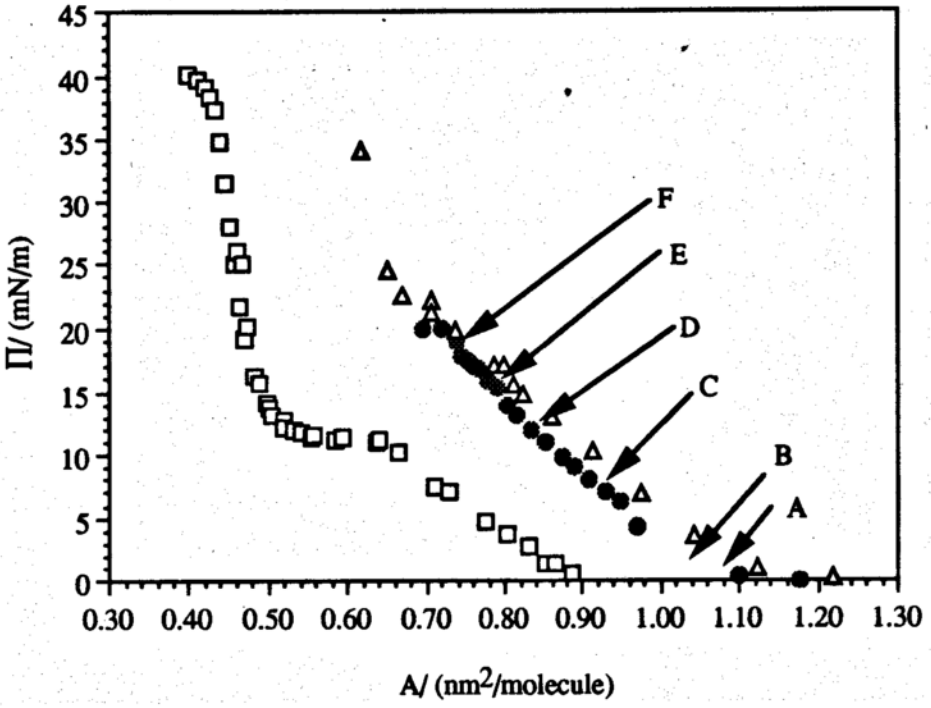

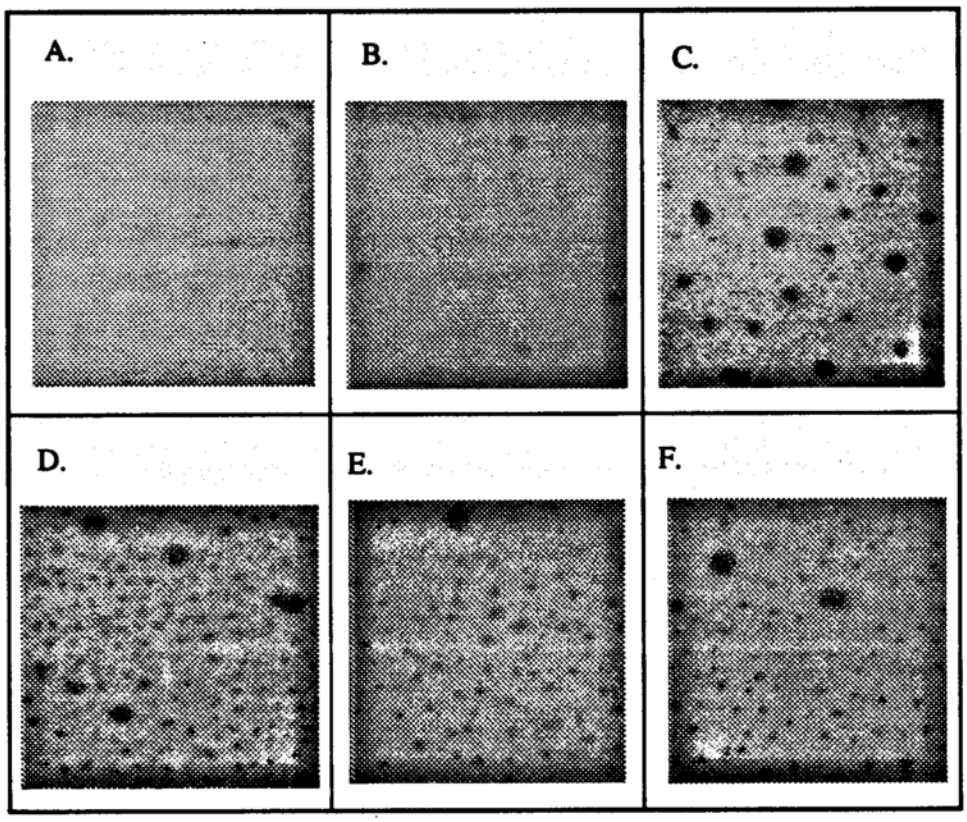

Figure 28. The π-A isotherm (top) and fluorescence images for DPPC/POPG (1:1) spread on 10 mM Tris-HCl, pH 7.4, 25°C and 15 mM NaCl. The images are obtained at (A.) 1.0 mN/m, (B.) 1.5 mN/m, (C.) 8.0 mN/m, and (D.) 12.8 mN/m, (E.) 15.8 mN/m, (F.) 17.8 mN/m.

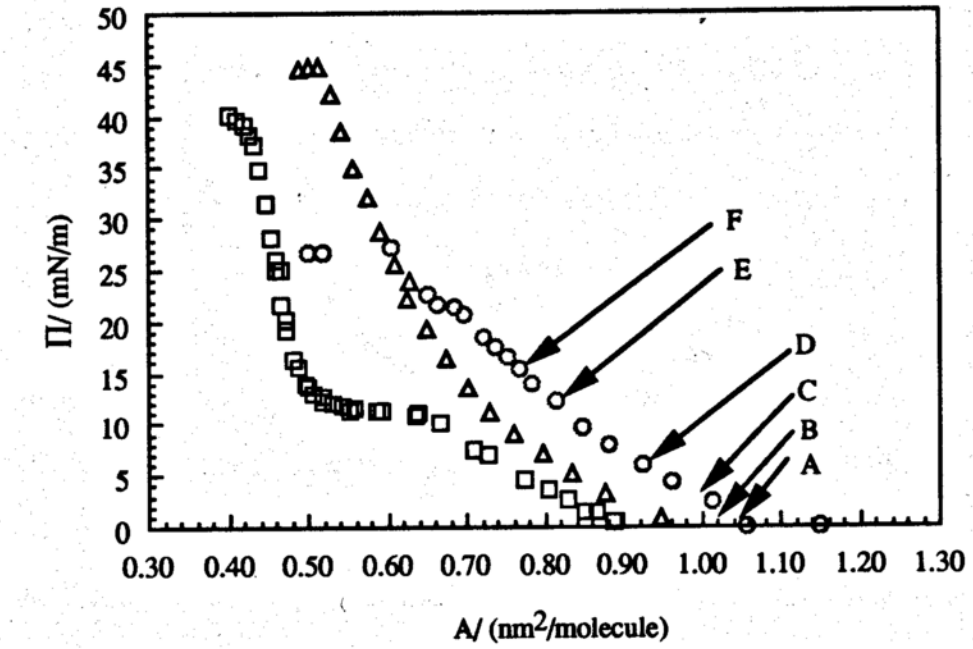

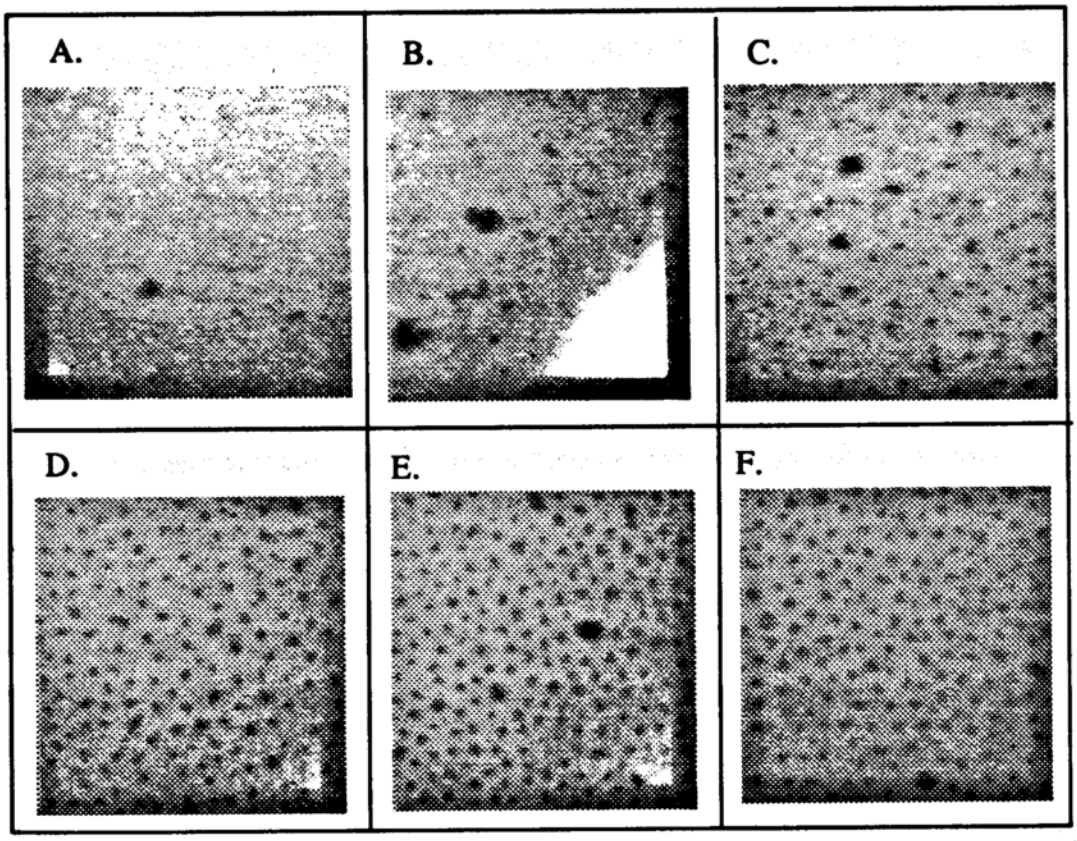

Figure 29. The π-A isotherm (top) and fluorescence images for DPPC/POPG (1:1) spread on 10 mM Tris-HCl, pH 7.4, 25°C and 5 mM $CaCl_2$. The images are obtained at (A.) 0.3 mN/m, (B.) 0.5 mN/m, (C.) 1.5 mN/m, and (D.) 4.0 mN/m, (E.) 9.8 mN/m, (F.) 14.0 mN/m.

separation was found to increase as surface pressure increased up to the collapse of the monolayer. The time dependence of the growth of the domains was monitored for the mixture at low and high surface pressures and in the absence and presence of $CaCl_2$ and found to remain essentially constant in size and shape for up to 16 hours. The reversibility and stability of domain formation was studied using a DPPC/POPG (1:1) monolayer spread on 10 mM Tris-HCl, pH 7.4, 25°C and 5 mM $CaCl_2$ at $\pi = 18$ mN/m (Figure 30). After equilibration of the monolayer (Figure 30A), a portion of the trough was partitioned and the monolayer material was removed. Upon removing the partition, the monolayer was allowed to expand, resulting in a lower measured surface pressure and a corresponding decrease in phase separation (Figure 30B). More DPPC/POPG (1:1) mixture was added to the monolayer to attempt to regain the initial surface pressure (Figure 30C). This monolayer had a surface pressure of 20 mN/m and there, indeed, was an increase in the amount of phase separated material. Furthermore, the domains were found to be stable at least up to 16 hours (Figure 30D). This experiment provides evidence that the domains formed in the binary monolayers are thermodynamically stable phases.

The fluorescence microscopic images of equimolar mixed monolayers of DPPC/DOPG in the absence (Figure 31) and presence (Figure 32) of 5 mM $CaCl_2$ also show phase separation. However, with this mixture, stable domain formation did not occur until the surface pressure exceeded 7 and 10 mN/m in the absence or presence of calcium ions, respectively. This suggests that DPPC is able to pack better with DOPG than POPG at the air/water interface at low surface pressure so as to remain homogeneously mixed. The amount of phase separation was also found to increase with surface pressure.

To explore this surface behavior in more detail, the amount of phase separation was quantified in both mixtures by analyzing the extent of total area covered by dark

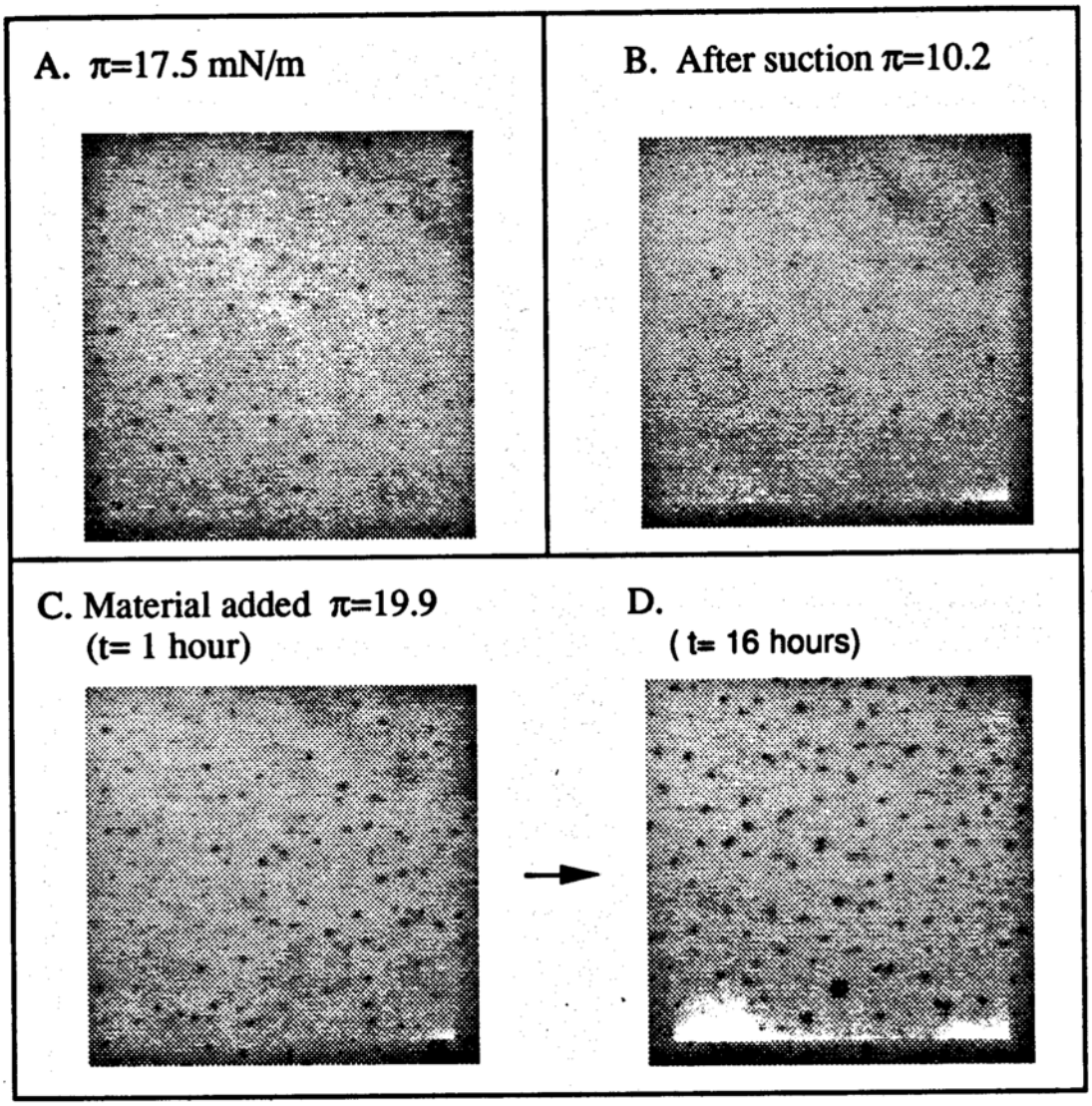

Figure 30. A. A DPPC/POPG (1:1) monolayer spread on 10 mM Tris-HCl, pH 7.4, 25°C and 5 mM $CaCl_2$ spread to a surface pressures of 17.5 mN/m. B. A portion of the monolayer was partition and some of the monolayer material was removed. C. More material was added to regain the monolayers original state (as in A). D. The kinetics and stability of domain formation was monitored.

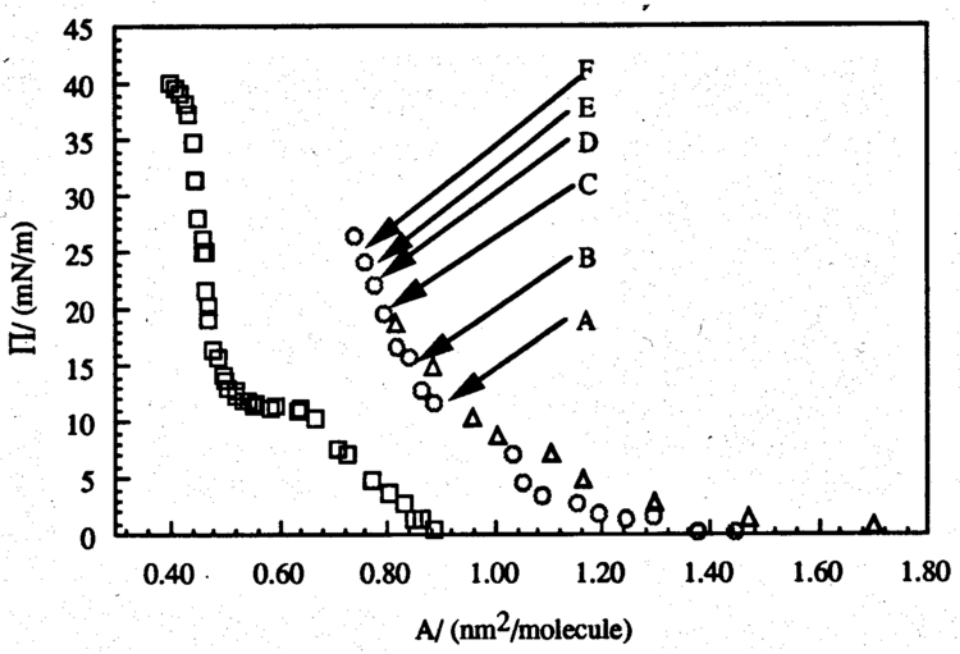

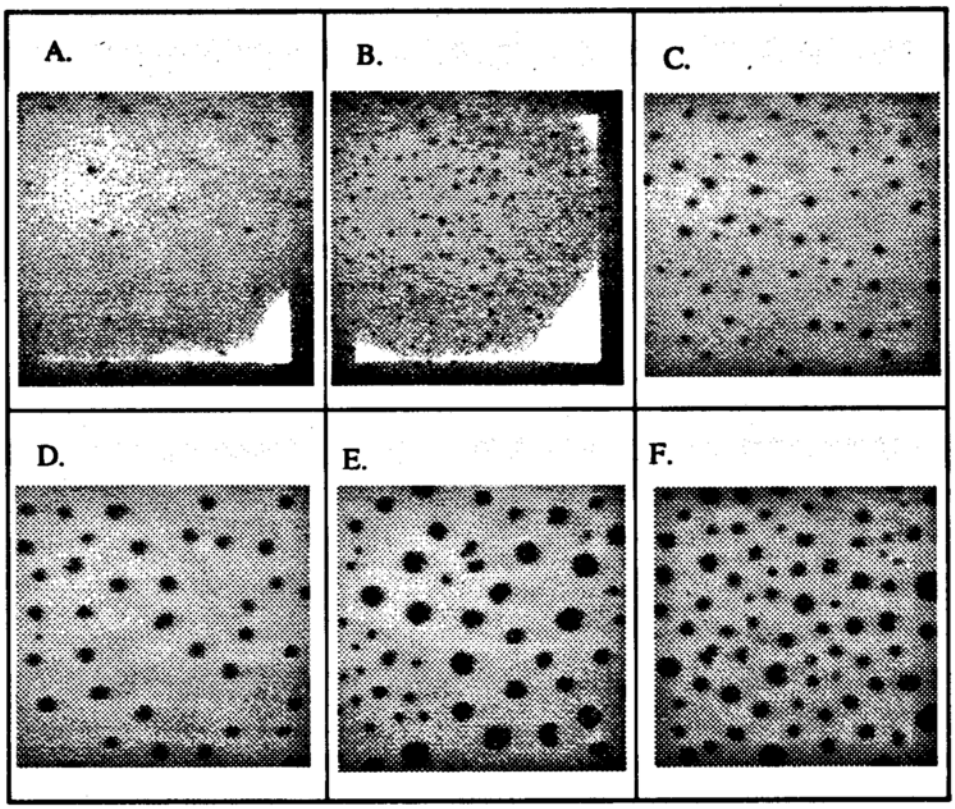

Figure 31. The π-A isotherm (top) and fluorescence images for DPPC/DOPG (1:1) spread on 10 mM Tris-HCl, pH 7.4, 25°C and 15 mM NaCl. The images are obtained at (A.) 11.3 mN/m, (B.) 14.8 mN/m, (C.) 17.8 mN/m, and (D.) 20.7 mN/m, (E.) 24.3 mN/m, (F.) 23.1 mN/m.

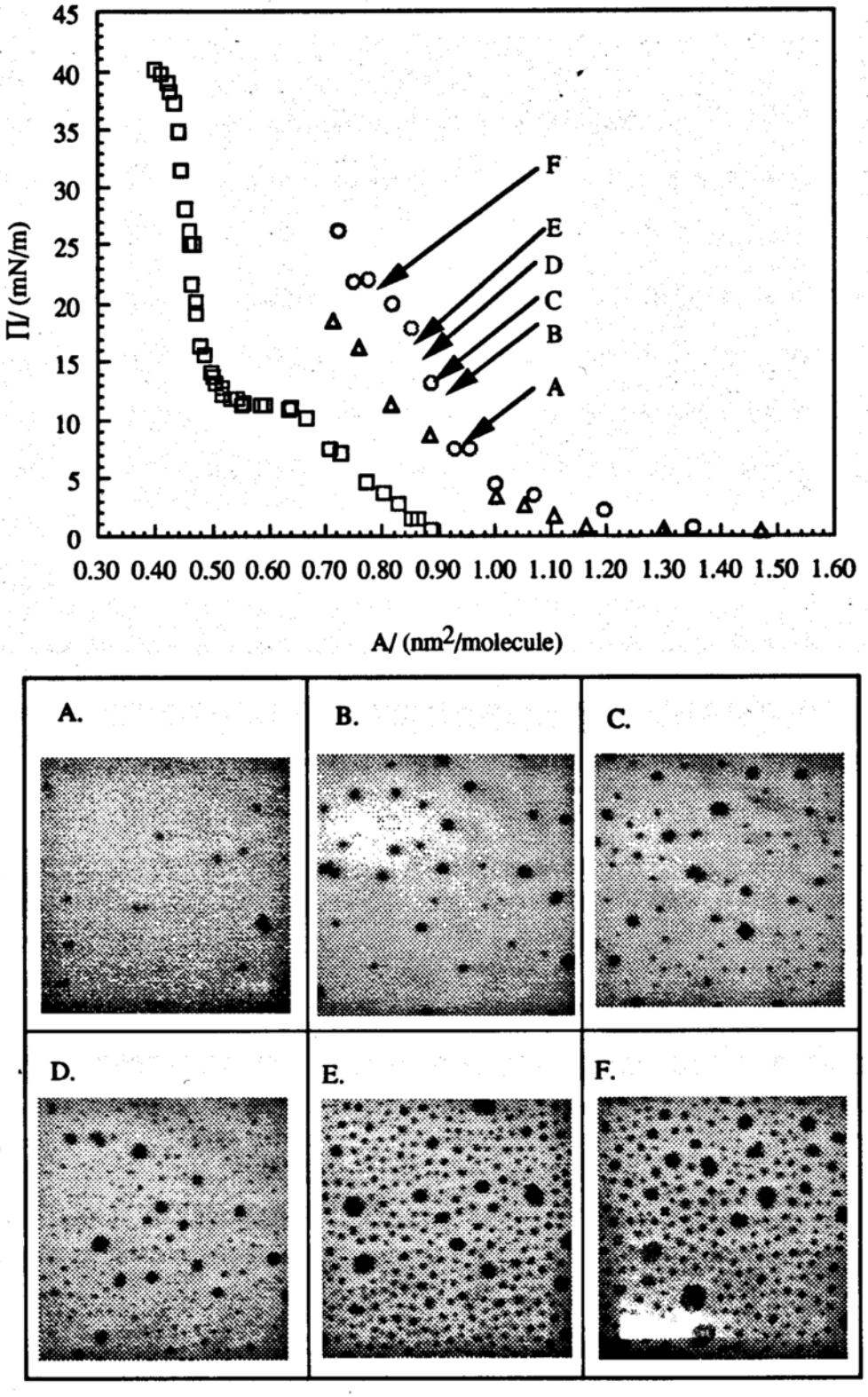

Figure 32. The π-A isotherm (top) and fluorescence images for DPPC/POPG (1:1) spread on 10 mM Tris-HCl, pH 7.4, 25°C and 5 mM $CaCl_2$. The images are obtained at (A.) 7.7 mN/m, (B.) 11.9 mN/m, (C.) 12.5 mN/m, and (D.) 13.6 mN/m, (E.) 16.0 mN/m, (F.) 19.6 mN/m.

domains using the NIH Image computer software (Figures 33 and 34). Interestingly, the amount of phase separated material was found to increase as π increased to approximately 10% or 20% in the absence and presence of calcium ions, respectively. Decreasing the dye concentration by half in the DPPC/POPG mixtures resulted in a negligible change in the amount of dark domains observed. Further studies were carried out by varying the molar ratios of DPPC/POPG and DPPC/DOPG in the monolayer. As shown in Figure 35 and 36, negligible amounts (<1%) of phase separation occurred in both DPPC/POPG and DPPC/DOPG 3:7 mixtures. Comparison of DPPC/POPG mixtures at molar ratios of 3:7, 1:1, 6:4 and 7:3 revealed that extensive phase separation occurs in the mixtures that contain higher percentages of DPPC (Figure 37) under the same conditions. The domains formed in the 6:4 and 7:3 mixtures were found to be highly irregular in shape and number, and therefore, quantitation of the amount of condensed domains was difficult and was therefore deemed unreliable.

As stated above, quantitation of the fluorescence micrographs of the mixtures revealed that the amount of phase separated material increases with surface pressure and never reaches a value of 50% indicating that most likely, complete immiscibility is not occurring but that there is a finite miscibility of one lipid in the other (to be discussed below). The phase that appears to be separating out is dark and thus depleted of fluorescent dye. This phase, therefore, most likely consists of a high percentage of DPPC, the lipid that forms more condensed monolayers.

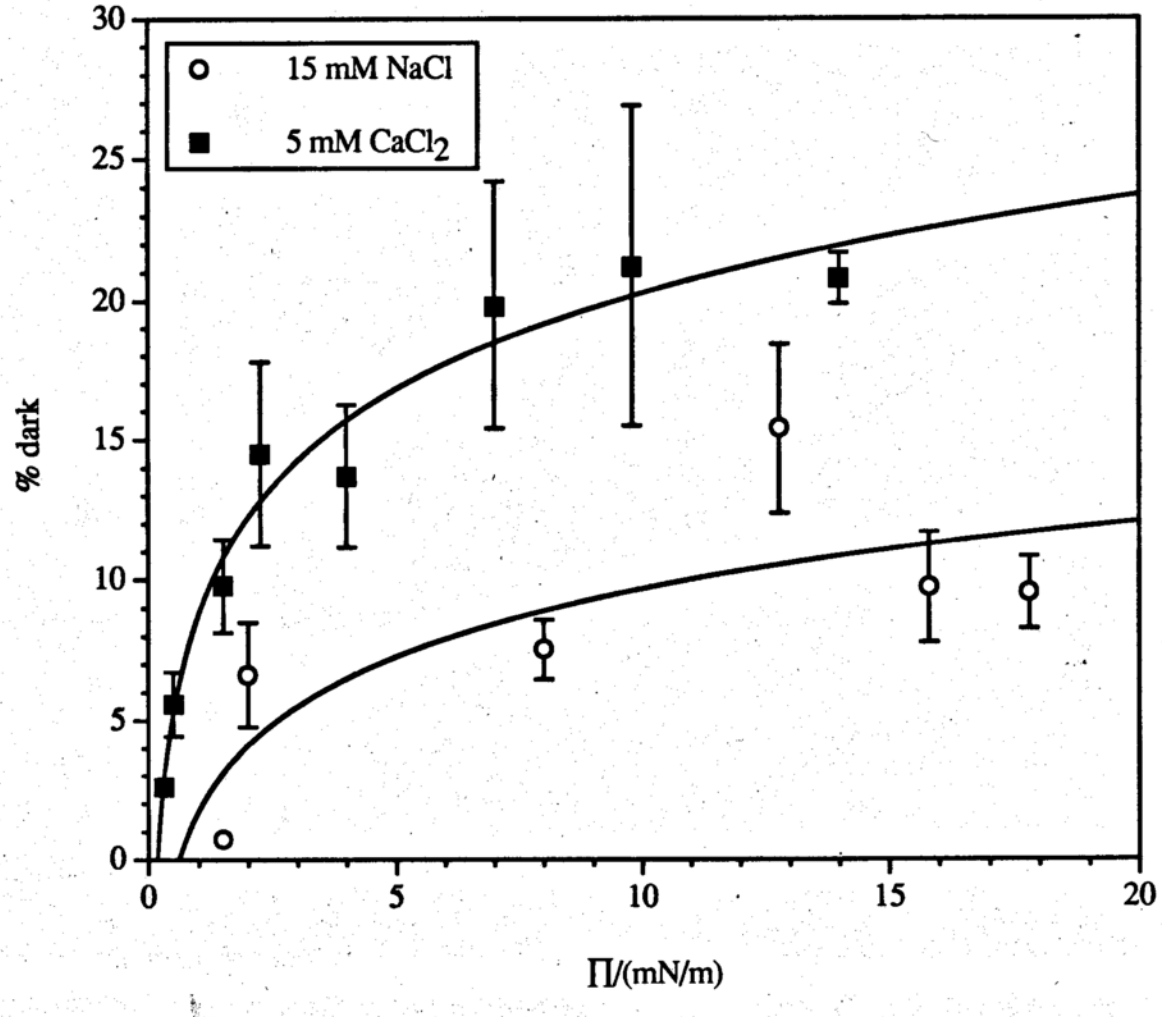

Figure 33. The percentage of dark domains as a function of surface pressure for DPPC/POPG (1:1) monolayers spread on 10 mM Tris-HCl, pH 7.4, 25°C in the presence of 15 mM NaCl (circles) or 5 mM CaCl2 (filled squares). The error bars indicate the standard deviation of at least three measurements.

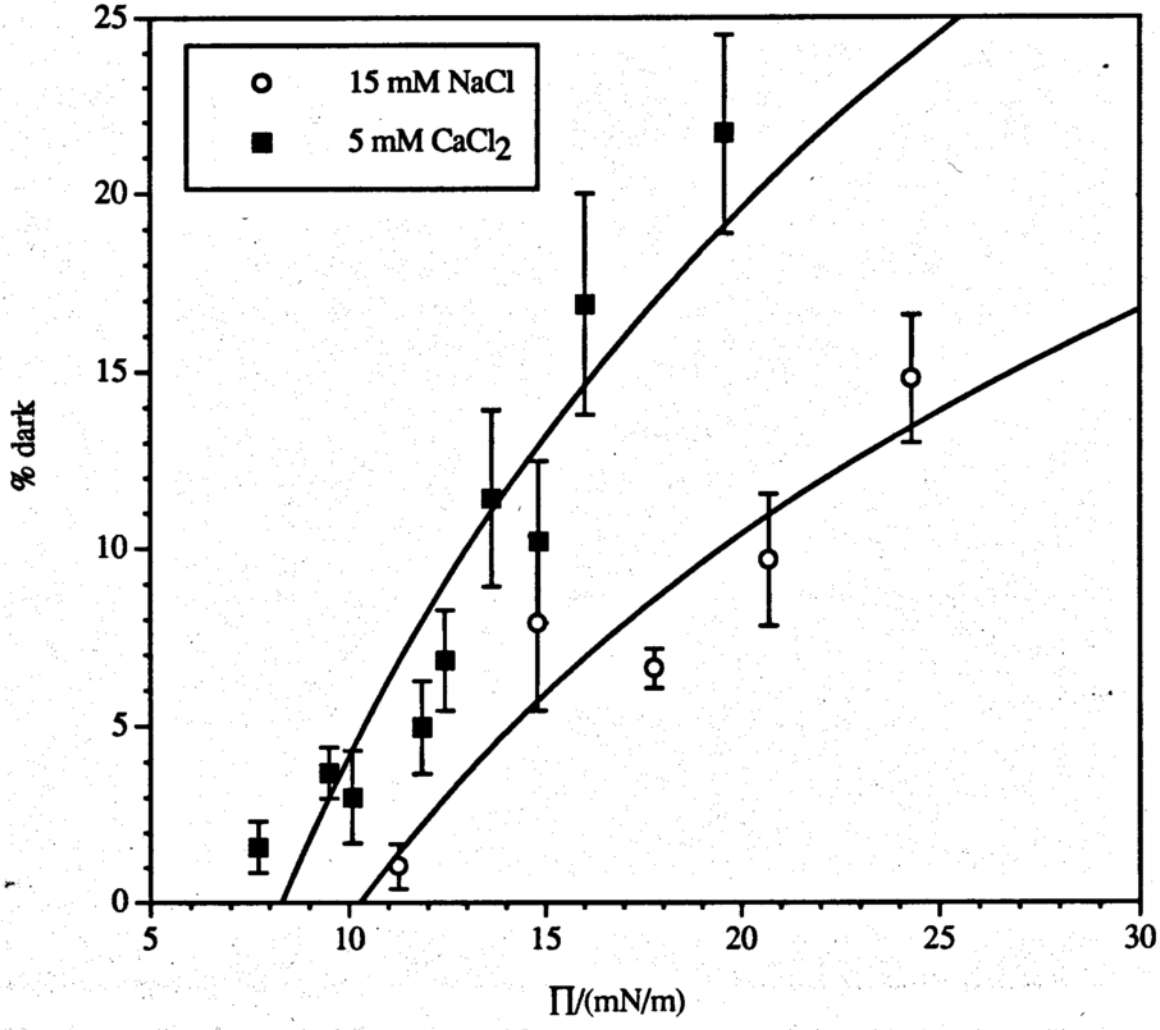

Figure 34. The percentage of dark domains as a function of surface pressure for DPPC/DOPG (1:1) monolayers spread on 10 mM Tris-HCl, pH 7.4, 25°C in the presence of 15 mM NaCl (circles) or 5 mM CaCl2 (filled squares). The error bars indicate the standard deviation of at least three measurements.

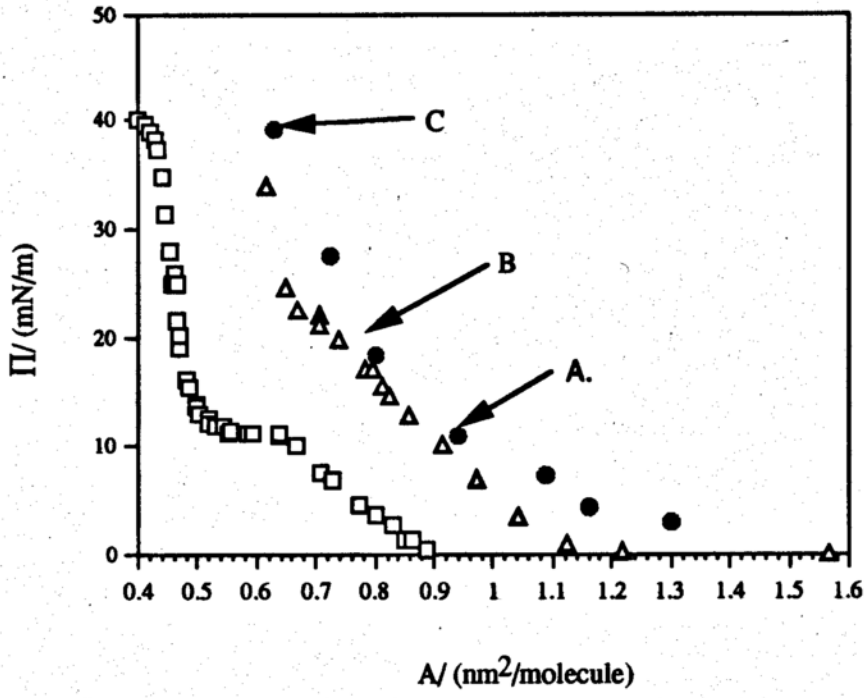

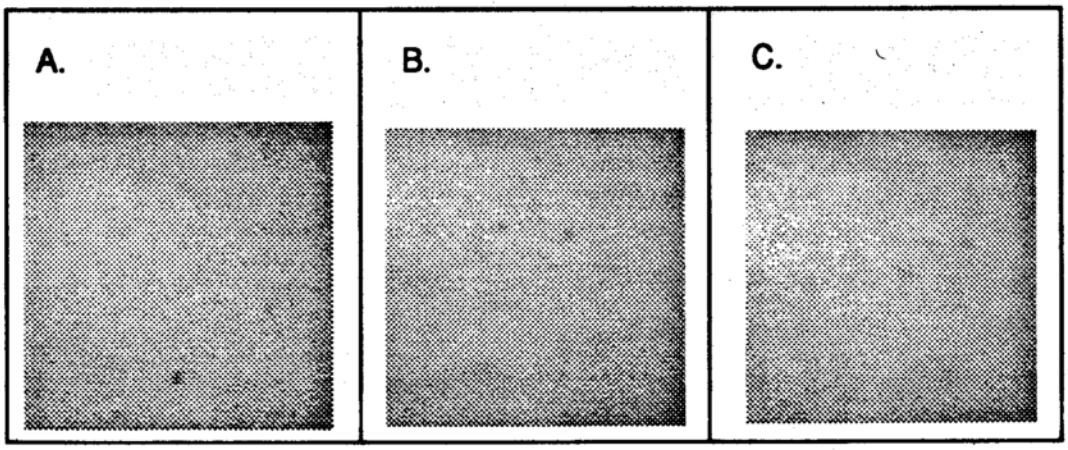

Figure 35. The π-A isotherm (top) and fluorescence images for DPPC/POPG (3:7) spread on 10 mM Tris-HCl, pH 7.4, 25°C and 15 mM NaCl. The images are obtained at (A.) 11.9 mN/m, (B.) 20.7 mN/m, (C.) 39.1 mN/m.

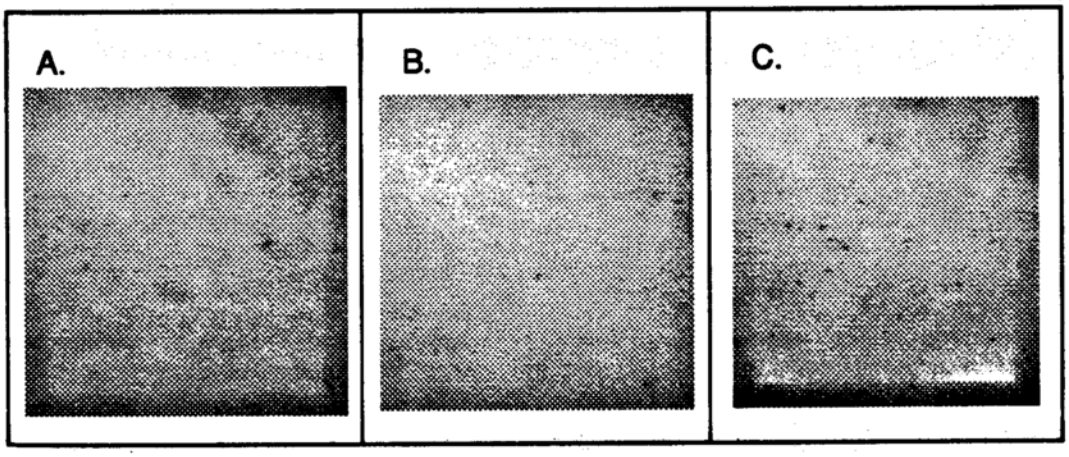

Figure 36. The fluorescence images for DPPC/DOPG (3:7) spread on 10 mM Tris-HCl, pH 7.4, 25°C and 15 mM NaCl. The images are obtained at (A.) 20.1 mN/m, (B.) 23.1 mN/m, (C.) 32.8 mN/m.

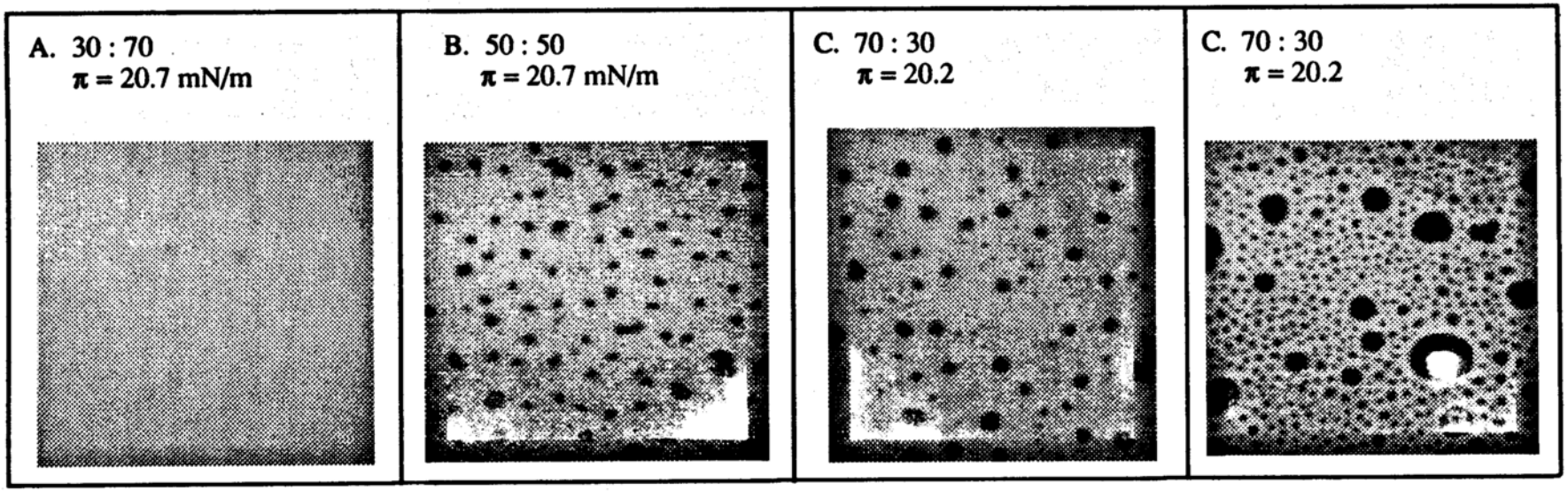

Figure 37. The fluorescence images for DPPC/POPG spread on 10 mM Tris-HCl, pH 7.4, 25°C and 15 mM NaCl at a surface pressure of 20 ± 1 mN/m. The images are for various molar ratios of lipids (A.) 3:7, (B.) 1:1, (C.) 6:4, and (D.) 7:3.

Discussion

The experiments outlined in the results chapter were designed to gain a better molecular understanding of the mixing of zwitterionic and anionic mixtures in the absence and presence of Ca^{2+} ions, in particular to establish to what extent such lipids form homogeneous mixtures and what factors govern their mixing tendencies. In order to do this, the surface phase behavior of mixtures of DPPC with various PG lipids, that have increasing amounts of unsaturation in their hydrocarbon chains, were studied. The phase behavior of these systems was then compared with their corresponding PC counterparts to isolate the individual contribution of the polar headgroup and hydrocarbon chains.

Same Acyl Chains/Different Headgroups

The π-A isotherm data in Figures 25 and 26 were analyzed by evaluating the excess area per molecule of the mixture, A^E, defined as (Gaines, 1966; Adamson, 1990)

$$A^E = A_{12} - (N_1A_1 + N_2A_2) \qquad (3)$$

where A_1 and A_2 are the area per molecule of each of the single components at a constant surface pressure, N_1 and N_2 are their corresponding mole fractions and A_{12} is the mean area per molecule of the mixed monolayer at the same surface pressure. As previously discussed (see Introduction), for mixtures of molecules of similar molecular shape and volume which exhibit either ideal mixing or complete immiscibility, $A^E=0$.

Deviations from zero, may be positive or negative indicating miscibility with positive or negative deviations from ideality. As expected, for mixtures of DPPC/DPPG the A^E values in both the LE and LC phases are close to zero in the absence of Ca^{2+}, with only small positive deviations in the presence of 5mM $CaCl_2$ (Figure 38). The presence of homogeneous images in Figures 25A, 25D, 26A and 26D in combination with the A^E data suggests nearly ideal mixing of these lipids in both the LE and LC phases. However, as stated above, an A^E value of zero could represent complete phase separation which may not be distinguishable from the homogeneously dark phase that is observed in the LC phase of the mixed monolayer. Confirmation of the state of these lipids in the LC phase can be made by the application of the Gibbs phase rule, as modified for application to insoluble monolayers by Crisp (Crisp, 1949);

$$F = C - P^B - P^S + 1 \qquad (4)$$

where F is the number of degrees of freedom in the system, C is the number of bulk and surface components and, P^B and P^S are the number of bulk and surface phases, respectively, at constant external pressure and temperature. Applying equation (4) in a region of coexistence in a binary mixed monolayer and assuming miscible components in both surface phases (i.e. C = 3 (water, DPPC,DPPG) P^B = 1 (water), P^S = 2 (mixed LE and mixed LC phases)), F=1. Thus, if components 1 and 2 are miscible, the surface pressure in the coexistence region, $\prod_t$, should vary continuously with changing area per molecule reflecting the changing composition of each phase, and it should also vary with the composition of the monolayer. If $\prod_t$ is invariant with composition, F=0 and in one of the surface phases the components must be immiscible and, therefore, another surface phase must be present (Motomura, Sekita et al., 1974). Application of the surface phase rule to the LE to LC phase transition of the DPPC/DPPG mixture in which the phase

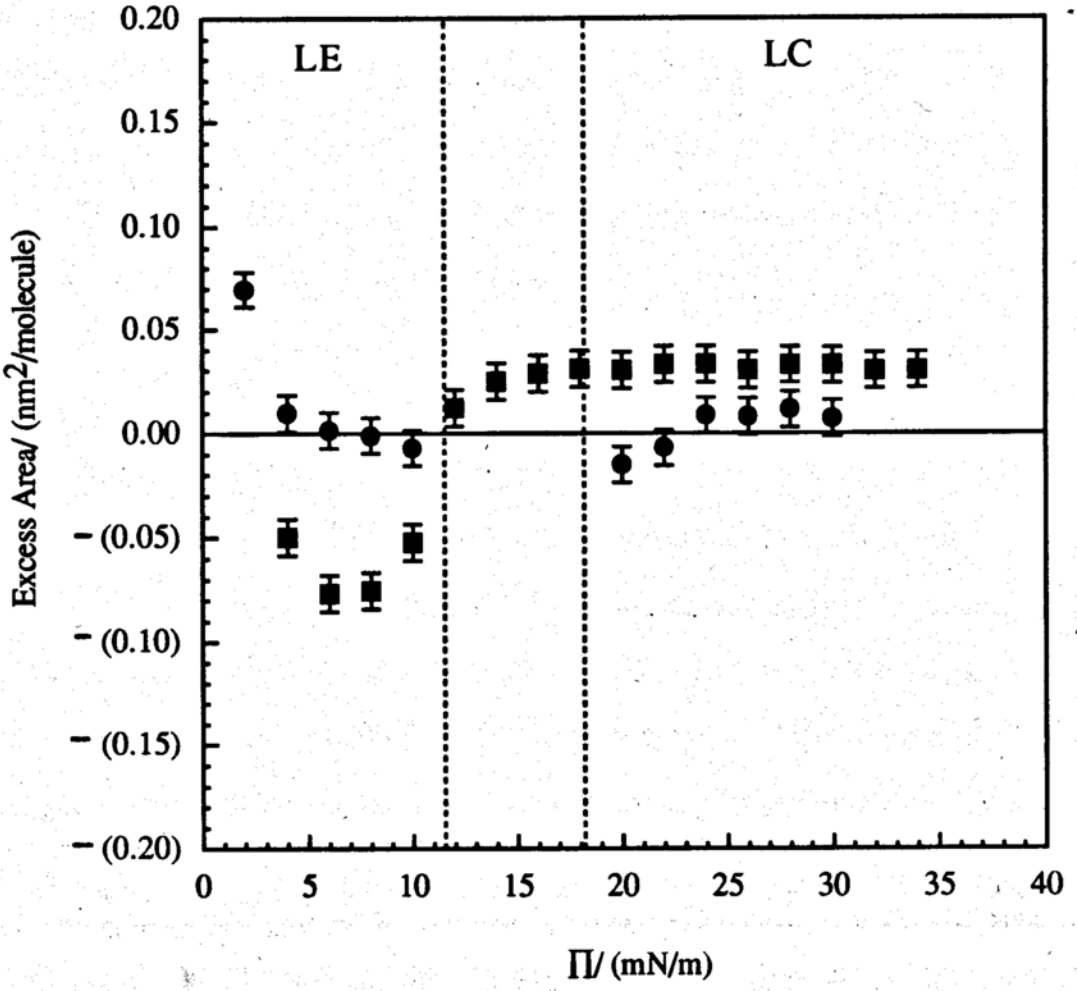

Figure 38. The excess area for DPPC/DPPG (1:1) mixtures spread on 10mM Tris-HCl, pH 7.4, 25°C with 15 mM NaCl (filled circles) or 5 mM $CaCl_2$ (filled squares). The dashed lines at 11.5mN/m and 18.2 mN/m are the phase transition pressures for DPPC and DPPG, respectively, on buffer containing 15 mM NaCl.

transition pressure changes with the LE/LC phase composition (F=1) and in which the composition of the LE and LC phases are changing as a function of area in a given mixture indicates that DPPC and DPPG are miscible in both the LE and LC phases. Thus, we can conclude that when the acyl chains of PC and PG lipids are identical as in the DPPC/DPPG system, in the absence of Ca^{2+} at a 1:1 mole ratio, ideal mixing in both the LE and LC phases occurs. The addition of Ca^{2+} introduces slightly nonideal mixing with positive deviations which are more significant in the LC phase however, it would appear that under these conditions DPPC and DPPG also remain miscible in the LC phase. These monolayer studies are in agreement with measurements made with mixed bilayers under similar conditions (Findlay and Barton, 1978).

Different Acyl Chains/Same Headgroups

A comparison of π_e and π_c for DPPC/POPC and DPPC/DOPC in Table II, provides strong support for the hypothesis that these compressed mixed monolayers reach their stability limit in a state of equilibrium with a separated bulk phase. The fact that the π_c (and π_e) for DPPC/POPC mixtures is the same as that for POPC alone strongly suggests that POPC leaves the monolayer phase, is "squeezed-out," to form a bulk phase at π_c, leaving behind a DPPC-enriched monolayer. The agreement of A_{min} in Table I and II for POPC and DPPC/POPC would support this conclusion. On the other hand for DPPC/DOPC we can see that π_e and π_c are higher (and the A_{min} lower) than that obtained for DOPC alone, suggesting a greater degree of compatibility between DPPC and DOPC than for DPPC and POPC. As mentioned in the introduction, earlier studies of the π-A behavior of DPPC/DOPC monolayers indicated miscibility in one study (Phillips and Chapman, 1968) as also suggested in

the present study, and the presence of phase separated domains in another study (Nag, Rich et al., 1994).

Miscibility in the monolayer may be determined from the calculation of A^E (see equation 3) from the π-A isotherms for DPPC/POPC and DPPC/DOPC mixtures. These values were found to be small with positive deviations from ideality occurring at surface pressures in excess of 10 mN/m (Figure 39). To further examine the miscibility of the surface phase, the phase equilibria at π_e can be determined by application of the phase rule (equation 4) to the measured equilibrium spreading pressure values. It has been reported in the literature that mixtures of DPPC with both POPC and DOPC that consist of 70 mol% or less of DPPC, at 25°C, exhibit bulk phase immiscibility in the gel state (Curatolo, Sears et al., 1985). Such immiscibility in the bulk phase is also implied by the π_c results above which suggests that "squeeze-out" of the less stable component occurs. The values for π_e for pure POPC and DOPC are close to those measured for their respective mixtures up to molar ratios of 7:3 of DPPC: unsaturated PC (Table I and II), indicating that there are no degrees of freedom in these systems or F=0. According to the phase rule, in order to obtain invariance, miscible components must exist in the surface film at the point of monolayer collapse (crisp) i.e. C = 3 (water, DPPC, PC), P^B = 3 (water, DPPC, PC) and P^S = 1 (mixed DPPC/PC) For both mixtures, miscibility is directly observed under the conditions of these experiments over the entire range of surface pressures below collapse thus, the experimental data are in complete agreement with the prediction of the surface phase rule.

It is interesting to note that while equimolar mixtures of DPPC/POPC and DPPC/DOPC mixtures are miscible in surface phases, bilayers of the same PC/PC mixtures are phase separated in the gel state as measured by thermal analysis (Curatolo, Sears et al., 1985). However, since the maximum surface pressure attained

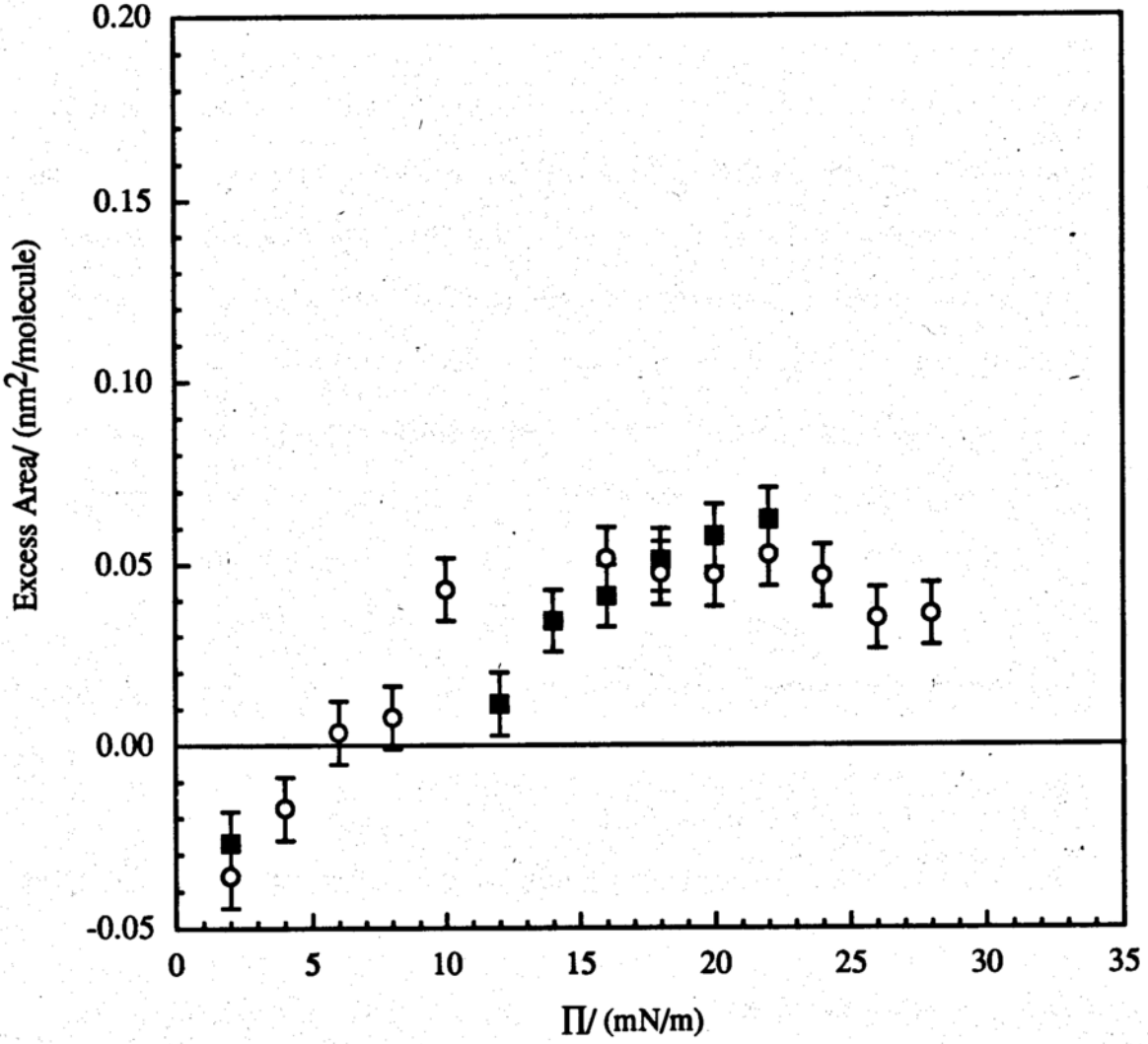

Figure 39. The excess area for DPPC/POPC (circles) and DPPC/DOPC (filled squares) (1:1) mixtures spread on 10mM Tris-HCl, pH 7.4, 25°C with 15 mM NaCl.

in this study was only on the order of 30 mN/m for both the DPPC/POPC and DPPC/DOPC mixtures, perhaps the degree of packing attainable (mean area per molecule) with the monolayer system is not representative of the bilayer system and the surface pressures attainable in these monolayers are less than the surface pressures found in a separated bilayer bulk phase. Previous results reported (Nag, Rich et al., 1994) domain formation in the DPPC/POPC mixture obtained with continuously compressed monolayers. With regard to this difference, in our experiments, upon initial compression to a particular area per molecule, below 30 mN/m, dark domains were obtained however, they disappeared as the surface pressure relaxed to its equilibrium value. The appearance of domains in continuously compressed monolayers, as reported by Nag and Keough (Nag, Rich et al., 1994), therefore, may be consistent with transient locally overcompressed monolayers of these phospholipids which may mimic the bulk phase separation observed in the bilayer systems.

Different Acyl Chains/Different Headgroups

The A^E (equation 3) values were calculated from the π-A isotherms for equimolar mixtures and it was found that the mixture of DPPC/POPG in both the absence and presence of 5 mM $CaCl_2$ (Figure 40), exhibit large positive deviations at surface pressures where DPPC would be expected to be in its LE phase indicating the tendency of this mixture to phase separate even at low surface pressures. Interestingly at higher pressures, above 10 mN/m, the excess area values decrease to zero just before monolayer collapse, the value of A^E expected if there was complete surface phase immiscibility. In the case of DPPC/DOPG mixtures the A^E values (Figure 41) were also large and positive, again suggesting the tendencies for surface phase

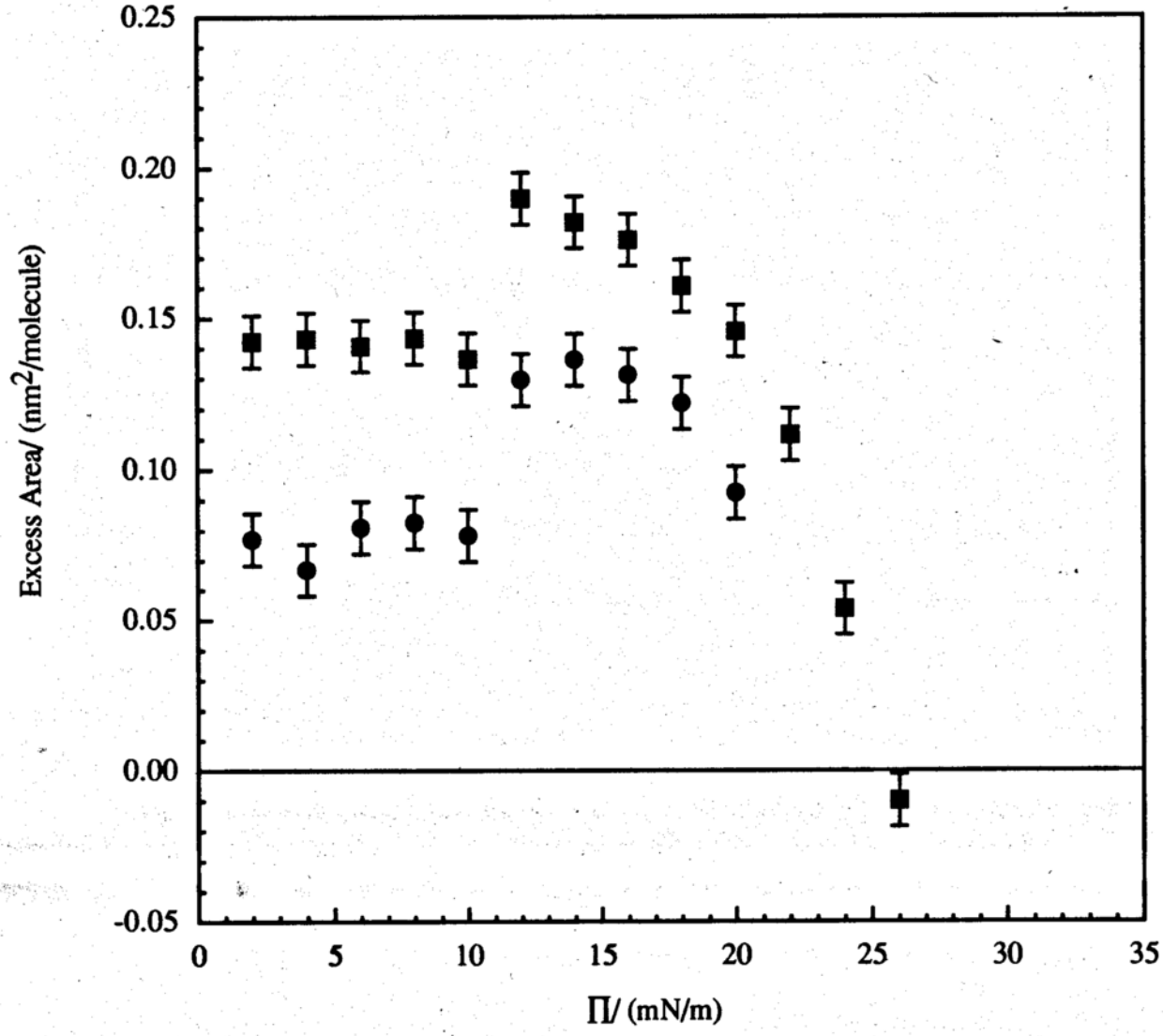

Figure 40. The excess area for DPPC/POPG (1:1) mixtures spread on 10 mMTris-HCl, pH 7.4, 25°C with 15 mM NaCl (filled circles) or 5 mM $CaCl_2$ (filled squares).

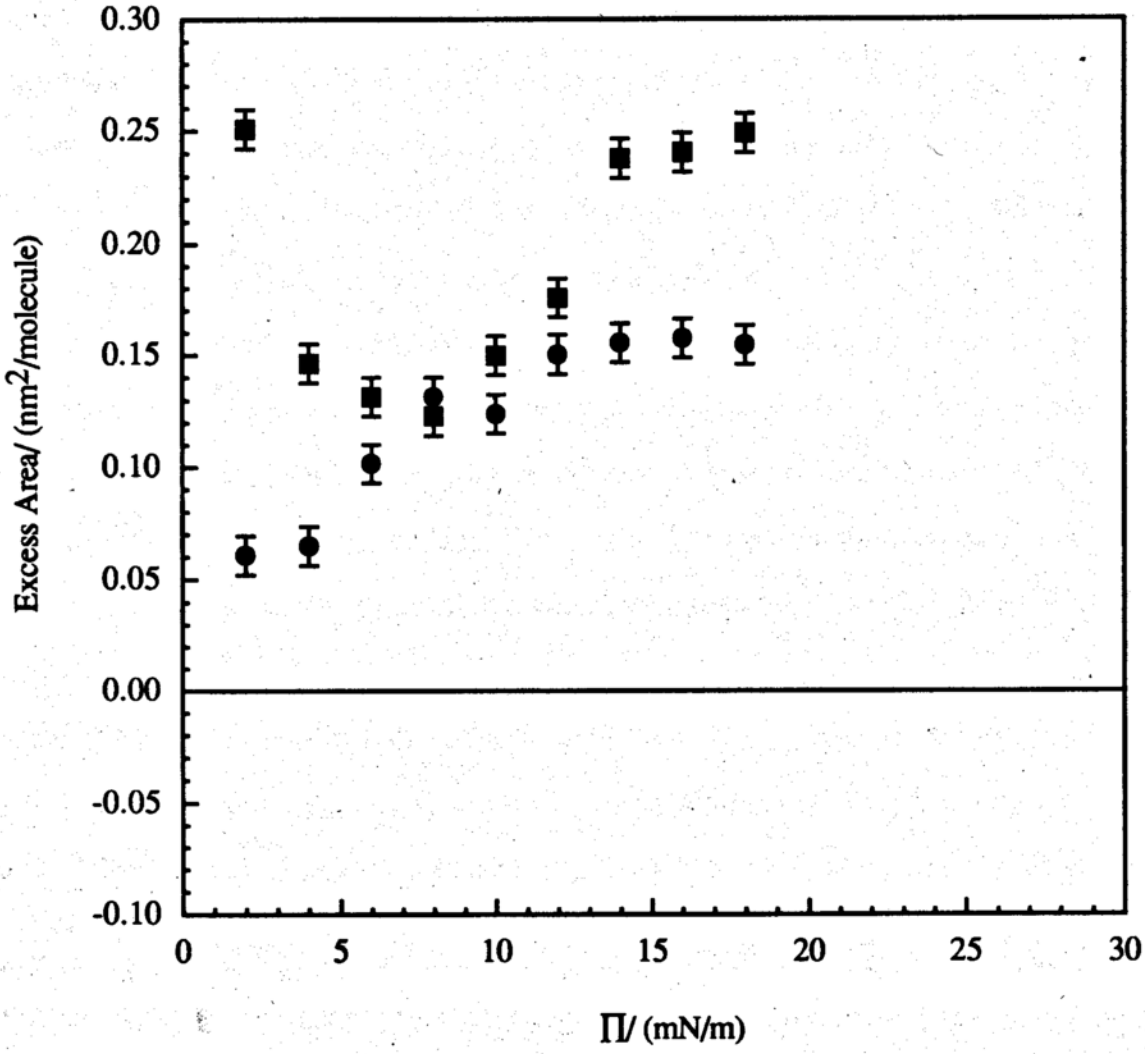

Figure 41. The excess area for DPPC/DOPG (1:1) mixtures spread on 10 mMTris-HCl, pH 7.4, 25°C with 15 mM NaCl (filled circles) or 5 mM $CaCl_2$ (filled squares).

separation, however in contrast to the DPPC/POPG mixture the values of A^E did not decrease toward zero at higher surface pressures suggesting a greater degree of compatibility between DPPC and DOPG than for DPPC and POPG. The similar observation made above for the DPPC/PC mixtures suggests that a greater compatibility exists between phospholipids that are symmetric, i.e. phospholipids whose acyl chains are identical in molecular structure.

Miscibility in this system can also be investigated by applying the phase rule (equation 4) to the π_c and π_e data in Table II for various mixtures of DPPC/POPG and DPPC/DOPG. The reported values were obtained in the absence of calcium, however, they are in agreement within experimental error with values obtained in the presence of 5 mM $CaCl_2$. As in the DPPC/PC systems, good agreement was found between the π_c and π_e, indicating equilibrium in the monolayer. However, compared to the PC/PC mixtures, the PC/PG mixtures collapse at significantly reduced maximum pressures relative to the corresponding pure lipids alone, indicative of the instability of PC/PG mixtures. To analyze these observations, the surface phase rule was applied to π_e values measured for several DPPC/POPG compositions. The equilibrium spreading pressure was found to be invariant (F=0) with composition in mixtures that contain 30 mol% DPPC or less (Figure 42). Experiments in bulk systems (using thermal analysis (unpublished results from this lab) and NMR (Wiedmann, Salmon et al., 1993)) performed at this composition indicate that such system exhibit immiscibility. Using this information (i.e. F = 0, P^B = 3 (water, DPPC, POPG) and C = 3 (water, DPPC, POPG)) the phase rule predicts a single surface phase (i.e. P^S = 1) exists and therefore DPPC and POPG, at this composition, must be miscible at π_e. Using fluorescence microscopy, the presence of a miscible surface phase in mixtures composed of 30 mol% or less of DPPC was observed to surface pressures as high as 39 mN/m, in complete agreement with the prediction of the phase rule. At compositions higher

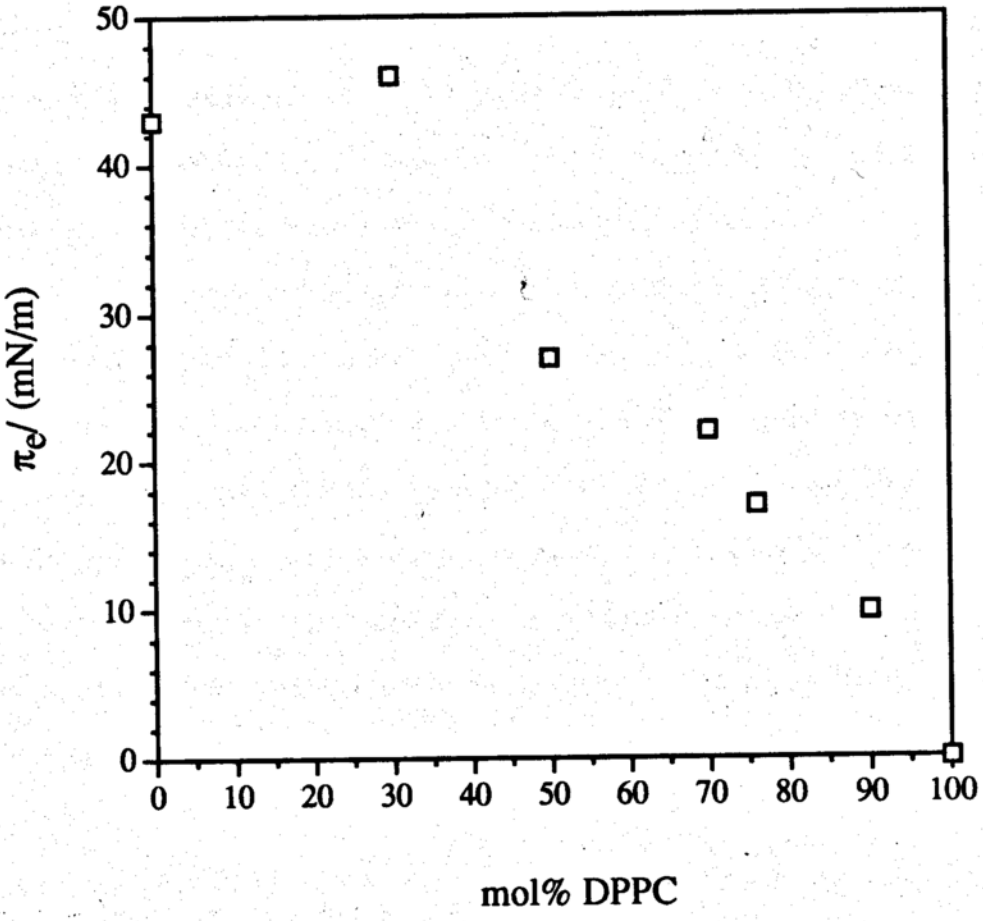

Figure 42. The equilibrium surface pressure for DPPC/POPG mixtures spread on 10 mM Tris-HCl, pH 7.4, 25°C.

than 50 mol% DPPC, πe is a function of composition so that at each surface composition there is a characteristic value for π_e (F=1). Thermal analysis of dispersions of DPPC and POPG performed in this lab (unpublished results) and which have been reported in the literature (Wiedmann, Salmon et al., 1993) have shown that at high concentrations of DPPC (> 50 mol%), these lipids appear to be miscible in the bulk phase. These data (i.e. F = 1, $P^B = 2$ (water. mixed DPPC/POPG bulk phase) and C = 3 (water, DPPC, POPG)) combined with the surface phase rule predict that in such mixtures of DPPC and POPG, the surface phase should be miscible at π_e. However, in mixtures containing higher amounts of DPPC, experiments revealed the presence of two surface phases up to surface pressures of 18 mN/m and that phase separation increased with increasing surface pressure, although the phase rule would predict that a miscible surface phase is present. There are a few possible explanations for this discrepancy. First, the two-dimensional phase rule may not be able to predict phase equilibria in such complicated systems i.e. systems which contain multiple bulk and surface phases. This is not likely since it has been applied to complicated systems in the literature that contain both bulk and surface phases (Crisp, 1949) and because it appears to be applicable to the DPPC/PC systems and to the DPPC/POPG system at low concentrations of POPG. Most likely, in mixtures that contain large amounts of DPPC, the presence of phase separation creates an unstable film and the DPPC-rich condensed domains serve as nucleation sites for early monolayer collapse, i.e. before the collapse of either component as a pure monolayer (see Table I). The bulk phase being formed is likely a DPPC-rich phase which leaves behind a mixed monolayer that is POPG-rich, and therefore miscible as the phase rule would predict at π_e.

Since phase separation may play an important role in biological events, it was of interest to further analyze the immiscibility of DPPC and unsaturated PGs as a

function of π using the fluorescence microscope. In these mixtures, most likely, the dark domains that occur at various surface pressures consist of an LC surface phase rich in DPPC (schematically shown in Figure 43). In a sense, therefore, we might think of phase separation as one in which the solubility of DPPC in the unsaturated PG is exceeded. From Figure 37, it appears as though the solubility is exceeded somewhere between a molar ratio of 3:7 and 1:1.

The effect of pressure on miscibility or the solubility of a condensed phase in a fluid phase has not been described in the monolayer literature and has only been studied to a limited extent in bulk systems due to the difficulty in performing such experiments. Bulk 3D solubility theory (Hendrickson, Fan et al., 1983) gives the relationship between the equilibrium solubility, x, and pressure, P,

$$\frac{d\ln x}{dP} = \frac{\overline{V^s} - \overline{V}}{RT\left(\frac{\partial \ln a}{\partial \ln x}\right)_P} \qquad (3)$$

where "a" is activity, $\overline{V^S}$ is the molar volume of the solid and $\overline{V}$ is the molar volume of the solution. If Raoult's law holds and since (for most substances) $\overline{V^S} < \overline{V}$, $\frac{d\ln x}{dP}$ is negative and thus, solubility decreases as pressure increases.

The corresponding two-dimensional analog may be written as:

$$\frac{d\ln x}{d\Pi} = \frac{\overline{A^s} - \overline{A}}{RT\left(\frac{\partial \ln a}{\partial \ln x}\right)_\Pi}$$

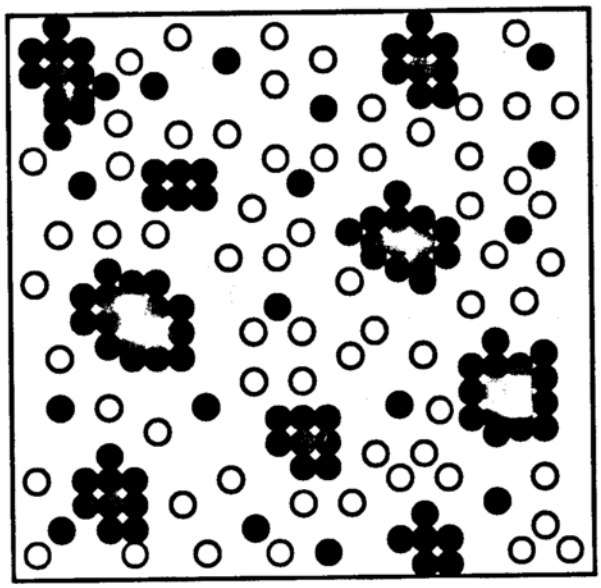

Figure 43. Schematic illustration of phase separation in DPPC/POPG mixtures as viewed from the top of the trough. The filled circles represent DPPC and the empty circles are POPG.

where $\overline{A^s}$ is the area per mole of the lipid at closest packing and $\overline{A}$ is the mean area per mole of lipid at a given surface pressure. A value for x can be calculated by assuming that the dark domains are exclusively DPPC, the more condensed lipid, and introducing a factor to take into account the difference in the densities between the more solid-like DPPC domains and the liquid-like solution of DPPC in POPG or DOPG. This factor can be obtained from the π-A isotherms at the various surface pressures of interest.

$$\begin{pmatrix}\%\text{dark} \\ \text{domains}\end{pmatrix} \times (N_1) \times \left(\frac{\Gamma^{\pi}_{DPPC}}{\Gamma^{\pi}_{mixture}}\right) = \text{moles of DPPC insoluble}$$

where N_1 is the moles of DPPC in the monolayer and thus the equilibrium solubility of DPPC can be calculated,

$$x_1 = \frac{\text{molesDPPC}_{soluble}}{\text{molesDPPC}_{soluble} + N_2}$$

where N_2 is the moles of component 2 in the monolayer. Based on this analysis, the solubility of DPPC in either POPG or DOPG was found to decrease with increasing surface pressure (Figures 44 and 45) as would be expected. Further, the solubility of DPPC in POPG is less than that in DOPG. It appears, therefore, that the disaturated chains of DPPC are able to interact and mix to a greater extent with lipids that contain chains which are the same as was also suggested by the A^E data and observations with the DPPC/DOPC mixture. The slope of the lines for both mixtures are similar with solubility decreasing to a greater extent with pressure in the presence of calcium ions especially in the DPPC/POPG mixture. The decrease in solubility upon addition of calcium is thought to take place due to the selective interaction of calcium ions with

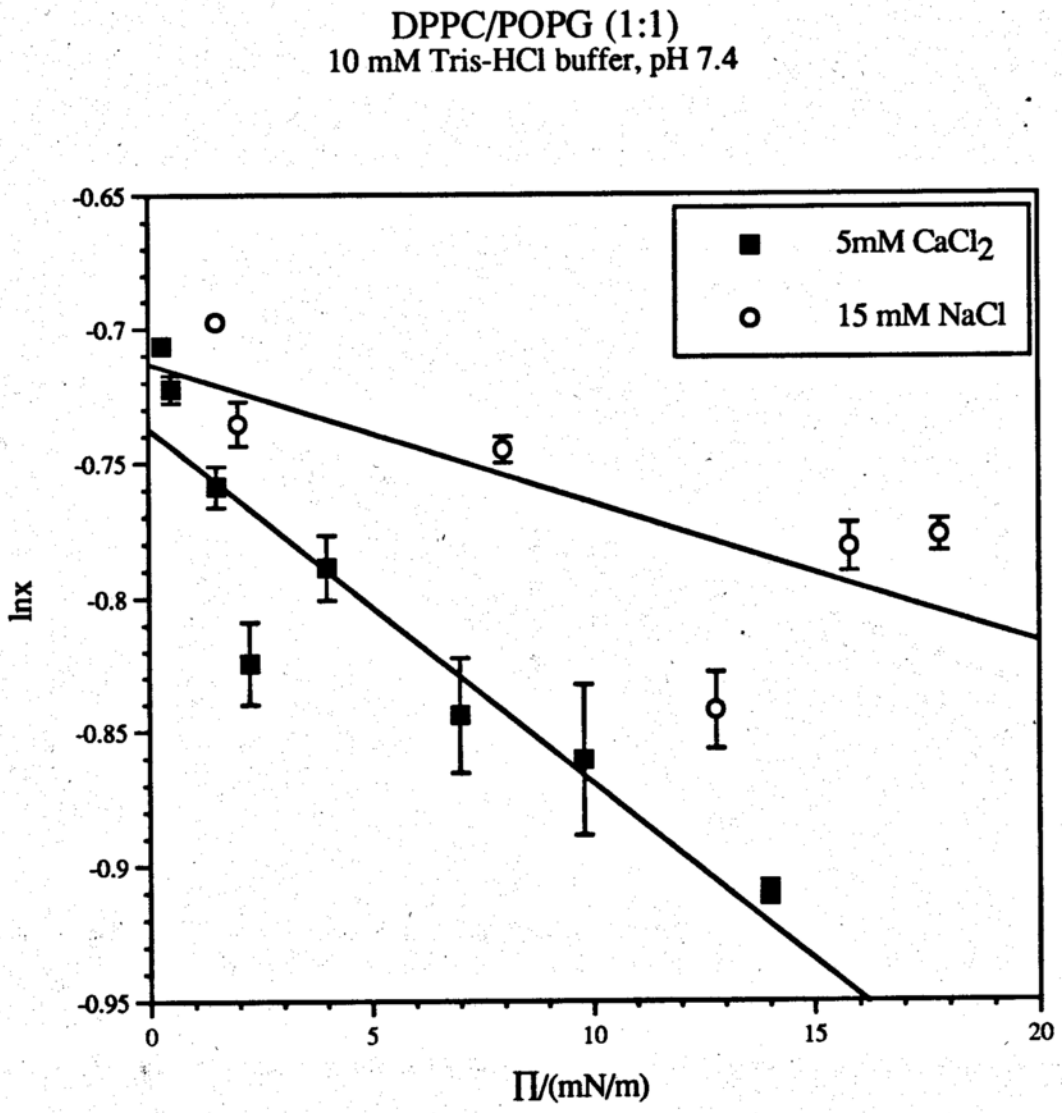

figure 44. Solubility plot for DPPC/POPG (1:1) monolayers spread on 10 mM Tris-HCl, pH 7.4, 25°C with 15 mM NaCl (circles) or 5 mM $CaCl_2$ (filled squares).

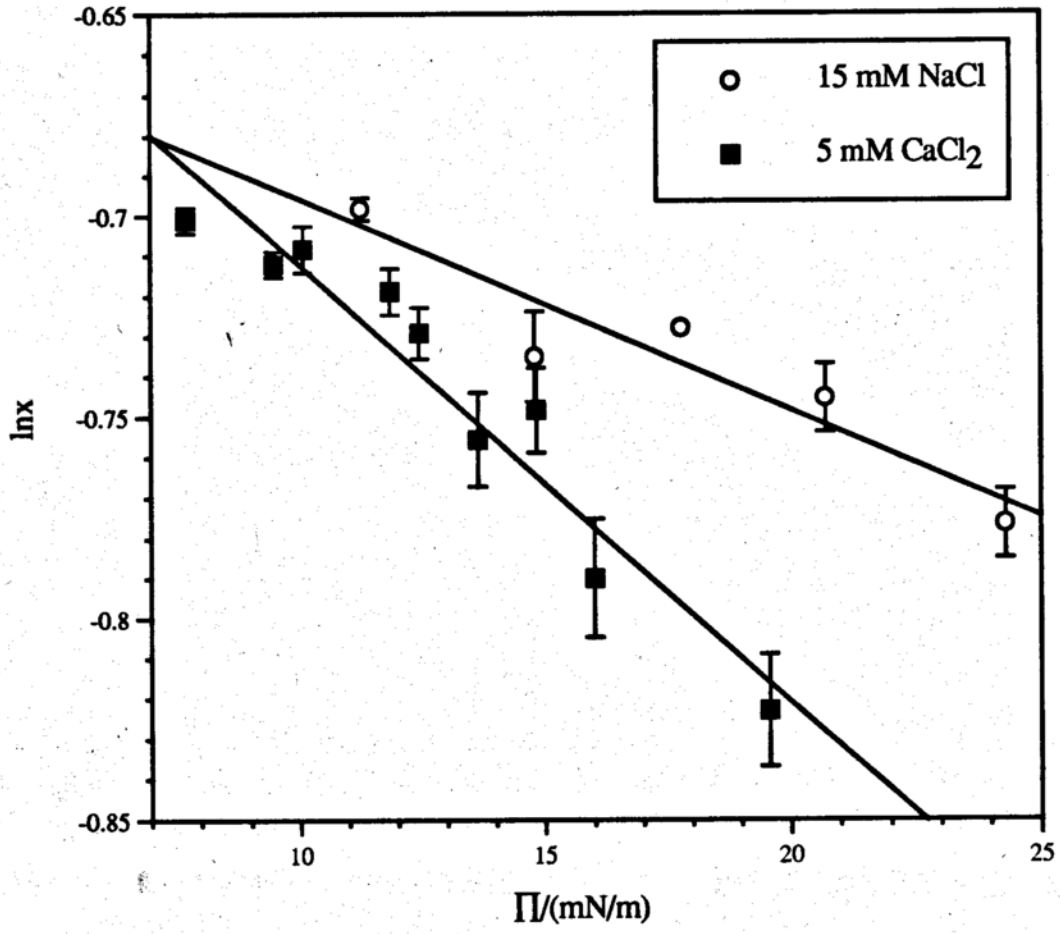

Figure 45. Solubility plot for DPPC/DOPG (1:1) monolayers spread on 10 mM Tris-HCl, pH 7.4, 25°C with 15 mM NaCl (circles) or 5 mM $CaCl_2$ (filled squares).

the negatively charged PG lipids causing condensation of these lipids, forcing more of the DPPC to precipitate out of the surface solution.

Chapter IV

Interaction of Lung Annexin I with Phospholipid Monolayers

Results

Surface pressure change in phospholipid monolayers caused by lung annexin I

Effects of lung annexin I concentration

Various amounts of LAI were injected into 10 mM Tris-HCl, pH 7.4, 5μM $CaCl_2$ at 25°C in the presence of a DPPG monolayer at $\pi = 5.0 \pm 0.5$ mN/m with stirring and the resulting change in surface pressure, $\Delta\pi$, was measured (Figure 46). As seen in Figure 46, the data points follow a sigmoidal curve which appears to begin to level off at approximately 5nM. Higher concentrations of LAI were not investigated because of the limited supply of purified protein. Interestingly, no change in surface pressure was measured in the absence of a monolayer even at a concentration of 4 nM of LAI. This indicates that the presence of the monolayer significantly enhances the surface activity of LAI.

Effects of calcium ion concentration

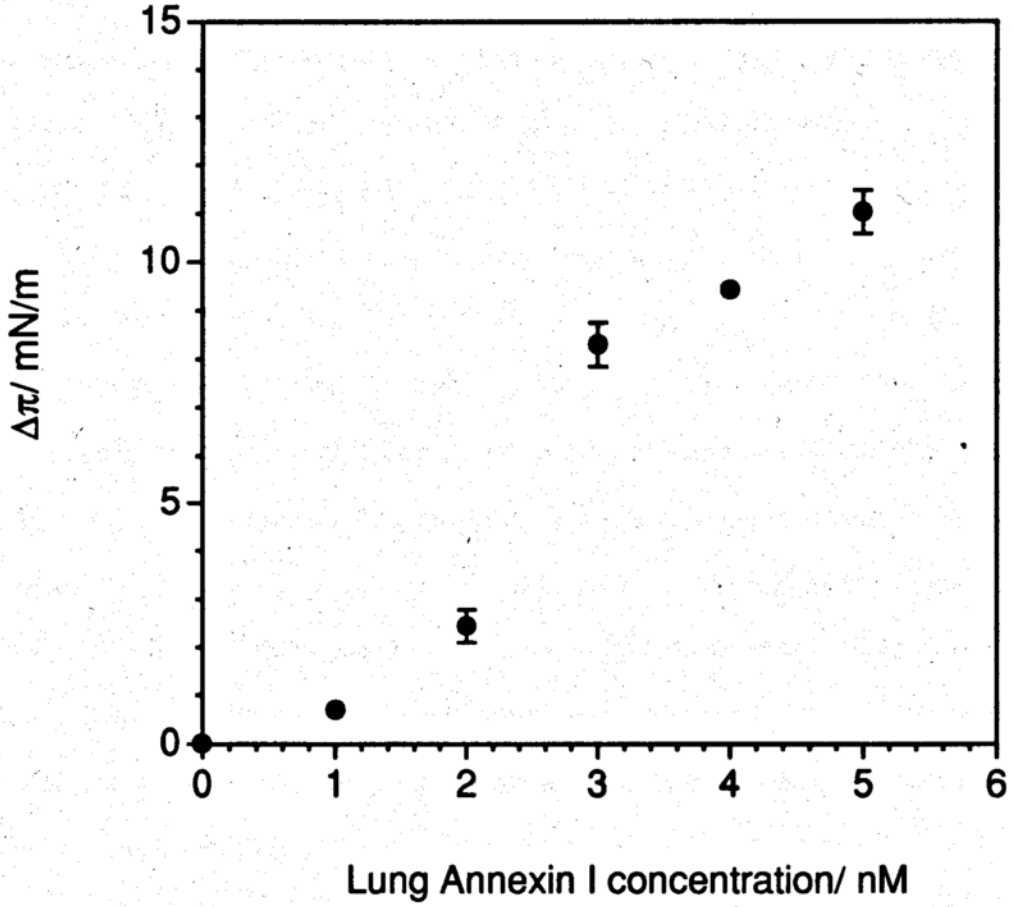

Figure 46. Change in π after injection of various amounts of lung annexin I below a DPPG monolayer spread on 10 mM Tris-HCl, pH 7.4, 25°C and 5 μ M $CaCl_2$, $\pi_i = 5.0 \pm 0.5$ mN/m.

Previous experiments performed in this laboratory using C^{14} radiolabelled protein had shown that the intrinsic surface activity of LAI at the air/water interface is significantly enhanced by the presence of calcium ions in the subphase(Tsao, Gau et al., 1993). Figures 47 and 48 show the change in surface pressure measured after injection of LAI (5μg) into a 10 mM Tris-HCl, pH 7.4, 25°C subphase below either a DPPG or POPG monolayer which contained various concentrations of calcium ions. The error bars represent the range of data points based on at least two experiments. In the presence of sufficient EDTA to bind the majority of free Ca^{2+}, some non-calcium-dependent interaction of LAI still can be measured using $\Delta\pi$ measurements. These interactions produce $\Delta\pi$ values of approximately 2-3 mN/m for the DPPG monolayer ($\pi i \approx 10$ mN/m) and 7-8 mN/m in the case of the more expanded POPG monolayer ($\pi i \approx 5$ mN/m). Increasing the calcium concentration to 0.5 μM for both monolayers, significantly enhances LAI-phospholipid interactions, however, as the concentration of calcium is further increased, $\Delta\pi$ decreases, indicating an additional opposite role of calcium (discussed below). The rate of lung annexin I accumulation at the interface, as reflected in the rate of change of surface pressure, was also found to increase upon addition of calcium ions to the subphase. The change in surface pressure upon addition of LAI (5μg) below a DPPC monolayer spread on 10 mM Tris-HCl, pH 7.4, 25°C, and 1 mM EDTA was also measured. The change in surface pressure was 2.6 ± 0.3 mN/m, close to the value of 1.8 ± 0.4 mN/m obtained in the presence of 5 μM $CaCl_2$.

The specificity of the above observations for calcium was further tested by performing experiments on subphases that contained the divalent cations, magnesium or barium instead of calcium. As seen with the data presented in Table III, at a concentration of 5 μM, the interaction of LAI (5 μg) appears to be mediated to a greater extent by calcium, although both barium and magnesium do mediate

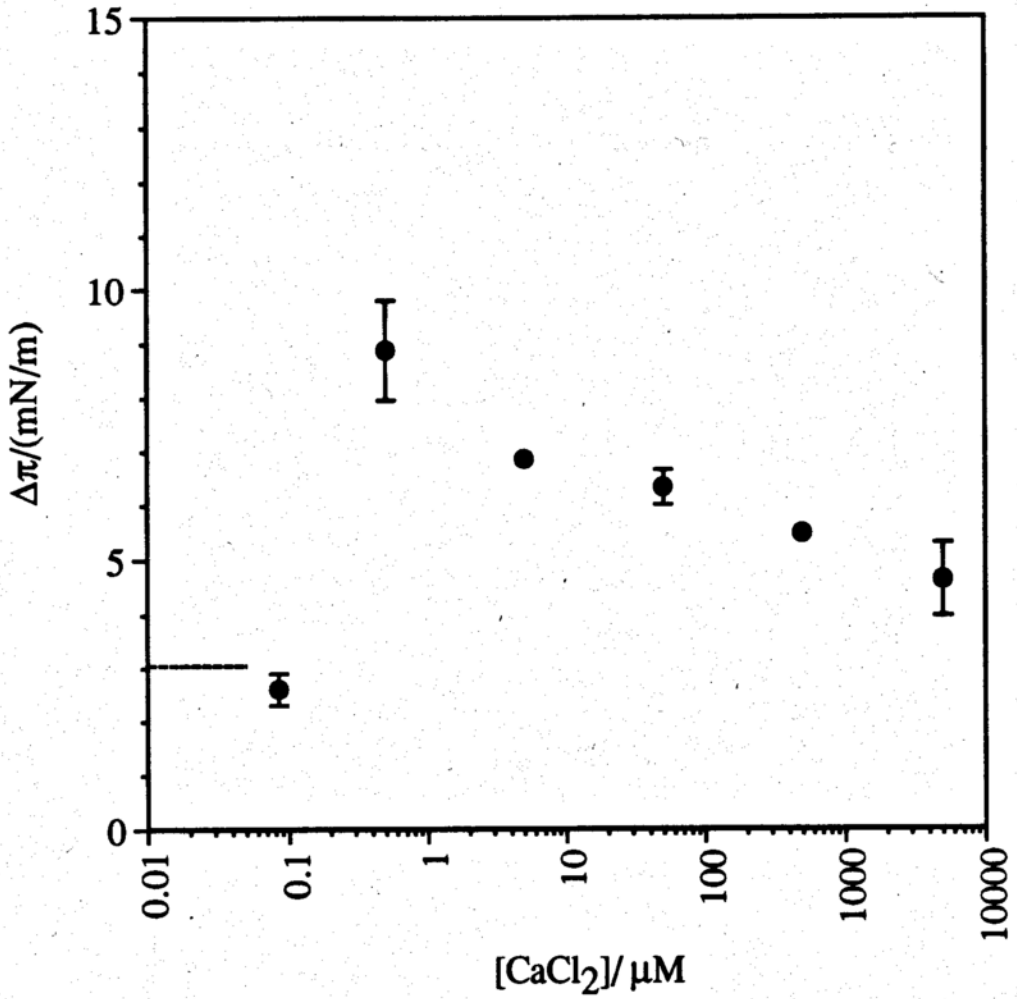

Figure 47. Change in surface pressure upon injection of 5μg of LA I below a DPPG monolayer at $\pi_i = 10.0 \pm 0.5$ mN/m spread on Tris-HCl, pH 7.4, subphase with various amounts of added $CaCl_2$. The dashed line is $\Delta\pi$ obtained in the presence of 1 mM EDTA in the subphase.

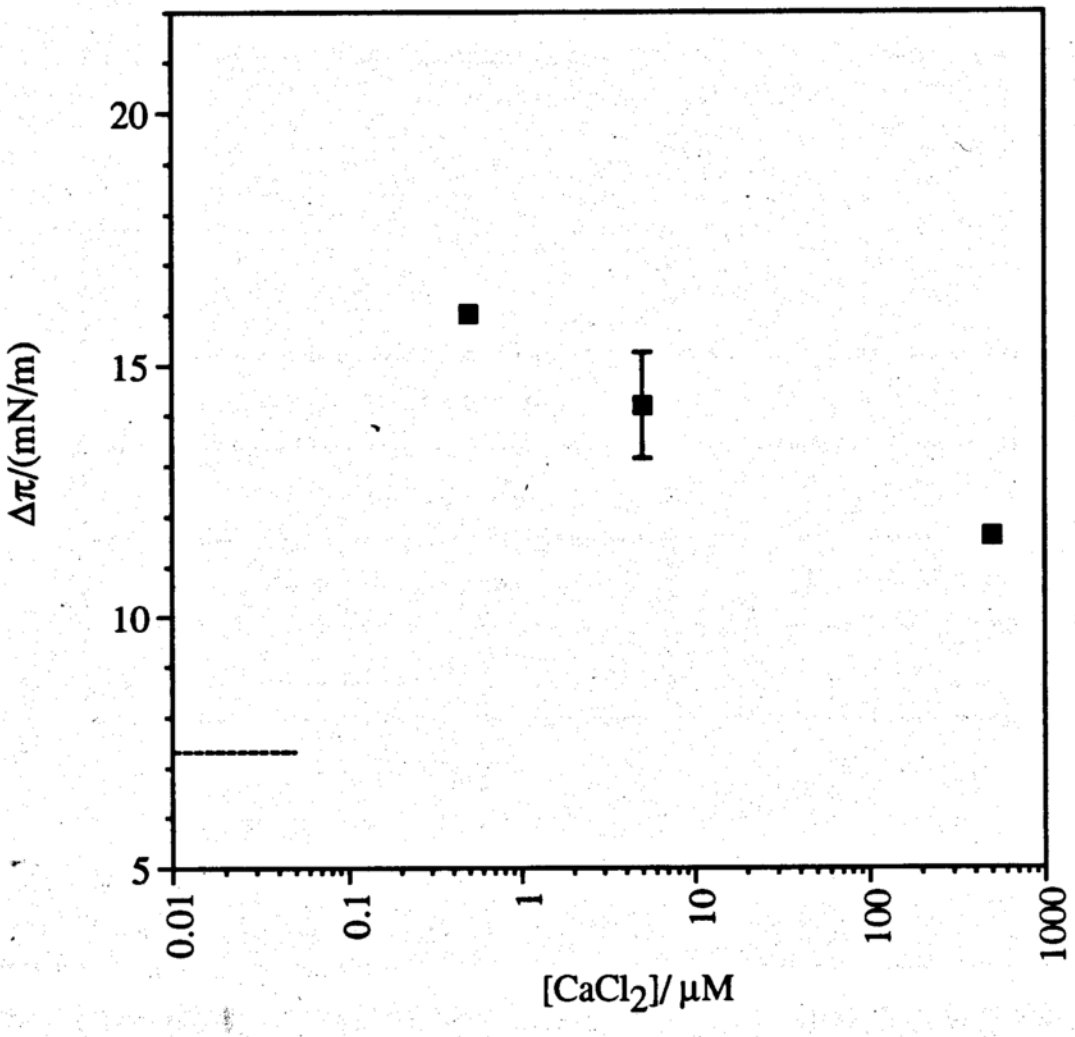

Figure 48. Change in surface pressure upon injection of 5μg of LA I below a POPG monolayer at $\pi_i = 5.0 \pm 0.5$ mN/m spread on Tris-HCl, pH 7.4, subphase with various amounts of added $CaCl_2$. The dashed line is $\Delta\pi$ obtained in the presence of 1 mM EDTA in the subphase.

Table III. Change in surface pressure upon injection of LAI (5μg) below a DPPG monolayer, $\pi_{initial} = 5.0 \pm 0.5$ mN/m spread on Tris-HCl, pH 7.4 subphase with added salts.

Subphase ion	$\Delta\pi$/(mN/m)
5μM Magnesium Chloride	5.0 ± 0.5
5μM Calcium Chloride	9.4 ± 0.0
5μM Barium Chloride	6.4 ± 0.3
1 mM EDTA	3.1 ± 0.3

interactions to a limited extent beyond what is observed in a subphase containing EDTA.

The reversibility of the calcium-dependent interaction of LAI with DPPG monolayers was examined by first spreading the DPPG monolayer on 10 mM Tris-HCl, pH 7.4, 25°C and 5μM $CaCl_2$ to a given π_i. After allowing the monolayer to equilibrate, LAI was injected below the monolayer and the system was again allowed to equilibrate. As seen above, the surface pressure increased dramatically upon addition of LAI to monolayers at a low π_i (≈ 5 mN/m) and decreased when added to monolayers equilibrated at a high π_i (≈ 30 mN/m) (Figure 49). A concentrated EDTA solution (0.5 M) was injected below the monolayer to form a subphase that contained a 1mM EDTA solution. No significant change in surface pressure was observed at either π_i indicating the irreversibility of LAI calcium-mediated interactions with DPPG monolayers under these conditions. The order of the addition of the calcium and EDTA solutions was then reversed. The experiment was conducted in a similar fashion except that the monolayer was initially equilibrated at a $\pi_i \approx 8$ mN/m on a subphase that contained 1mM EDTA. LAI was then injected below the monolayer and only a slight increase in surface pressure (2-3 mN/m) was measured as observed above for the non-calcium dependent interactions (Figure 47). Addition of $CaCl_2$ (a sufficient amount to increase the subphase $CaCl_2$ concentration to 5 μM in the absence of EDTA), did not enhance the LAI interaction as measured by $\Delta\pi$ (Figure 50).

Effects of phospholipid structure and initial surface pressure

The change in surface pressure upon addition of LAI (5 μg) as a function of the initial surface pressure was measured for a variety of lipid monolayers (Figure 51)

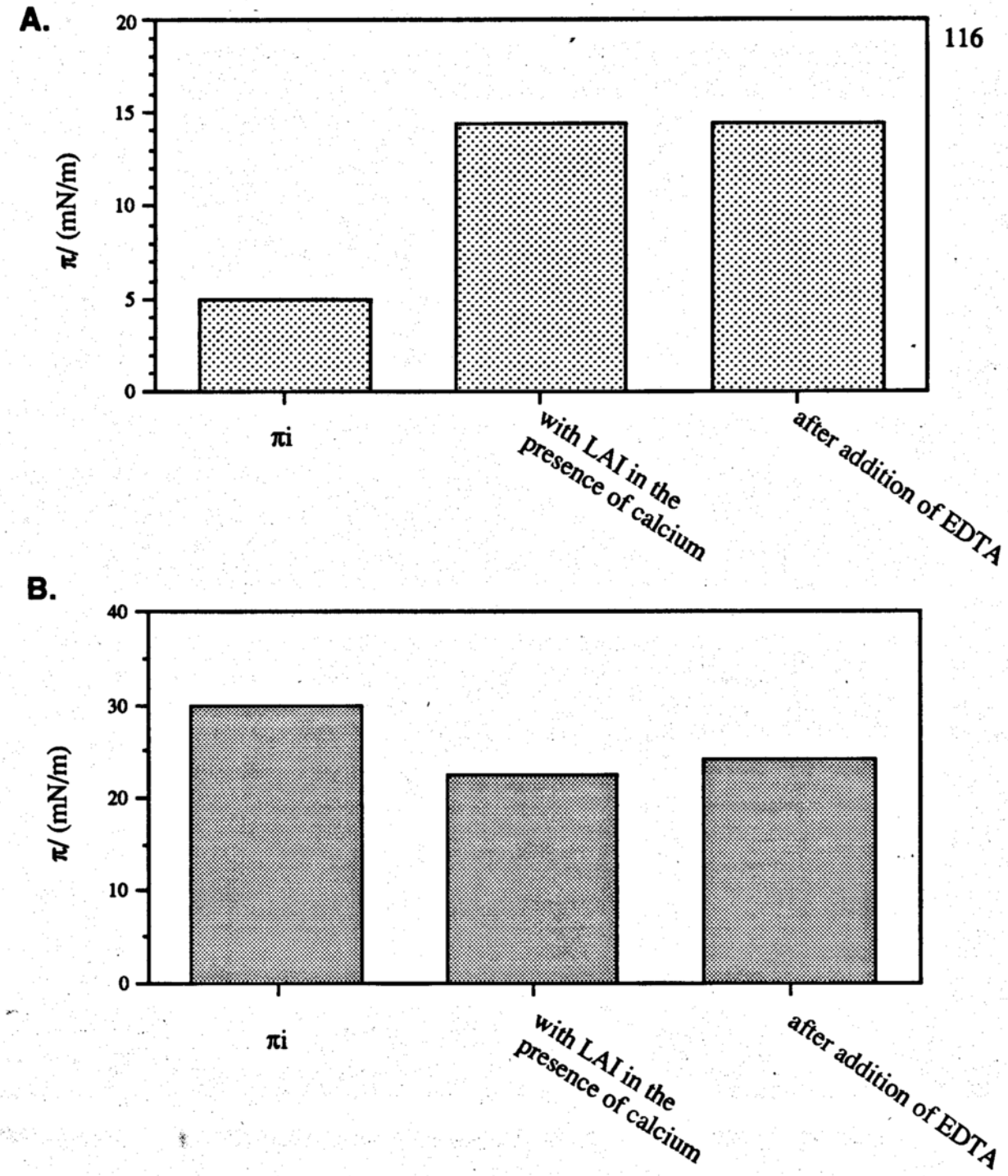

Figure 49. Surface pressure upon injection of LAI (5μg) below DPPG monolayers at π_i of (**A**) 5 mN/m or (**B**) 30 mN/m spread on 10 mM Tris-HCl, pH 7.4, 25°C and 5μM $CaCl_2$ and after subsequent addition of 1 mM EDTA.

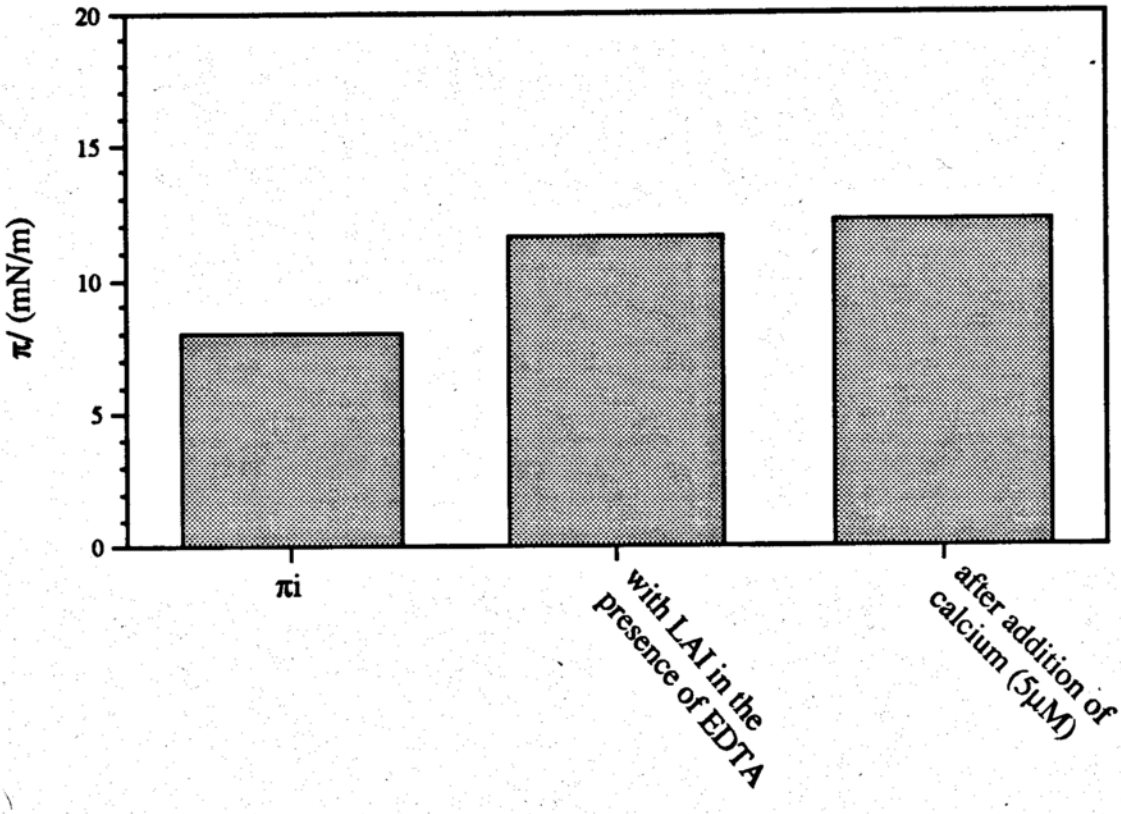

Figure 50. Surface pressure upon injection of LAI (5μg) below DPPG monolayers at π_i of 8 mN/m spread on 10 mM Tris-HCl, pH 7.4, 25°C and 1 mM EDTA and after subsequent addition of 5μM $CaCl_2$.

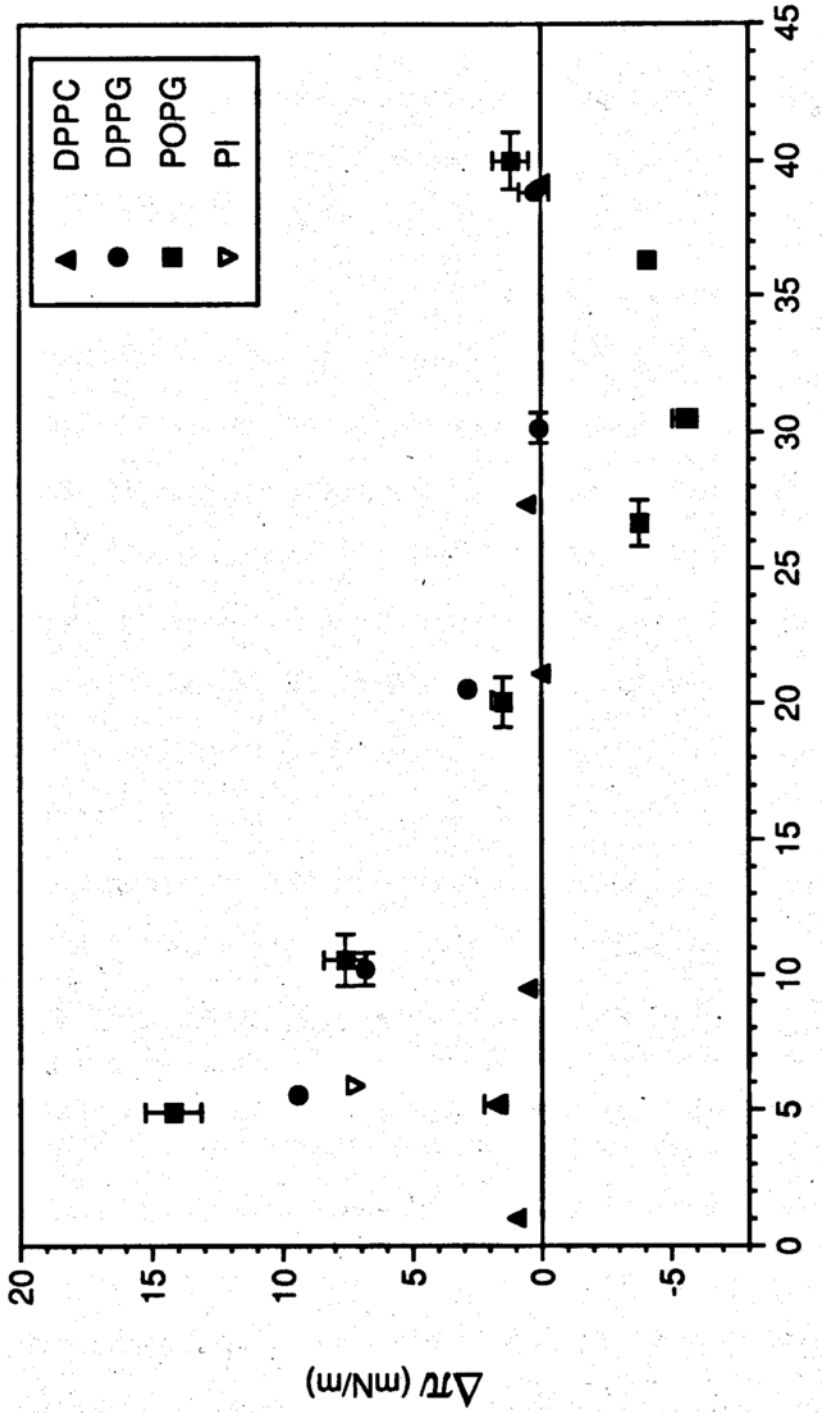

Figure 51. Change in surface pressure upon injection of LAI (5μg) below monolayers at various initial surface pressures spread on Tris-HCl, pH 7.4, 25°C and 5μM $CaCl_2$.

spread on 10 mM Tris-HCl, pH 7.4, 25°C, that also contained 5 μM or 5 mM $CaCl_2$. The relevant π-A diagrams for each phospholipid monolayer are given in Figure 52. The values of Δπ for the DPPC monolayer were all small, 2-3 mN/m or less, similar to the value observed when EDTA is used as a subphase in the experiments performed with DPPG. This would appear to indicate only nonspecific interaction between LAI and DPPC. For the PG lipids, as π_i increased, the corresponding values of Δπ decreased. In all cases, the Δπ values reach zero somewhere in the region $20 < \pi_i < 30$ mN/m. Interestingly, at $25 < \pi_i < 35$ mN/m, negative Δπ values were measured with the POPG monolayer (to be discussed below). Finally, at π_i of ≈40 mN/m, Δπ is zero for all lipids and either the protein is no longer interacting with the monolayer or, Δπ measurements are no longer sensitive to the perturbations caused by the interaction of the protein with the monolayer at this surface pressure. The measured Δπ value for the anionic PI monolayer at π_i of ≈ 5 mN/m was less than that measured for any of the PG monolayers at the same π_i. However, due to the highly variable distribution of lipid acyl chain structure in the PI sample, direct comparison of the PI results with those obtained for pure POPG monolayers cannot be made. Finally, a similar $\Delta\pi$-π_i profile was obtained for a DPPG monolayer spread on 10 mM Tris-HCl, pH 7.4, 25°C, and 5mM $CaCl_2$ (Figure 53). The Δπ values below 20 mN/m were slightly lower as was previously observed at the higher $CaCl_2$ concentration (Figure 47), however Δπ still became zero at $\pi_i \approx 20$ mN/m.

The ability to reversibly remove LAI that had penetrated a DPPG monolayer was investigated using an analogous set of experiments with a DPPG monolayer spread on 10 mM Tris-HCl, pH 7.4, 25°C, and 5 μM $CaCl_2$ (Figure 54). In these experiments, the surface pressure at which the protein is "squeezed-out," i.e. excluded from the monolayer, was measured by first allowing LAI (5 μg) to penetrate the DPPG monolayer (point **a** in Figure 54) at a surface pressure of ≈ 5mN/m. More lipid then

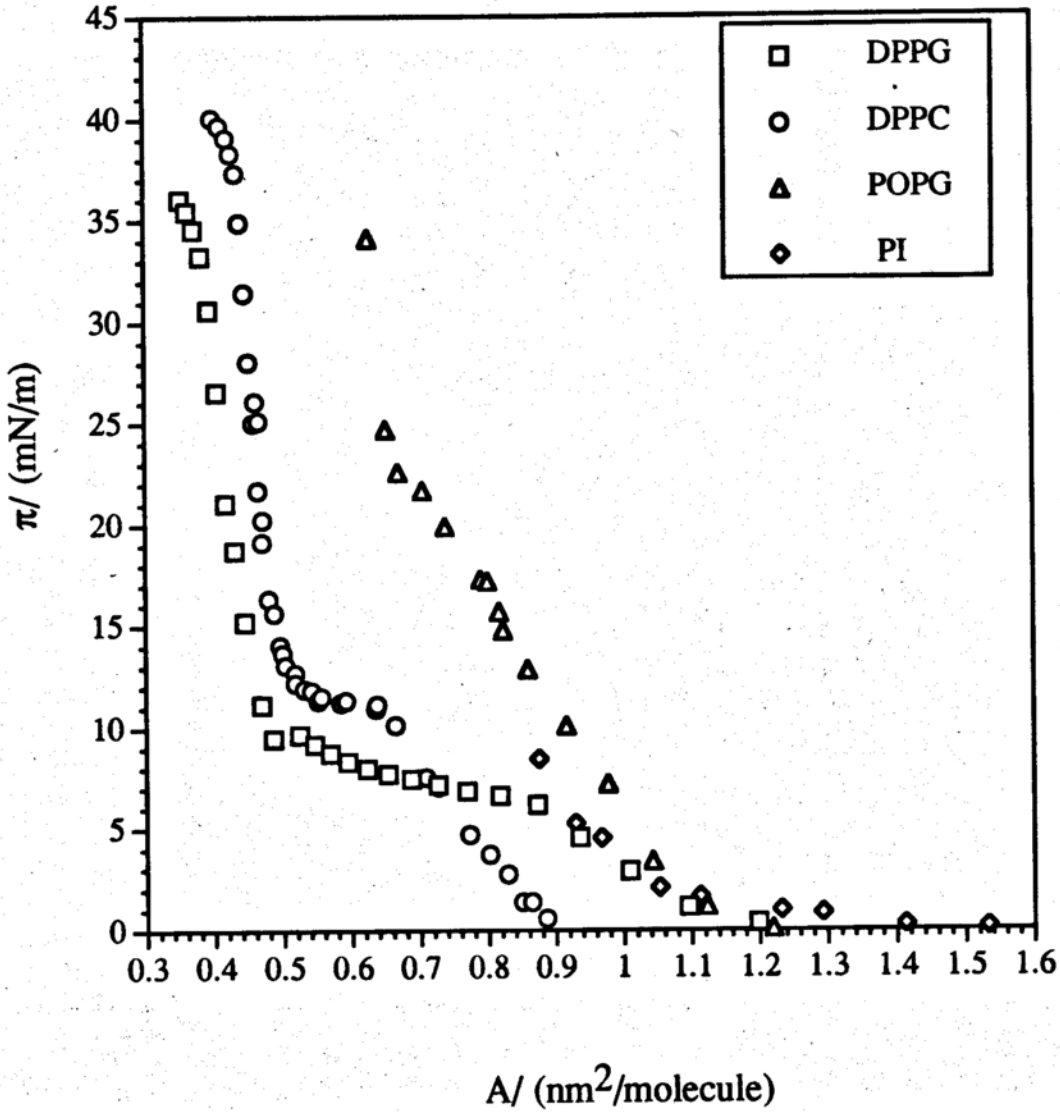

Figure 52. Surface pressure versus area diagram for various lipids spread on 10 mM Tris-HCl, pH 7.4, 25°C, and 5μM $CaCl_2$.

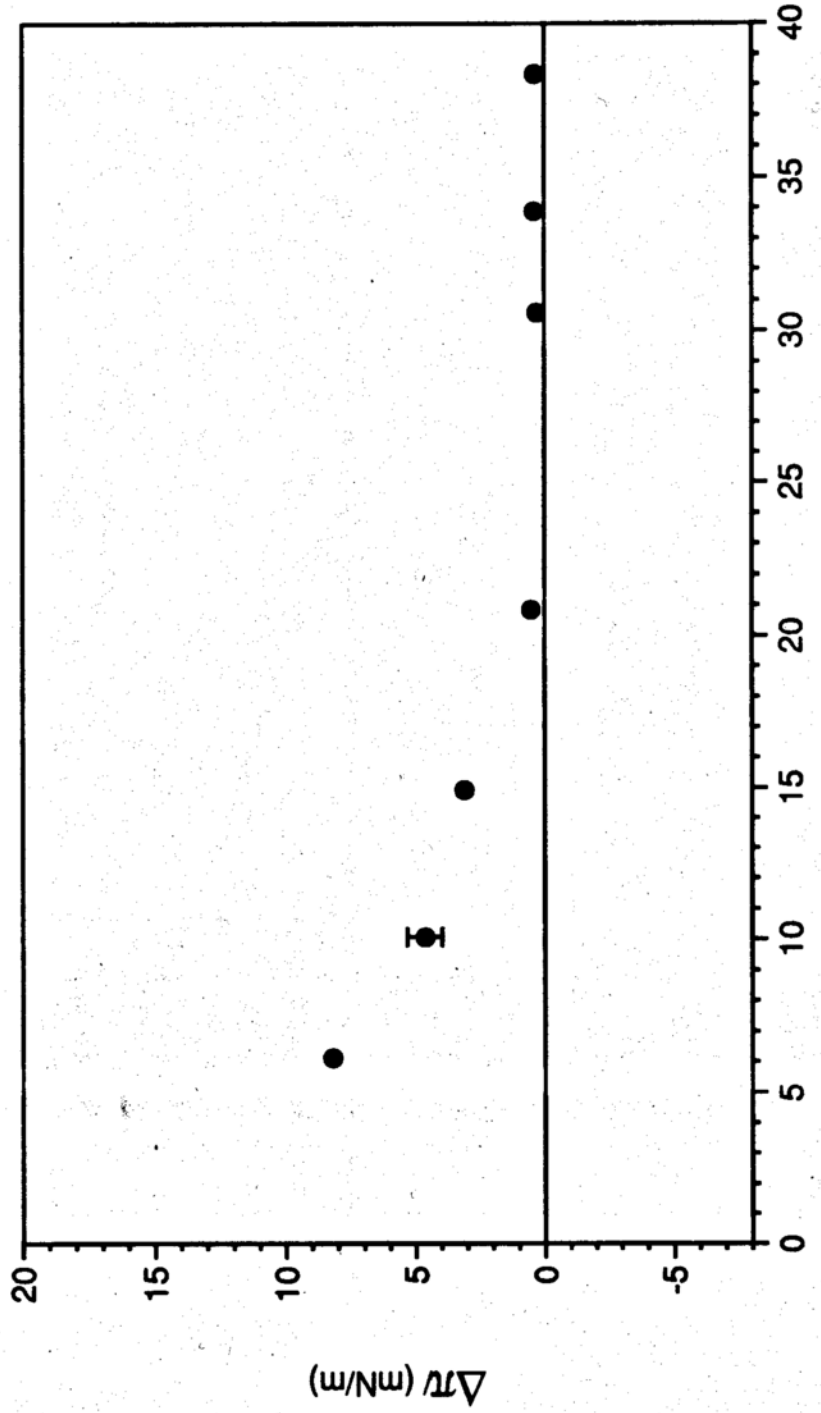

Figure 53. Change in surface pressure upon injection of LAI (5μg) below DPPG monolayers at various initial surface pressures spread on Tris-HCl, pH 7.4, 25°C and 5mM $CaCl_2$.

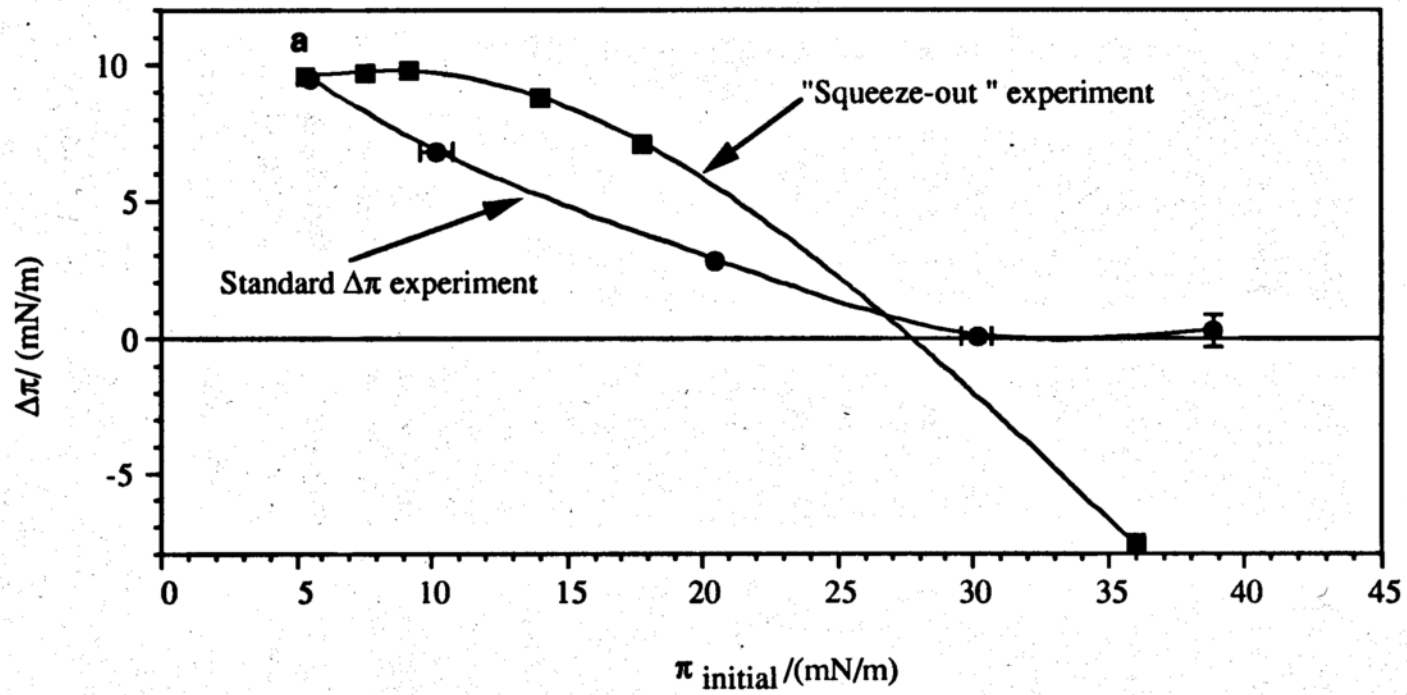

Figure 54. "Squeeze-out" experiment (filled squares). Initially, a DPPG monoayer is spread, (5.0 ± 0.5) mN/m on 10 mM Tris-HCl, pH 7.4, 25°C, and 5μM $CaCl_2$. The monolayer is allowed to equilibrate and LAI is injected into the subphase and Dπ is measured (point **a** in graph). Known amounts of DPPG solution are added to the monolayer and the resulting π is measured. The π_i is obtained from the π-A isotherm for DPPG at the calculated area/molecule based on the amount spread. More DPPG solution is added and the calculations are repeated.

was added successively to the surface (π_i was obtained from the π-A diagram from the known amount of lipid spread at the interface), thus increasing the surface pressure, until the protein was believed to be "squeezed-out" from the interface, i.e. $\Delta\pi = 0$. Slightly higher $\Delta\pi$ values were obtained at different levels of added lipid in these experiments as opposed to those obtained by performing separate penetration experiment (Figure 51) below π_i of ≈ 25mN/m. However, the $\Delta\pi$ value became zero at approximately the same π_i. Interestingly, a negative value was obtained in the "squeeze-out" experiment providing evidence that the protein still interacts with the monolayer even at initial surface pressures of ≈ 35mN/m (to be discussed below).

Studies with mixed DPPC/PG monolayers

Lung surfactant is a complex mixture of anionic and zwitterionic lipids therefore, it is of importance to study the interaction of LAI with mixed lipid monolayers. The changes in surface pressure upon injection of LAI (5 μg) below mixed DPPC/PG monolayers spread on 10 mM Tris-HCl, pH 7.4, 25°C, and 5 μM $CaCl_2$ at an $\pi_i \approx$ 5mN/m were measured at various surface compositions as shown in Figure 55. A small $\Delta\pi$, 2-3 mN/m, was measured in mixtures that only contained 10 mol% of anionic lipid, close to the value obtained for DPPC monolayers alone. Increasing the anionic lipid content to 30 mol%, however, significantly increased $\Delta\pi$ and the $\Delta\pi$ values increased further as the anionic lipid content of the mixed monolayer was increased. The $\Delta\pi$ values for the mixed DPPC/POPG monolayer were consistently higher than those obtained for the mixed DPPC/DPPG monolayers. A $\Delta\pi$ vs. π_i profile was obtained for the DPPC/POPG monolayer spread on 10 mM Tris-HCl, pH 7.4, 25°C, and 5 μM $CaCl_2$ (Figure 56). The $\Delta\pi$ values decrease to zero at $\pi_i \approx$ 15mN/m, which is a much smaller surface pressure than was previously measured for

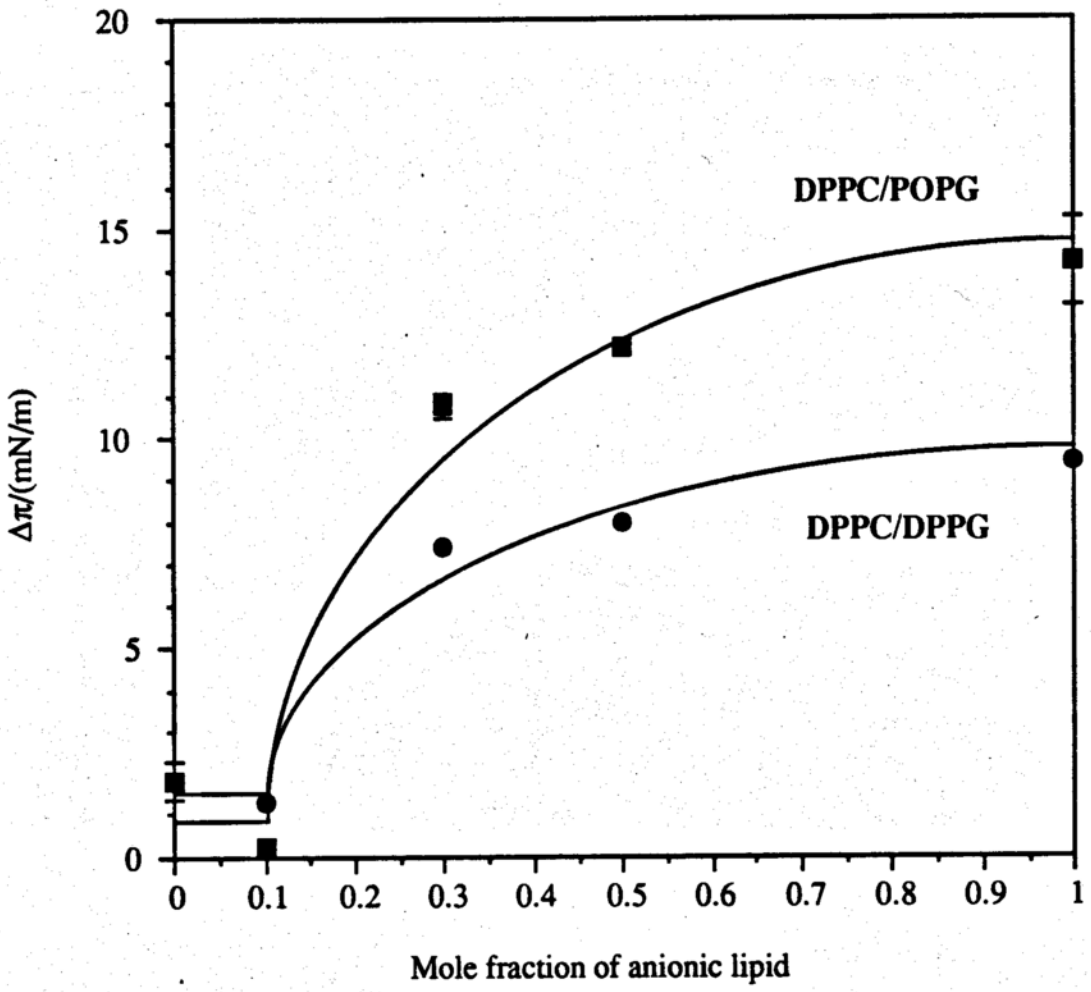

Figure 55. Change in surface pressure upon injection of LAI (5μg) below mixed DPPC/PG monolayers, $\pi_i = 5.0 \pm 0.5$ mN/m spread on Tris-HCl, pH 7.4, 25°C, and 5μM $CaCl_2$.

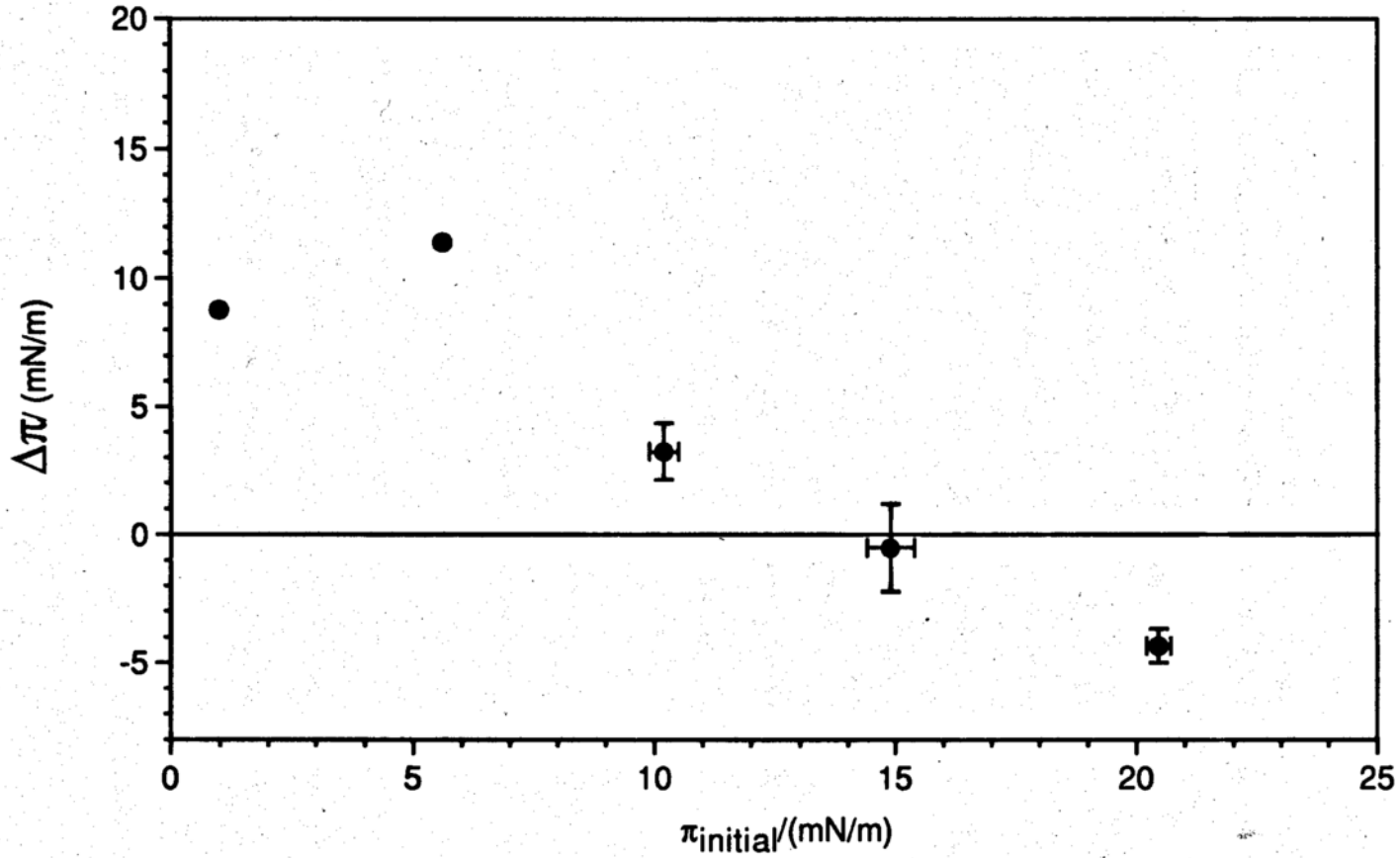

Figure 56. Change in surface pressure upon injection of LAI (5μg) below DPPC/POPG (1:1) monolayers at various initial surface pressures spread on Tris-HCl, pH 7.4, 25°C and 5μM $CaCl_2$.

the single-component monolayers. Negative $\Delta\pi$ values, as were observed for the pure POPG monolayer (Figure 51), were obtained at surface pressures as low as 20 mN/m.

The interaction of 33 kDa PLBP and LAI-bp with the DPPC/POPG binary monolayers at three values of π_i was also studied. Table IV compares the changes in the surface pressure for each protein at approximately the same π_i. The 33 kDa protein increased the surface pressure of the monolayer significantly at $\pi_i \approx 1$ mN/m but, to a lesser extent at a $\pi_i \approx 6$ mN/m. LAI-bp appeared to interact with the binary monolayers in a non-specific fashion yielding very small $\Delta\pi$ values even at π_i as low as 1 mN/m. Negative $\Delta\pi$ values were measured for both the 33 kDa PLBP and LAI-bp at higher π_i (to be discussed below).

Effects of various proteins on phase equilibria in mixed DPPC/POPG mixtures as measured by fluorescence microscopy

The changes in the phase equilibria of mixed DPPC/POPG monolayers, (with 1 mol% NBD-PC) spread on 10 mM Tris-HCl, pH 7.4, 25°C, and 5 μM $CaCl_2$, after injection of protein (5 μg) into the underlying subphase were examined using fluorescence microscopy at various π_i for LAI (Figures 57 and 58) LAI-bp (Figures 59 and 60), and for 33kDa PLBP (Figures 61 and 62). The images both before and after introduction of the protein were recorded and the percentage of dark domains in each field were quantitated using the NIH Image software (Table V). At low π_i (up to $\pi i \approx 6$ mN/m) the addition of LAI increased surface pressure as observed above. As expected, based on observations presented in the previous results section above, an increase in the amount of phase separated material from 2- to 10-fold accompanied the increase in surface pressure (Figure 57). At higher π_i, however, a decrease in surface pressure was measured and an unusually large loss (i. e the presence of a lesser

Table IV. Change in surface pressure upon injection of protein (5μg) below a DPPC/POPG (1:1) mixture spread on 10 mM Tris-HCl, pH 7.4, 25°C, and 5μM $CaCl_2$.

	Δπ/ (mN/m)		
π_i /(mN/m)	L AI	L AI bp	33 kDa PLBP
1.2 ± 0.2	8.8	3.3	7.4
5.8 ± 1.0	11.4	2.3	3.2
16.0 ± 0.5	- 2.8	- 2.3	-0.5

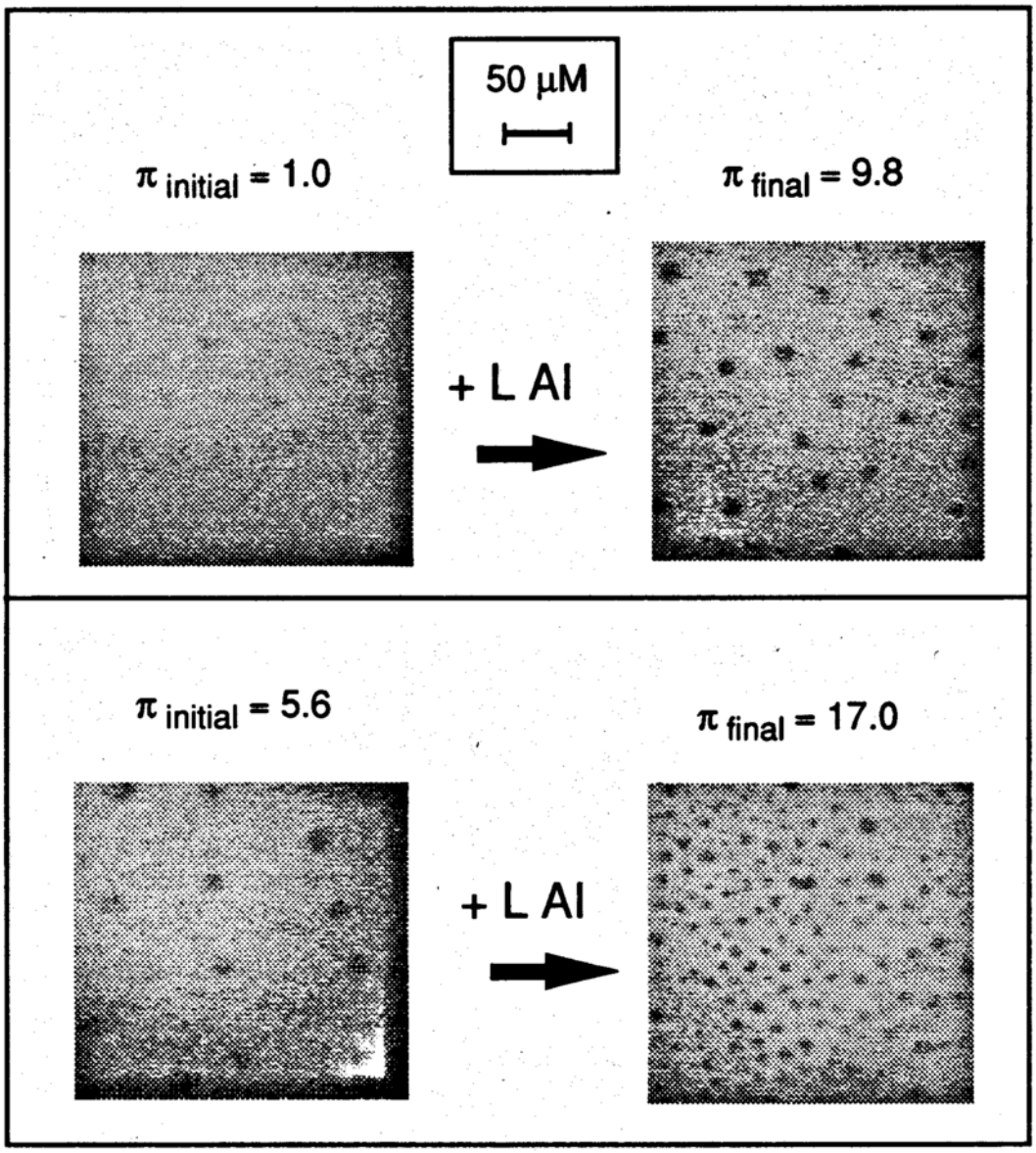

Figure 57. Fluorescence images of DPPC/POPG (1:1) spread on 10 mM Tris-HCl, pH 7.4, 25°C, and 5μM $CaCl_2$ before and after the injection of LAI (5μg).

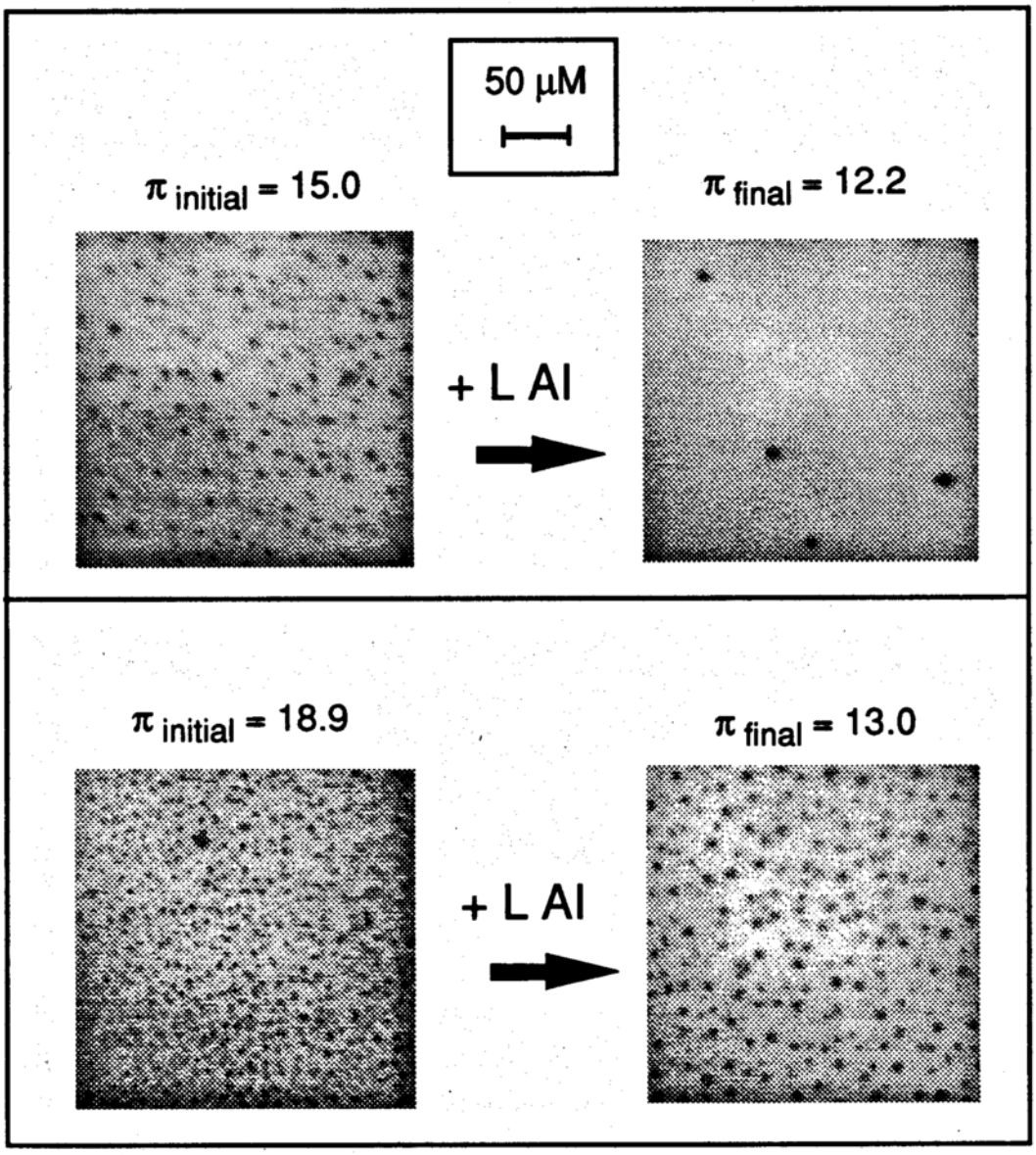

Figure 58. Fluorescence images of DPPC/POPG (1:1) spread on 10 mM Tris-HCl, pH 7.4, 25°C, and 5μM $CaCl_2$ before and after the injection of LAI (5μg).

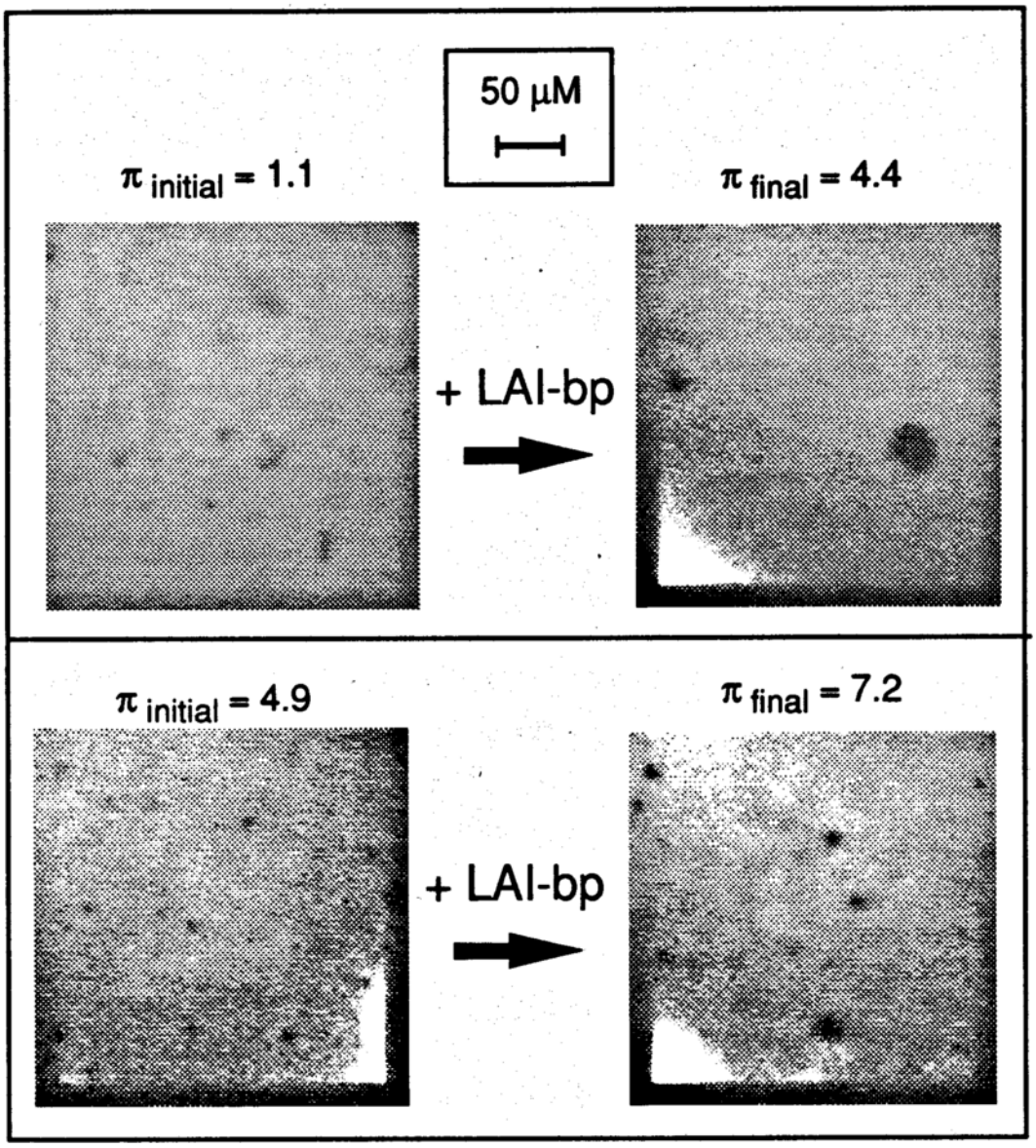

Figure 59. Fluorescence images of DPPC/POPG spread on 10 mM Tris-HCl, pH 7.4, 25°C, and 5μM CaCl before and after the injection of LAI-bp (5μg).

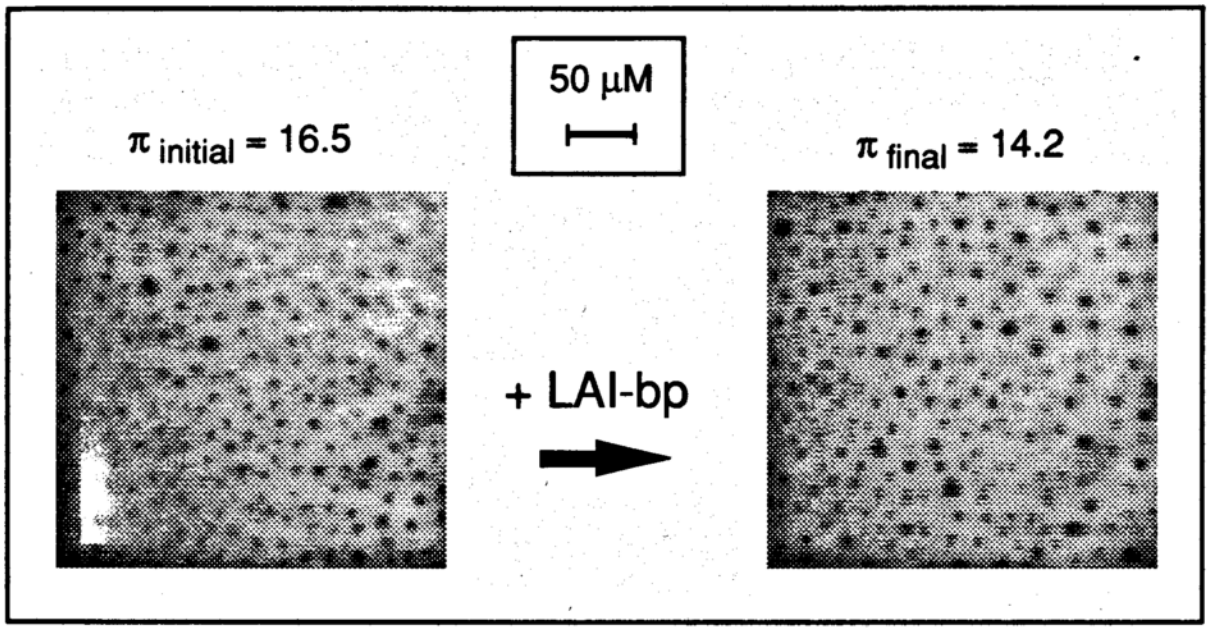

Figure 60. Fluorescence images of DPPC/POPG spread on 10 mM Tris-HCl, pH 7.4, 25°C, and 5μM CaCl before and after the injection of LAI-bp (5μg).

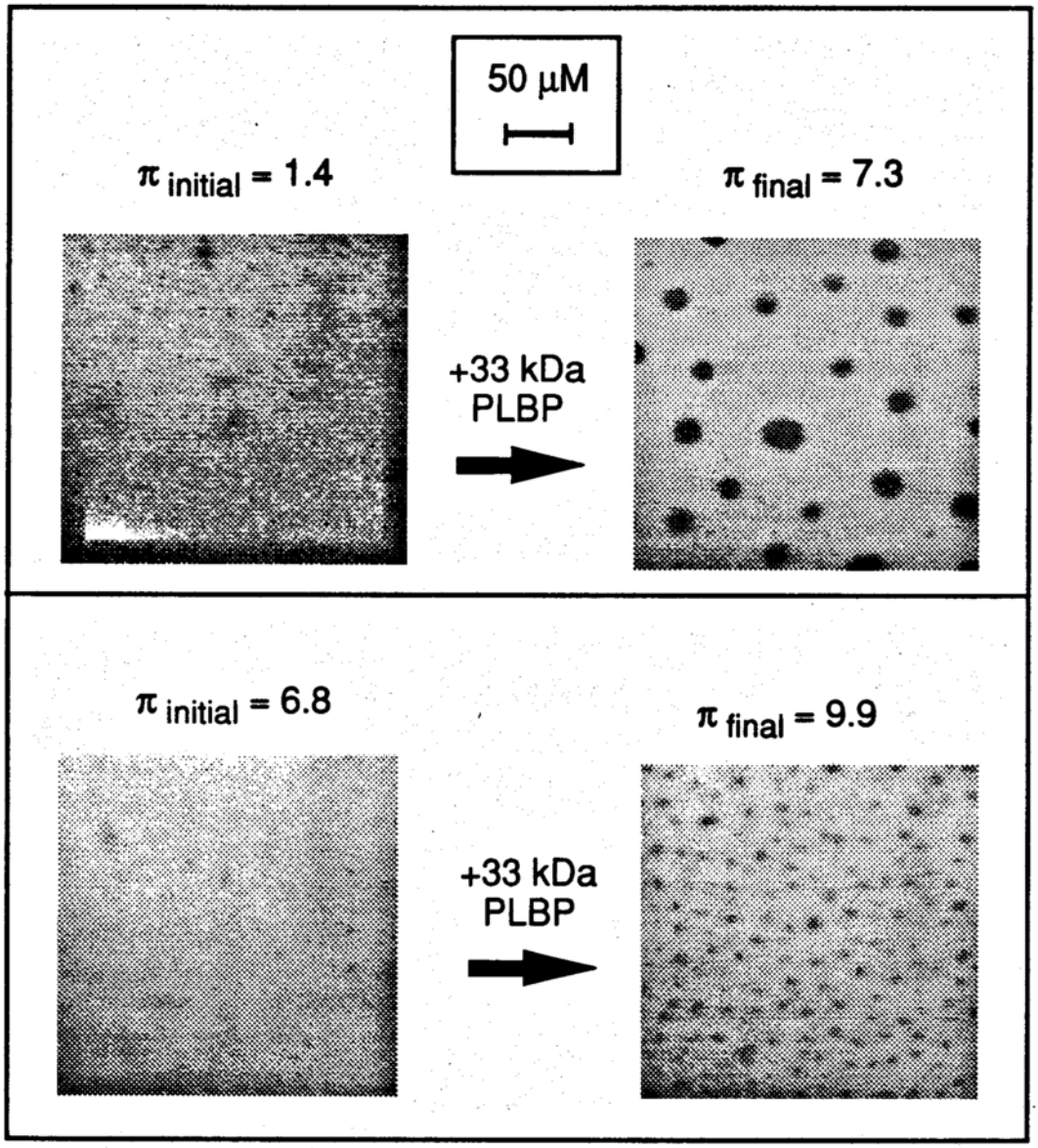

Figure 61. Fluorescence images of DPPC/POPG spread on 10 mM Tris-HCl, pH 7.4, 25°C, and 5μM CaCl before and after the injection of 33 kDa PLBP (5μg).

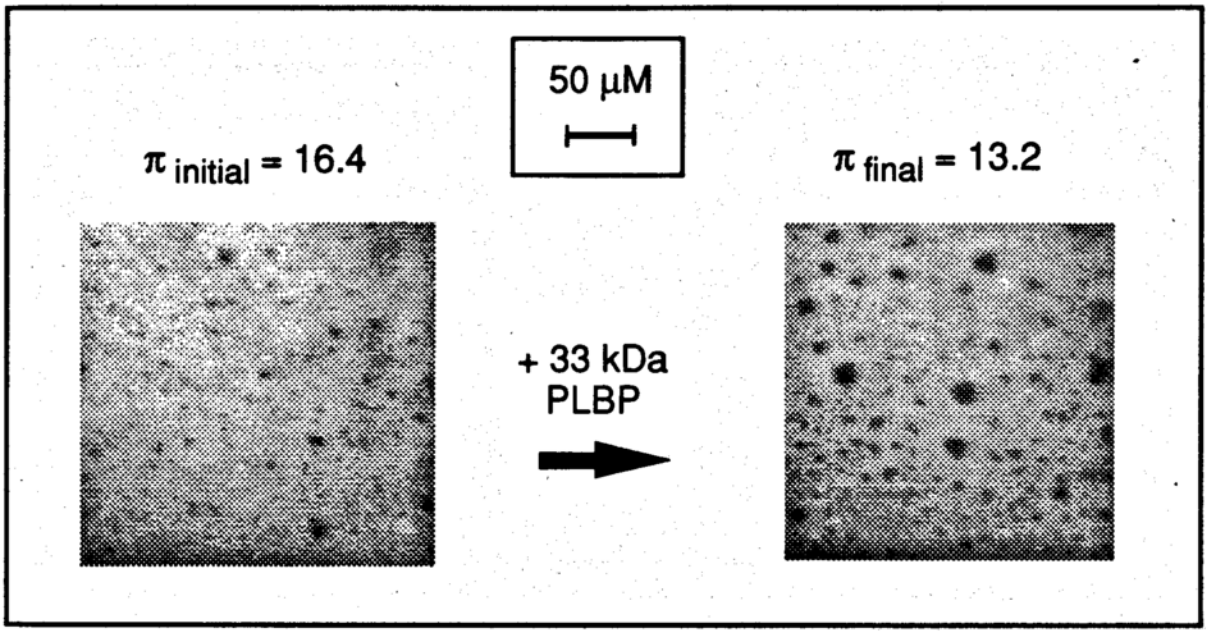

Figure 62. Fluorescence images of DPPC/POPG spread on 10 mM Tris-HCl, pH 7.4, 25°C, and 5μM CaCl before and after the injection of 33 kDa PLBP (5μg).

Table V. The changes in the percentage of dark domains before and after the injection of protein (5μg) below DPPC/POPG (1:1) binary monolayers spread on 10 mM Tris-HCl, pH 7.4, 25°C, and 5μM $CaCl_2$,at various initial surface pressures. (The error in the surface pressure is expected to be in the range of ± 0.5 mN/m while errors of the analysis of the percentage of dark domains is not more than 10% of the reported value.

Protein	π_i/(mN/m)	π_f/(mN/m)	% dark (π_i)	% dark (π_f)
LAI	1.0	9.8	0.86	10.3
	5.5	17.0	4.5	9.3
	15.0	12.2	6.8	1.8
	18.9	13.0	13.2	7.1
LAI-bp	1.1	4.4	2.0	4.2
	4.9	7.2	1.1	1.7
	16.5	14.2	8.4	10.9
33 kDa PLBP	1.4	7.3	1.3	7.4
	6.8	9.9	4.9	12.9
	12.6	13.2	12.9	13.6

amount of domains at the same surface pressure in the absence of protein) in the amount of phase separated material was observed (Figure 58). The breakdown protein, in contrast, only changed the surface pressure by small amounts, ≈2 to 3 mN/m regardless of π_i. Correspondingly, no change in the appearance of dark domains was observed for any π_i examined (Figures 59 and 60 and Table V). The 33 kDa PLBP increased surface pressure of the mixed DPPC/POPG monolayers spread at low surface pressures (i.e. $\pi_i \approx 7$ mN/m or less) which led to a 3- to 7-fold increase in the amount of dark domains. At higher π_i, a decrease in surface pressure was measured however, no large changes in the extent of phase separation were observed as was in the case of LAI (Figures 61 and 62).

Lung annexin I interactions with supported planar DPPG bilayers

DPPG, which forms highly condensed monolayers at the air/water interface at high surface pressures, was transferred to mica as a bilayer at a surface pressure of ≈ 35 mN/m. The films were observed by atomic force microscopy (AFM) with and without added protein using the fluid cell attachment. The first experiment performed attempted to investigate any nonspecific binding of LAI to a freshly cleaved mica surface. Figure 63 is the image obtained of the freshly cleaved mica in 10 mM Tris-HCl, pH 7.4, and 5μM $CaCl_2$ (the buffer used in all of these experiments unless otherwise noted). At resolutions down to 10 nm in the z-direction, the mica appears smooth. LAI was then introduced to the fluid cell at the same concentration used in the above experiments (≈ 5μg/ 35 ml). Figures 64 and 65 present the images obtained 20 and 40 minutes, respectively, after incubation of the mica with the LAI solution. Tall, broad peaks appeared on the surface of the mica in a random fashion indicating the likely presence of adsorbed protein. The mica was washed by passing solutions

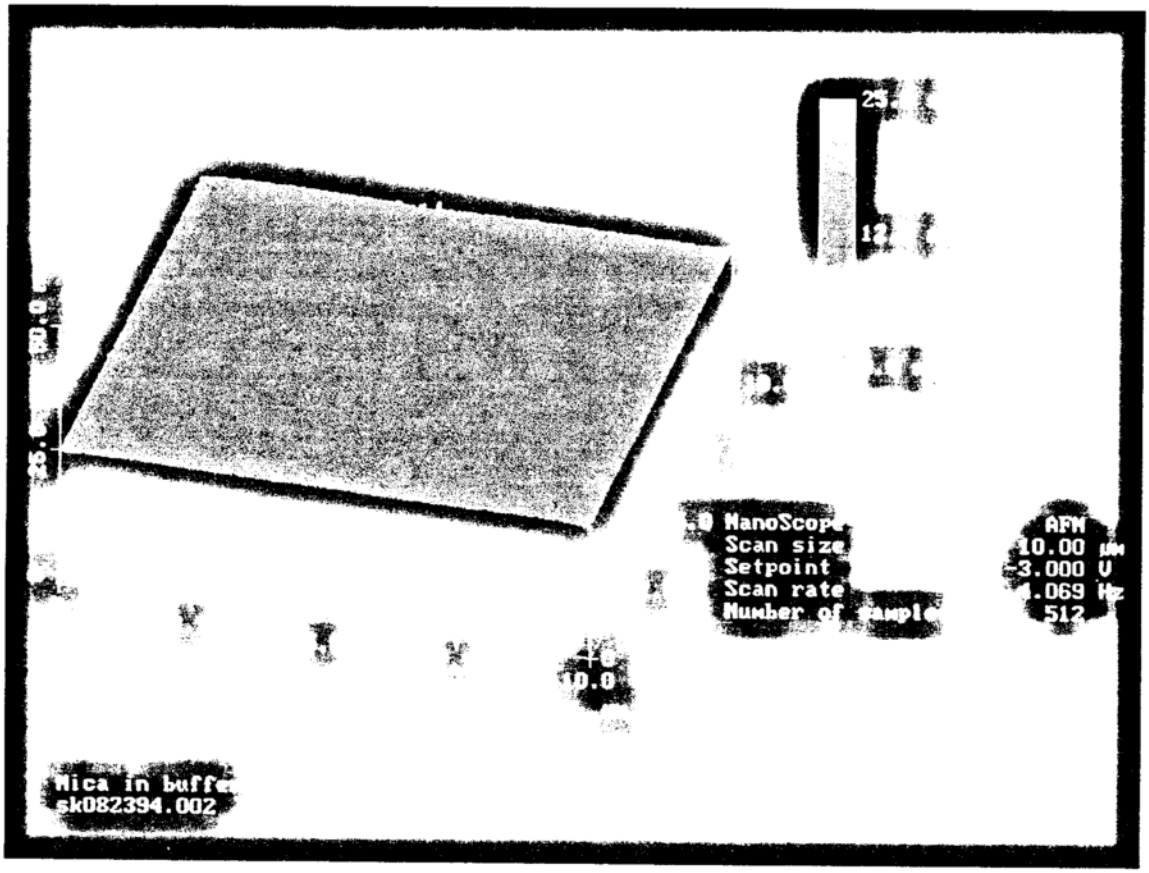

Figure 63. AFM image of freshly cleaved mica in 10 mM Tris-HCl, pH 7.4, 5µM $CaCl_2$ at 25°C.

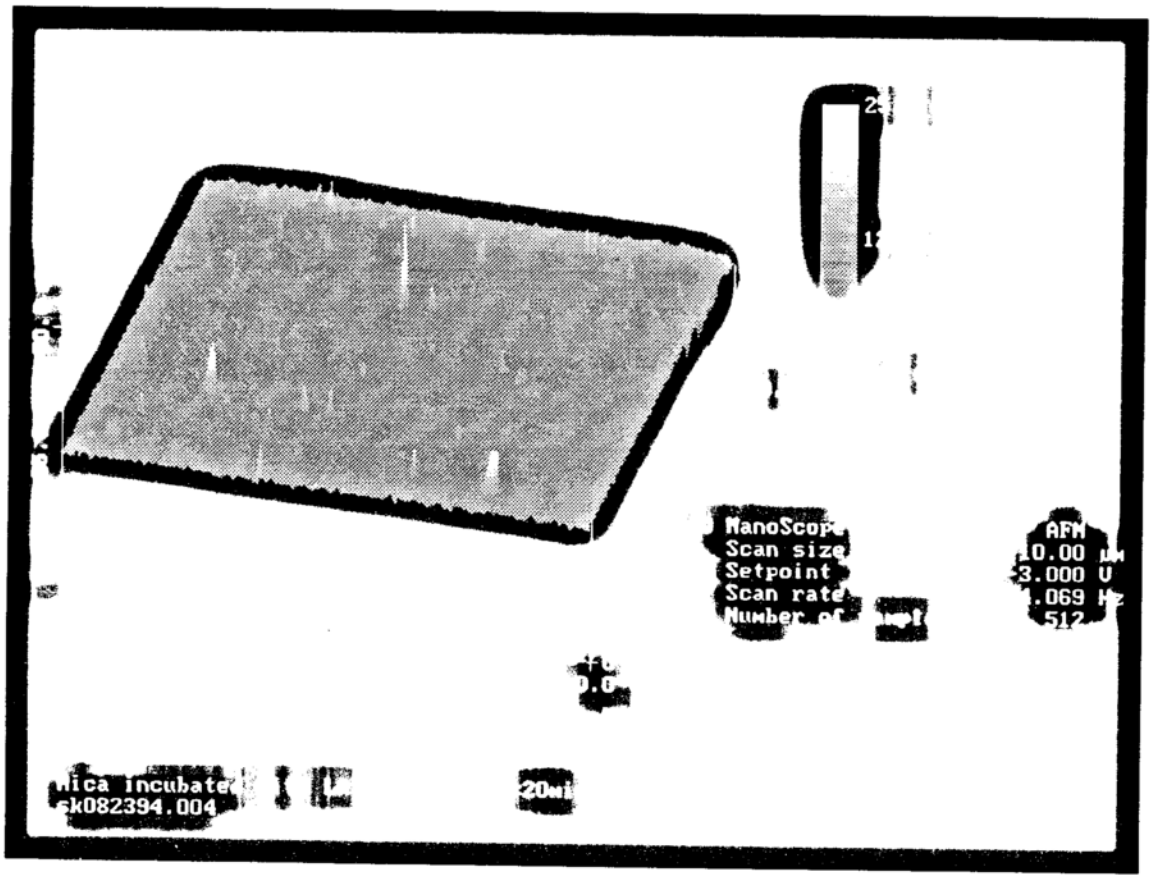

Figure 64. AFM image of mica incubated with LAI (5µg/35 ml) in 10 mM Tris-HCl, pH 7.4, 5µM $CaCl_2$ at 25°C after 20 minutes.

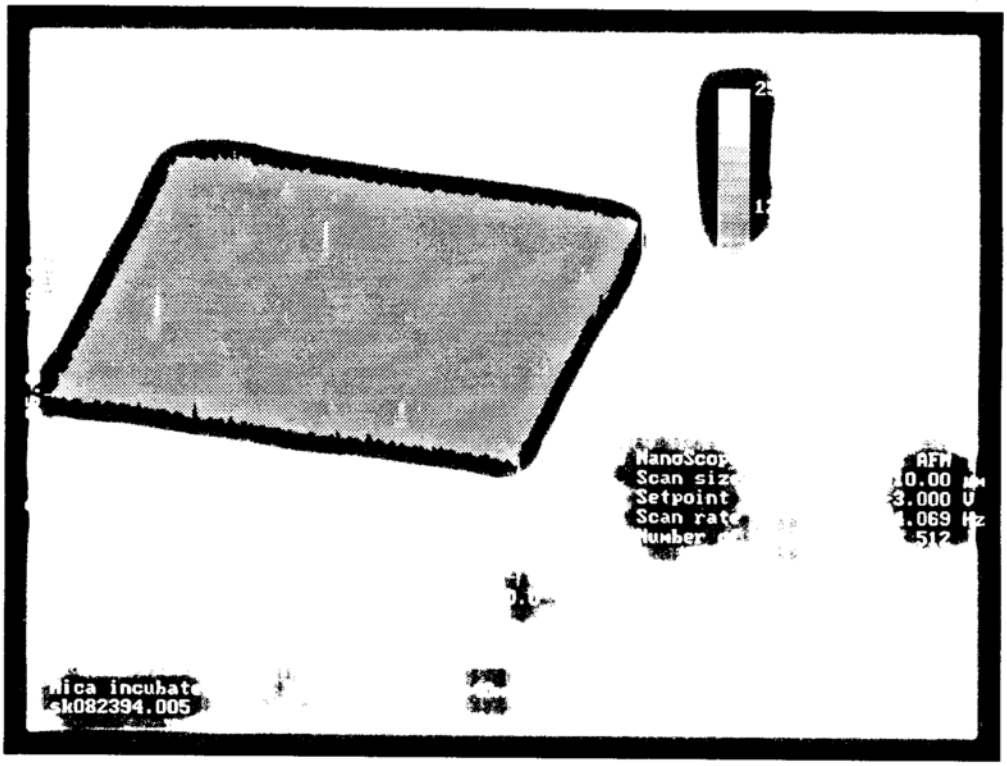

Figure 65. AFM image of mica incubated with LAI (5µg/35 ml) in 10 mM Tris-HCl, pH 7.4, 5µM $CaCl_2$ at 25°C after 40 minutes.

through the fluid cell to be sure that the peaks that appeared were not instrument-induced artifacts. Five washings were performed with the buffer and the resulting image which shows the presence of residual adsorbed protein is presented in Figure 66. Therefore, washing the mica with buffer alone does not remove all of the deposited material. Figure 67 contains the image obtained after the mica was washed with a 10% SDS (sodium dodecyl sulfate) detergent solution. The clean mica surface was recovered indicating that the observed peaks in the previous images were, in fact, deposited material and not an artifact of the experiment. The maximum height change (peak to valley distance in the z-direction) in the various images is given in Table VI, an increase of 16 nm over the maximum height in the mica in buffer value is observed upon addition of LAI. The baseline height is recovered after the SDS wash.

Figures 69 through 76 present images obtained upon incubating a DPPG planar bilayer on mica to LAI solution for various amounts of time. Although the DPPG bilayer could not be directly imaged at areas as small as 500 nm^2 (Figure 68), the transfer is believed to have been successful since a reduction in trough area occured upon transfer of the monolayer at constant surface pressure (see experimental above). Incubating the film with LAI solution for 15 (Figures 69 to 72) or 30 (Figures 73 to 76) minutes resulted in significant amounts of protein becoming adsorbed to the solid surface, certainly more than that adsorbed to mica alone. The contrast in the amount of protein adsorbed to the presumably bilayer coated mica and the clean mica provides further evidence of the presence of the deposited DPPG bilayer. Images at reduced areas (Figures 71 and 75) and the corresponding images as viewed from the top (Figures 70, 72, 74, and 76) suggest that the protein is adsorbing in an ordered fashion into long branch-like structures that extend anywhere from 1 to 4 μm in length. The adsorbed protein forms tall, broad peaks that extend beyond monolayer coverage of the DPPG lipids. The protein could only be removed with an 10% SDS wash, as

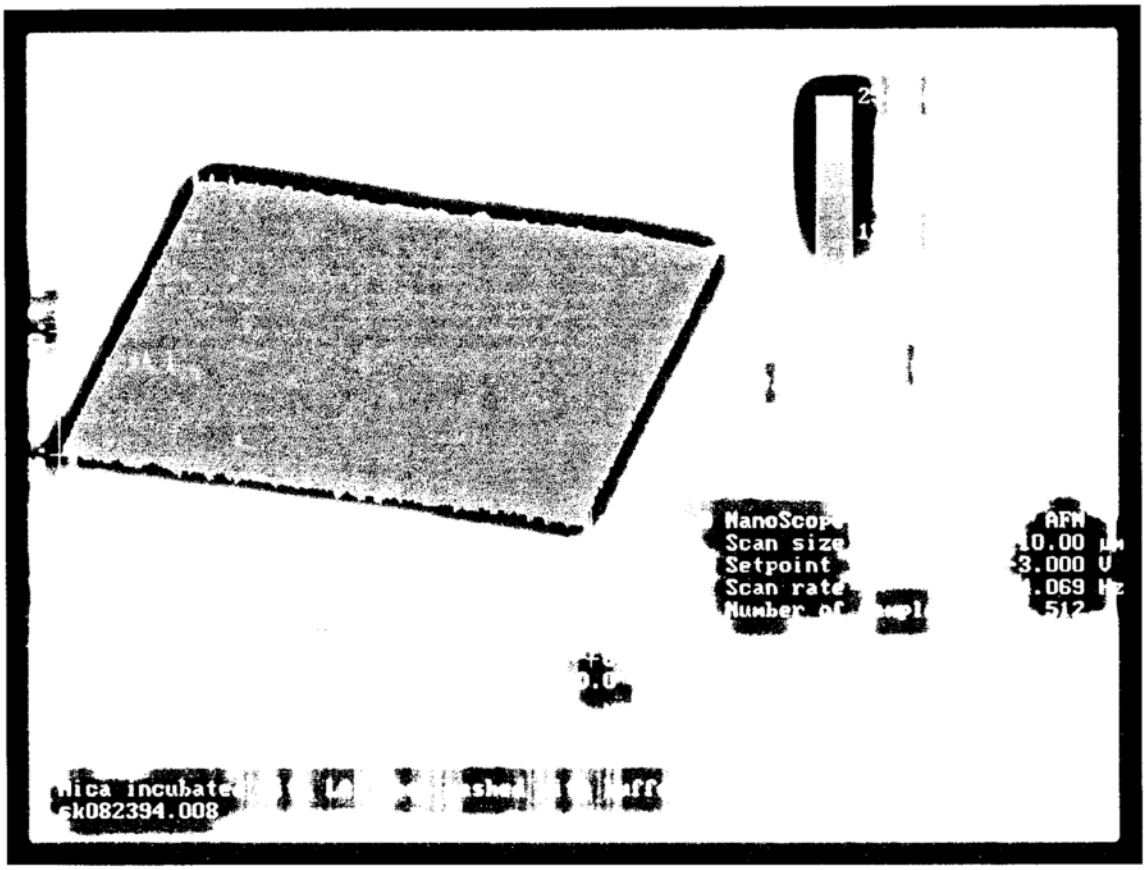

Figure 66. AFM image of mica incubated with LAI (5μg/35 ml) in 10 mM Tris-HCl, pH 7.4, 5μM $CaCl_2$ at 25°C then washed with 10 mM Tris-HCl, pH 7.4, 1 mM EDTA.

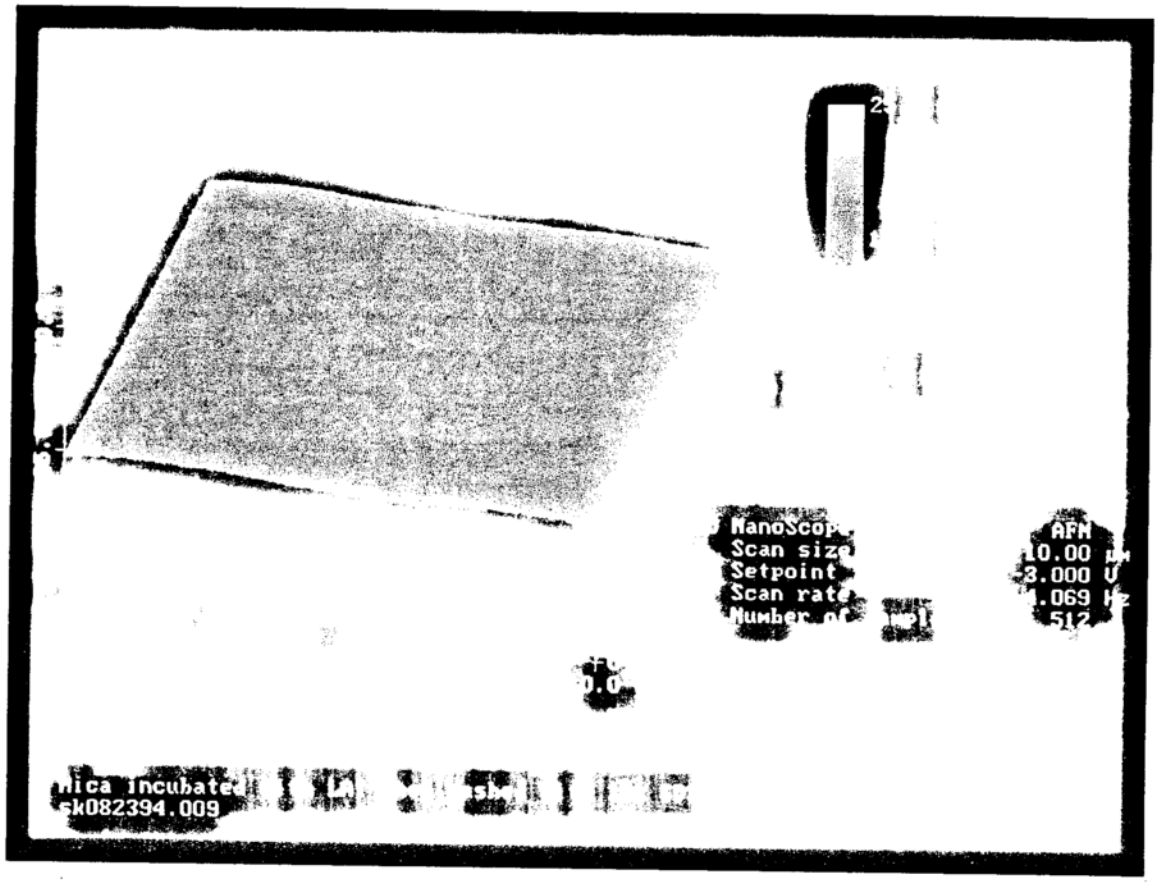

Figure 67. AFM image of mica incubated with LAI (5µg/35 ml) in 10 mM Tris-HCl, pH 7.4, 5µM $CaCl_2$ at 25°C then washed with 10 % SDS.

Table VI. Maximum height change analysis

Image	Maximum height change (nm)
Mica in air	16.5
Mica in buffer	17.8
Mica + LAI solution	34.1
10 % SDS wash	20.1

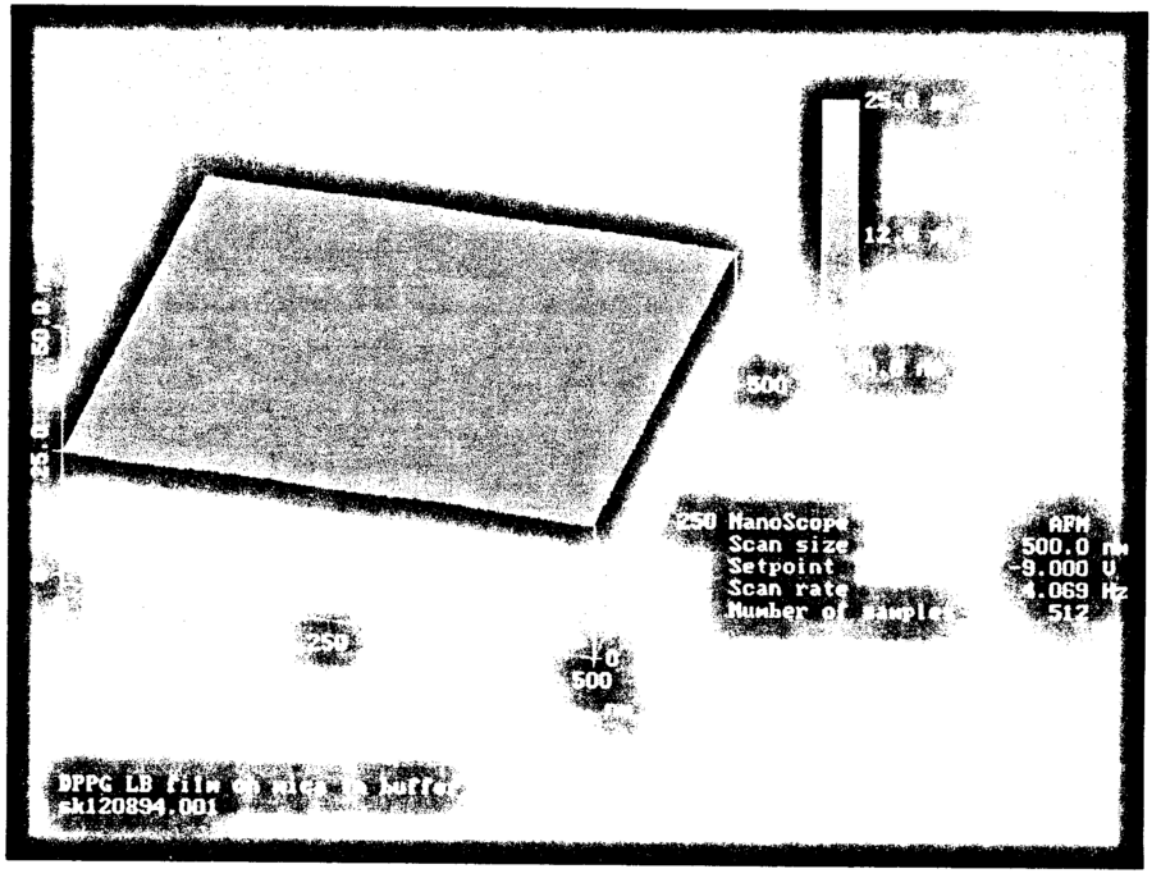

Figure 68. AFM image of a DPPG bilayer supported on mica in 10 mM Tris-HCl, pH 7.4, 5μM $CaCl_2$ at 25°C.

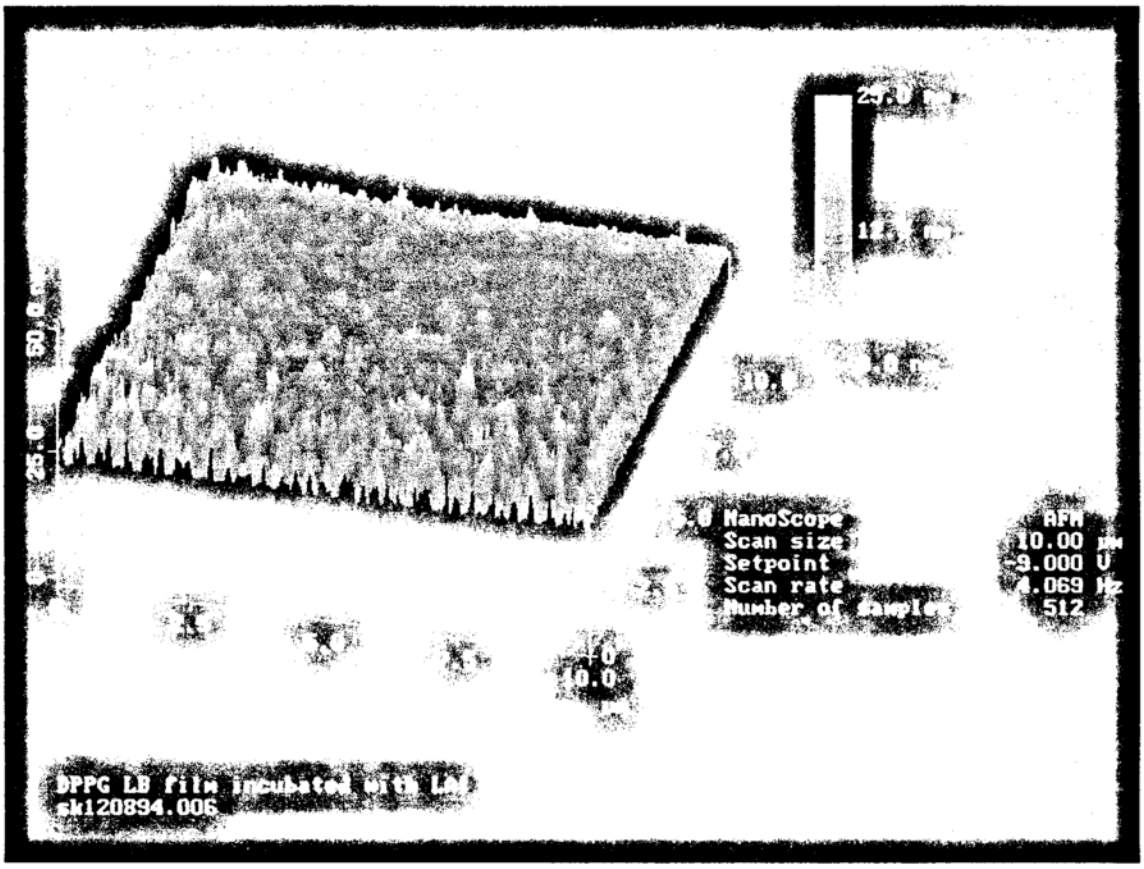

Figure 69. AFM image of a DPPG bilayer supported on mica incubated with LAI (5μg/35 ml) in 10 mM Tris-HCl, pH 7.4, 5μM $CaCl_2$ at 25°C after 15 minutes.

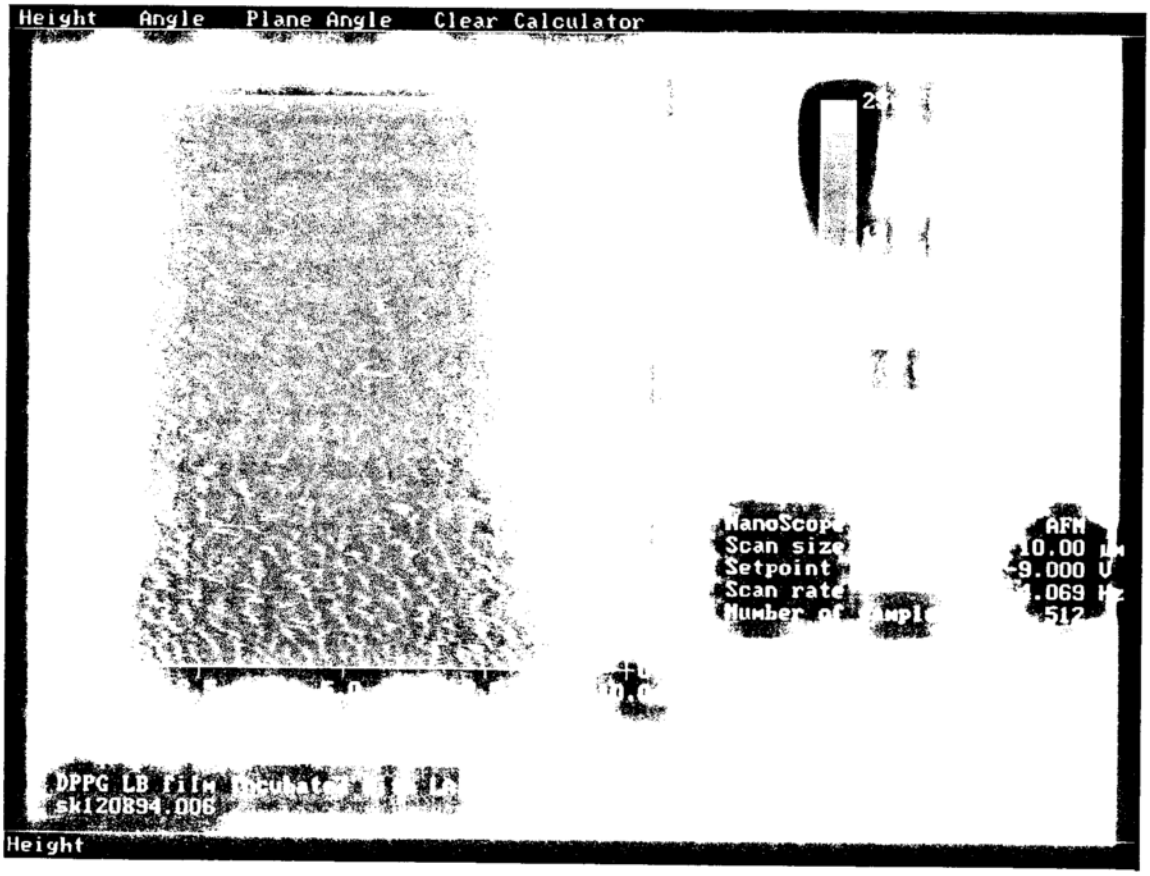

Figure 70. AFM image of a DPPG bilayer supported on mica incubated with LAI (5μg/35 ml) in 10 mM Tris-HCl, pH 7.4, 5μM $CaCl_2$ at 25°C after 15 minutes (top view).

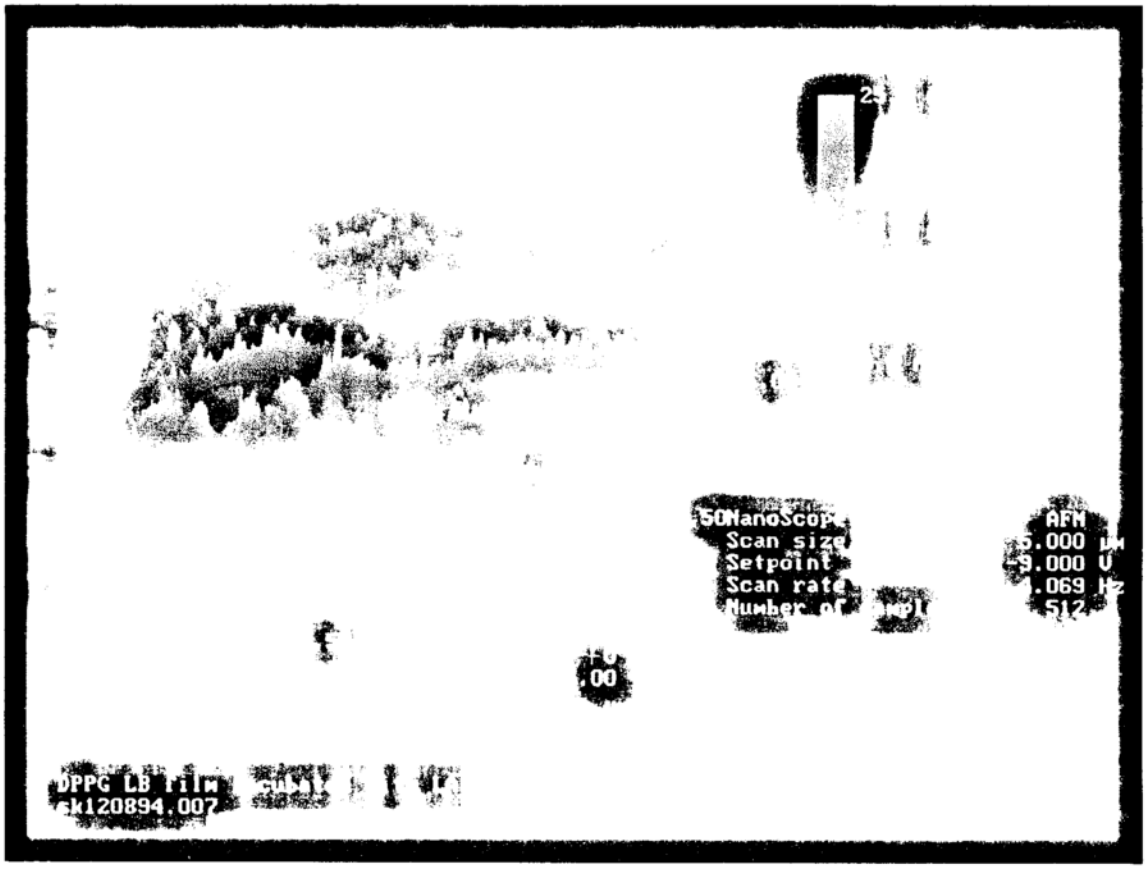

Figure 71. AFM image of a DPPG bilayer supported on mica incubated with LAI (5μg/35 ml) in 10 mM Tris-HCl, pH 7.4, 5μM $CaCl_2$ at 25°C after 15 minutes.

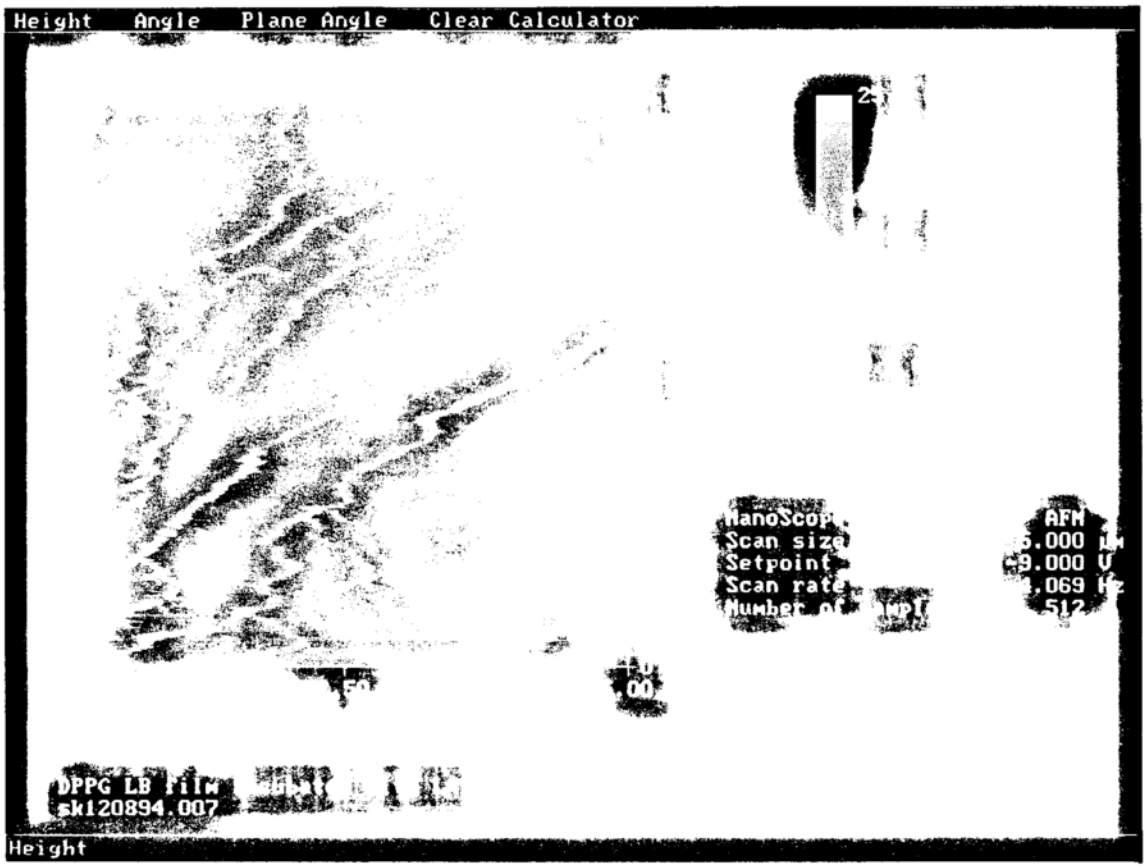

Figure 72. AFM image of a DPPG bilayer supported on mica incubated with LAI (5μg/35 ml) in 10 mM Tris-HCl, pH 7.4, 5μM $CaCl_2$ at 25°C after 15 minutes (top view).

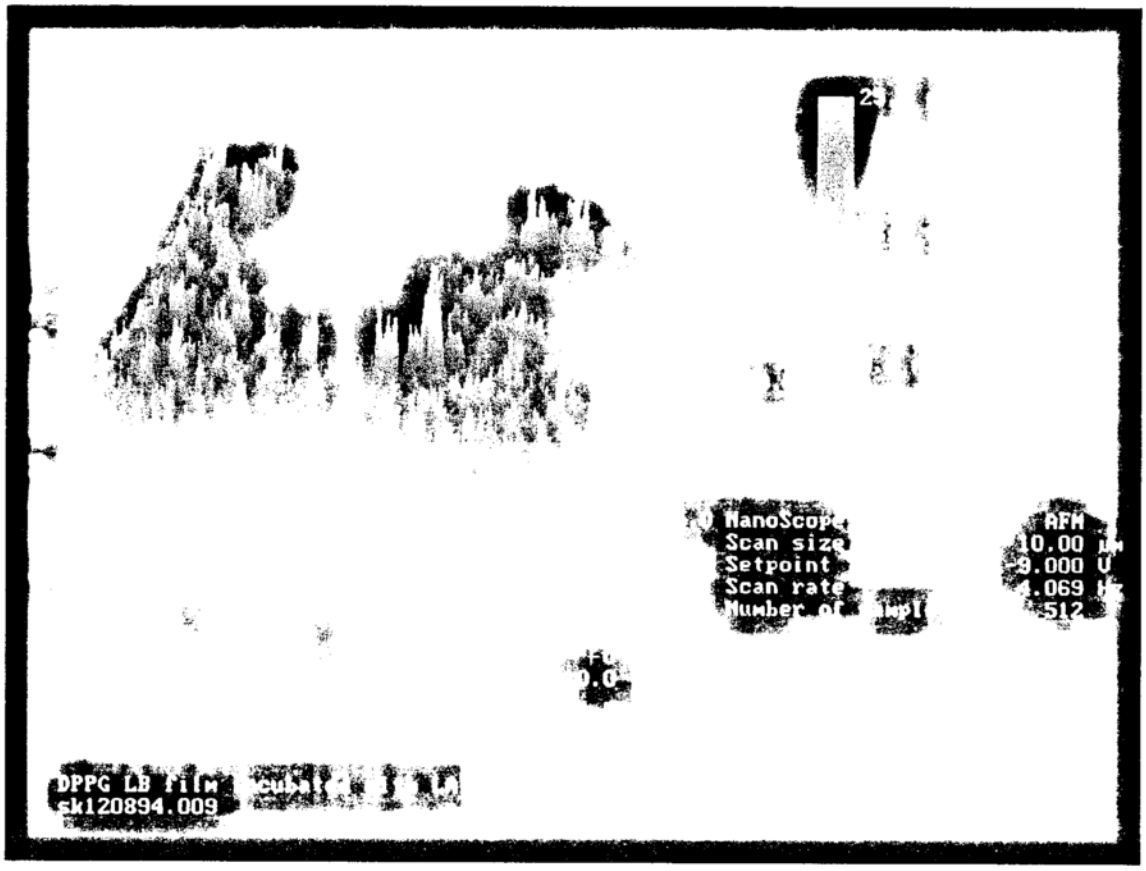

Figure 73. AFM image of a DPPG bilayer supported on mica incubated with LAI (5μg/35 ml) in 10 mM Tris-HCl, pH 7.4, 5μM $CaCl_2$ at 25°C after 30 minutes.

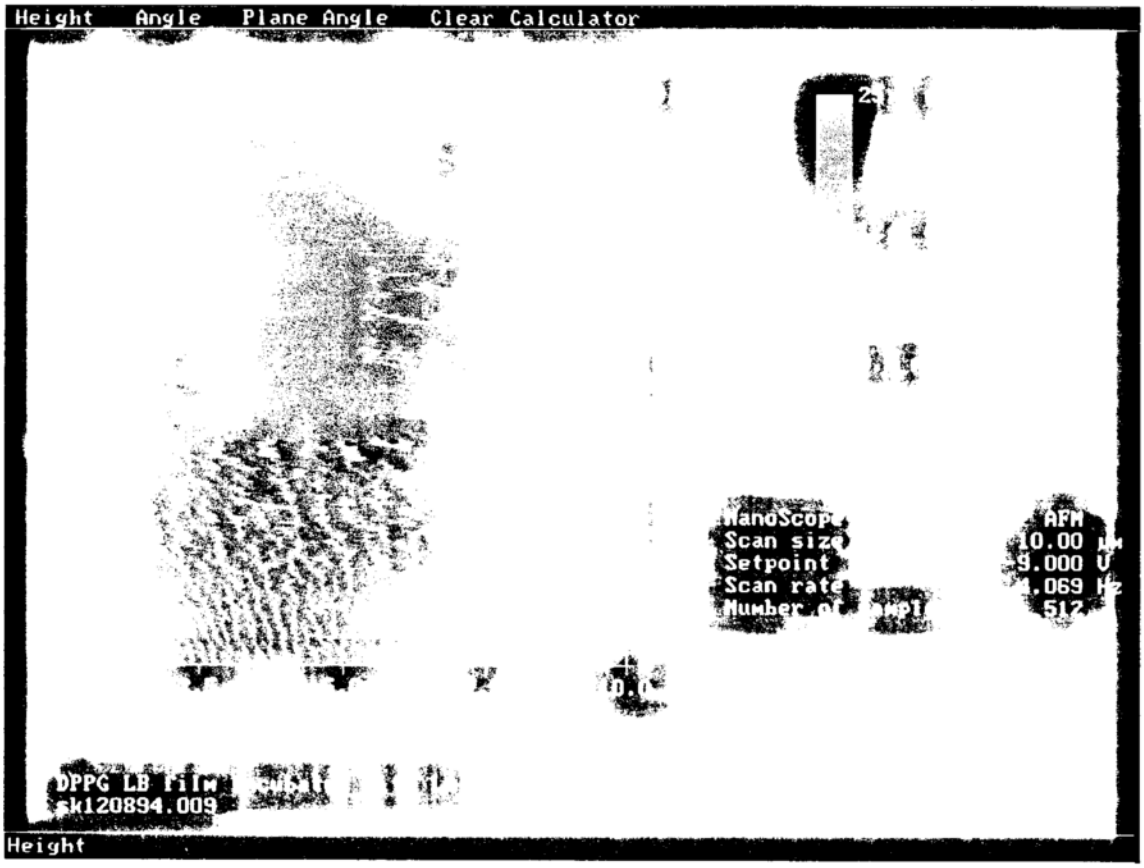

Figure 74. AFM image of a DPPG bilayer supported on mica incubated with LAI (5μg/35 ml) in 10 mM Tris-HCl, pH 7.4, 5μM $CaCl_2$ at 25°C after 30 minutes (top view).

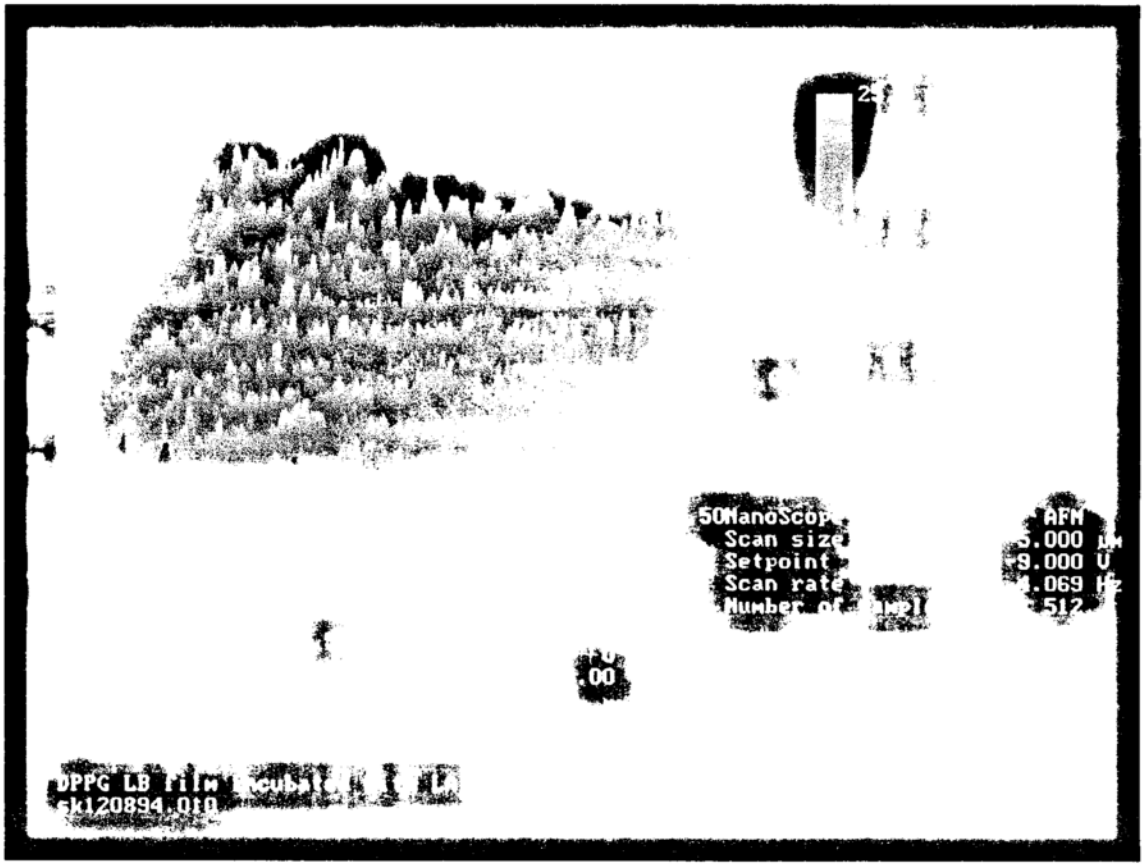

Figure 75. AFM image of a DPPG bilayer supported on mica incubated with LAI (5μg/35 ml) in 10 mM Tris-HCl, pH 7.4, 5μM $CaCl_2$ at 25°C after 30 minutes.

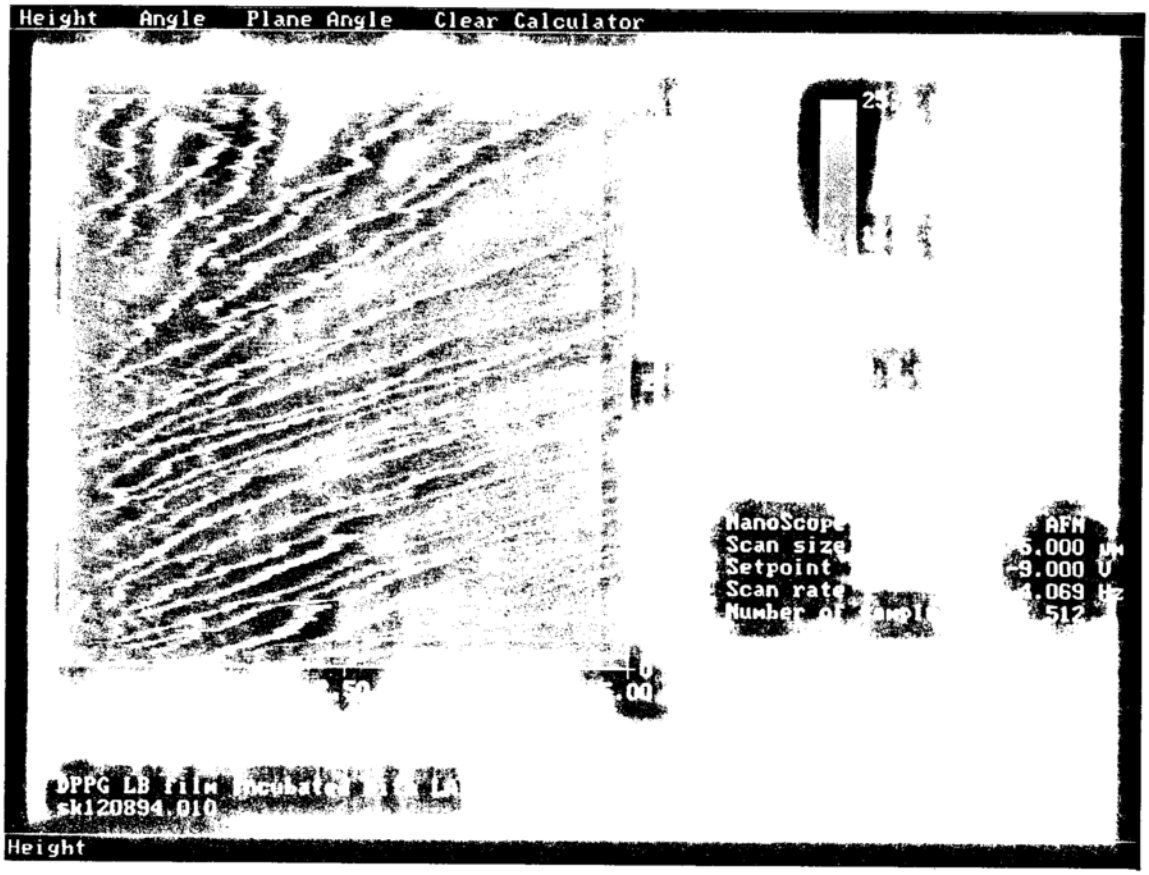

Figure 76. AFM image of a DPPG bilayer supported on mica incubated with LAI (5μg/35 ml) in 10 mM Tris-HCl, pH 7.4, 5μM $CaCl_2$ at 25°C after 30 minutes (top view).

above (Figure 77). The maximum height analysis (Table VII) shows a change of 27 nm upon addition of LAI over the maximum height of 2 nm measured with the DPPG film alone providing additional evidence for the presence of significant amounts of adsorbed protein. The SDS removed the majority of the adsorbed protein and reduced the maximum height in the sample back down to 7 nm, within experimental error of the original value obtained in the presence of the DPPG bilayer alone. It is unclear from these experiments if the DPPG bilayer is intact after the SDS wash although it would be expected to be removed as well due to the possible strong ionic interactions between SDS and mica.

The next series of experiments investigated the ability to reverse protein adsorption by washing with an EDTA containing buffer. The DPPG planar bilayer on mica (Figure 78) was incubated with LAI solution and the resulting adsorption of protein was imaged after 15 minutes (Figures 79) and after 40 minutes (Figure 80). There appeared to be significant amounts of protein adsorption as was reported above for an identical system (Figures 68 to 76). The system was then washed with 10 mM Tris-HCl, pH 7.4 and 1 mM EDTA solution in order to see if protein adsorption could be reversed. No significant loss in the amount of adsorbed protein could be observed as can be seen in Figure 81 and no change in the height analysis results could be measured (Table VIII). However, the 10% SDS solution was able to remove the adsorbed protein (Figure 82). The maximum height change analysis (Table VIII) revealed that an increase of 9 nm over the measured value in the absence of protein occurred upon adsorption of the protein. Washing with SDS returned the maximum height back to the baseline value within experimental error. It is therefore concluded that LAI adsorption mediated by calcium can not be reversed by the subsequent addition of EDTA in agreement with $\Delta\pi$ experiments performed above which demonstrated the irreversibility of the calcium-mediated interactions.

Table VII. Maximum height change analysis

Image	Maximum height change (nm)
Mica with bilayer in buffer	1.9
Mica with bilayer + LAI solution	29.4
10 % SDS wash	6.9

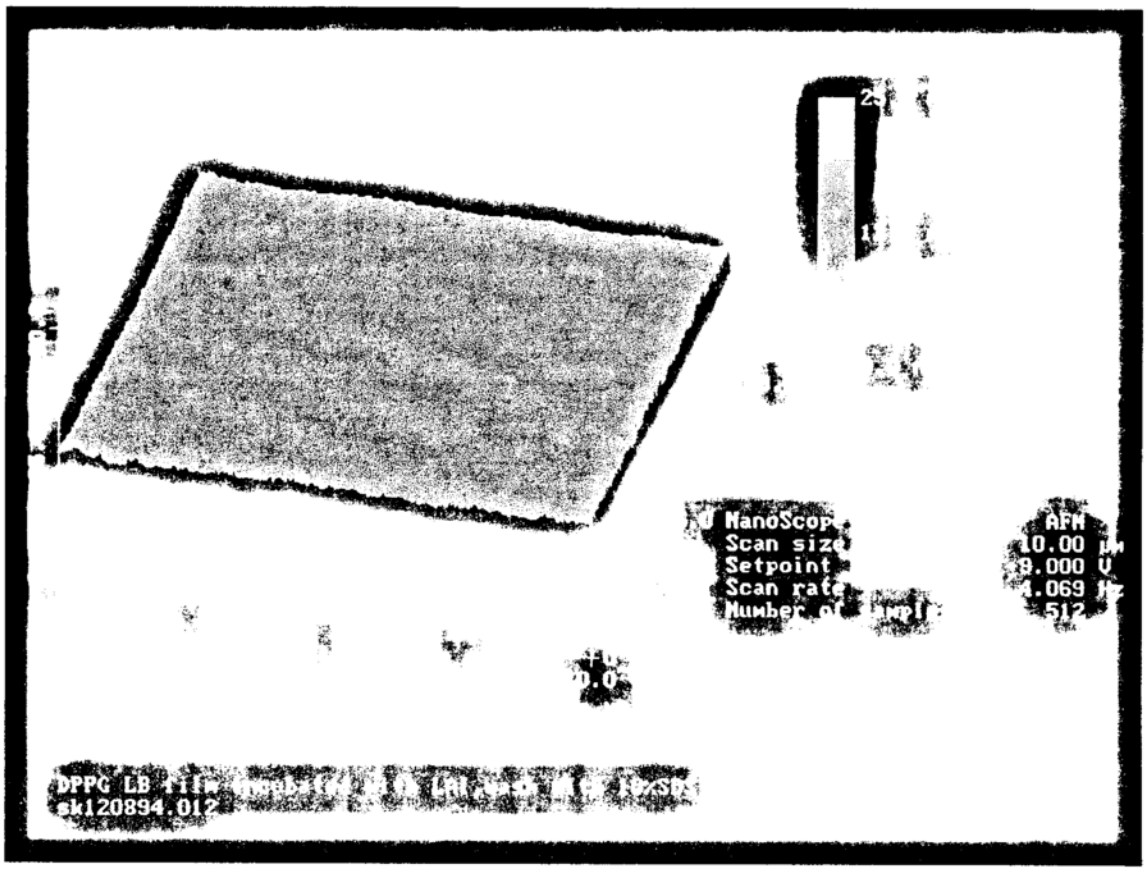

Figure 77. AFM image of a DPPG bilayer supported on mica incubated with LAI (5μg/35 ml) in 10 mM Tris-HCl, pH 7.4, 5μM $CaCl_2$ at 25°C and then washed with 10% SDS.

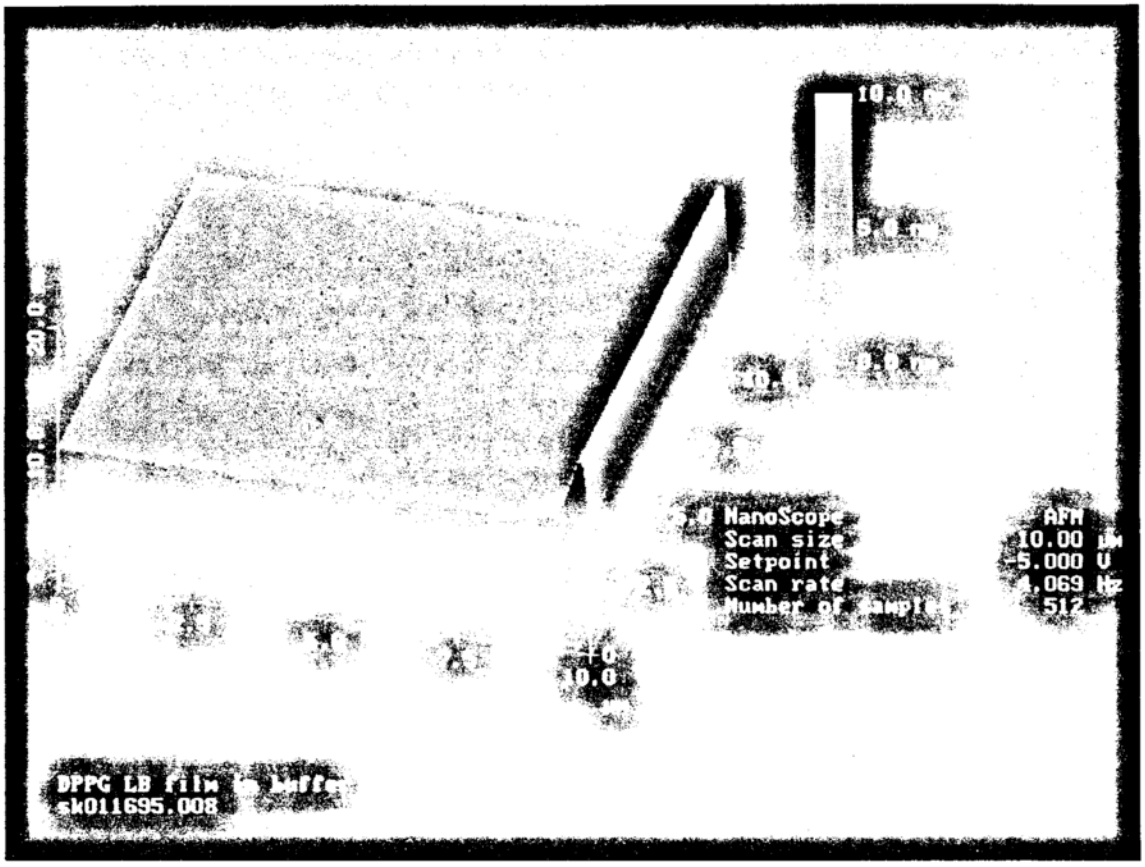

Figure 78. AFM image of a DPPG bilayer supported on mica in 10 mM Tris-HCl, pH 7.4, 5µM $CaCl_2$ at 25°C.

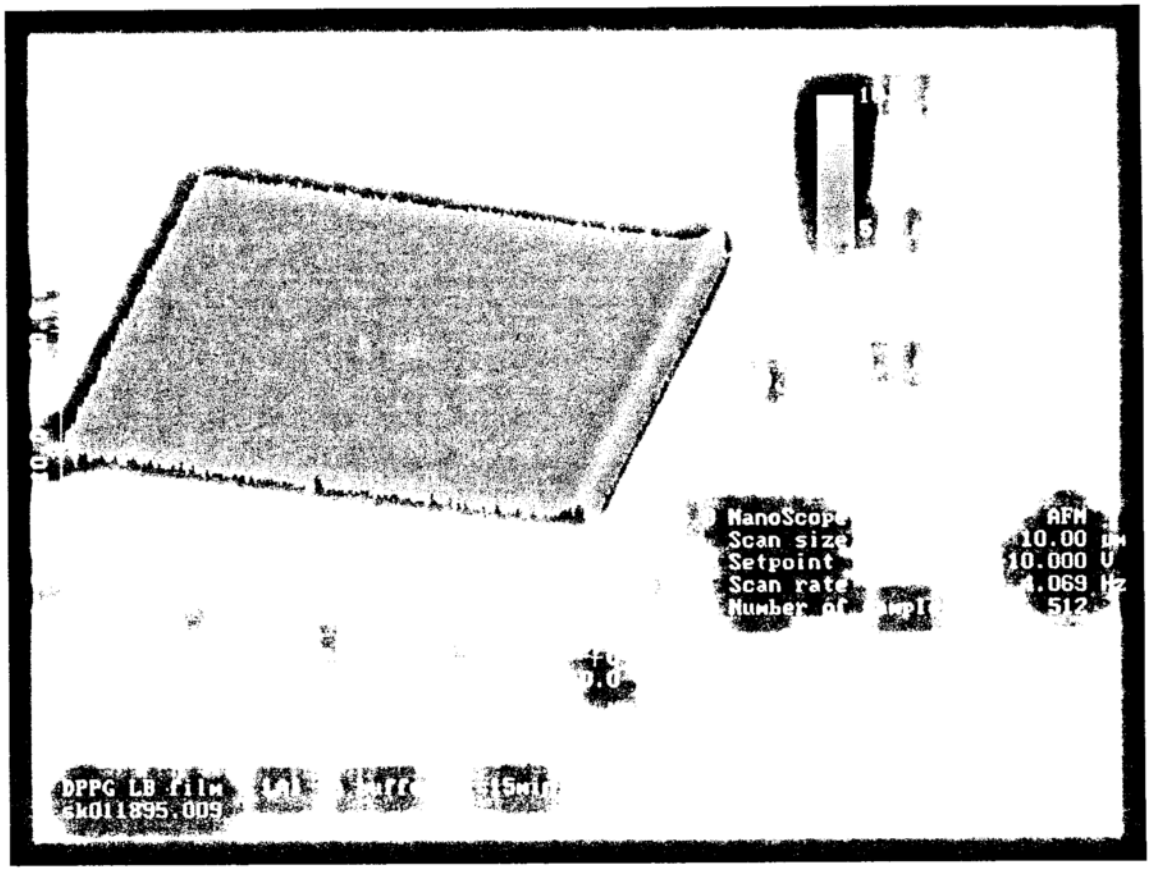

Figure 79. AFM image of a DPPG bilayer supported on mica incubated with LAI (5μg/35 ml) in 10 mM Tris-HCl, pH 7.4, 5μM $CaCl_2$ at 25°C after 15 minutes.

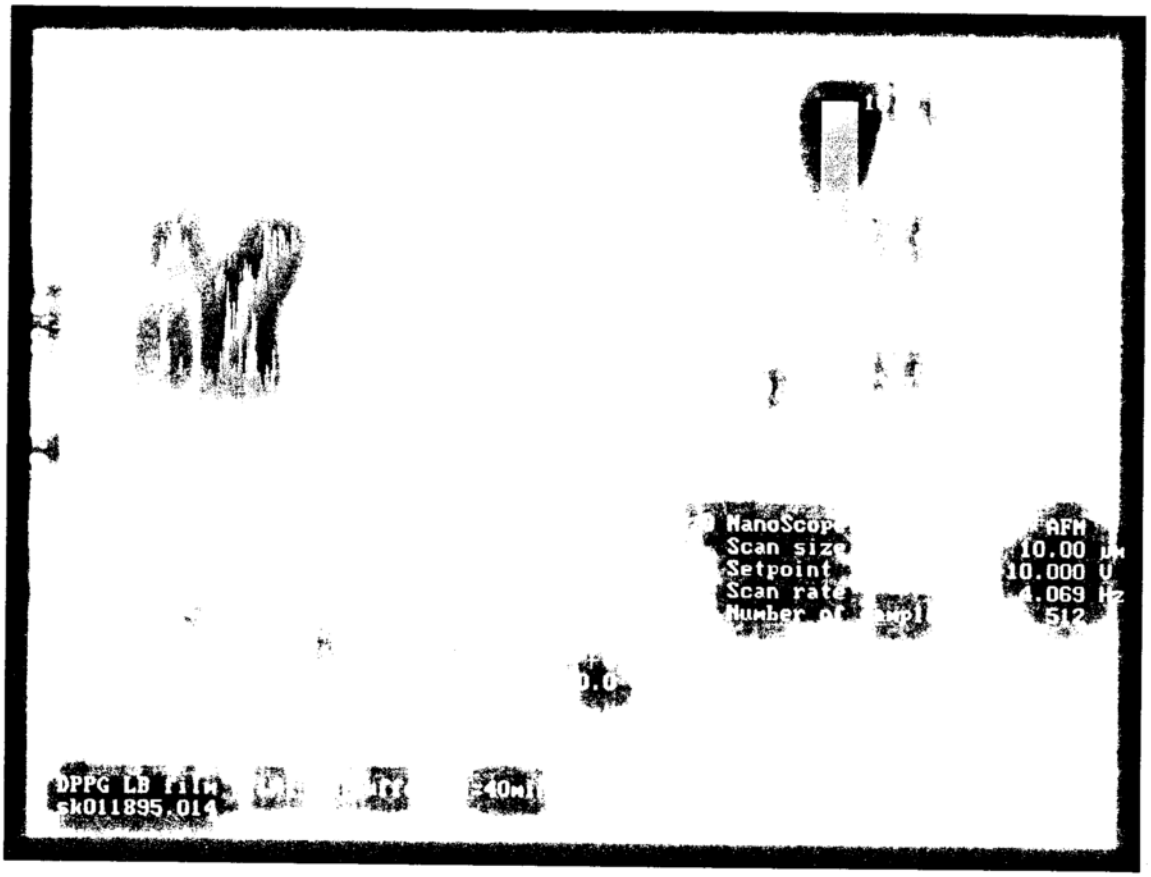

Figure 80. AFM image of a DPPG bilayer supported on mica incubated with LAI (5μg/35 ml) in 10 mM Tris-HCl, pH 7.4, 5μM $CaCl_2$ at 25°C after 40 minutes.

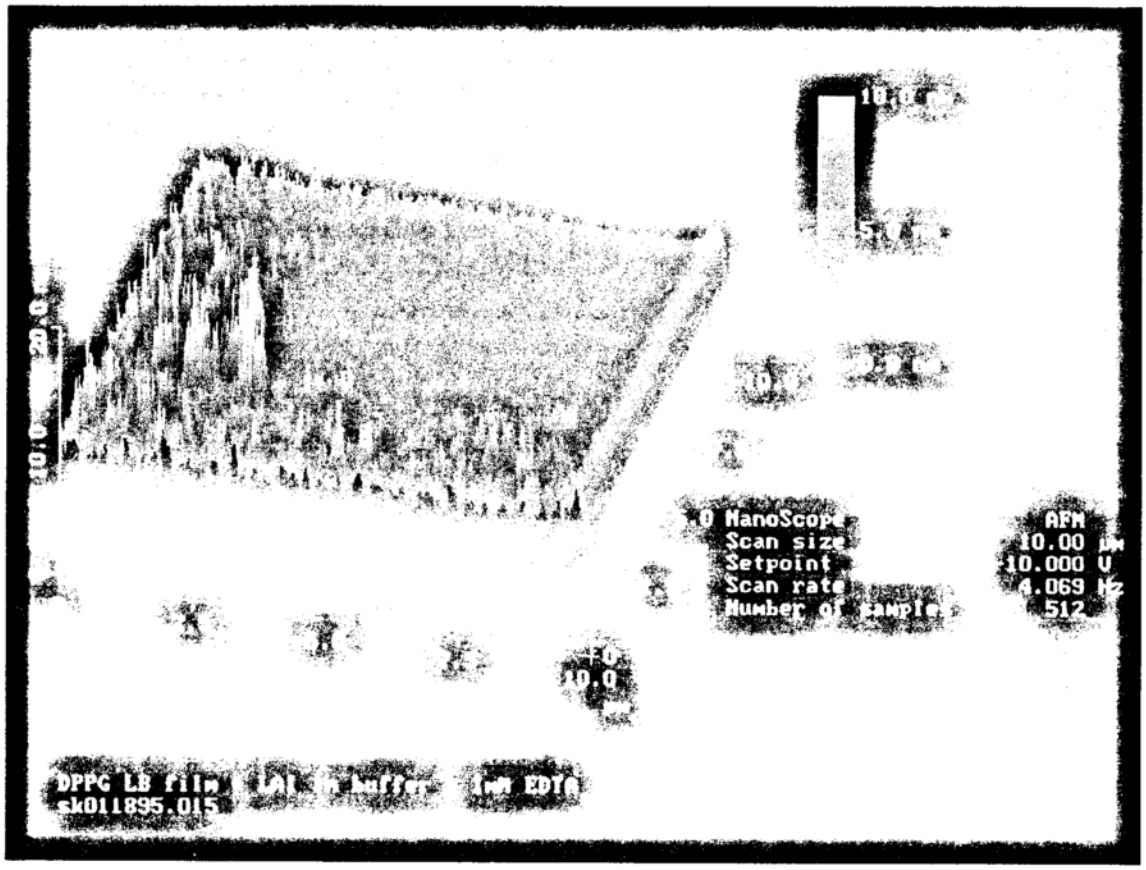

Figure 81. AFM image of a DPPG bilayer supported on mica incubated with LAI (5µg/35 ml) in 10 mM Tris-HCl, pH 7.4, 5µM $CaCl_2$ at 25°C then washed with 10 mM Tris-HCl, pH 7.4,1 mM EDTA.

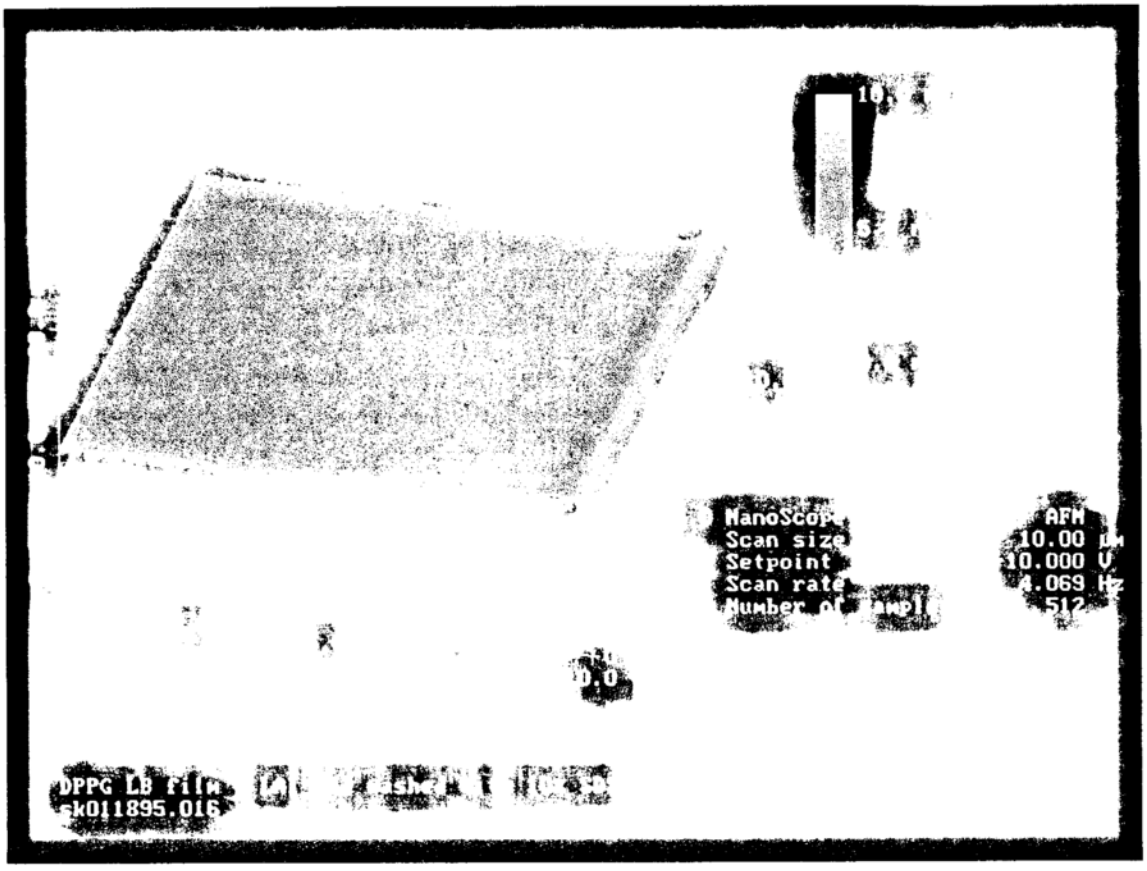

Figure 82. AFM image of a DPPG bilayer supported on mica incubated with LAI (5µg/35 ml) in 10 mM Tris-HCl, pH 7.4, 5µM $CaCl_2$ at 25°C then washed with 10% SDS.

Table VIII. Maximum height change analysis

Image	Maximum height change (nm)
Mica with bilayer in buffer	6.4
Mica with bilayer + LAI solution	15.0
1 mM EDTA wash	15.0
10 % SDS wash	4.2

The last experiment performed with LAI probed the role of calcium in the adsorption of the protein to the bilayer covered mica surface. Figure 83 is the image of the bilayer on mica which again shows no significant features at a resolution of 25 nm in the z-direction. This bilayer was then incubated with LAI in an EDTA containing buffer. Figures 84 to 86 are the images obtained 30, 45, and 60 minutes after addition of the protein solution. Tall, broad peaks distributed in a random fashion were imaged and are similar in appearance to those obtained in Figures 64 and 65, indicative of nonspecific binding. A small increase in the maximum height in the sample was observed upon addition of the protein and the baseline value was recovered upon washing with SDS (Table IX). The above experiments demonstrate that, although some non-calcium-dependent binding of LAI to mica or DPPG bilayer coated mica occurs, strong LAI binding to supported DPPG bilayers requires the presence of calcium. This conclusion assumes that the EDTA buffer did not affect the DPPG supported bilayer, which is reasonable given the experiment described above in Figures 79 to 81 which showed that EDTA was not able to remove any adsorbed material.

Similar experiments were performed with the 33 kDa PLBP. The DPPG supported bilayer was formed (Figure 88) in buffer and then incubated with the 33 kDa solution (5μg/35 ml). Images obtained 15 (Figure 89) and 30 (Figure 90) minutes after introduction of the protein were obtained and tall, broad peaks, in excess of that expected for nonspecific adsorption (i.e. Figures 64, 65, and 84 to 86), were observed in the presence of protein presumably due to the adsorption of the protein. Once again, the material could only be removed upon washing with a 10% SDS solution (Figure 91). The maximum height analysis (Table X) shows a height change of approximately 20 nm upon addition of the protein and a return back to the baseline value after washing with SDS (Table X). This preliminary AFM imaging

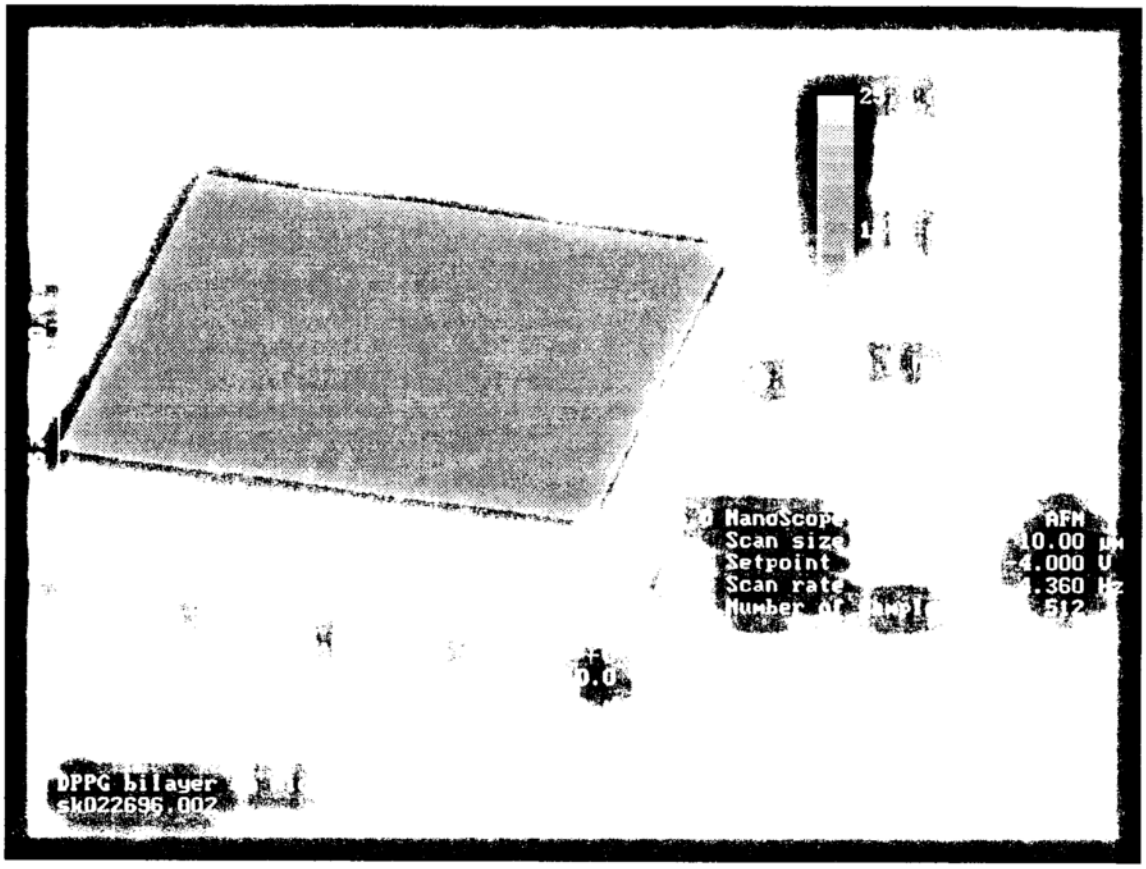

Figure 83. AFM image of a DPPG bilayer supported on mica in 10 mM Tris-HCl, pH 7.4, 1 mM EDTA at 25°C.

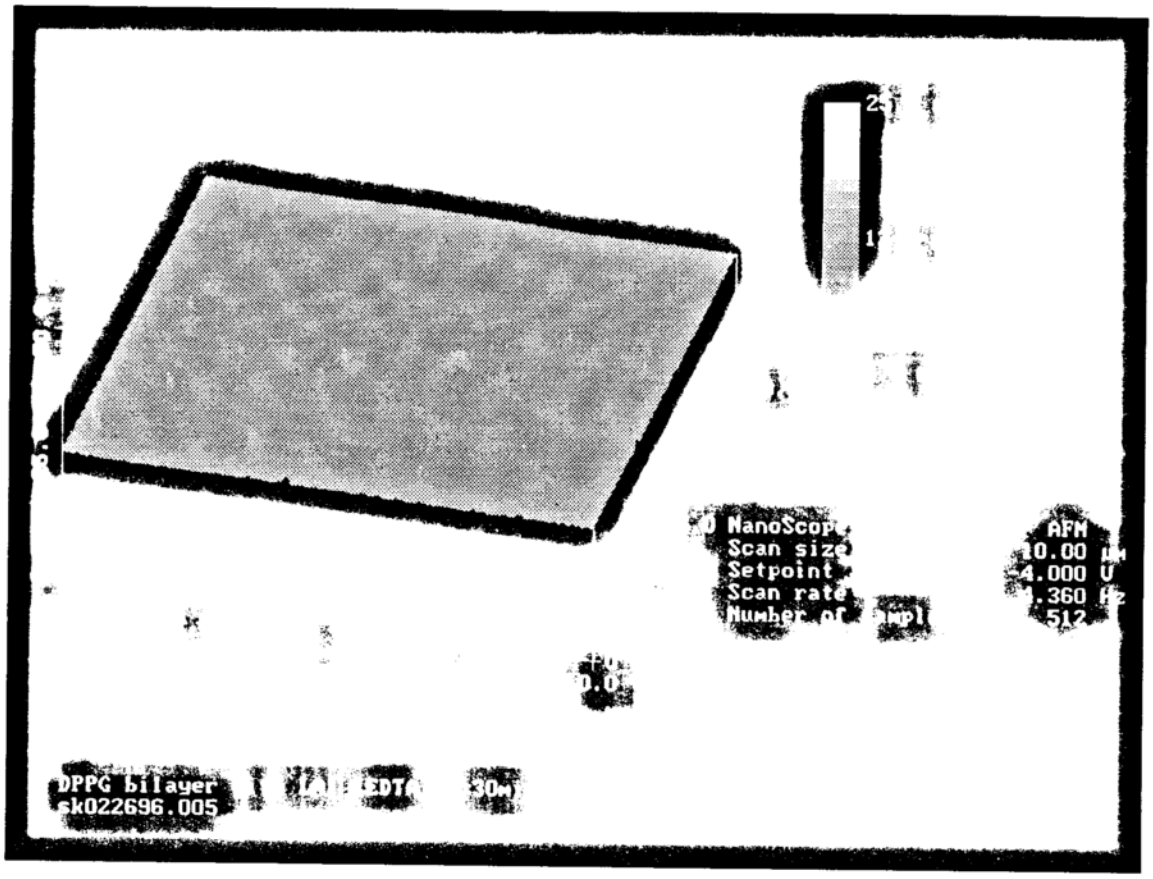

Figure 84. AFM image of a DPPG bilayer supported on mica incubated with LAI (5μg/35 ml) in 10 mM Tris-HCl, pH 7.4, 1 mM EDTA at 25°C after 30 minutes.

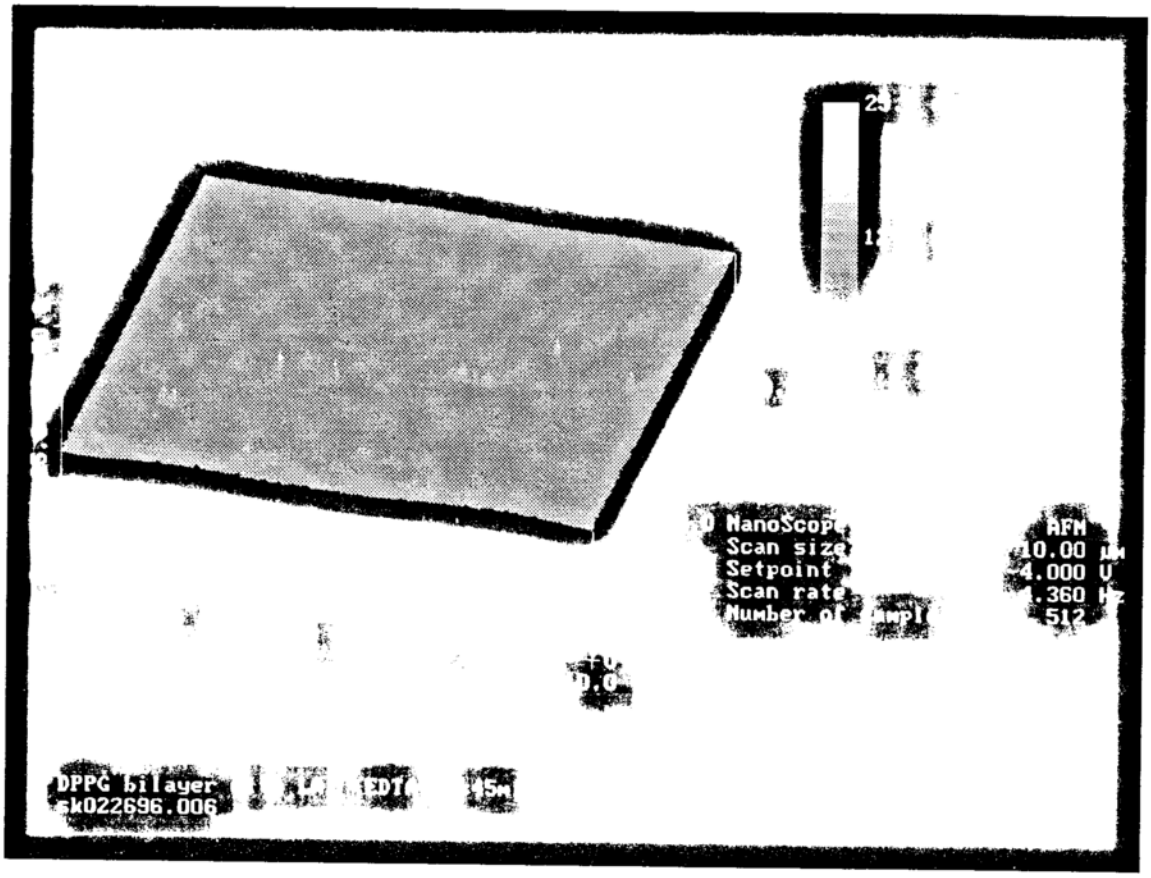

Figure 85. AFM image of a DPPG bilayer supported on mica incubated with LAI (5μg/35 ml) in 10 mM Tris-HCl, pH 7.4, 1 mM EDTA at 25°C after 45 minutes.

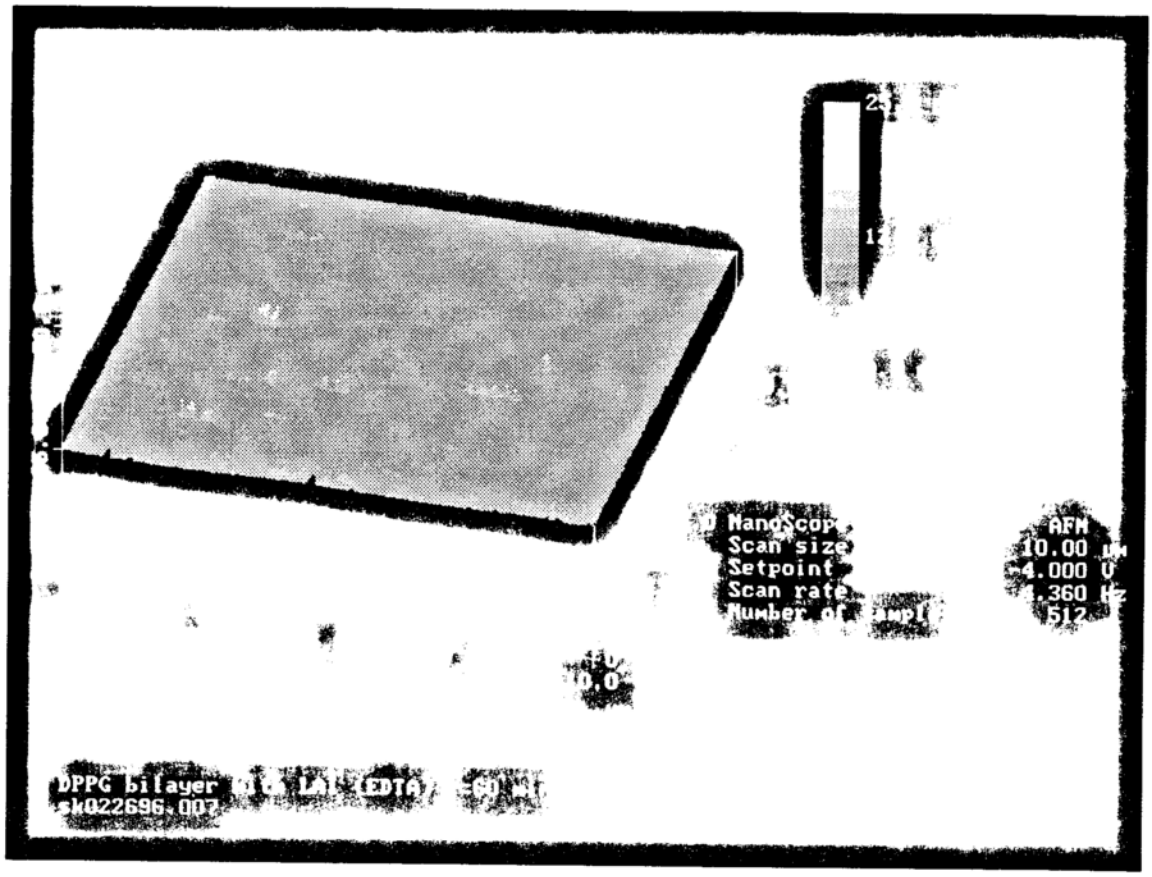

Figure 86. AFM image of a DPPG bilayer supported on mica incubated with LAI (5μg/35 ml) in 10 mM Tris-HCl, pH 7.4, 1 mM EDTA at 25°C after 60 minutes.

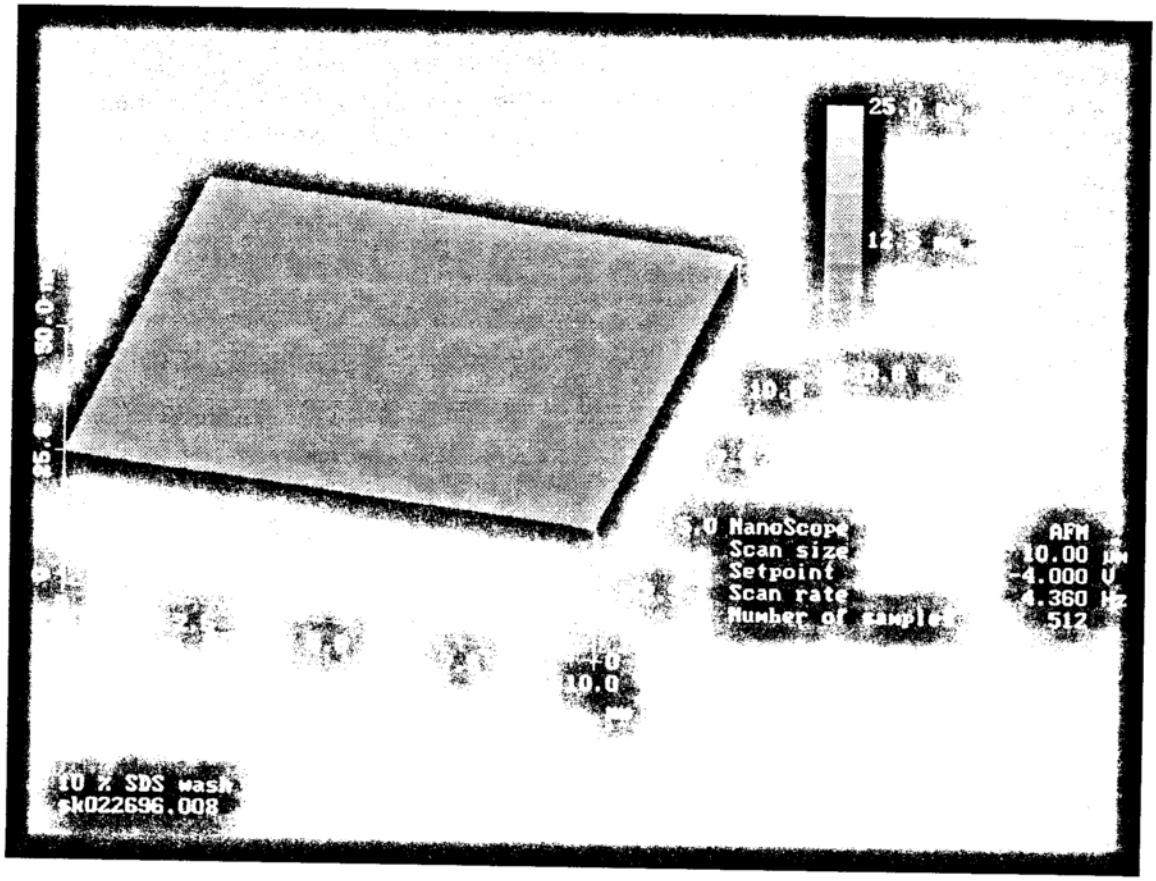

Figure 87. AFM image of a DPPG bilayer supported on mica incubated with LAI (5µg/35 ml) in 10 mM Tris-HCl, pH 7.4, 1 mM EDTA at 25°C then washed with 10% SDS.

Table IX. Maximum height change analysis

Image	Maximum height change (nm)
Mica with bilayer in EDTA buffer	2.6
Bilayer + LAI solution in EDTA buffer	7.3
10 % SDS wash	1.0

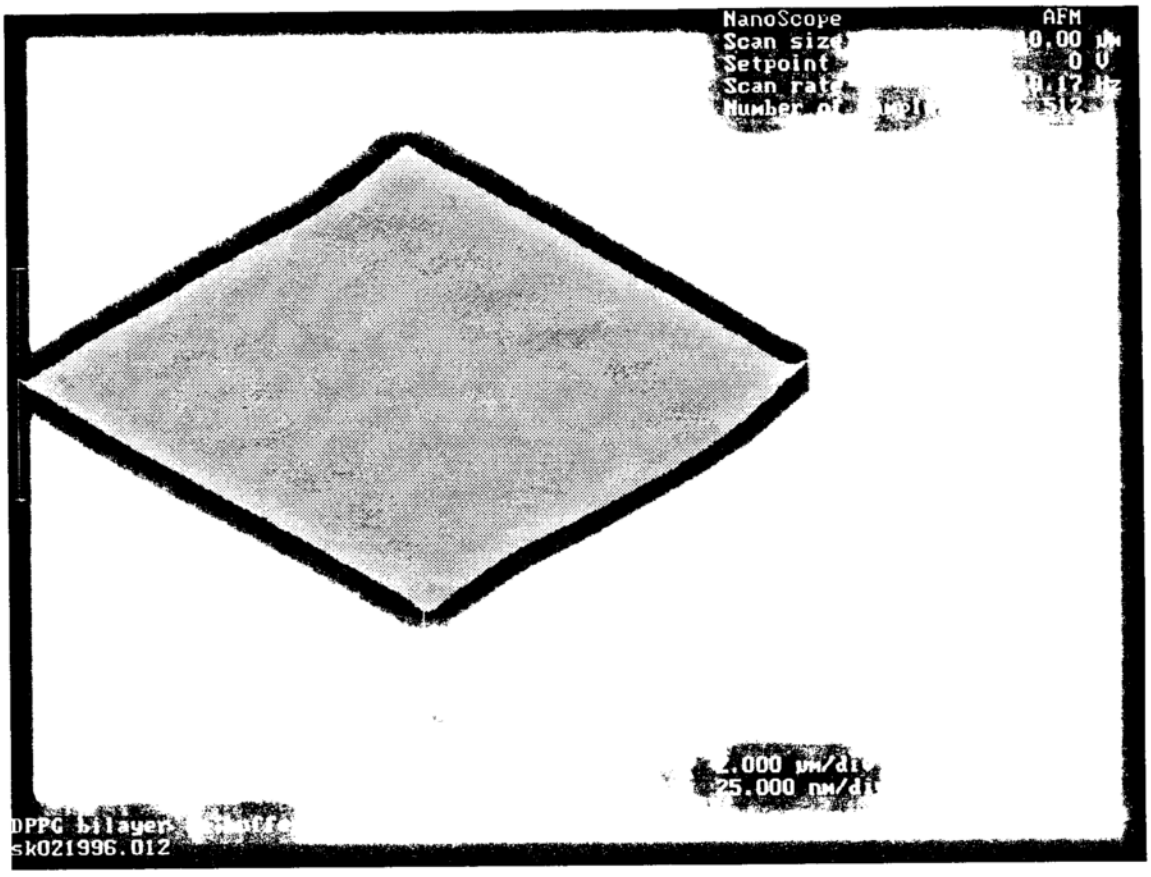

Figure 88. AFM image of a DPPG bilayer supported on mica in 10 mM Tris-HCl, pH 7.4, 5 µM $CaCl_2$ at 25°C.

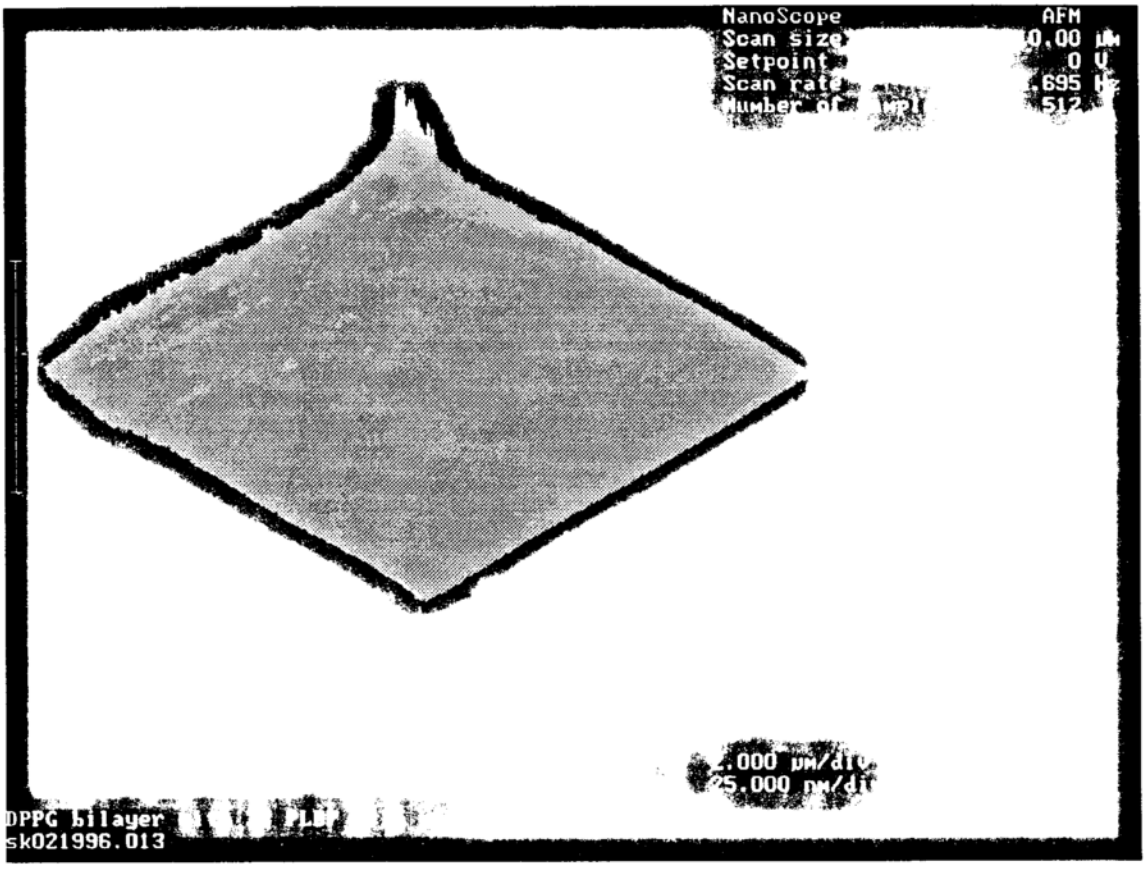

Figure 89. AFM image of a DPPG bilayer supported on mica incubated with 33 kDa PLBP (5μg/35 ml) in 10 mM Tris-HCl, pH 7.4, 5 μM $CaCl_2$ at 25°C after 15 minutes.

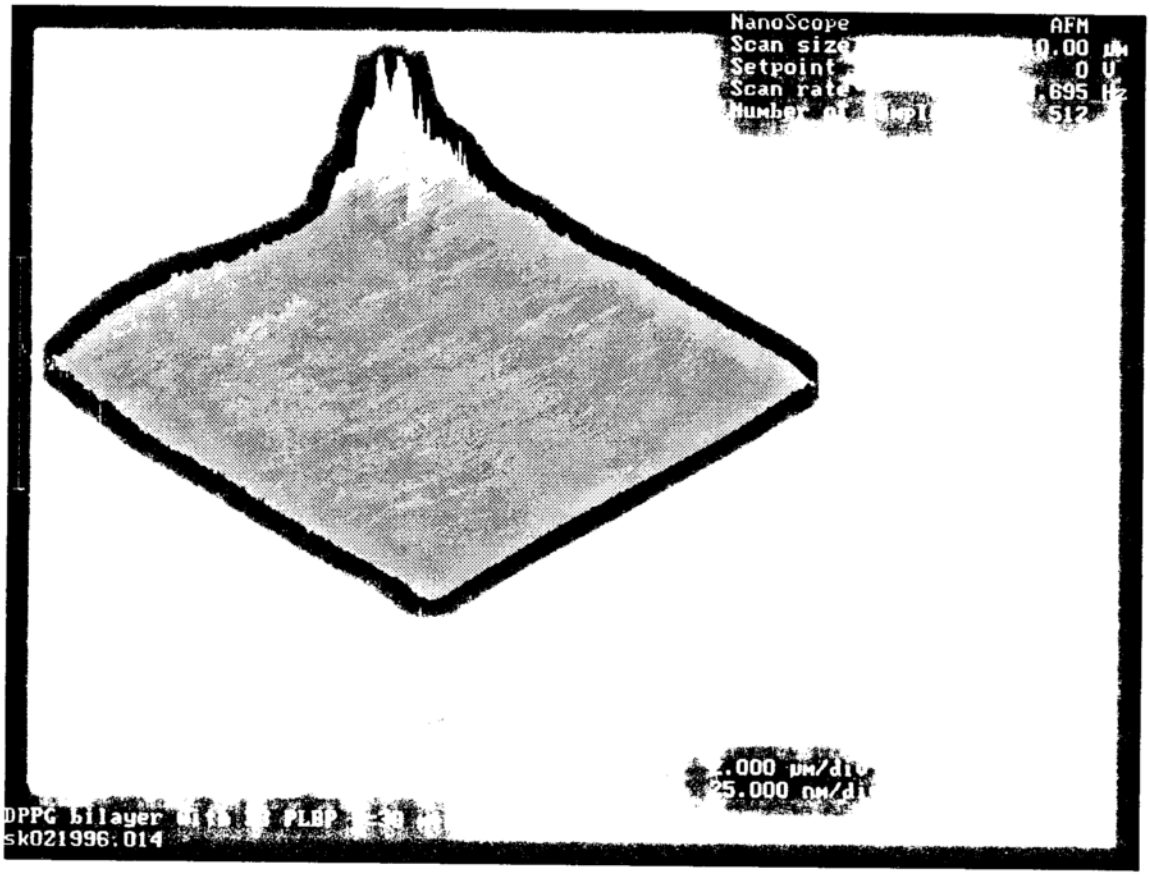

Figure 90. AFM image of a DPPG bilayer supported on mica incubated with 33 kDa PLBP (5µg/35 ml) in 10 mM Tris-HCl, pH 7.4, 5 µM $CaCl_2$ at 25°C after 30 minutes.

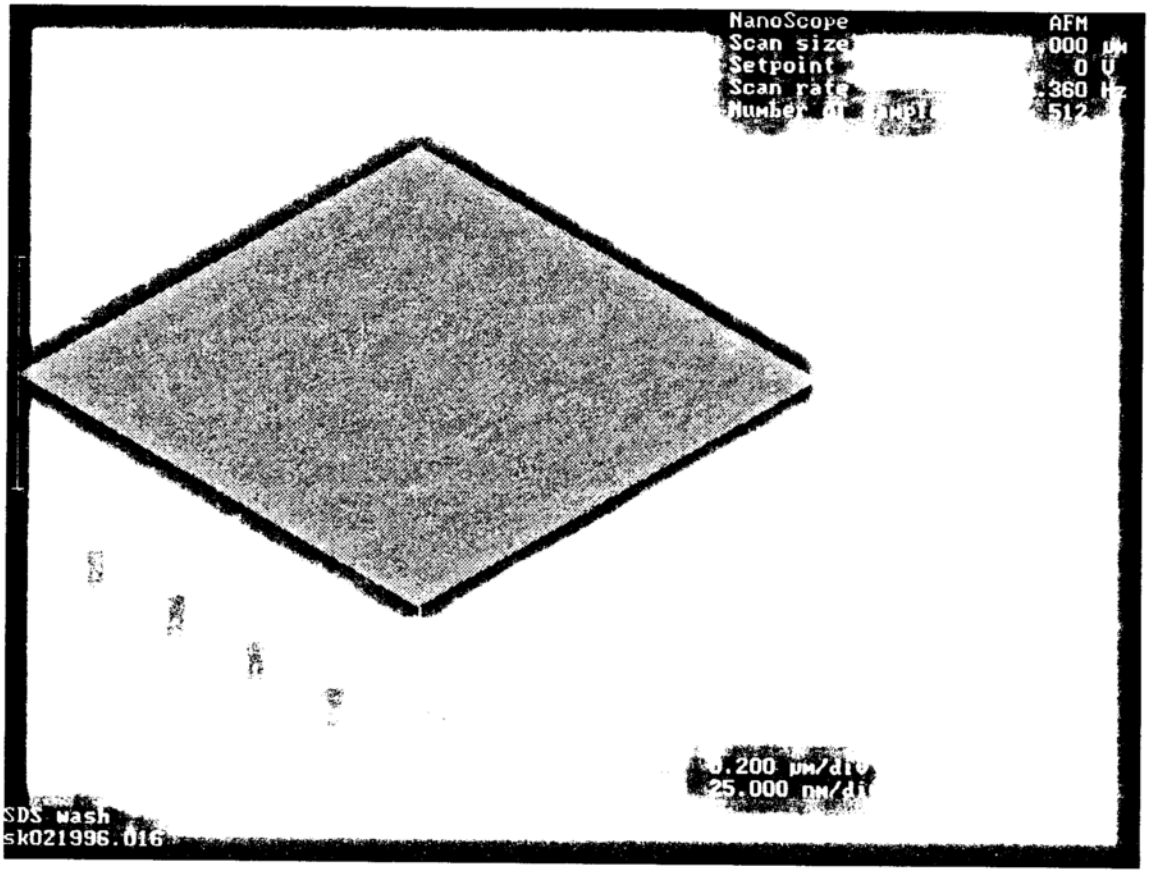

Figure 91. AFM image of a DPPG bilayer supported on mica incubated with 33 kDa PLBP (5µg/35 ml) in 10 mM Tris-HCl, pH 7.4, 5 µM $CaCl_2$ at 25°C after washing with 10% SDS.

Table X. Maximum height change analysis

Image	Maximum height change (nm)
Mica with bilayer in buffer	45.1
Mica with bilayer + 33 kDa solution	66.3
10 % SDS wash	1.4

experiment is the first piece of data collected which provides evidence that the 33 kDa PLBP interacts with DPPG monolayers even at surface pressures as high as 35 mN/m.

Discussion

The experiments reported in the previous results section were primarily aimed at determining the affinity and specificity of LAI for phospholipids, the factors that govern these interactions and, finally, the influence LAI-phospholipid interactions on certain structural features of model phospholipid monolayers that may relate to the ability of LAI to affect lipid storage and release in the lung. In addition, a comparison was made between LAI and another lung-associated annexin-like protein, 33 kDa PLBP, and an inactive breakdown product of LAI, LAI-bp.

LAI-Phospholipid Interactions

The affinity and specificity of LAI for phospholipids was investigated by measuring the change in surface pressure, $\Delta\pi$, upon injection of LAI beneath a variety of single-component and binary monolayers at a low initial surface pressure of 5mN/m. Table XI lists the $\Delta\pi$ values in the absence of a monolayer and for several lipids and lipid mixtures (taken from Figures 51 and 55) all at an initial surface pressure of 5 mN/m. In the absence of a monolayer, no $\Delta\pi$ can be measured, while in the presence of a lipid monolayer the addition of LAI appears to have an increased affinity for the interface. The $\Delta\pi$ value for zwitterionic DPPC was found to be significantly smaller than DPPG or any of the other phospholipid monolayers containing the anionic lipid, PG. This supports the hypothesis that there are indeed, specific interactions that occur between LAI and anionic phospholipids.

Further evidence was gathered supporting the hypothesis that LAI interacts specifically with anionic lipids from the experiments performed with the mixed

Table XI. Change in surface pressure upon injection of LAI (5μg) into the subphase (10 mM Tris, pH 7.4 with 5μM $CaCl_2$, 25°C) in the absence and presence of phospholipid monolayers. The initial area/molecule, A_i, is listed at the initial surface pressure, π_i, of 5.0 ± 0.5 mN/m for all monolayers.

Lipid	$\Delta\pi$/(mN/m)	A_i,/(nm^2/molecule)
None	0	-----
DPPC	1.8 ± 0.4	0.767
DPPG	9.4 ± 0.0	0.462
POPG	14.2 ± 1.1	0.834
DOPG	7.9 ± 1.3	0.968
DPPC/DPPG	8.0 ± 0.2	0.535
DPPC/POPG	12.2 ± 0.2	0.918

DPPC/PG monolayers. Figure 55 shows that low $\Delta\pi$ values $\approx$ 2 mN/m were obtained in the presence of only 10 mol% anionic lipid, the same value expected when a pure DPPC monolayers is spread, thus indicative of non-specific interactions. The interactions, as measured by $\Delta\pi$, however, are significantly increased by increasing the amount of anionic lipid to 30 mol%. Increases above 50 mol% did not increase $\Delta\pi$ significantly suggesting that there may be a specific stoichiometry that exists between LAI and the number of anionic lipids necessary to maximize LAI-anionic phospholipid interactions.

Beyond ionic interactions, it is of interest to determine the important surface structural parameters that govern the LAI-phospholipid interactions. Comparison of results for the three PG lipids at a relatively low π_i (5mN/m) suggests that the interaction of LAI with anionic PG lipid monolayers is not governed by the area/ molecule of the monolayer film. It can be observed, for example, that although DOPG is the most expanded monolayer (Table XI), with the largest area/molecule for a given surface pressure, the $\Delta\pi$ value is actually less than that measured for either DPPG or POPG. In addition, although the $\Delta\pi$ values for DPPG and POPG are close to their mixed counterparts, i.e. DPPC/DPPG and DPPC/POPG, the corresponding areas /molecule are very different.

In order for LAI to penetrate a monolayer covered interface, one would assume that there must be sufficient void space to accommodate the protein. Therefore, an attempt was made to correlate the measured $\Delta\pi$ values with free area, A_f, which is defined as,

$$A_f = A - A_0 \qquad (9)$$

Table XII. The occupied area/molecule, A_0, for phospholipid monolayersspread on 10 mM Tris, pH 7.4, 25°C and 5μM $CaCl_2$.

Lipid	A_0,/(nm^2/molecule)
DPPC	0.420
DPPG	0.420
POPG	0.520
DOPG	0.720

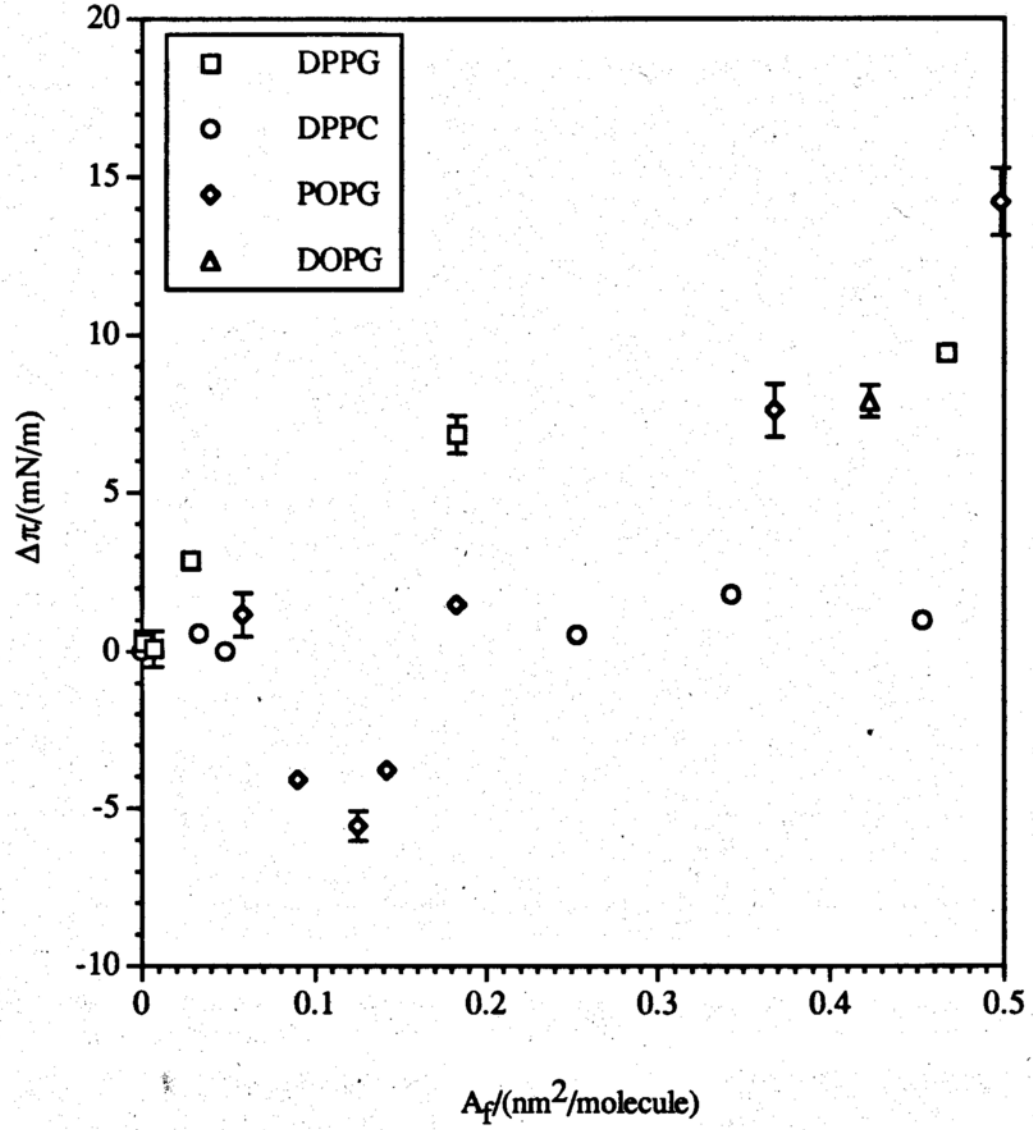

Figure 92. The change in surface pressure upon injection of LAI (5μg) below monolayers spread on 10 mM Tris-HCl, pH 7.4, 25°C and 5μM $CaCl_2$.as a function of the free area in the monolayer.

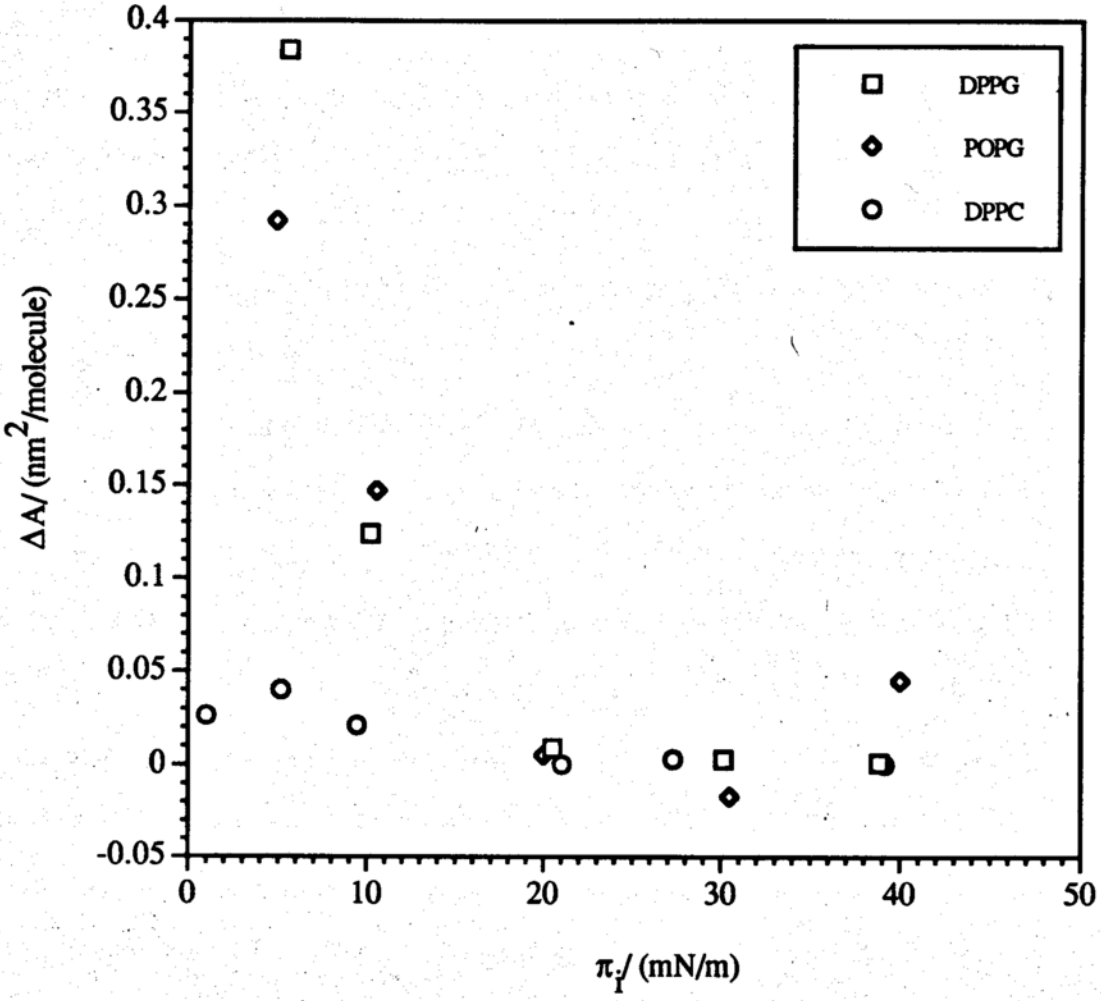

Figure 93. The change in area/molecule upon injection of LAI (5μg) below monolayers at various initial surface pressures spread on 10 mM Tris-HCl, pH 7.4, 25°C and 5μM $CaCl_2$.

where A is the calculated area/molecule and A_0 is the occupied area, or the area/molecule at closest packing. The A_0 is obtained from the π-A isotherm at the point of monolayer collapse, and values for the various lipids are listed in Table XII. The results of $\Delta\pi$ experiments (Figure 51) were plotted as a function of the free area available in the monolayer (Figure 92.) and comparing DPPC and any of the PG lipids at large A_f (low π_i) it is apparent that $\Delta\pi$ is not controlled by free area alone. However, at large A_f (i.e. > 0.2) it appears as though a correlation may exist between A_f and $\Delta\pi$ with the three molecules in the PG lipid series. This suggests that LAI-phospholipid monolayer interactions at low π_i are driven both specific interaction with anionic lipids and free area.

A similar correlation was also found to exist between ΔA and π_i (Figure 93), where ΔA is the corresponding change in area for the given $\Delta\pi$ measured, as calculated from the π-A isotherms. This relationship between ΔA and π_i suggests that LAI penetrates anionic lipid monolayers to produce the same ΔA, penetrates to the same extent at a given surface pressure, regardless of the amount of free area. The ΔA values change with surface pressure suggesting that there are different extents of penetration of the protein.

The last parameter to be investigated in this analysis was the effect of monolayer surface pressure itself on the interaction of LAI. The ability of LAI to penetrate anionic lipid monolayers decreases with increasing surface pressure (Figure 51) and is completely excluded at a π_i of 20 to 25 mN/m and higher, regardless of the lipid identity or the amount of available free area (Figure 92 and 51). Thus, it appears as though there is an interfacial pressure barrier to penetration of the protein. Beyond 25 mN/m, $\Delta\pi$ experiments are of limited utility in detecting protein-lipid interactions especially with more condensed lipid monolayers such as DPPG and therefore other methods, such as direct imaging (to be described below) or indirect detection i.e. via

radiolabelling the protein, must be used. On the other hand, the interaction of the protein with the POPG monolayer is still detectable with $\Delta\pi$ experiments since from Figure 51, it can be seen that negative $\Delta\pi$ values are obtained for POPG monolayers at 25 mN/m $\leq \pi i \leq$ 35mN/m. A decrease in surface pressure at a constant area under such conditions appears to be indicative of condensation of the monolayer. Therefore at these surface pressures, although the protein is no longer able to penetrate the monolayer, it is able to persist beneath the monolayer and condense the monolayer film. It is interesting to note that a condensation was not observed, in this experiment for DPPG monolayers at π_i = 35 mN/m. Condensation of the DPPG monolayer is not observed most likely because of the limited compressibility of the monolayer. The compressibility (or elasticity) of the monolayer is defined,

$$\text{Compressibility} = \frac{1}{\text{elasticity}} = -\frac{1}{A}\frac{dA}{d\pi}$$

Table XIII lists the compressibilities for a DPPG monolayer and a POPG monolayer at a surface pressure of 30 mN/m. The DPPG, at a surface pressure of 30 mN/m is less compressible than the POPG monolayer at the same surface pressure and therefore we might expect the interaction of the protein not to cause any significant change in the area/molecule within the monolayer and thus does not affect surface pressure. The POPG monolayer, in contrast, is relatively compressible and in this case we might expect the interaction of the protein to reduce the area/molecule of the lipid film, causing a drop in surface pressure. For all of the monolayers studied, no interactions of the protein with the lipid monolayer could be detected at π_i of $\approx$ 40 mN/m or greater using $\Delta\pi$ experiments. Direct measurement of protein adsorption at these higher surface pressures will be required to study this further.

Table XIII. The compressibility of PG monolayers spread on 10 mM Tris-HCl, pH 7.4, 25°C, and 5μM $CaCl_2$, at a surface pressure of 30 mN/m.

Lipid	Area/molecule/ (nm^2/molecule)	Compressibility/ (mN^{-1})
DPPG	0.402	0.000711
POPG	0.618	0.00719

To further assess the effects of π or A on protein penetration additional lipid was added to an existing DPPG monolayer in which protein penetration had already occurred (Figure 54). In this experiment, it was observed that larger $\Delta\pi$ values were obtained for a given π_i than in an experiment where protein was added at a fixed π_i. This would indicate that the protein is able to resist expulsion from the monolayer if it had been already incorporated when the monolayer was formed. This observation may have relevance on short time scales, on the order of several hours, as was the case in this experiment however, it is expected that the $\Delta\pi$ values would equilibrate back to those obtained in the standard experiment given an longer time frame. In other words, these observations are most likely meta-stable states that would return back to the equilibrium values measured above in the standard experiment (Figure 51). These kinetic effects could not be studied further at this time due to experimental limitations, but interestingly, the π_i at which "squeeze-out" or expulsion of LAI from the DPPG monolayer occurs is approximately at the same surface pressure regardless of how the experiment is carried out, emphasizing the significance of surface pressure as the barrier to LAI penetration. The negative $\Delta\pi$ value at a surface pressure of 35 mN/m in this "squeeze-out" experiment (Figure 54) is a further indication that LAI is still associated with the DPPG monolayer. This was not observed in the standard experiment described previously (Figure 51) and is most likely also a kinetic phenomenon, since surface diffusion of molecules at these surface pressures is small (Kim and Yu, 1992).

The AFM images reported above provide further evidence that both LAI and the 33kDa PLBP still interact with condensed and ordered DPPG layers, even at surface pressures as high as 35 mN/m, the pressure at which the DPPG monolayer was transferred for imaging experiments. While some nonspecific adsorption of protein was observed on mica, the presence of the DPPG bilayer significantly enhanced the

amount of adsorbed protein (i.e. Figures 68 to 76). The protein appears to engage in lateral protein contacts so that large (2 to 4 μm) branch-like structures are formed. At this protein concentration, aggregation of protein appears to occur, resulting in large peaks in the AFM images. Further experiments need to be done to test the feasibility of using a DPPG bilayer as a template for the growth of three-dimensional crystals of LAI.

The interaction of LAI with phase separated DPPC/POPG (1:1) binary monolayers was found to be significantly different from the observations made above for single component monolayers. In both systems, the interaction of LAI caused an increase in surface pressure at relatively small π_i and $\Delta\pi$ decreased with increasing surface pressure. However, "squeeze-out" or expulsion of LAI occurs at π_i of only 15 mN/m and a condensation of the monolayer is noticed at pressures as low as 20 mN/m. A likely cause for these large discrepancies is the difference in the homogeneity of the monolayer. While the single component anionic monolayers are homogeneous in charge distribution throughout the monolayer, the binary monolayer is highly phase separated and would necessarily have an inhomogeneous distribution of charges which could effect the interaction of the protein with the monolayer (to be discussed below).

An important question in any study of a surface active material concerns the amount of material that has accumulated at the interface i.e. the surface concentration, Γ. Although the application of any form of the Gibbs adsorption equation to LAI-anionic phospholipid interactions is of questionable utility because of the existence of specific interactions (as described above), an attempt was made to calculate the apparent surface excess of LAI beneath a DPPG monolayer at a π_i of 5 mN/m using the data in Figure 46 and equations (10), (11) and (12). The plot of π versus concentration is given in Figure 94. A reasonable linear fit is obtained for $5 < \pi < 17$ mN/m. Using the area/molecule at a surface pressure of 5 mN/m for $\hat{A}_I$ and at 15

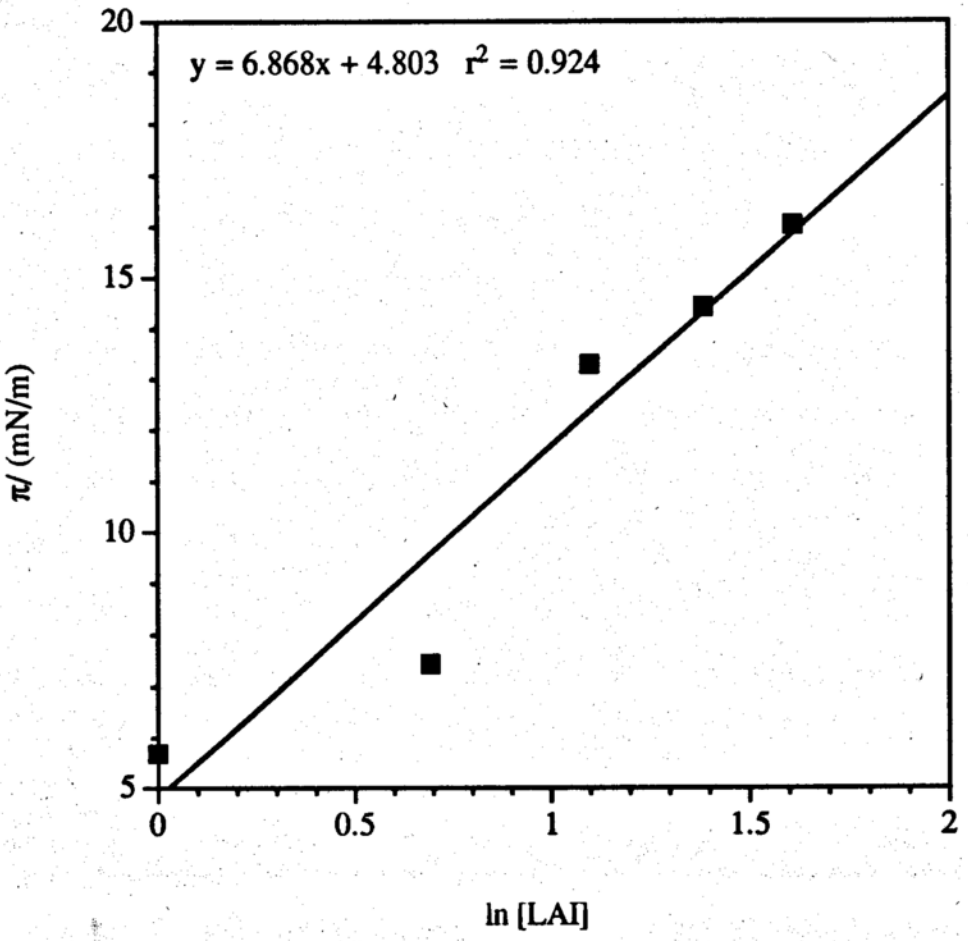

Figure 94. A plot of the final surface pressure as a function of the logarithm of LAI concentration (nM). Data taken from Figure 46.

mN/m for $\overline{A}_I$. Equation (10) gives a Γ_S of 23 mg/m^2 and A_S of 60 Å^2/molecule, while equation (11) gives a Γ_S of 12 mg/m^2 and A_S of 109 Å^2/molecule. The surface concentration values are an order of magnitude greater than what is expected at the bulk LAI concentrations from previos studies (Tsao, Gau et al., 1993). At a bulk concentration of 137 nM, in the absence of a monolayer, Tsao et. al. (Tsao, Gau et al., 1993) measured a surface concentration of LAI of 1.91 mg/m^2. Given the trough area, the amount of LAI necessary to yield surface concentrations of 10 to 20 mg/m^2 , 30 to 60 μg would need to be added to the subphase, and all of it would have to be associated with the surface. The maximum amount of material used in these experiments was 10 μg, so it is clear that the assumptions made in the equations (10) and (11) do not hold for this system i.e. that the surface concentration of DPPG is not sufficiently low, the perturbations due to the monolayer can not be ignored, the LAI concentration can not be interchanged with activity, and that $\overline{A}_I$ and $\overline{A}_S$ are constants.

Calcium dependence of LAI-phospholipid monolayer interactions

The calcium-dependent nature of annexin-phospholipid interactions has been well documented in the literature (Raynal and Pollard, 1994). Therefore, it would be expected that calcium would play an important role in LAI-phospholipid interactions as measured in this study. Experiments with PG monolayers in the absence and presence of calcium have shown that some non-calcium-dependent interaction of LAI with anionic monolayers occurs. However, small amounts of calcium (0.5 μM) significantly enhance these interactions (Figures 47 and 48). The decrease in surface pressure observed at higher levels of calcium (>5 μM) in Figures 47 and 48 most likely occurs because of the ability of calcium to simultaneously affect the DPPG

monolayer, causing it to become more condensed. To understand this more clearly it is helpful to refer back to the Gibbs equation;

$$d\pi = RT\Gamma_I d\log a_I + RT\Gamma_S d\log a_S \qquad (9)$$

Calcium has been shown to increase the intrinsic nonspecific surface activity of the LAI (Tsao, Gau et al., 1993). Therefore the change in surface activity would be expected to affect the second term in equation (9) at low calcium concentrations, and have very little effect on the first term in equation (9). Therefore an increase in surface pressure would be expected as the surface concentration of the species being adsorbed, Γ_S, increases upon being introduced to the sub-solution. At higher calcium concentrations, however, the calcium also has a significant effect on the state of the monolayer. It has been previously observed, for example, that 5 mM $CaCl_2$ significantly condenses both DPPG and POPG monolayers (Koppenol, 1993). This would have a large affect on the first term in equation (9), and thus the initial increases in $\Delta\pi$ shown in Figures 47 and 48 are most likely due to an increase in the surface activity of LAI causing the second term in equation (9) to dominate while the decrease in $\Delta\pi$ is most likely due to the condensation of the monolayer, caused by the higher calcium concentration. This in turn would decrease the protein's ability to penetrate the monolayer.

Additional evidence for the calcium-dependent nature of the LAI-phospholipid interactions is provided by the AFM experiments with DPPG bilayers. Figures 83 through 87 show that adsorption of the protein, to a large extent, is abolished in the presence of EDTA. Only a small amount of non-specific adsorption could be observed in the images, similar to the results obtained in the absence of a bilayer (Figures 63 through 66).

Two independent sets of experiments have illustrated that the calcium-mediated interaction between LAI and anionic phospholipids is not completely reversible upon the addition of EDTA. Experiments were performed where EDTA was introduced into the subphase beneath a monolayer after the system had first been allowed to equilibrate in the presence of calcium, i.e. the experiment outlined in Figure 49, and when similar experiments were carried out with the supported bilayer systems, as seen in the AFM images shown in Figures 78 through 82. In both cases the interaction of the protein with the lipid layer could not be reversed once EDTA was introduced over the time scales of these experiments (up to 8 hours) suggesting that the binding constant of Ca^{2+} is lower for LAI than the dissociation constant for EDTA and Ca^{2+} which is reported to be 10^6 M(Schwarzenbach and Flaschka, 1965). However, if EDTA was added before addition of the protein, specificity of the interaction was lost.

Effects of LAI-phospholipid interactions on the phase equilibria of the phospholipid monolayer

The ability of LAI to mediate fusion of phospholipid vesicles is most likely related to the protein's ability to interact with the lipids (as was shown above), to perturb the lipid organization, in some way, and to facilitate the fusion event. Fluorescence microscopy of the mixed monolayers, in this study, was performed to detect changes in phase equilibria that may occur upon introduction of the protein. For LAI at low surface pressures, when the monolayer is "loosely" packed, the protein appears to interact specifically with the anionic PG lipids in a Ca^{2+}-dependent manner by inserting into the monolayer, causing it to expand and increasing π. The resulting increase in surface pressure shifts the phase equilibria of the monolayer so that it now exhibits properties characteristic of the new surface pressure, i.e. increased phase

separation in the DPPC/POPG mixed monolayers (Figure 57) as was observed in the Results section of this chapter. This is schematically illustrated in Figure 95A. At high surface pressure, when the monolayer is relatively "tightly" packed, the protein is no longer able to penetrate the monolayer but it is able to interact with the monolayer from the subphase side, and condense the anionic PG lipids. This allows the expansion of the other species within the film, thus reducing the surface pressure at the constant area and decreasing the phase separation in the DPPC/POPG mixed monolayers (Figure 58). This is schematically illustrated in Figure 95B.

Comparison of LAI with other lung-associated annexin-like proteins

Finally, the interaction of LAI-bp and 33kDa PLBP was investigated and compared to that of LAI under a few conditions using the binary DPPC/POPG monolayer. The 33 kDa PLBP did interact with the mixed monolayer to a significant extent, beyond the value of 2 to 3 mN/m expected when only non-specific interactions take place but, it did not reach the $\Delta\pi$ values obtained for LAI. The interactions, as measured by $\Delta\pi$, also decreased with increasing π_i, and changes in the phase equilibria of the monolayer, accompanying the increase in surface pressure were observed with LAI. However, in contrast to LAI, no significant condensation or loss in the amount of phase separation was observed at higher π_i with 33 kDa PLBP. Further experiments, when more protein is available, should be carried out to investigate the possible role of calcium in mediating these interactions since it has been previously reported in the literature that the calcium sensitivity of 33 kDa PLBP is different than that of LAI (Tsao, 1990). The LAI-bp interactions resulted in $\Delta\pi$ values that were indicative of non-specific interactions i.e. 2mN/m. This observation strongly suggests that the N-terminus, although it may not be directly involved with phospholipid-

A.

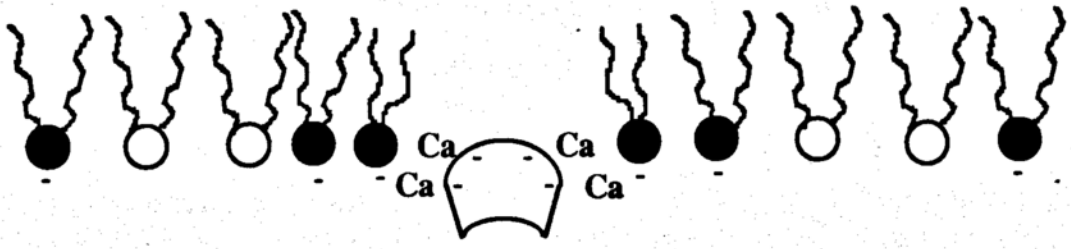

B.

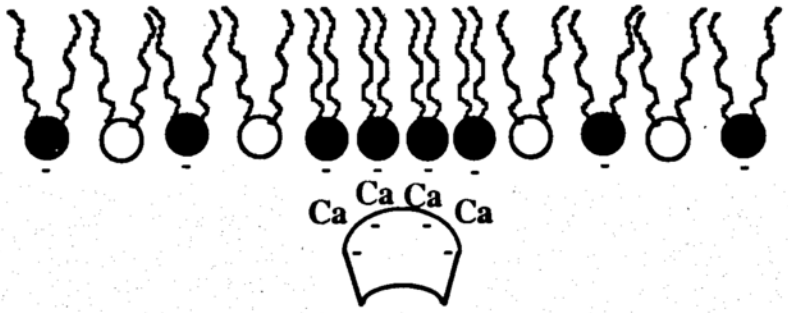

Figure 95. Schematic illustration of LAI interactions at (A) low surface pressure and (B) high surface pressure.

binding, does play a significant role in determining the specificity of LAI-anionic phospholipid interactions. In contrast to both LAI and 33 kDa PLBP, LAI-bp did not change the phase equilibria in the monolayer to any extent. The nonspecific interaction of LAI-bp with DPPC/POPG monolayers and its inability to elicit any structural changes in the monolayer may explain the lack of aggregation and fusion activity of this protein as observed by Tsao.

Chapter V. Summary and Conclusions

1. Through the measurement of πe, π-A and fluorescence microscopy, at pH 7.4, 25°C, it has been possible to study mixed monolayers of dipalmitoylphosphatidylcholine (DPPC), a key ingredient of lung surfactant, with various other phosphatidylcholines containing unsaturated acyl chains and phosphatidylglycerols (PG) likewise containing other types of acyl chains. In the latter case the effects of Ca^{2+} were also evaluated.

2. Mixtures of DPPC with a PC lipid having acyl chains containing unsaturation, POPC and DOPC, form nonideal miscible monolayers at the air/water interface. Mixtures in which the acyl chains of DPPC and the PG lipid are identical, i.e. DPPC and DPPG, form ideally miscible monolayers at the air/water interface. However, mixtures of DPPC (in excess of 50 mol%) with unsaturated PGs formed phase separated monolayers in which the amount of phase separation increased with increasing amounts of the saturated lipid, DPPC. At a concentration of DPPC between 30 and 50 mol%, the solubility of DPPC in the unsaturated PG lipid is exceeded and DPPC-enriched domains are formed. The solubility of DPPC decreases with surface pressure, as would be expected from the known effects of pressure on three-dimensional solubility of solids.

3. The surface phase rule has been used to analyze the nature of the equilibrium between the bulk mixed phospholipid systems and corresponding monolayers at πe. For DPPC/POPC and DPPC/DOPC, over all compositions up to 70 mol% of DPPC,

πe is constant, consistent with an equilibrium between separated bulk phases and miscible monolayer phases, as observed experimentally and independently via thermal analysis of the bulk phases and π-A analysis and fluorescence microscopy for the surface phases. Likewise, for DPPC/POPG at concentrations less than 30 mol% of DPPC, πe is constant, indicating that a similar equilibrium at πe exists between an immiscible bulk system and a miscible monolayer system. However, at and above 50 mol% DPPC, πe decreases with increasing DPPC. If the data reported in the literature for DPPC/POPG bilayers is correct and these systems are miscible, the phase rule would predict surface phase miscibility at these higher mole fractions of DPPC. However direct measurement up to, but not at πe indicate immiscibility of the monolayer system. Possible explanations for such results are discussed.

4. The monolayer technique was used to study the interaction of lung annexin I, LAI, with the DPPC/PG systems examined above. The penetration of LAI into monolayers at various initial surface pressures, π_i, was monitored by measuring the change in surface pressure, $\Delta\pi$. The effects of LAI on monolayer phase behavior were followed using fluorescence microscopy. The presence of LAI at the monolayer surface at high π_i was directly observed by atomic force microscopy, AFM, using Langmuir-Blodgett (LB) films of DPPG deposited on mica.

5. LAI interacts specifically with the anionic PG lipids, DPPG, POPG, and DOPG, in a calcium-dependent manner as opposed to zwitterionic DPPC which shows only limited nonspecific interactions. Penetration of the PG monolayers at $\pi < 20$ mN/m occurs and the extent of penetration is governed by the availability of free area in the monolayer. Exclusion of the protein from the monolayer occurs at a surface pressure of between 20 and 30 mN/m regardless of the lipid however, with POPG monolayers

at surface pressures in excess of 25 mN/m, the protein appears to adsorb beneath the lipid layer to cause the condensation of phospholipid monolayer films that have not reached their closest packing dimensions, and hence produce negative values of $\Delta\pi$. AFM measurements with DPPG LB films formed by monolayers at $\pi = 35$ mN/m, support the conclusion that LAI remains associated with the PG even when excluded from the monolayer.

6. LAI interaction with phase separated mixtures of DPPC and POPG increases as the PG composition increases and the interactions significantly affected the phase equilibria of these mixtures. At surface pressures of 6 mN/m or less, LAI penetrated the monolayer, increased surface pressure and thus promoted phase separation. At higher surface pressures a significant decrease in phase separation was observed. In order for phase separation to decrease in this latter system, condensed DPPC-enriched domains must have dissolved by expanding into some of the free area created upon interaction of LAI with the monolayer. This creation of less ordered regions could play an important role in the ability of LAI to promote fusion and aggregation.

7. Preliminary experiments with another lung protein, 33 kDa PLBP, indicate that this protein and LAI have similar interactions with mixed DPPC/POPG monolayers. The 33 kDa PLBP appears to also interact specifically with these monolayers and to have the ability to alter the phase equilibria by enhancing phase separation at low initial surface pressures. Preliminary experiments with the LAI breakdown protein, which does not have the aggregation and fusion activity possessed by LAI and 33 kDa PLBP, showed that this protein did not have any specific affinity for the binary DPPC/POPG monolayers and did not have the ability to alter the phase equilibria. This suggests

that the amino-terminus is involved in regulating the protein's ability to mediate specific interactions with anionic phospholipid monolayers.

Chapter VI. Appendix A

BCA Protein Assay in the Presence of Sulfhydryl Reagents*

(modified from Hill, H.D. and Straka, J.G., *Protein Determination Using Bicinchoninic Acid in the Presence of Sulfhydryl Reagents*. Analytical Biochemistry, 1988. **170**: p. 203-208.)

*Thiol reagents (such as 2-mercaptoethanol and dithiothreitol (DTT)) will reduce the copper in the BCA protein reagent resulting in marked increases in absorbance at 562nm. This method involves reaction of the thiols with iodoacetamide prior to addition of the BCA reagents.

Reagent A:

Aqueous solution (w/v %)of:

1% BCA-Na_2

2% $Na_2CO_3 \cdot H_2O$

0.16% Na_2 tartrate

0.2% NaOH

0.95% $NaHCO_3$

adjust to pH 11.25 with NaOH (50%)

Reagent B:

4 (w/v)% $CuSO_4 \cdot 5H_2O$ in deionized water

NOTE: Reagents A and B are commercially available from Pierce Chemical Co. (Rockford, IL).

1. Prepare fresh S-WR according to the standard BCA protocol.

   100 volume of Reagent A

   2 volume Reagent B

   S-WR should be apple green in color.

2. Prepare a 1 mM iodoacetamide solution in 0.01 M Tris-HCl, pH 7.4. Protect solution from light and store refrigerated.

3. Into test tubes, pipette the unknown protein sample (that contains the sulfhydryl reagent) and the protein standards (i.e. BSA). Add the same amount of the sulfhydryl reagent to the standards.

4. Add enough iodoacetamide to all test tubes so that there are at least 2 moles of iodoacetamide per mole of thiol. Prepare a blank that contains the same amount of iodoacetamide.

5. Bring the volume of protein unknown and standards to 50 µl with buffer (volume can be larger but, be sure to add the appropriate amount of S-WR).

6. Incubate for 15 minutes at 60°C.

7. Mix 1 volume of sample (standard or unknown) with 20 volume of S-WR, i.e. if the sample volume is 50 µl, add 1 ml of S-WR.

8. Incubate for 30 minutes at 60°C.

9. Cool samples to room temperature.

10. Measure absorbance at 562 nm versus the reagent blank that only contains iodoacetamide, buffer, and the S-WR.

A typical standard curve for bovine serum albumin is shown below .

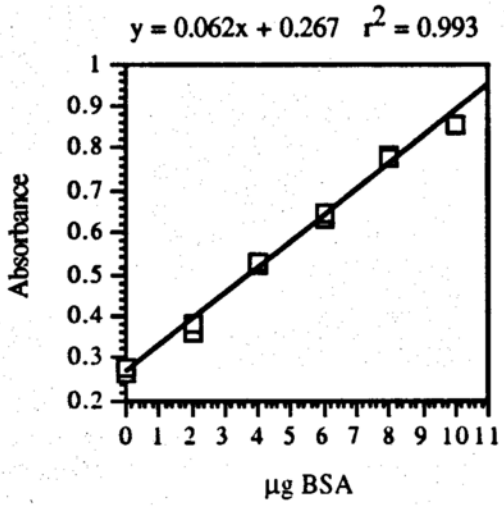

Chapter VII. Appendix B

The primary sequence for rabbit lung annexin I isolated from alveolar type II cells has been reported by Tsao, F.H.C, Wen, C., and Hu, J.

MAMVSEFLKQAWFIDNEEQDYINTVKTYKGGPGSAVSPYPAFNPSSDVAALHQ
AIMVKGVDEATIIDILTKRNNAQRQQIKAAYLQEKGKPLDEVLKKALTGHLEEV
VLALLKTPAQFDADELRAAMKGLGTDEDTLIEILASRNNKEIREINRVYREELK
RDLAKDIASDTSGDFQKALLSLAKGDRSEDFGVNEDLADTDARALYEAGERRK
GADVNVFTTILTTRSYLHLRRVFQKYSKYSQHDMNKVLDLELKGDIEKCLTAI
VQCATCKPAYFAEKLYQAMKGAGTRHKALIRIMVSRSEVDMNDIKAFYQKKY
GVSLCQAILDETKGDYEKILVALCGGN

Chapter VIII. Appendix C

Abbreviations

a	activity
A	area/molecule
A^E	excess area
A_f	free area/molecule
A_{min}	minimum area to which the monolayer can be compressed
A_o	occupied area/molecule
AFM	atomic force microscopy
C	components
DPPC	1, 2-dipalmitoyl-*sn*-glycero-3-phosphocholine
DPPG	1, 2-dipalmitoyl-*sn*-glycero-3-phospho-rac-glycerol
DOPC	1, 2-dioleoyl-*sn*-glycero-3-phosphocholine
DOPG	1, 2-dioleoyl-*sn*-glycero-3-phospho-rac-glycerol
F	number of degrees of freedom
Γ	surface concentration
γ	surface tension
LAI	lung annexin I
LAI-bp	lung annexin I breakdown protein
LB	Langmuir-Blodgett
LC	liquid condensed
LE	liquid expanded
NBD-PC	1-palmitoyl-2-[12-[(7-nitro-2-1,3-benzoxadiazol-4-yl)amino] dodecanoyl-*sn*- glycero-3-phosphocholine

π	surface pressure
π_c	film collapse pressure
π_e	equilibrium spreading pressure
π_f	final surface pressure
π_i	initial surface pressure
π_{max}	film collapse pressure
^pB	bulk phases
^pS	surface phases
PA	phosphatidic acid
PC	phosphatidylcholine
PE	phosphatidylethanolamine
PI	soy plant phosphatidylinositol
PG	phosphatidylglycerol
PS	phosphatidylserine
PLA_2	phospholipase A_2
PLBP	phospholipid-binding protein
POPC	1-palmitoyl-2-oleoyl-*sn*-glycero-3-phosphocholine
POPG	1-palmitoyl-2-oleoyl-*sn*-glycero-3-phospho-rac-glycerol
r	radius
R	gas constant
T	temperature

Chapter VII. References

Adamson, A. W. (1990). Physical Chemistry of Surfaces. New York, Wiley-Interscience.

Alexander, D. M. and G. T. Barnes (1980)."Use of the Gibbs Equation to Calculate Adsorpteion into Monolayer-covered Surfaces." *J.C.S. Faraday I* , **76**, 118-125.

Ando, Y., S. Imamura, Y.-M. Hong, et al. (1989)."Enhancement of Calcium Sensitivity of Lipocortin I in Phospholipid Binding Induced by Limited Proteolysis and Phosphorylation at the Amino Terminus as Analyzed by Phospholipid Affinity Column Chromatography." *J. Biol. Chem.* , **264**, 6948-6955.

Andree, H. A. M., C. P. M. Reutelingsperger, R. Hauptmann, et al. (1990)."Binding of Vascular Anticoagulant α (VACα) to Planar Phospholipid Bilayers." *J. Biol. Chem.* ; **265**, 4923-4928.

Andree, H. A. M., M. C. A. Stuart, W. T. Hermens, et al. (1992)."Clustering of Lipid-Bound Annexin V May Explain Its Anticoagulant Effect." *J. Biol. Chem.* , **267**, 17907-17912.

Andree, H. A. M., G. M. Willems, R. Hauptmann, et al. (1993)."Aggregation of Phospholipid Vesicles by a Chimeric Protein with the N-Terminus of Annexin I and the Core of Annexin V." *Biochemistry* , 4634-4640.

Bangham, A. D., C. J. Morley and M. C. Phillips (1979)."The Physical Properties of an Effective Lung Surfactant." *Biochim. Biophys. Acta* , **573**, 552-556.

Batenburg, J. J. (1992)."Surfactant Phospholipids: Synthesis and Storage." *Am. J. Physiol.* , **262**, L367-L385.

Bewley, M. C., C. M. Boustead, J. H. Walker, et al. (1993)."Structure of Chicken Annexin V at 2.25-Å Resolution." *Biochemistry* , **32**, 3923-3929.

Binnig, G., C. F. Quate and C. Gerber (1986)."Atomic Force Microscope." *Phys. Rev. Lett.* , **56**, 930-933.

Birdi, K. S. (1989). Lipid and Biopolymer Monolayers at Liquid Interfaces. New York, Plenum Press.

Blackwood, R. A. and J. D. Ernst (1990)."Characterization of Ca2+ -Dependent Phospholipid Binding, Vesicle Aggregation and Membrane Fusion by Annexins." *Biochem. J.* , **266**, 195-200.

Boonman, A., F. H. J. Machiels, A. F. M. Snik, et al. (1987)."Squeeze-Out from Mixed Monolayers of Dipalmitoylphosphatidylcholine and Egg Phosphatidylglycerol." *J. Colloid Interface Sci.* , **120**, 456-468.

Bourdieu, L., O. Ronsin and D. Chatenay (1993)."Molecular Positional Order in Langmuir-Blodgett Films by Atomic Force Microscopy." *Science* , **259**, 798.

Brian, A. A. and H. M. McConnell (1984)."*Proc. Natl. Acad. Sci. USA* , **81**, 6159-6163.

Brisson, A., G. Mosser and R. Huber (1991)."Structure of Soluble and Membrane-Bound Human Annexin V." *J. Mol. Biol.* , **220**, 199-203.

Burgoyne, R. D. and A. Morgan (1992)."Phospholipid-Binding Proteins in Calcium-Dependent Exocytosis." *Biochem. Soc. Trans.* , **20**, 834-836.

Chen, Y. L., M. Sano, M. Kawaguchi, et al. (1986)."*Langmuir* , **2**, 352.

Chi, L. F., M. Anders, R. R. Johnston, et al. (1993)."Domain Structures in Langmuir-Blodgett Films Investigated by Atomic Force Microscopy." *Science* , **259**, 213-216.

Chi, L. F., H. Fuchs, R. R. Johnston, et al. (1994)."Investigations of Phase Separated Langmuir-Blodgett Films by Atomic Force Microscopy." *Thin Solid Films* , **242**, 151-156.

Colacicco, G. (1968)."Lipid Monolayers: Mechanisms of Protein Penetration With Regard to Membrane Models." *Lipids* , **5**, 636-649.

Concha, N. O., J. F. Head, M. A. Kaetzel, et al. (1993)."Rat Annexin V Crystal Structure: Ca2+ -Induced Conformational Changes." *Science* , **261**, 1321-1324.

Crisp, D. J. (1949). A Two Dimensional Phase Rule. I. Derivation of a Two Dimensional Phase Rule for Plane Interfaces. II. Some Applications of a Two Dimensional Phase Rule for a Single Interface. Surface Chemistry. London, 17-35.

Curatolo, W., B. Sears and L. J. Neuringer (1985)."A Calorimetry and Deuterium NMR Study of Mixed Model Membranes of 1-palmitoyl-2-oleylphosphatidylcholine and saturated phosphatidylcholines." *Biochim. Biophys. Acta* , **817**, 261-270.

Davidson, F. F. and E. A. Dennis (1992)."Limitations of Phosphatidylcholine/Deoxycholate Mixtures for the Analysis of Phospholipase A_2 Inhibition and Activation: Illustration with Annexins." *Biochim. Biophys. Acta* , **1127**, 270-276.

Davis, P. J., K. P. Coolbear and K. M. W. Keough (1980)."Differential Scanning Calorimetric Studies of the Thermotropic Phase Behaviour of Membranes Composed of Dipalmitoyllecithin and Mixed-Acid Unsaturated Lecithins." *Can. J. Biochem.* , **58**, 851-858.

Dörfler, H. D. (1990)."Mixing Behavior of Binary Insoluble Phospholipid Monolayers. Analysis of the Mixing Properties of Binary Lecithin and Cephalin Systems By Application of Several Surface and Spreading Techniques." *Advances in Colloid and Interface Science* , **31**, 1-110.

Driessen, H. P. C., R. H. Newman, P. S. Freemont, et al. (1992)."A Model of the Structure of Human Annexin VI Bound to Lipid Monolayers." *FEBS* , **306**, 75-79.

Eklund, K. K., J. Vuorinen, J. Mikkola, et al. (1988)."Ca^{2+}-Induced Lateral Phase Seperation in Phosphatidic Acid/Phosphatidylcholine Monolayers As Revealed by Fluorescence Microscopy." *Biochemistry* , **27**, 3433-3437.

El Mashak, E. M., F. Lakhdar-Ghazal and J. F. Tocanne (1982)."Effect of pH, Mono- and Divalent Cations on the Mixing of Phosphatidylglycerol with Phosphatidylcholine. A Monolayer (Π, ΔV) and Fluorescence Study." *Biochim. Biophys. Acta* , **688**, 465-474.

Ernst, J. D., A. Mall and G. Chew (1994)."Annexins Possess Functionally Distinguishable Ca2+ and Phospholipid Binding Domains." *Biochem. Biophys. Res. Comm.* , **200**, 867-876.

Fare, T. L., C. A. Palmer, C. G. Silvestre, et al. (1992)."Langmuir-Blodgett Studies and Atomic Force Microscope Images of Nicotinic Acetylcholine Receptor Films." *Langmuir* , **8**, 3116-3121.

Findlay, E. J. and P. G. Barton (1978)."Phase Behavior of Synthetic Phosphatidylglycerols and Binary Mixtures with Phosphatidylcholines in the presence and Absence of Calcium Ions." *Biochemistry* , **17**, 2400-2405.

Fleming, B. D. and K. M. W. Keough (1988)."Surface Respreading After Collapse of Monolayers Containing Major Lipids of Pulmonary Surfactant." *Chem. Phys. Lipids* , **49**, 81-86.

Francis, J. W., K. J. Balazovich, J. E. Smolen, et al. (1992)."Human Neutrophil Annexin I Promotes Granule Aggregation and Modulates Ca^{2+} -Dependent Membrane Fusion." *J. Clin. Invest.* , **90**, 537-544.

Frommer, J. and E. Meyer (1991)."Atomic Force Microscopy: A Tool for Surface Science." *J. Phys.: Condens. Matter* , **3**, S1-S9.

Gaines, G. L., Jr. (1966). Insoluble Monolayers at the Liquid-Gas Interfaces. New York, Wiley-Interscience.

Garnaes, J., D. K. Schwartz, R. Viswanathan, et al. (1992)."Domain Boundaries and Buckling Superstructures in Langmuir-Blodgett Films." *Nature* , **357**, 54-57.

Geisow, M. J., J. H. Walker, C. Boustead, et al. (1987)."Annexins - New Family of Ca2+ -Regulated-Phospholipid Binding Protein." *Bioscience Reports* , **7**, 289-298.

Gilmanshin, R., C. E. Creutz and L. K. Tamm (1994)."Annexin IV Reduces the Rate of Lateral Lipid Diffusion and Changes the Fluid Phase Structure of the Lipid Bilayer When It Binds to Negatively Charged membranes in the Prescence of Calcium." *Biochemistry* , **33**, 8225-8232.

Goddard, E. D. and J. H. Schulman Molecular Interaction in Monolayers. I. Complex Formation." 309-340.

Goerke, J. (1974)."Lung Surfactant." *Biochim. Biophys. Acta* , **344**, 241-261.

Goodrich, F. C. (1957). Molecular Interactions in Mixed Monolayers. Proc. 2nd Int. Congr. Surface Activity. London, Butterworths. 85-91.

Gould, S. A. C., B. Drake, C. B. Prater, et al. (1990)."From Atoms to Integrated Circuit Chips, Blood Cells, and Bacteria with the Atomic Force Microscope." *J. Vac. Sci. Technol. A.* , **8**, 369-373.

Green, J. P., M. C. Phillips and G. G. Shipley (1973)."Structural investigations of Lipid, Polypeptide and Protein Multilayers." *Biochim. Biophys. Acta* , **330**, 243-253.

Hall, D. G. (1986)."Thermodynamics of Monolayer Penetration." *Langmuir* , **2**, 809-812.

Hallman, M., G. Enhorning and F. Possmayer (1985)."Composition and Surface Activity of Normal and Phosphatidylglycerol-Deficient Lung Surfactant." *Pediatr. Res.* , **19**, 286-291.

Hansma, H. G., S. A. C. Gould, P. K. Hansma, et al. (1991)."Imaging Nanometer Scale Defects in Langmuir-Blodgett Films with the Atomic Force Microscope." *Langmuir* , **7**, 1051-1054.

Hansma, P. K., V. B. Elings, O. Marti, et al. (1988)."Scanning Tunneling Microscopy and Atomic Force Microscopy: Application to Biology and Technology." *Science* , **242**, 209-216.

Hawco, M. W., K. P. Coolbear, P. J. Davis, et al. (1981)."Exclusion of Fluid Lipid During Compression of Monolayers of Mixtures of Dipalmitoylphosphatidylcholine with Some Other Phosphatidylcholines." *Biochim. Biophys. Acta* , **646**, 185-187.

Hawco, M. W., P. J. Davis and K. M. W. Keough (1981)."Lipid Fluidity in Lung Surfactant: Monolayers of Saturated and Unsaturated Lecithins." *J. Applied Physiol.: Respirat. Environ. Exercise Physiol.* , **51**, 509-515.

Hawgood, S. and J. A. Clements (1990)."Pulmonary Surfactant and Its Apoproteins." *J. Clin. Invest.* , **86**, 1-6.

Hendrickson, H. S., P. C. Fan, D. K. Kaufman, et al. (1983)."The Effect of a Phase Transition on Penetration of Phospholipid Monolayers by Melittin and Glucagon." *Arch. Biochem. Biophys.* , **227**, 242-247.

Hifeda, Y. F. and G. W. Rayfield (1992)."Evidence for First-Order Phase Transitions in Lipid and Fatty Acid Monolayers." *Langmuir* , **8**, 197-200.

Hill, H. D. and J. G. Straka (1988)."Protein Determination Using Bincinchoninic Acid in the Presence of Sulfhydryl Reagents." *Analytical Biochemistry* , **170**, 203-208.

Hills, B. A. (1990)."The Role of Lung Surfactant." *British J. Anaesthesia* , **65**, 13-29.

Hoekstra, D., R. Buist-Arkema, K. Klappe, et al. (1993)."Interaction of Annexins with Membranes: The N-Terminus as a Governing Parameter As Revealed with a Chimeric Annexin." *Biochemistry* , **32**, 14194-14202.

Huber, R., R. Berendes, A. Burger, et al. (1992). Annexin V: Crystal Structure and its Implications on Function. The Annexins. London, Portland Press. 105-124.

Huber, R., R. Berendes, A. Burger, et al. (1992)."Crystal and Molecular Structure of Human Annexin V After Refinement. Implications for Structure, Membrane Binding and Ion Channel Formation of the Annexin Family of Proteins." *J. Mol. Biol.*, **223**, 683-704.

Egger, M., F. Ohnesorge, A. L. Weisenhorn, et al. (1990)."Wet Lipid-Protein Membranes Imaged at Submolecular Resolution by Atomic Force Microscopy." *J. Struct. Biol.*, **103**, 89-94.

Jalal, I. M., G. Zografi, A. K. Rakshit, et al. (1980)."Monolayer Properties of Fatty Acids. I. Thermodynamics of Spreading." *J. Colloid Interface Sci.*, **76**, 146-156.

Junker, M. and C. E. Creutz (1993)."Endonexin (Annexin IV)-Mediated Lateral Segregation of Phosphatidylglycerol in Phosphatidylglycerol/Phosphatiddylcholine Membranes." *Biochemistry*, **32**, 9968-9974.

Junker, M. and C. E. Creutz (1994)."Ca^{2+}-Dependent Binding Of Endonexin (Annexin IV) to Membranes: Analysis of the Effects of Membrane Lipid Composition and Development of a Predictive Model for the Binding Interaction." *Biochemistry*, **33**, 8930-8940.

Kajiyama, T., Y. Oishi, F. Hirose, et al. (1994)."Direct Observation of Molecular Arrangements in Fatty Acid Monolayers with an Atomic Force Microscope." *Langmuir* , **10**, 1297-1299.

Keough, K. M. W. (1984)."Physical Chemical Properties of Some Mixtures of Lipids and Their Potential for Use as Exogenous Pulmonary Surfactants." *Prog. Resp. Res.* , **18**, 257-262.

Keough, K. M. W. (1985). Lipid Fluidity and Respiratory Distress Syndrome. Membrane Fluidity in Biology. New York, Academic Press, Inc. 39-84.

Kim, K. M., D. K. Kim, Y. M. Park, et al. (1994)."Annexin-I Inhibits Phospholipase A2 by Specific Interaction, Not By Substrate Depletion." *FEBS Lett.* , **343**, 251-255.

Kim, S. and H. Yu (1992)."Lateral Diffusion of Amphiphiles and Macromolecules at the Air/Water Interface." *J. Phys. Chem.* , **96**, 4034-4040.

Klee, C. B. (1988)."Ca2+ -Dependent Phospholipid- (and Membrane-) Binding Proteins." *Biochemistry* , **27**, 6645-6653.

Koppenol, S. (1993). Phase Equilibria in Binary Mixtures of Phospholipid Monolayers at the Air/Water Interface. University of Wisconsin-Madison.

Lal, R. and S. A. John (1994)."Biological Applications of Atomic Force Microscopy." C1-C21.

Lecompte, M.-F., G. Bouix and K. G. Mann (1994)."Electrostatic and Hydrophobic Interactions Are Involved in Factor Va Binding to Membranes Containing Acidic Phospholipids." *J. Biol. Chem.* , **269**, 1905-1910.

Luecke, H., B. T. Chang, W. S. Mailliard, et al. (1995)."Crystal Structure of the Annxin XII Hexamer and Implications for Bilayer Insertion." *Nature* , **378**, 512-515.

MacRitchie, F. (1990). Chemistry at Interfaces. New York, Academic Press, Inc.

Marti, O., B. Drake and P. K. Hansma (1987)."Atomic Force Microscopy of Liquid-Covered Surfaces: Atomic Resolution Images." *Appl. Phys. Lett.* , **51**, 484-486.

McConnell, H. M. (1991)."Structures and Transitions in Lipid Monolayers at the Air-Water Interface." *Annu. Rev. Phys. Chem.* , **42**, 171-195.

McConnell, H. M., T. H. Watts, R. M. Weis, et al. (1986)."Supported Planar Membranes in Studies of Cell-Cell Recognition in the Immune System." *Biochim. Biophys. Acta* , **864**, 95-106.

Meers, P., D. Daleke, K. Hong, et al. (1991)."Interactions of Annexins with Membrane Phospholipids." *Biochemistry* , **30**, 2903-2908.

Meers, P. and T. Mealy (1994)."Phospholipid Determinants for Annexin V Binding Sites and the Role of Tryptophan 187." *Biochemistry* , **33**, 5829-5837.

Meers, P., T. Mealy, N. Pavlotsky, et al. (1992)."Annexin I-Mediated Vesicular Aggregation: Mechanism and Role in Human Neutrophils." *Biochemistry* , **31**, 6372-6382.

Meers, P., T. Mealy and A. I. Tauber (1993)."Annexin I Interactions with Human Neutrophil Specific Granules: Fusogenicity and Coaggregationwith Plasma Membrane Vesicles." *Biochim. Biophys. Acta* , **1147**, 177-184.

Meller, P. (1988)."Computer-Assisted Video Microscopy for the Investigation of Monolayers on Liquid and Solid Substrates." *Rev. Sci. Instrum.* , **59**, 2225-2231.

Meyer, E., L. Howald, R. M. Overney, et al. (1991)."Molecular-Resolution Images of Langmuir-Blodgett Films Using Atomic Force Microscopy." *Nature* , **349**, 398-400.

Mittler-Neher, S. and W. Knoll (1989)."Phase Seperation in Bimolecular Mixed Lipid Membranes Induced by Polylysine." *Biochem. Biophys. Res. Comm.* , **162**, 124-129.

Möhwald, H. (1990)."Phospholipid and Phospholipid-Protein Monolayers at the Air/Water Interface." *Annu. Rev. Phys. Chem.* , **41**, 441-476.

Mosser, G., C. Ravanat, J.-M. Freyssinet, et al. (1991)."Sub-Domain Structure of Lipid-Bound Annexin-V Resolved by Electonic Image Analysis." *J. Mol. Biol.* , **217**, 241-245.

Motomura, K. (1980)."Thermodynamics of Interfacial Monolayers." *Adv. Colloid Interface Sci.* , **12**, 1-42.

Motomura, K., K. Sekita and R. Matuura (1974)."Thermodynamics of Multicomponent Monolayers. II. Phase Transitions in Two-Component Monolayers." *J. Colloid Interface Sci.*, **48**, 319-326.

Nag, K., C. Boland, N. Rich, et al. (1991)."Epifluorescence Microscopic Observation of Monolayers of Dipalmitoylphosphatidylcholine: Dependence of Domain Size on Compression Rates." *Biochim. Biophys. Acta* , **1068**, 157-160.

Nag, K., C. Boland, N. H. Rich, et al. (1990)."Design and Construction of an Epifluorescence Microscopic Surface Balance for the Study of Lipid Monolayer Phase Transitions." *Rev. Sci. Instrum.*, **61**, 3425-3430.

Nag, K., N. H. Rich and K. M. W. Keough (1994)."Interaction Between Dipalmitoylphosphatidylglycerol and Phosphatidylcholine and Calcium." *Thin Solid Films* , **244**, 841-844.

Newman, R., A. Tucker, C. Ferguson, et al. (1989)."Crystallization of p68 on Lipid Monolayers and as Three-Dimensional Single Crystals." *J. Mol. Biol.*, **206**, 213-219.

Pagano, R. E. and N. L. Gershfeld (1972)."Physical Chemistry of Lipid Films at the Air-Water Interface. II. Binary Lipid Mixtures. The Principles Governing Miscibility of Lipids in Surfaces." *J. Phys. Chem.*, **76**, 1238-1243.

Pallas, N. R. and B. A. Pethica (1985)."Liquid-Expanded to Liquid-Condensed Transitions in Lipid Monolayers at the Air/Water Interface." *Langmuir* , **1**, 509-513.

Pallas, N. R. and B. A. Pethica (1985)."Liquid-Expanded to Liquid-Condensed Transitions in Lipid Monolayers at the Air/Water Interface." *Langmuir* , **1**, 509-513.

Pastrana, B., A. J. Mautone and R. Mendelsohn (1991)."Fourier Transform Infared Studies of Secondary Structure and Orientation of Pulmonary Surfactant SP-C and Its Effect on the Dynamic Surface Properties of Phospholipids." *Biochemistry* , **30**, 10085-10064.

Peltonen, J. P. K., P. He and J. B. Rosenholm (1992)."Order and Defects of Langmuir-Blodgett Films Detected with the Atomic Force Microscope." *J. Am. Chem. Soc.* , **114**, 7637-7642.

Perretti, M. (1994)."Lipocortin-Derived Peptides." *Biochem. Pharmacol.* , **47**, 931-938.

Peters, R. and K. Beck (1983)."Translational Diffusion in Phospholipid Monolayers Measured by Fluorescence Microphotolysis." *Proc. Natl. Acad. Sci. USA* , **80**, 7183-7187.

Pethica, B. A. (1955)."The Thermodynamics of Monolayer Penetration at Constant Area." *Trans. Faraday Soc.* , **51**, 1402-1411.

Phillips, M. C. and D. Chapman (1968)."Monolayer Characteristics of Saturated 1,2-Diacyl Phosphatidylcholines (Lecithins) and Phosphatidylethanolamines at the Air-Water Interface." *Biochim. Biophys. Acta* , **163**, 301-313.

Pigault, C., A. Follenius-Wund, M. Schmutz, et al. (1994)."Formation of Two-Dimensional Arrays of Annexin V on Phosphatidylserine-Containing Liposomes." *J. Mol. Biol.*, **236**, 199-208.

Pollard, H. B., H. R. Guy, N. Arispe, et al. (1992)."Calcium Channel and Membrane Fusion Activity of Synexin and Other Members of the Annexin Gene Family." *Biophys. J.*, **62**, 15-18.

Quinn, P. J. and R. M. C. Dawson (1970)."An Analysis of the Interaction of Protein with Lipid Monolayers at the Air/Water Interface." *Biochem. J.*, **116**, 671-680.

Radmacher, M., R. W. Tillmann, M. Fritz, et al. (1992)."From Molecules to Cells: Imaging Soft Samples with the Atomic Force Microscope." *Science*, **257**, 1900-1905.

Rana, F. R., A. J. Mautone and R. A. Dluhy (1993)."Surface Chemistry of Binary Mixtures of Phospholipids in Monolayers. Infrared Studies of Surface Composition at Varying Surface Pressures in a Pulmonary Surfactant Model System." *Biochemistry*, **32**, 3169-3177.

Raynal, P. and H. B. Pollard (1994)."Annexins: The Problem of Assessing the Biological Role for a Gene Family of Multifunctional Calcium- Phospholipid-Binding Proteins." *Biochim. Biophys. Acta*, **1197**, 63-93.

Reichert, A., H. Ringsdorf and A. Wagenknecht (1992)."Spontaneous Domain Formation of Phospholipase A_2 at Interfaces: Fluorescence Microscopy of the

Interaction of Phospholipase A_2 with Mixed Monolayers of Lecithin, Lysolecithin and Fatty Acid." *Biochim. Biophys. Acta* , **1106**, 178-188.

Riegler, J. E. (1988)."Fluorescence Microscope for Real-Time Studies of Langmuir-Blodgett Layer Deposition." *Rev. Sci. Instrum.* , **59**, 2220-2224.

Roberts, G., Ed. (1990). Langmuir-Blodgett Films. New York, Plenum Press.

Rojas, E., N. Arispe, H. T. Haigler, et al. (1992)."Identification of Annexins as Calcium Channels in Biological Membranes." *Bone and Mineral* , **17**, 214-218.

Romisch, J. and E. P. Paques (1991)."Annexins: Calcium-Binding Proteins of Multi-Functional Importance." *Med. Microbiol. Immunol.* , **180**, 109-126.

Ruger, D. and P. Hansma (1990)."Atomic Force Microscopy." *Physics Today* , 23-30.

Sacchetti, M., H. Yu and G. Zografi (1993)."A Canal Surface Viscometer for the In-Plane Steady Shear Viscosity of Monolayers at the Air/Water Interface." *Rev. Sci. Instrum.* , **64**, 1941-1946.

Sackmann, E. (1996)."Supported Membranes: Scientific and Practicle Applications." *Science* , **271**, 43-48.

Schlaepfer, D. D. and H. T. Haigler (1987)."Characterization of Ca2+ -Dependent Phospholipid Binding and Phosphorylation of Lipocortin I." *J. Biol. Chem.* , **262**, 6931-6937.

Schlame, M., C. Casals, B. Rustow, et al. (1988)."Molecular Species of Phosphatidylcholine and Phosphatidylglycerol in Rat Lung Surfactant and Different Pools of Pneumocytes Type II." *Biochem. J.* , **253**, 209-215.

Schwarzenbach, G. and H. Flaschka (1965). Complexometric Titrations. London, Methuen and Company, LTD.

Shah, D. O. and R. W. Capps (1968)."On Thermodynamics of Mixed Monolayers." *J. Colloid Interface Sci.* , **27**, 319-320.

Shah, D. O. and J. H. Schulman (1968)."Influence of Induced Dipoles, Metal Ions, and Cholesterol on the Characteristics of Phospholipid Monolayers." *ACS: Advances in Chemistry Series* , **84**, 189-209.

Smith, P. K., R. I. Krohn, G. T. Hermanson, et al. (1985)."Measurement of Protein Using Bincinchoninic Acid." *Analytical Biochemistry* , **150**, 76-85.

Sopkova, J., J. Gallay, M. Vincent, et al. (1994)."The Dynamic Behavior of Annexin V as a Function of Calcium Ion Binding: A Circular Dichroism, UV Absorption, and Steady-State and Time-Resolved Fluoerescence Study." *Biochemistry* , **33**, 4490-4499.

Sopkova, J., M. Renouard and A. Lewit-Bentley (1993)."The Crystal Structure of a New High-Calcium Form of Annexin V." *J. Mol. Biol.* , **234**, 816-825.

Stine, K. J. (1994)."Investigations of Monolayer by Fluorescence Microscopy." *Microsc. Res. Tech.* , **27**, 439-450.

Stine, K. J. and C. M. Knobler (1992)."Fluorescence Microscopy: A Tool for Studying the Physical Chemistry of Interfaces." *Ultramicroscopy* , **47**, 23-34.

Stine, K. J. and D. T. Stratmann (1992)."Fluorescence Microscopy Study of Langmuir Monolayers of Stearylamine." *Langmuir* , **8**, 2509-2514.

Tait, J. F., D. Gibson and K. Fujikawa (1989)."Phospholipid Binding Properties of Human Placental Anticoagulant Protein-I, a Member of the Lipocortin Family." *J. Biol. Chem.* , **264**, 7944-7949.

Thunnissen, M. M. G. M., E. AB, K. H. Kalk, et al. (1990)."X-Ray Structure of Phospholipase A2 Complexed with a Substrate-Derived Inhibitor." *Nature* , **347**, 689-691.

Trave, G., J.-F. Quignard, C. Lionne, et al. (1994)."Interdependence of Phospholipid Specificity and Calcium Binding in Annexin I as Shown by Site-Directed Mutagenesis." *Biochim. Biophys. Acta* , **1205**, 215-222.

Trurnit, H. J. (1960)."A Theory and Method for the Spreading of Protein Monolayers." *J. Colloid Sci.* , **15**, 1-13.

Tsao, F. H. C. (1990)."Purification and Characterization of Two Rabbit Lung Ca^{2+} -Dependent Phospholipid-Binding Proteins." *Biochim. Biophys. Acta* , **1045**, 29-39.

Tsao, F. H. C., X. Chen, X. Chen, et al. (1994)."Immunocharacterization and Developmental Regulation of Rabbit Lung Calcium-Dependent Phospholipid-Binding Proteins." *Biochim. Biophys. Acta* , **1213**, 91-99.

Tsao, F. H. C., T. K. F. Foo, P. M. DeLuca Jr., et al. Inhibition of Phospholipase A2 by Lung CA2+ -Dependent Phospholipid Binding Proteins." ,

Tsao, F. H. C., T. K. F. Foo, P. M. DeLuca Jr., et al. (1990)."The Use of a Multichannel Scaling Method to Detect Radioactive Species in Spread Monolayers." *Anal. Biochem.* , **188**, 1-4.

Tsao, F. H. C., C. S. Gau, H. Yu, et al. (1993)."The Surface Properties of Lung 36kDa Ca^{2+} -Dependent Phospholipid-Binding Protein." *Biochim. Biophys. Acta* , **1166**, 39-47.

Tsao, F. H. C., W. M. Hull, M. S. Strickland, et al. (1991)."Lung Calcium-Dependent Phosphilipid-Binding Proteins: Structure and Function." *Biochim. Biophys. Acta* , **1081**, 141-150.

Van Golde, L. M. G., J. J. Batenburg and B. Robertson (1988)."The Pulmonary Surfactant System: Biochemical Aspects and Functional Significance." *Phys. Rev.* , **68**, 374-455.

Van Iwaarden, F., B. Welmers, J. Verhoef, et al. (1990)."Pulmonary Surfactant Protein A Enhances the Host-Defense Mechanism of Rat Alveolar Macrophages." *Am. J. Respir. Cell. Mol. Biol.* , **2**, 91-98.

Van Liempd, J. P. J. G., A. A. H. Boonman, R. A. Demel, et al. (1987)."Nonselective Squeeze-out of Dioleoylphosphatidylcholine and Dioleoylphosphatidylglycerol from Binary Mixed Monolayers with Dipalmitoylphosphatidylcholine." *Biochim. Biophys. Acta* , **897**, 495-501.

Voges, D., R. Berendes, A. Burger, et al. (1994)."Three-Dimensional Structure of Membrane-Bound Annexin V. A Correlative Electron Microscopy-X-Ray Crystallography Study." *J. Molec. biol.* , **238**, 199-213.

Von Tscharner, V. and H. M. McConnell (1981)."Physical Properties of Lipid Monolayers on Alkylated Planar Glass Surfaces." *Biophys. J.* , **36**, 421-427.

Wang, W. and C. E. Creutz (1994)."Role of the Amino-Terminal Domain in Regulating Interactions of Annexin I with Membranes: Effects of Amino-Terminal Truncation and Mutagenesis of the Phosphorylation Sites." *Biochemistry* , **33**, 275-282.

Watkins, J. C. (1968)."The Surface Properties of Pure Phospholipids in Relation to Those of Lung Extracts." *Biochim. Biophys. Acta* , **152**, 293-306.

Weng, X., H. Luecke, I. S. Song, et al. (1993)."Crystal Structure of Human Annexin I at 2.5Å Resolution." *Protein Science* , **2**, 448-458.

Wiedmann, T., A. Salmon and V. Wong (1993)."Phase Behavior of Mixtures of DPPC and POPG." *Biochim. Biophys. Acta* , **1167**, 114-120.

Wright, J. R. and J. A. Clements (1987)."Metabolism and Turnover of Lung Surfactant." *Am. Rev. Respir. Dis.* , **135**, 426-444.

Yazdanian, M. (1990). Ionic Interactions of Fatty Acid Monolayers at the Air/Water Interface. University of Wisconsin.

Yu, S.-H. and F. Possmayer (1992)."Effect of Pulmonary Surfactant Protein B (SP-B) and Calcium on Phospholipid Adsorption and Squeeze-Out of Phosphatidylglycerol from Binary Phospholipid Monolayers Containing Dipalmitoylphosphatidylcholine." *Biochim. Biophys. Acta* , **1126**, 26-34.

Zaks, W. J. and C. E. Creutz (1990)."Evaluation of the Annexins as Potential Mediators of Membrane Fusion in Exocytosis." *J. Bioenergetics Biomembranes* , **22**, 97-120.

Zasadzinski, J. A., R. Viswanathan, L. Madsen, et al. (1994)."Langmuir-Blodgett Films." *Science* , **263**, 1726-1733.